frontiers

RESEARCH TOPICS

TRAUMATIC INJURIES IN THE NERVOUS SYSTEM

Hosted by
Mårten Risling

frontiers in
NEUROLOGY

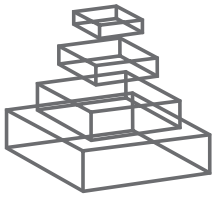

frontiers

Cover image provided by Ibbl sarl, Lausanne CH

ISSN 1664-8714
ISBN 978-2-88919-018-8
DOI 10.3389/978-2-88919-018-8

ABOUT FRONTIERS

Frontiers is more than just an open-access publisher of scholarly articles: it is a pioneering approach to the world of academia, radically improving the way scholarly research is managed. The grand vision of Frontiers is a world where all people have an equal opportunity to seek, share and generate knowledge. Frontiers provides immediate and permanent online open access to all its publications, but this alone is not enough to realize our grand goals.

FRONTIERS JOURNAL SERIES

The Frontiers Journal Series is a multi-tier and interdisciplinary set of open-access, online journals, promising a paradigm shift from the current review, selection and dissemination processes in academic publishing.
All Frontiers journals are driven by researchers for researchers; therefore, they constitute a service to the scholarly community. At the same time, the Frontiers Journal Series operates on a revolutionary invention, the tiered publishing system, initially addressing specific communities of scholars, and gradually climbing up to broader public understanding, thus serving the interests of the lay society, too.

DEDICATION TO QUALITY

Each Frontiers article is a landmark of the highest quality, thanks to genuinely collaborative interactions between authors and review editors, who include some of the world's best academicians. Research must be certified by peers before entering a stream of knowledge that may eventually reach the public - and shape society; therefore, Frontiers only applies the most rigorous and unbiased reviews.
Frontiers revolutionizes research publishing by freely delivering the most outstanding research, evaluated with no bias from both the academic and social point of view.
By applying the most advanced information technologies, Frontiers is catapulting scholarly publishing into a new generation.

WHAT ARE FRONTIERS RESEARCH TOPICS?

Frontiers Research Topics are very popular trademarks of the Frontiers Journals Series: they are collections of at least ten articles, all centered on a particular subject. With their unique mix of varied contributions from Original Research to Review Articles, Frontiers Research Topics unify the most influential researchers, the latest key findings and historical advances in a hot research area!
Find out more on how to host your own Frontiers Research Topic or contribute to one as an author by contacting the Frontiers Editorial Office: researchtopics@frontiersin.org

TRAUMATIC INJURIES IN THE NERVOUS SYSTEM

Hosted By
Mårten Risling, Karolinska Institutet, Sweden

This Research Topic surrounds the information presented at the upcoming conference Neurotrama Symposium held at the Centre for Trauma Research, September 15-16 2010. Traumatic injury to the central nervous system (CNS) is the leading cause of death and disability for people up to about 40 years of age. Examples and experiences of CNS trauma and medical care during historic and ongoing wars will be given, referring to the early history of KarolinskaInstitutet (KI).

Table of Contents

04 ***Traumatic Injuries in the Nervous System***
Mårten Risling, Bo-Michael Bellander and Staffan Cullheim

06 ***Karolinska Institutet 200-Year Anniversary. Symposium on Traumatic Injuries in the Nervous System: Injuries to the Spinal Cord and Peripheral Nervous System – Injuries and Repair, Pain Problems, Lesions to Brachial Plexus***
Mattias K. Sköld, Mikael Svensson, Jack Tsao, Thomas Hultgren, Thomas Landegren, Thomas Carlstedt and Staffan Cullheim

11 ***Selectivity in the Reinnervation of the Lateral Gastrocnemius Muscle after Nerve Repair with Ethyl Cyanoacrylate in the Rat***
Thomas Landegren, Mårten Risling, Henrik Hammarberg and Jonas K. E. Persson

20 ***The Importance of Systemic Response in the Pathobiology of Blast-Induced Neurotrauma***
Ibolja Cernak

29 ***Low Level Primary Blast Injury in Rodent Brain***
Pamela B. L. Pun, Enci Mary Kan, Agus Salim, Zhaohui Li, Kian Chye Ng, Shabbir M. Moochhala, Eng-Ang Ling, Mui Hong Tan and Jia Lu

44 ***Stress and Traumatic Brain Injury: A Behavioral, Proteomics, and Histological Study***
Sook-Kyung C. Kwon, Erzsebet Kovesdi, Andrea B. Gyorgy, Daniel Wingo, Alaa Kamnaksh, John Walker, Joseph B. Long and Denes V. Agoston

58 ***A New Model to Produce Sagittal Plane Rotational Induced Diffuse Axonal Injuries***
Johan Davidsson and Marten Risling

69 ***"Studying Injured Minds" – The Vietnam Head Injury Study and 40 Years of Brain Injury Research***
Vanessa Raymont, Andres M. Salazar, Frank Krueger and Jordan Grafman

82 ***Physics of IED Blast Shock Tube Simulations for mTBI Research***
Jesus Mediavilla Varas, M. Philippens, S. R. Meijer, A. C. van den Berg, P. C. Sibma, J. L. M. J. van Bree and D. V. W. M. de Vries.

96 ***Report of a Consensus Meeting on Human Brain Temperature After Severe Traumatic Brain Injury: Its Measurement and Management During Pyrexia***
Charmaine Childs, Tadeusz Wieloch, Fiona Lecky, Graham Machin, Bridget Harris and Nino Stocchetti

104 ***Pivotal Role of Anterior Cingulate Cortex in Working Memory after Traumatic Brain Injury in Youth***
Fabienne Cazalis, Talin Babikian, Christopher Giza, Sarah Copeland, David Hovda and Robert F. Asarnow

frontiers in
NEUROLOGY

EDITORIAL
published: 24 February 2012
doi: 10.3389/fneur.2012.00026

Traumatic injuries in the nervous system

Mårten Risling*, Bo-Michael Bellander and Staffan Cullheim

Karolinska Institutet, Stockholm, Sweden
**Correspondence: marten.risling@ki.se*

A BRIEF HISTORY OF KAROLINSKA INSTITUTET

Like many other countries in Europe, nineteenth century Sweden had suffered from an extensive period of wars. After a devastating Finnish war against Russia 1808–1809, the Swedish king Karl XIII decided to start a new training facility for Army surgeons. This new institute was named "Medico-Chirurgiska Institutet," but soon the prefix "Karolinska" was added. The word "Karoliner" had been used to denote soldiers during the reign of the warrior kings Karl XI and Karl XII. After 200 years of peace, this word has fortunately become more associated with a medical university.

Originally, the institute was located in central Stockholm close to the Royal castle, but it moved in the late 1940s to Solna, on the north side of the city. Karolinska institutet is now Sweden's third oldest medical school and is associated with the Karolinska University Hospital. A committee at the institute appoints the laureates for the Nobel Prize in Physiology or Medicine. Several laureates have been awarded for outstanding studies on the nervous system, including Camillo Golgi, Santiago Ramón y Cajal, Charles Scott Sherrington, Otto Loewi, Joseph Erlanger, Herbert Spencer Gasser, Andrew Fielding Huxley, Julius Axelrod, Ulf von Euler, Bernard Katz, Roger Sperry, Ragnar Granit, David Hubel, Torsten Wiesel, Arvid Carlsson, Paul Greengard, Eric Kandel, Richard Axel, and Linda Buck.

Neuroscience research has been a strong area for a substantial amount of time at both Karolinska institutet and Karolinska University Hospital. Future neurotrauma research at this location has a solid foundation to rest upon. It is impossible to name all the distinguished neuroscientists from Karolinska institutet in this editorial, but a few examples can be noted.

One early example is "Studien in der Anatomie des Nervensystems und des Bindegewebes" by Axel Key and Gustaf Retzius in the 1870s. Ulf von Euler's studies on storage mechanisms of adrenergic neurotransmitters were succeeded by the work of Nils Hillarp and his successful followers Kjell Fuxe, Tomas Hökfelt, and many others. Hökfelt is also well-known for his studies on neuropeptides, many of which had been discovered by von Euler or Viktor Mutt. Neurophysiology has a long and strong tradition with scientists like Ragnar Granit, Curt von Euler, and Sten Grillner, who demonstrated the importance of circuits for locomotion in the spinal cord. The late Håkan Persson and his associates Patrik Ernfors and Carlos Ibáñez have studied and identified neurotrophic growth factors. Jonas Frisén and Ernst Arenas have conducted pioneering work with neuronal stem cells. Lars Olson has been active in many areas, including experiments with surgical reconstruction after spinal cord lesions. The methodological development by Fritiof Sjöstrand started an era of ultrastructure research at the Department of Anatomy that provided details on the fine structure of the nervous system.

Herbert Olivecrona had an instrumental role in developing neurosurgery into a modern specialty at Karolinska institutet. After Lars Leksell's description of the gamma motor system, he continued with clinical work and became a professor of neurosurgery, succeeding Olivecrona. He developed instruments for stereotactic surgery and the Gamma Knife for non-invasive treatment of brain tumors. Thomas Carlstedt started his work on surgical replantation of avulsed spinal nerve roots at Karolinska institutet and the hospital. Sweden's largest trauma center is now located at Karolinska sjukhuset in Solna. A new modern hospital building will replace the old hospital in 2016, adjacent to new research buildings at the campus of Karolinska institutet.

NEUROTRAUMA

The seminal works of Ramon y Cajal demonstrated that on a cellular level, the central and peripheral nervous system (CNS and PNS), share many injury response patterns. He also provided a detailed description of the general lack of regeneration in the central nervous system. Furthermore, Cajal predicted the importance of neurotrophic factors and also showed a few examples of regenerative growth in the CNS. Research has not yet been able to drastically improve regeneration in the CNS, in spite of current knowledge regarding growth factors, inhibitory molecules, axon guidance mechanisms, and stem cells. Traumatic brain injuries (TBI) also face the problem of limited space inside the scull, which means that an edema or bleeding rapidly can become lethal. To the complexity of the CNS adds a complex cascade of secondary injury mechanisms. Development and testing of curative drugs is complicated due to the great variation among patients and injury patterns. The only factor that can improve this situation is more research. For obvious reasons, research must be carefully planned and significant efforts are required to ensure a good translation between experimental and clinical work.

THE 200 YEAR ANNIVERSARY NEUROTRAUMA SYMPOSIUM

The three sessions of the symposium covered a number of themes in current neurotrauma research, such as injury mechanisms and new injury models for experimental work. A couple of the lectures provided detailed information on the influence small differences in genetic background, such as single nucleotide polymorphism, can have on the outcome of an injury. Current trends in diagnosis and drug development were discussed. Army Col. Jamie Grimes, MD, national director of the

Defense and Veterans Brain Injury Center (DVBIC) introduced a session on military related neurotrauma. Keynote speakers for the three sessions were Andrew Maas, Thomas Carlstedt, and Jordan Grafman.

We are delighted to present a cross section of the presentations from the Karolinska anniversary symposium in this Research Topic and its associated book.

Received: 10 February 2012; accepted: 10 February 2012; published online: 24 February 2012.
Citation: Risling M, Bellander B-M and Cullheim S (2012) Traumatic injuries in the nervous system. Front. Neur. ***3****:26. doi: 10.3389/fneur.2012.00026*
This article was submitted to Frontiers in Neurotrauma, a specialty of Frontiers in Neurology.

frontiers in NEUROLOGY

PERSPECTIVE ARTICLE
published: 12 May 2011
doi: 10.3389/fneur.2011.00029

Karolinska Institutet 200-year anniversary. Symposium on traumatic injuries in the nervous system: injuries to the spinal cord and peripheral nervous system – injuries and repair, pain problems, lesions to brachial plexus

Mattias K. Sköld[1,2]*, Mikael Svensson[3], Jack Tsao[4,5], Thomas Hultgren[6], Thomas Landegren[6], Thomas Carlstedt[6,7] and Staffan Cullheim[1]

[1] *Department of Neuroscience, Karolinska Institutet, Stockholm, Sweden*
[2] *Department of Clinical Neuroscience, Department of Neurosurgery, Uppsala University Hospital, Uppsala, Sweden*
[3] *Department of Clinical Neuroscience, Department Neurosurgery and Neurology, Karolinska Institutet, Karolinska University Hospital, Stockholm, Sweden*
[4] *United States Navy Bureau of Medicine and Surgery, Wounded, Ill and Injured, Washington, DC, USA*
[5] *Department of Neurology, Uniformed Services University of the Health Sciences, Bethesda, MD, USA*
[6] *Section of Hand Surgery, Department of Clinical Science and Education, Karolinska Institutet, Södersjukhuset, Stockholm, Sweden*
[7] *The Peripheral Nerve Injury Unit, The Royal National Orthopaedic Hospital, University College London, London, UK*

Edited by:
Marten Risling, Karolinska Institutet, Sweden

Reviewed by:
Marcus Ohlsson, Karolinska Institutet, Sweden
Leif A. Havton, University of California, Los Angeles, USA

****Correspondence:***
Mattias K. Sköld, Department of Neuroscience, Karolinska Institutet, S-171 77 Stockholm, Sweden.
e-mail: mattias.skold@ki.se

The Karolinska Institutet 200-year anniversary symposium on injuries to the spinal cord and peripheral nervous system gathered expertise in the spinal cord, spinal nerve, and peripheral nerve injury field spanning from molecular prerequisites for nerve regeneration to clinical methods in nerve repair and rehabilitation. The topics presented at the meeting covered findings on adult neural stem cells that when transplanted to the hypoglossal nucleus in the rat could integrate with its host and promote neuron survival. Studies on vascularization after intraspinal replantation of ventral nerve roots and microarray studies in ventral root replantation as a tool for mapping of biological patterns typical for neuronal regeneration were discussed. Different immune molecules in neurons and glia and their very specific roles in synapse plasticity after injury were presented. Novel strategies in repair of injured peripheral nerves with ethyl-cyanoacrylate adhesive showed functional recovery comparable to that of conventional epineural sutures. Various aspects on surgical techniques which are available to improve function of the limb, once the nerve regeneration after brachial plexus lesions and repair has reached its limit were presented. Moreover, neurogenic pain after amputation and its treatment with mirror therapy were shown to be followed by dramatic decrease in phantom limb pain. Finally clinical experiences on surgical techniques to repair avulsed spinal nerve root and the motoric as well as sensoric regain of function were presented.

Keywords: spinal cord, peripheral nerves, nerve injury, mirror therapy, neural stem cell

ADULT NEURAL STEM/PROGENITOR CELLS TRANSPLANTED TO THE HYPOGLOSSAL NUCLEUS OF RAT INTEGRATES WITH THE HOST CNS AND PROMOTES MOTOR NEURON SURVIVAL

Michael Fagerlund, Cynthia Perez Estrada, Nasren Jaff, Lou Brundin and Mikael Svensson

Transplantation of neural stem cells and the mobilization of endogenous neuronal precursors in the adult brain have been proposed as therapeutic strategies for a large range of central nervous system disorders and injuries. The aim of the present study was to investigate the possible survival and integration of grafted neural progenitor cells (NPCs) from the subventricular zone (SVZ) in a hypoglossal nerve avulsion model with substantial neuronal loss.

Adult NPCs from the SVZ were cultured from inbred transgenic eGFP Lewis rats and transplanted to the hypoglossal nucleus of inbred Lewis rat from the same family but that were not carrying the eGFP strain after avulsion of the hypoglossal nerve. Grafted cells survived in the host more than 3 months and differentiated into neurons (β-III tubulin) with fine axon- and dendrite-like processess as well as astrocytes (GFAP) and oligodendrocytes (O4) with typical morphology. Stainings for synaptic structures (synaptophysin and bassoon) indicated integration of differentiated cells from the graft with the host CNS. Furthermore, transplantation of NPCs increased the number of surviving motor neurons in the hypoglossal nucleus after nerve avulsion that, if untreated, result in substantial neuronal death. The NPCs used in this study expressed VEGF *in vitro* as well as *in vivo* following transplantation that may promote neuronal survival.

PLEASE MIND THE GAP – AN UPDATE ON EXPERIMENTAL CNS–PNS BRIDGING EFFORTS IN VENTRAL SPINAL CORD

Mattias K. Sköld, T. Ochsman, T. Carlstedt, H. Lindå, S. Plantman, E. Rostami, M. Angeria and M. Risling

Replantation of avulsed spinal ventral roots has been shown to enable significant and useful regrowth of motor axons in both experimental animals and in human clinical cases, making up an interesting exception to the rule of unsuccessful neuronal regeneration in CNS.

The CNS/PNS transitional zone is a region normally relatively scarce of blood vessels, with few capillaries crossing the CNS/PNS border, but it has been shown that lesions to this area is followed by upregulation of vascular growth factors and angiogenesis (Skold et al., 2000). Increasing interest during recent years has focused on the fact that blood vessels and nerves share common growth factors and growth patterns during development and in disease (Carmeliet and Tessier-Lavigne, 2005). Therefore we investigated the vascular supply in the area of ventral root avulsion and replantation. The left L5 ventral root was identified and avulsed by gentle traction of the root followed by replantation of the avulsed root into the lateral funiculus of the spinal cord. We found an increased number of capillaries in the CNS/PNS transitional zone after replantation and in addition that these capillaries overgrow the CNS/PNS border but also that astrocytes in this scar area are organized alongside the blood vessels, typically in a cone shaped fashion resembeling of the normal morpholgy in the trasitional zone. At the replantation site and in the more central parts of the spinal cord just adjacent to the replantation site, axons and astrocytes were seen growing alongside each other, a pattern that could also be observed in more peripheral parts of the replanted ventral root where axons and astrocytic processess do align (**Figure 1A**). Furthermore, we can show that neurites do regrow from the spinal cord ventral horn, through the scar tissue and out into the ventral roots and that these regrowing axons are organized alongside blood vessels growing from the central parts of the spinal cord bridging the border between CNS and PNS and growing in to the replanted ventral root (**Figure 1B**). In conclusion it seems that the normally rather avascular zone between the CNS–PNS at the transitional zone is vascularized after replantation of avulsed ventral roots and that the vessels, together with astrocytes and neurites do grow from CNS to PNS. Further experiments are needed to analyze the possible interplay between these different cell types in this kind of injury.

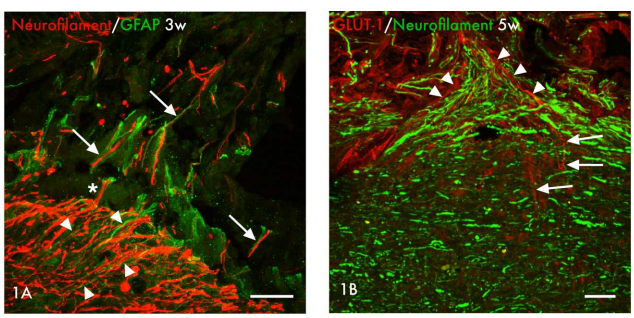

FIGURE 1 | (A) Axons (neurofilament, red) and astrocytes (GFAP, green) are seen at the border between the central and peripheral parts of the spinal cord at the site of replantation of the avulsed ventral root at 3 weeks after injury. In the more central parts astrocyte processes can be seen growing alongside axons (arrowheads) in a pattern that can also be found in the more peripheral parts where axons and astrocytic processess do align (arrows). Marked is also one single axon that seemingly grow from the central parts of the cord in to the peripheral nerve graft alongside astrocytic processess (asterisk*). Scale bar 50 µm. **(B)** Micrographs showing the relation between regenerating blood vessels, shown with marker for GLUT-1 (red), and regenerating axons, shown with marker for neurofilament (green), at the replantation site at 5 weeks after replantation of avulsed ventral roots. Note how blood vessels grow from the CNS compartment (arrows) to the PNS compartment (arrowheads) alongside the axons (green). Scale bar 50 µm.

We did also analyze the acute response to ventral root avulsion and replantation in the ventral quadrant of spinal cord tissue at the injured side from adult rats with gene arrays in combination with cluster analysis of gene ontology search terms and can show significant differences between rats subjected to ventral replantation compared to avulsion only. The number of genes related to cell death is similar in the two models after 24 h, but a significantly larger number of genes related to neurite growth and development are regulated in rats treated with ventral root replantation, possibly reflecting intrinsic neuroregenerative capacity in the replantation model. In addition, regulation of genes related to synaptic transmission was much more pronounced after replantation than after avulsion without replantation. These data indicate that the axonal regenerative response from replantation is initiated at an earlier stage than differences in terms of neuron survival (Risling et al., 2011). An analysis such as this could possibly facilitate the comparison of the regenerative response in different kind of neurotraumatic injuries.

IMMUNE MOLECULES IN NEURONS AND GLIA – IMPLICATIONS FOR SYNAPTIC PLASTICITY AFTER NERVE LESION

Staffan Cullheim

There is accumulating evidence that immune molecules are used by neurons and glia in the CNS to modulate synaptic function and plasticity during development and after nerve injury. Spinal motoneurons in rat and mouse constitutively express mRNAs for the major histocompatibility complex (MHC) class I and beta2-microglobulin (beta2m), which is necessary for surface expression of MHC class I. One classical response to lesion of motor axons is the shedding of synapses from the cell surface of severed motoneurons. We have shown that mice lacking the beta2m gene display a more extensive synaptic elimination from the cell bodies of axotomized spinal motoneurons compared with wild-type (WT) mice. This surplus elimination is directed toward synaptic terminals with a putative inhibitory function (Oliveira et al., 2004).

The complement system is a part of the innate immune system. Mice lacking complement proteins C1q or C3 exhibit large defects in the organization of synapses in the development of the retinogeniculate pathway, resembling the picture seen in the absence of MHC class I (Stevens et al., 2007). We therefore studied the synaptic elimination from axotomized motoneurons in mice deficient in C3. In these mice the elimination was much less prominent than in WT animals, which lends support to the idea that complement proteins are "tagging" synapses to be eliminated.

Astrocytes and, in particular, microglia have been attributed important roles in the synaptic elimination response after axon lesion. In mice, mRNAs for classical MHC class I (H2-Kb/Db) was upregulated in both motoneurons and microglia after lesion, while non-classical MHC class I (H2-T22) was upregulated only in motoneurons. In contrast, C1q mRNA was upregulated solely in activated microglia, with no neuronal expression. The general pattern of activation, as revealed by GFAP and Iba 1 immunoreactivity for astrocytes and microglia, respectively, did not reveal any major differences between WT animals and mice with gene deletions for MHC class I or complement proteins. We conclude that the effects exerted by the immune molecules are very specific, probably involves glia but are not mirrored by the general activation pattern of glia.

LONG-TERM RESULTS OF PERIPHERAL NERVE REPAIR: A COMPARISON OF NERVE ANASTOMOSIS WITH ETHYL-CYANOACRYLATE AND EPINEURAL SUTURES

Thomas Landegren, Anders Sondén, Mårten Risling and Jonas K. Persson

There is a need for complementary surgical techniques which offers rapid and reliable primary repair of transected nerves. Anastomosis of a nerve with synthetic adhesive following a lesion has previously been shown to indicate recovery to an extent comparable to that of conventional techniques. The aim of this study was to quantify the morphological and functional recovery and evaluate the selectivity of muscle reinnervation after transection and repair of rat sciatic nerve, and compare epineural sutures with a synthetic ethyl-cyanoacrylate tissue adhesive.

Six months after repair, when reinnervation had well been completed the tibial branch to the lateral gastrocnemius muscle and the caudal sural cutaneous nerve were examined with electrophysiological measurements of motor and sensory conduction velocity, motor nerve action potentials, and quantitative histological examinations. Furthermore, cholera toxin B technique of retrograde axonal tracing was used to evaluate the morphology, the number, and the three-dimensional location of a-motoneurons in L5 spinal cord, innervating the lateral gastrocnemius muscle and the results were put in relation to the recorded wet weight of the muscle.

There was functional reinnervation of motor and sensory nerves in both groups, as shown by equivalent recovery of motor and sensory conduction velocities, and motor nerve action potentials. Histological examination showed no significant difference in the mean diameter, fiber density, or the number of regenerated myelinated motor and sensory axons distal to the repair site between the two groups. Moreover, independent of repair method, the redistribution of the motoneuron pool were markedly disorganized, had increased apparently in number, and were scattered throughout a larger volume of the spinal cord gray matter with a decrease in the synaptic coverage compared to controls. A reduction in muscle weight was observed as well. Differences compared to controls were statistically significant.

We conclude that anastomosis of the nerve with ethyl-cyanoacrylate adhesive supports morphological and functional recovery comparable to that of conventional epineural sutures after a unilateral lesion of the sciatic nerve in adult rats.

SURGICAL TREATMENT OF RESIDUAL IMPAIRMENT AFTER BRACHIAL PLEXUS LESIONS

Tomas Hultgren

The basic strategies and techniques for surgical repair of brachial plexus lesions using multiple nerve grafts were essentially established in the 1980s. Additional techniques such as nerve transfer ("neurotization"), and spinal root reimplantation as pioneered by Prof. Carlstedt, have led to improved results. Even so, these often very extensive nerve injuries can be expected to leave major functional loss. This presentation will outline some of the surgical techniques which are available to improve function of the limb, once the nerve regeneration has reached its limit.

The functional impairment following obstetric plexus (OBP) lesions differs somewhat from the adult injuries. Contractures are common, and hypoplasia, dysplasia, and joint subluxations are often seen in the growing child as sequels to an OBP lesion. The shoulder joint is particularly susceptible to such deformities. Contractures and deformities of the shoulder in OBP patients were described already 100 years ago, and yet there is no consensus regarding treatment. I will present results from our ongoing prospective studies which aim to provide a scientific basis for optimal surgical treatment of these patients.

USE OF MIRROR THERAPY FOR THE TREATMENT OF PHANTOM LIMB PAIN

Jack W. Tsao, Ilana R. Yurkiewicz, Brett Monson, Brenda L. Chan, Lindsay Hussey-Andersen, Katie E. Hughes, Richard Witt, Kenneth M. Heilman and Paul F. Pasquina

INTRODUCTION

At least 90% of amputees experience phantom limb pain (PLP; Melzack, 1990). This pain can manifest as a variety of sensations, including burning, stabbing, and squeezing (Jensen et al., 1985). One proposed explanation for PLP is the presence of a conflict between visual and proprioceptive inputs to the brain. Mirror therapy intends to reduce this conflict by having an amputee perform specific movements with the phantom limb while viewing the reflected image of the intact limb executing actual movements (Ramachandran and Hirstein, 1998). While this therapy was shown to treat chronic phantom limb pain in 60% of upper limb amputees (Ramachandran and Rogers-Ramachandran, 1996), studies with lower limb amputees were limited. Moreover, it remains unclear whether the therapy's efficacy varies in response to the diverse manifestations of PLP. We performed a randomized, sham-controlled study to explore the efficacy of short-term use of mirror therapy for reducing PLP in lower extremity amputees (Chan et al., 2007). This paper expands upon our findings and examines which types of PLP are most responsive to mirror therapy.

MATERIALS AND METHODS

We randomly assigned 22 unilateral lower limb amputees with PLP to three treatment groups. Mirror group subjects performed movements with the phantom limb while viewing the reflected image of their intact limb moving (**Figure 2**). Covered mirror group subjects performed the exercise with the mirror covered by an opaque sheet. Mental visualization group subjects had no mirror, but simply imagined performing the movements with the phantom limb. All subjects engaged in the exercises for 15 min daily. Each day for 4 weeks, subjects monitored the duration and intensity of pain episodes using a 100-mm visual analog scale (VAS) and reported their specific manifestation of pain with the McGill Pain Assessment Questionnaire Short-Form. After the first month, subjects in the covered mirror and mental visualization groups were crossed over to mirror therapy.

RESULTS

Eighteen subjects completed the study. All six subjects (100%) in the mirror group experienced a reduction in PLP, in contrast with one patient (17%) in the covered mirror group and two patients (33%) in the mental visualization group. After crossing over to mirror therapy, PLP decreased in in 8 of 9 subjects (89%) at 2 months, yielding a total of 14 of 15 subjects (93.3%) who used the mirror ultimately reported

FIGURE 2 | Right above-knee amputee using the mirror.

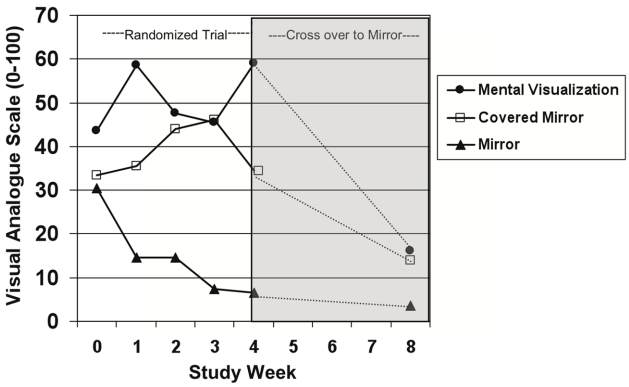

FIGURE 3 | Change in pain in subjects measured using the VAS. Group medians are depicted for each time point. After the first month (week 4), subjects in the covered mirror and mental visualization groups were switched to using the uncovered mirror. $N = 6$ per group after accounting for dropouts. Reprinted with permission from the New England Journal of Medicine (Chan et al., 2007).

decreased PLP (**Figure 3**; Chan et al., 2007). We found a significant effect of the number of mirror treatment days ($p < 0.0001$), with efficacy seen starting at 5 days ($p = 0.023$). A treatment effect was seen for four types of pain: shooting ($p = 0.007$), stabbing ($p = 0.003$), sharp ($p < 0.0001$), and aching ($p < 0.0001$; **Figure 4**). Throbbing, cramping, gnawing, hot-burning, heavy, tender, and splitting pain also decreased, but these did so independently from the number of treatment days. In addition, length of PLP episodes decreased

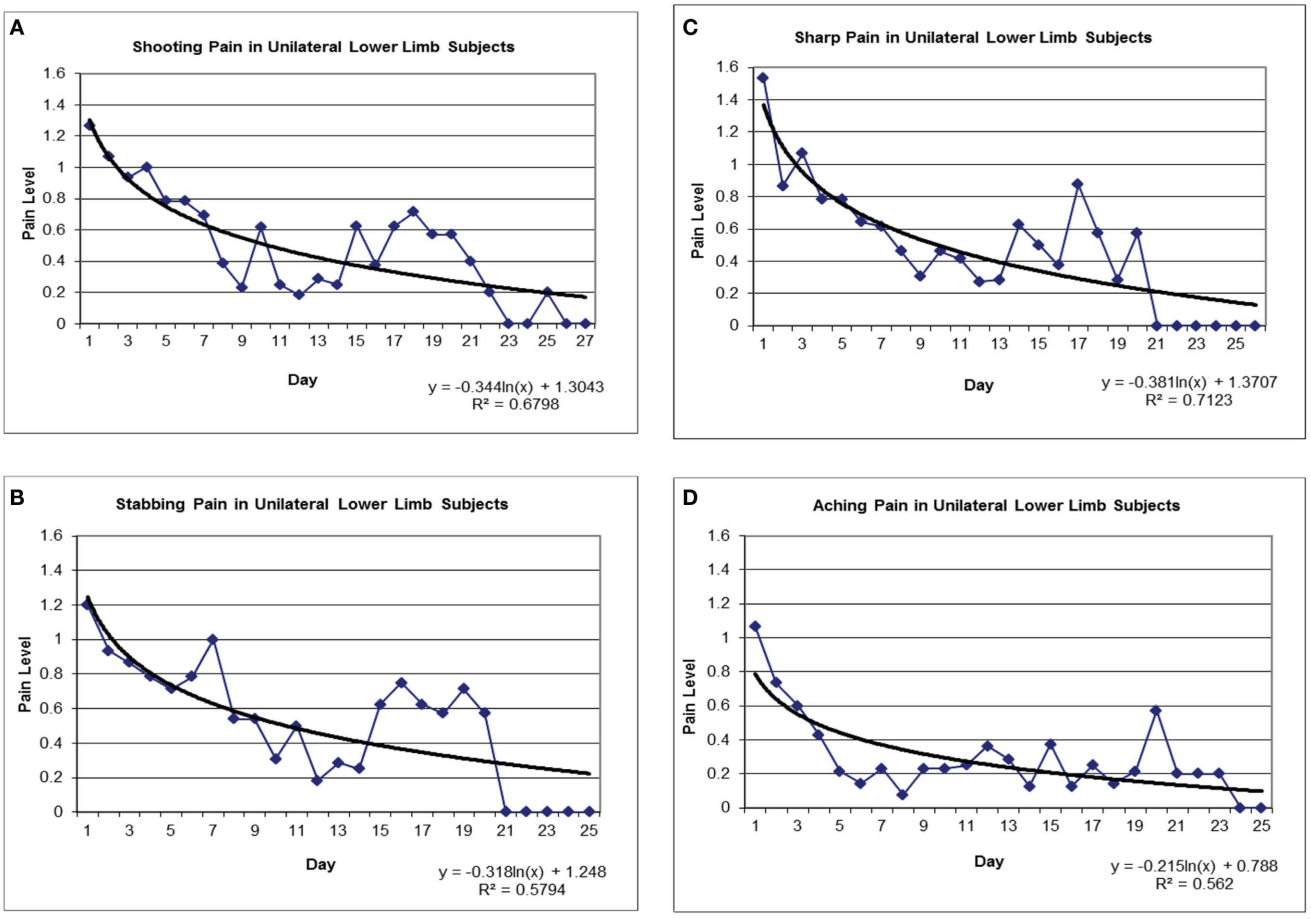

FIGURE 4 | Treatment effect for shooting pain (A), stabbing pain (B), sharp pain (C), and aching pain (D).

after the first week while the number of daily PLP episodes did not begin to decrease until the third week (data not shown). Of those who reported improvement in pain, pain levels at 4 months after starting therapy were minimal or non-existent, and several subjects seen in routine clinical follow-up 2 years later remained pain-free.

CONCLUSION

These results suggest that visual input is necessary for mirror therapy to be effective, providing additional support for a causative role for mismatch between visual and proprioceptive signals in the brain in the etiology of PLP. Our findings are also the first to offer insight into the efficaciousness of mirror therapy broken down by specific phantom pain type. We hope this information may be valuable for tailoring mirror therapy to those who will benefit most.

SPINAL CORD SURGERY AFTER ROOT AVULSION INJURY IN MAN RESULTS IN MOTOR AND SENSORY RECOVERY

Thomas Carlstedt

Spinal nerve root avulsion is a longitudinal spinal cord injury that affects mainly the final common motor pathway and the primary sensory medullary trajectories. In humans this occurs most frequently in traction injuries to the brachial plexus but also in trauma to the lumbosacral plexus and cauda equina as well as conus medullaris. This injury has serious effects on the pertinent spinal cord segment with the breakdown of connections and networks, death of motor, autonomic and sensory neurons, and the development of a spinal cord scar. This injury often occurs as a result of road traffic accidents or violent acts. About 1000 patients are affected annually in the UK. The functional consequence of such injury is lower motoneuron syndromes, associated with autonomic paralysis including dysfunctional internal organs, limb muscle atrophy, sensory impairment, and chronic pain. Spinal nerve root injury has been associated with an overall poor clinical outcome as a successful surgical repair would require axonal regrowth within the central nervous system as spinal cord regeneration. A surgical technique for the repair of this spinal cord injury was developed from basic science experiments and successfully translated to humans (Havton and Carlstedt, 2009).

Today, the reimplantation of avulsed ventral roots to the spinal cord in total brachial plexus avulsion injury restores useful proximal limb function and is the method of choice in the treatment of such devastating injuries. Even hand function can be restored by this technique. By means of functional magnetic resonance imaging (fMRI) it was established that the restored hand function relayed on pre-injury established cortical sensory program (Carlstedt et al., 2009).

Sensory roots are not possible to replant with functional recovery. Sensory recovery is therefore not occurring. In some cases as an expression of plasticity there are phenomenona observed as referrals of sensation to the denervated limb as well as hypersensitivity at border zones between normal and denervated dermatomes. When nerve graft has been implanted into the dorsal part of the spinal cord it has been possible to record return of some aspects of sensation. There was in such a case possible to elicit a biceps reflex and also record by means of electrophysiology a H-reflex proving that by this surgical technique it has been possible to restore a sensory-motor spinal cord reflex. However, neither quantitative sensory testing (QST), nor contact heat evoked potential stimulation (CHEPs) could demonstrate any exteroceptive sensory qualities.

Pain, which is most severe and excruciating in most cases of brachial plexus avulsion injuries, was found to be alleviated in conjunction with motor recovery after motor (but not sensory) root replantation. The mechanisms behind this are elusive but recent observations have indicated that there is retrograde transneuronal degeneration into the spinal cord dorsal horn following ventral root avulsion. This is reversed by ventral root replantation.

These observations achieved by spinal cord surgery will serve as baseline data when assessing the effects of future application of adjuvant therapies.

REFERENCES

Carlstedt, T., Hultgren, T., Nyman, T., and Hansson, T. (2009). Cortical activity and hand function restoration in a patient after spinal cord surgery. *Nat. Rev. Neurol.* 5, 571–574.

Carmeliet, P., and Tessier-Lavigne, M. (2005). Common mechanisms of nerve and blood vessel wiring. *Nature* 436, 193–200.

Chan, B. L., Witt, R., Charrow, A. P., Magee, A., Howard, R., Pasquina, P. F., Heilman, K. M., and Tsao, J. W. (2007). Mirror therapy for phantom limb pain. *N. Engl. J. Med.* 357, 2206–2207.

Havton, L. A., and Carlstedt, T.(2009). Repair and rehabilitation of plexus and root avulsions in animal models and patients. *Curr. Opin. Neurol.* 22, 570–574.

Jensen, T. S., Krebs, B., Nielsen, J., and Rasmussen, P. (1985). Immediate and long-term phantom limb pain in amputees: incidence, clinical characteristics and relationship to pre-amputation limb pain. *Pain* 21, 267–278.

Melzack, R.(1990). Phantom limbs and the concept of a neuromatrix. *Trends Neurosci.* 13, 88–92.

Oliveira, A. L., Thams, S., Lidman, O., Piehl, F., Hokfelt, T., Karre, K., Linda, H., and Cullheim, S. (2004). A role for MHC class I molecules in synaptic plasticity and regeneration of neurons after axotomy. *Proc. Natl. Acad. Sci. USA,* 101, 17843-17848.

Ramachandran, V. S., and Hirstein, W.(1998). The perception of phantom limbs. The D. O. Hebb lecture. *Brain* 121, 1603–1630.

Ramachandran, V. S., and Rogers-Ramachandran, D. (1996). Synaesthesia in phantom limbs induced with mirrors. *Proc. Biol. Sci.* 263, 377–386.

Risling, M., Ochsman, T., Carlstedt, T., Linda, H., Plantman, S., Rostami, E., Angeria, M., and Skold, M. K. (2011). On acute gene expression changes after ventral root replantation. *Front. Neur.* 1: 159. doi: 10.3389/fneur.2010.00159

Skold, M., Cullheim, S., Hammarberg, H., Piehl, F., Suneson, A., Lake, S., Sjogren, A., Walum, E., and Risling, M. (2000). Induction of VEGF and VEGF receptors in the spinal cord after mechanical spinal injury and prostaglandin administration. *Eur. J. Neurosci.* 12, 3675–3686.

Stevens, B., Allen, N. J., Vazquez, L. E., Howell, G. R., Christopherson, K. S., Nouri, N., Micheva, K. D., Mehalow, A. K., Huberman, A. D., Stafford, B., Sher, A., Litke, A. M., Lambris, J. D., Smith, S. J., John, S. W., and Barres, B. A. (2007). The classical complement cascade mediates CNS synapse elimination. *Cell* 131, 1164–1178.

Conflict of Interest Statement: The authors declare that the research was conducted in the absence of any commercial or financial relationships that could be construed as a potential conflict of interest.

Received: 02 February 2011; paper pending published: 23 February 2011; accepted: 25 April 2011; published online: 12 May 2011.

Citation: Sköld MK, Svensson M, Tsao J, Hultgren T, Landegren T, Carlstedt T and Cullheim S (2011) Karolinska Institutet 200-year anniversary. Symposium on traumatic injuries in the nervous system: injuries to the spinal cord and peripheral nervous system – injuries and repair, pain problems, lesions to brachial plexus. Front. Neur. ***2****:29. doi: 10.3389/fneur.2011.00029 This article was submitted to Frontiers in Neurotrauma, a specialty of Frontiers in Neurology.*

frontiers in NEUROLOGY

ORIGINAL RESEARCH ARTICLE
published: 27 April 2011
doi: 10.3389/fneur.2011.00025

Selectivity in the reinnervation of the lateral gastrocnemius muscle after nerve repair with ethyl cyanoacrylate in the rat

Thomas Landegren[1]*, Mårten Risling[2], Henrik Hammarberg[1] and Jonas K. E. Persson[3]

[1] Section of Hand Surgery, Department of Clinical Science and Education, Södersjukhuset, Karolinska Institutet, Stockholm, Sweden
[2] Retzius Laboratory, Experimental Traumatology Unit, Department of Neuroscience, Karolinska Institutet, Stockholm, Sweden
[3] Department of Clinical Neuroscience, Karolinska Institutet, Karolinska Universitetssjukhuset Solna, Stockholm, Sweden

Edited by:
Mattias Skšld, Uppsala University, Sweden

Reviewed by:
Ching-Hsiang Wu, National Defense Medical Center, Taiwan
Eng-Ang Ling, National University of Singapore, Singapore

***Correspondence:**
Thomas Landegren, Section of Hand Surgery, Department of Clinical Science and Education, Södersjukhuset, Karolinska Institutet, SE-118 83 Södersjukhuset, Stockholm, Sweden.
e-mail: thomas.landegren@ki.se

There is a need for complementary surgical techniques that enable rapid and reliable primary repair of transected nerves. Previous studies after peripheral nerve transection and repair with synthetic adhesives have demonstrated regeneration to an extent comparable to that of conventional techniques. The aim of this study was to compare two different repair techniques on the selectivity of muscle reinnervation after repair and completed regeneration. We used the cholera toxin B technique of retrograde axonal tracing to evaluate the morphology, the number, and the three-dimensional location of α-motoneurons innervating the lateral gastrocnemius muscle and compared the results after repair with either ethyl cyanoacrylate (ECA) or epineural sutures of the transected parent sciatic nerve. In addition, we recorded the wet weight of the muscle. Six months after transection and repair of the sciatic nerve, the redistribution of the motoneuron pool was markedly disorganized, the motoneurons had apparently increased in number, and they were scattered throughout a larger volume of the spinal cord gray matter with a decrease in the synaptic coverage compared to controls. A reduction in muscle weight was observed as well. No difference in morphometric variables or muscle weight between the two repair methods could be detected. We conclude that the selectivity of motor reinnervation following sciatic nerve transection and subsequent repair with ECA is comparable to that following conventional micro suturing.

Keywords: nerve repair, cyanoacrylate, synthetic adhesive, retrograde tracing, gastrocnemius muscle, spinal misdirection, sciatic nerve, peripheral nerve

INTRODUCTION

Experimental and clinical results of neural anastomosis using microsutures have been shown to be less than satisfactory in adults (Sullivan, 1985; Vertruyen et al., 1994; Siemionow and Brzezicki, 2009). Nevertheless, the repair technique using interrupted nylon microsutures is currently accepted as the golden standard of peripheral nerve repair (Millesi, 1973; Dvali and Mackinnon, 2007). Moreover, this technique with repeated tissue handling and consequent trauma has been shown to injure the nerve tissue, hinder the sprouting of axons, and compress the blood supply to the fascicles. This may hamper the growth of regenerating axons and ultimately impede complete nerve function recovery (Brushart et al., 1983; Bertelli and Mira, 1993; Suri et al., 2002).

To improve the functional outcome of peripheral nerve repair, a sutureless seam with synthetic adhesive has been proposed as an option to microsutures for achieving proper coaptation of the nerve endings. Data from previously published experimental reports have demonstrated recovery after repair of transected peripheral nerves using cyanoacrylate (CA) to an extent comparable to that after conventional microsurgical suturing (Choi et al., 2004; Pineros-Fernandez et al., 2005; Landegren et al., 2006).

However, irrespective of the operative method, functional restoration following nerve injury and subsequent repair is often disappointing. The type of injury, injury location, time delay from injury to surgery, age, and physical condition of the individual are factors that have been suggested to influence the results of nerve regeneration (Fu and Gordon, 1995a,b; Verdu et al., 2000). Misdirection of regenerating axons is also a factor that may explain poor functional recovery. When reinnervation of a repaired motor nerve has been completed, misdirected reinnervation of the target muscle can lead to involuntary muscular movements accompanying voluntary movements (e.g., synkinesis; Fu and Gordon, 1995a,b; Sumner, 1990). After reinnervation of a sensory nerve, misdirection may similarly result in persistent sensory dysfunction (Galtrey and Fawcett, 2007).

Different retrograde tracing techniques, including single-labeling, have been used to investigate the accuracy of motor and sensory nerve regeneration after experimental nerve repair. The results of these studies all suggest that there is a preferential reinnervation of the original target muscle (Brushart, 1993), but the specificity of reinnervation is limited (Zhao et al., 1992). However, little is known about the effect of applying synthetic adhesive on motoneuron regeneration specificity.

Since sensory and motor Schwann cell phenotypes differ in their patterns of trophic factor expression, it seems possible that this circumstance could help regrowing axons to find proper motor or sensory fascicles in the distal stump (Hoke et al., 2006). Adding synthetic materials to the lesioned nerve endings might possibly

exert a negative influence on the recognition of such trophic guidance cues. In this study we have assessed whether nerve repair with CA would impair the precision in reinnervation, compared to conventional nerve suturing.

The aim of the present study was to compare two different repair techniques: micro suturing versus coaptation with ethyl cyanoacrylate (ECA) in the process of reinnervating the lateral gastrocnemius muscle (LGC) following sciatic nerve transection and subsequent repair. After reinnervation had been completed, retrograde neuronal tracing with single- and double-labeling techniques was performed to evaluate quantitatively and descriptively the accuracy of motor axons for regeneration to the original target. In addition, the weight of the lateral LGC was determined at the end of the experiment, and the results were correlated with those obtained after retrograde axonal labeling.

MATERIALS AND METHODS

ANIMALS

Eighteen female Sprague-Dawley rats weighing 180–200 g and obtained from B & K Universal, Sollentuna, Sweden, were used in the experiments. The animals were caged in small groups and their environment was maintained at room temperature with 12-h light–dark, day–night cycles. They had free access to standard rodent food and water. All experiments were carried out with the approval of the Ethics Committee for Animal Research in Southern Stockholm.

SURGICAL PROCEDURES AND POSTOPERATIVE CARE

Animals were anesthetized by injection of Hypnorm vet® (fentanyl 0.05 mg/ml and fluanisone 2.50 mg/ml, Janssen Animal Health Ltd) 0.4 ml/kg intraperitoneally and midazolam 2 mg/kg intraperitoneally. One surgeon did all the operations using an aseptic technique and microsurgical dissection under an operating stereomicroscope (ZEISS OPMI-9, Carl Zeiss, Göttingen, Germany). The animals were kept on a thermostat-adjusted heating pad to maintain normal body temperature during all procedures. The left sciatic nerve of each rat was exposed through a dorsal gluteal-splitting approach between the gluteal muscle and the femoral biceps muscle. The nerve was transected at the mid-thigh level and repaired immediately by direct coaptation of the nerve ends with ECA ($n = 10$) and epineural sutures ($n = 10$), respectively. The ECA used in this study is commercially available (Evobond®, Tong Shen Enterprise Co., Ltd, Taiwan) and supplied in a 2-ml plastic ampoule with a stiff-tip applicator at one end. In this configuration, it is impossible to apply the adhesive during a microsurgical procedure. For this reason, a couple of drops (0.2 ml) of the adhesive were transferred into a 1-ml syringe with a needle. After transection of the nerve, a minimal amount was applied gently to the proximal nerve ending which had just been dried to promote adhesion. Sealing was facilitated by a sterile sheet of absorbable gelatin sponge, 1 mm^2, placed under the nerve to avoid the spontaneous retraction of the proximal and distal segments of the nerve. The nerve endings were then carefully brought together microsurgically with two pairs of microforceps, after which the gelatin sponge was removed. On application, the liquid monomer formulation polymerises instantly to a thin polymer film that adheres to the two opposite nerve endings. Any surplus adhesive was removed. A single 9/0 monofilament nylon suture (Ethicon, J & J, Somerville, NJ, USA) marked the anastomotic site in the epineurium of the proximal nerve ending. The overlying muscles and skin were closed in layers with single 5/0 monofilament nylon sutures (Ethicon, Somerville, NJ, USA). Other rats had their transected nerve repaired with three 9/0 monofilament interrupted nylon sutures (Ethicon, J & J, Somerville, NJ, USA) evenly spaced in the epineurium and followed by skin closure. Buprenorphine hydrochloride (Schering-Plough, Kenilworth, NJ, USA) was administered subcutaneously 30 min after the repair for prevention of pain. The rats in the two groups recovered from the anesthetic and were allowed to move freely immediately after the operation.

Three months after the repair, four rats in each group were chosen at random and reanesthetized. The anastomosis in the sciatic nerve was explored and examined under the operating stereomicroscope. The tissues were then closed and the animals were allowed to survive until the end of the predetermined postoperative period.

TRACING OF LGC NEURONS

Six months postoperatively, the animals were reanesthetized and the sciatic nerve and tibial branch of the LGC were exposed bilaterally. The tibial branch of the left LGC was identified and cut at a location just before it entered the muscle. The proximal nerve ending was inserted into a polyethylene capsule containing a solution of 1% cholera toxin subunit B low salt (CTB; List Biological Laboratories, Campbell, CA, USA) and left in place for 30 min. The capsule was then removed, and the surrounding area was rinsed with saline. Subsequently, the tibial branch of the opposite LGC at the corresponding site was processed by the same method and used as a control.

Three days later the animals were deeply reanesthetized and perfused via the ascending aorta with 200 ml saline at body temperature, followed by 700 ml of ice-cold 4% (w/v) paraformaldehyde in a 0.15-M phosphate buffer (pH 7.2–7.4). The spinal cord was exposed and the exit levels of the lumbar spinal roots were used to identify the individual lumbar spinal cord segments. The L5 spinal cord segment was carefully removed and the left side was marked by a longitudinal shallow groove. The L5 spinal cord segment was post-fixed for 4 h at +4°C and cryoprotected in sucrose (30% in 0.01 M PB, pH 7.3) at +4°C overnight.

Frozen cross-sections were cut at 14 μm with a Cryostat (Micram HM 560, Heidelberg, Germany) and every fifth section was thaw-mounted serially in a rostro-caudal sequence on gelatin-coated slides and prepared for the single-labeling process. Remaining sections were thaw-mounted serially in the same manner and stored for the double-labeling process. This resulted in neighboring sections on each slide taken from the L5 spinal cord segment at an interval of 70 μm.

IMMUNOHISTOCHEMISTRY

For the detection of CTB, the sections were preincubated with 5% bovine serum albumin and 0.3% Triton X-100 in 0.01 M PBS (pH 7.4) at room temperature for 30 min (all primary and secondary antisera were diluted in this solution) and then incubated in a humid atmosphere with goat anti-CTB (List Biological

Laboratories, Campbell, CA, USA, dilution 1:1000) overnight at 4°C. Thereafter, the sections were rinsed in PBS (2 × 10 min) and incubated with Cy3-conjugated donkey anti-goat IgG (Jackson ImmunoResearch, PA, USA, dilution 1:1000) for 1 h at room temperature, followed by rinsing in PBS (2 × 10 min). Single-labeling sections were then mounted in a 1:3 solution of glycerol and PBS.

In the cases of double-labeling, sections were labeled using two different fluorophores and processed for CTB immunohistochemistry as described, combined with immunoprocessing with one of the two following cellular markers: rabbit anti-CGRP (Bachem, Bubendorf, Switzerland, dilution 1:400), mouse anti-synaptophysin (Sigma, Saint Louis, MO, USA, dilution 1:400). After rinsing with PBS (2 × 10 min), the sections were incubated with Cy2-conjugated donkey anti rabbit IgG (Jackson ImmunoResearch, PA, USA, dilution 1:200) or donkey anti-mouse IgG (Jackson ImmunoResearch, PA, USA, dilution 1:200) for 1 h at room temperature. Subsequently, the sections were rinsed in PBS (2 × 10 min) and mounted in a 1:3 solution of glycerol and PBS.

IMAGING

The sections were examined using a fluorescence microscope and appropriate filter combinations for the fluorophores used (Nikon Eclipse E600, Nikon, Tokyo, Japan). Fluorescence microscopic images were captured with a digital camera (Nikon Digital Sight DS-U1), whereas confocal microscopic images were processed in software and digitalized (described later). Identical magnification was used for all the micrographs for each imaging technique.

The micrographs were imported into and edited in Adobe® Photoshop® CS software (version 7.0; Adobe Systems Inc., San Jose, CA, USA). The only digital manipulations done were limited contrast and/or brightness enhancement to allow adequate comparison of images and, if the size of a region of interest was too big to be captured in one frame, a series of adjacent overlapping frames was shot under the same conditions and montaged together. Retrogradely labeled motoneurons (RLMs), with a diameter of $\geq$30 μm, a clearly visible nucleus and polygonal in shape, were counted in order to selectively estimate the labeled population of α-motoneurons (α-MNs) and avoid inclusion of γ-motoneurons. Analyses, quantitative or descriptive, were performed bilaterally using digitalized images displayed on a computer monitor. Quantitative comparisons of the two repair methods were made as a percentage of the operated side proportionately to the unoperated control side (mean values, expressed as percentages, for the two repair methods were determined) unless otherwise indicated. All images were masked and, to avoid bias, the observer was blinded to the method of repair.

MORPHOLOGICAL EVALUATION

At the end of the predetermined postoperative period (6 months), immunofluorescently labeled α-MNs were evaluated with respect to nucleus and cell body shape, fluorescence intensity and neurite appearance.

QUANTITATIVE AND DESCRIPTIVE ESTIMATIONS OF RETROGRADELY LABELED MOTONEURON

To investigate the anatomical distribution of α-MNs innervating the LGC in the lateral ventral horn of the spinal cord, micrographs from every five of all serially cut 14-μm sections from the L5 spinal cord segment were transformed into separate layers using Adobe Photoshop 7.0. For each separate layer, the localization of every labeled α-MN was selected manually, using a computer mouse, and marked with a dot. The demarcation of the gray matter was also outlined in these layers. Micrograph layers representing L5 spinal cord sections, with the exception of dots and lines of anatomical boundaries, were then concealed and stacks of serially superimposed layers representing RLMs (and the outlined gray matter boundaries) only were reconstructed to form a two-dimensional digitized image. The transversal extensions of the RLM population, located in the lateral ventral horn of both sides, were then approximated to ellipses. The elliptical area was then measured using morphometric software (ImageJ 1.33u, National Institutes of Health, USA); see **Figure 1**. The distribution area of selected labeled neurons from the control side, which had been described as an ellipse, was delimited in a separate layer, reversed and superimposed as a template on the repaired side (dashed line) to facilitate estimations of the number of motoneurons located within or outside this assumed normal myotopic distribution area (**Figure 1**). The number of RLMs, identified by their localization in the lateral ventral horn of the L5 spinal cord sections, was determined bilaterally by manual counting in all serially cut 14-μm sections. Correlations between repaired and control sides, followed by quantitative comparisons between the two repair methods, were worked out for RLMs in total and for RLMs within the assumed normal myotopic distribution area (described above), respectively. From each specimen, five RLMs were randomly selected from the repair and control sides, respectively, for cross-sectional cell body area measurements. RLMs were identified as previously described. By assuming that RLMs were elliptical in the transversal section, the areas were calculated by using the morphometric software ImageJ, NIH.

DOUBLE-LABELING

Cy3-conjugated profiles (CTB-positive motoneurons) were counted as RLMs innervating LGCs, whereas Cy2-conjugated profiles (CGRP-positive motoneurons) were counted as indefinable sciatic nerve-mediated neurons in the lateral ventral horn (**Figure 2**). Three sections were randomly selected from each specimen and their content of α-MNs was counted bilaterally. The correlation between the number of RLMs and CGRP-labeled motoneurons was determined, whereupon quantitative comparisons between the two repair methods were made as described above.

CONFOCAL MICROSCOPY AND ANALYSIS

We used confocal microscopy to determine whether axons were synapsing on RLMs in the L5 spinal cord 6 months after sciatic nerve repair. Synaptophysin-immunoreactive (ir) profiles in the immediate vicinity of the cell bodies and proximal dendrites of RLMs were assessed quantitatively. From each repair method, six animals and five sections from each animal were randomly selected. Care was taken to choose all CTB-labeled α-MNs (described above) in the lateral ventral horn from the two opposite sides with the aid of a fluorescence microscope. The morphometric examinations were optimized, with a minimum

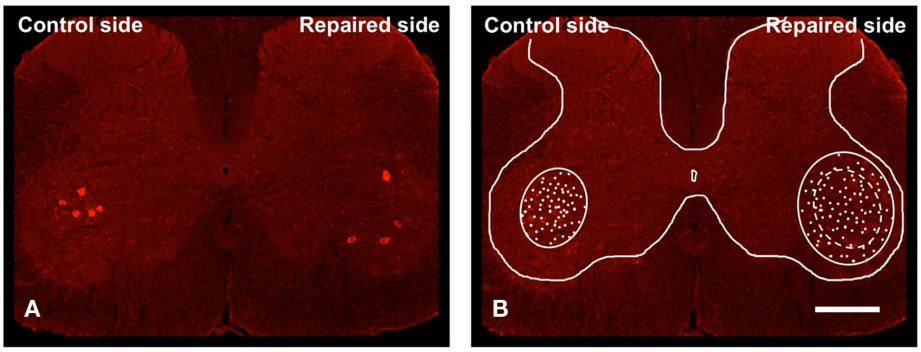

FIGURE 1 | Micrograph from a single separate transverse L5 spinal cord section showing RLMs bilaterally to the lateral gastrocnemius muscle (LGC) in the lateral ventral horn 6 months after transection and repair of the left rat sciatic nerve with ETC (A). The background image **(B)** has been manipulated in Photoshop to remove RLMs and artifacts. Scale bar = 500 μm.

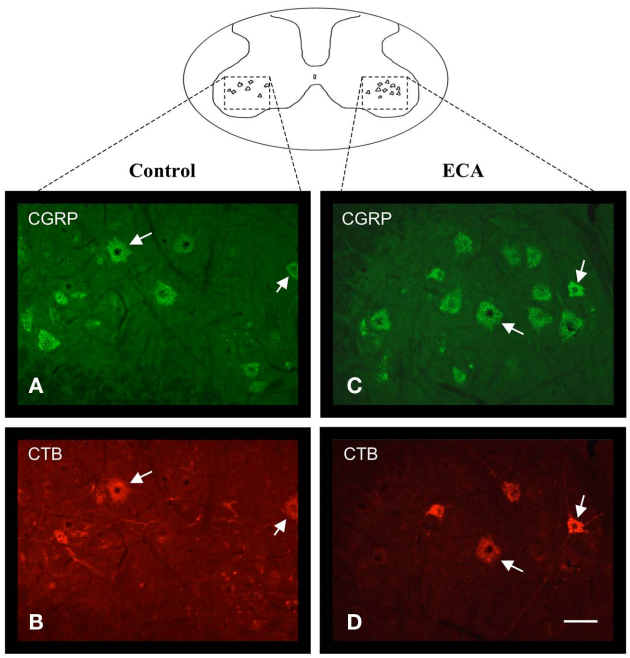

FIGURE 2 | Transverse L5 spinal cord sections 6 months after transection and repair of the left rat sciatic nerve with ECA, double-labeled with anti-CGRP (A,C) and anti-CTB (B,D). Two images, each with appropriate filter, were captured from identical visual fields. Note that all CTB-labeled α-motoneurons also demonstrate CGRP-positive labeling (arrows). Nor was any difference between repair and controls regarding shape, fluorescence intensity, or neurite appearance seen. Scale bar = 50 μm.

source of error, by reproducing each motoneuron in the microscope equipped with an e-C1 confocal system with an Argon Ion Laser 488 nm (40 mW) and a HeNe Laser 543 nm (1.0 mW). Fluorescence was filtered through a 500–530 nm band pass filter (green) and a 570-nm-long pass filter (red). Images were collected using an oil immersion (60×) Plan Apo objective. Stacks of three optical serial confocal sections taken at 0.15-μm intervals were reconstructed to produce two-dimensional digitized images using the volume rendering maximum paradigm in the EZ-C1 acquisition and analysis software (version 2.30, Nikon, Tokyo, Japan).

The two-dimensional digitized images were captured as TIFF files and imported into the morphometric software ImageJ, NIH. These laser scanning confocal images have been manipulated in Photoshop to adjust color values, remove artifacts, and increase sharpness. For each RLM (repair and control side), the total perimeter of the cell body outline was estimated and the total extension of the sections of the outlined circumference occupied by synaptophysin-immunoreactive profiles was measured. The ratio occupied by the labeled structure of interest was then calculated, the mean value for each specimen was also calculated and the percentage of repaired versus control side was generated, followed by quantitative comparisons (%) between the two repair methods.

LGC WEIGHT

The LGC of the repaired and control sides of each animal was dissected free from its origin and insertion and weighed immediately while still wet at the time of euthanasia. LGC weight data were calculated as percentages of those for the contralateral unaffected limb of the same rat to correct for individual differences.

STATISTICAL ANALYSIS

The statistical analysis was performed using one-way ANOVA, followed by Student's *t*-test for counts comparing the two repair groups. All statistical tests were performed using the software GraphPad Prism 4.0 (GraphPad Software, Inc., San Diego, CA, USA). Statistical significance was set at $P < 0.05$.

RESULTS

During the first postoperative month one rat from the adhesive group was killed because of a severe wound infection and one rat from the suture group was likewise killed because of clinical signs of far advanced self-harm.

FLUORESCENCE MICROSCOPY AND MORPHOLOGICAL EXAMINATION

Cell bodies labeled with CTB antibodies and/or CGRP antibodies were observed bilaterally in each of the 16 experimental rats and

Table 1 | Mean (SD) morphometric data on cross-sectional distribution area ($\mu m^2 \times 10^3$) and correlation (%) between repair and control, respectively, of RLMs representing the LGC in the lateral ventral horn throughout the L5 spinal cord segment 6 months after transection and repair of the left rat sciatic nerve with either ECA or epineurial sutures ($n = 8$ in each group).

	Suture	ECA	*P*-value
Repair	340 (53)	317 (58)	
Control	148 (22)	155 (40)	
Repair/ctrl %	232 (45)	210 (35)	0.29

were easily distinguished from unlabeled cells located in the gray matter of the lateral ventral horn extending through L5(**Figure 2**).

RETROGRADE TRACING OF REGENERATED MOTONEURON

Quantitative data showed a slightly more than a doubling of the anatomical cross-sectional distribution area of RLMs at the spinal L5 level in the suture group, compared to controls, whereas this increase were slightly less for the adhesions. Nevertheless, no significant differences were demonstrated (**Table 1**). The number of detected RLMs representing the LGC, located in the lateral ventral horn of the L5 spinal cord, was increased for both repair methods compared to the control side. No statistical difference was seen between the two repair methods (**Figure 3**). Without any detectable difference between the two repair methods, the number of RLMs located within the assumed normal anatomical distribution area in the gray matter was slightly more than half of the total number of RLMs distributed on the repair side. While the mean number of RLMs within the assumed normal myotopic area was slightly larger in the group repaired with ECA than in the sutured group, this difference was not significant (**Figure 3**).

In most controls, the RLMs appeared to merge so as to form one common column that occupied the described dorso-medial position in the lateral ventral horn of the gray matter. RLMs that were situated beyond the assumed normal myotopic area on the repair side could not be distinguished from corresponding profiles within this area or controls with respect to cell body shape, size (not shown), fluorescence intensity, or neurite appearance.

The measured mean cross-sectional area of RLMs in the lateral ventral horn was similar for the two repair methods but was somewhat increased compared to controls, although not significantly so (**Table 2**).

DOUBLE-LABELING

Retrogradely labeled motoneurons were assessed in the approximate ratio of 1 to 3 in relation to CGRP-labeled motoneurons (sciatic nerve-mediated neurons) in the lateral ventral horn irrespective of the repair method. A corresponding assessment of the contralateral control side showed an approximate ratio of 1 to 4. RLMs in all sections were also consistently found to be CGRP-positive when appropriate fluorophores and filter combinations for double-labeling were utilized. The ratio of CGRP-labeled motoneurons from the ipsilateral repair side and the contralateral

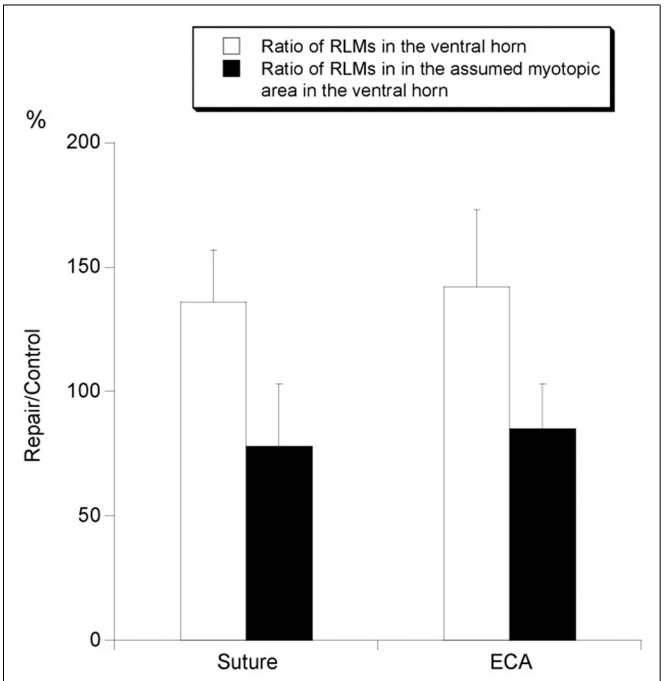

FIGURE 3 | Histograms representing quantification of RLMs, expressed as mean (SD), detected in the lateral ventral horn of the L5 spinal cord 6 months after transection and repair of the left rat sciatic nerve with either ECA or epineural sutures. Each column shows the relation of the number of RLMs between repaired and control side, calculated as a percentage value. RLMs were counted within the ventral horn in total or within the assumed normal myotopic distribution area ($n = 8$ in each group).

Table 2 | Mean (SD) morphometric data on cross-sectional soma size area (μm^2) and correlation (%) between repair and control, respectively, of RLMs representing the LGC in the lateral ventral horn of the L5 spinal cord 6 months after transection and repair of the left rat sciatic nerve with either ECA or epineurial sutures ($n = 8$ in each group).

	Suture	ECA	*P*-value
Repair	2210 (183)	2234 (80)	
Control	2136 (137)	2057 (153)	
Repair/ctrl %	103 (12)	109 (7)	0.31

control side was calculated to be approximately 89% (SD ± 5%) in the ECA repair group and 91% (SD ± 8%) in the suture repair group. Using fluorescence microscopy, the boundaries of cell bodies and proximal dendrites of RLMs, with a negligible number of exceptions, were found to be covered by synaptophysin-immunoreactive profiles. The major portion of the circumference was found to be coated by these profiles, although with an irregular degree of fluorescence intensity and a rough appearance along the outline (**Figure 4**). No difference in the extent of labeling or fluorescence intensity of immunoreactivity for synaptophysin between the two repair methods, or compared to controls, could be revealed by fluorescence microscopy.

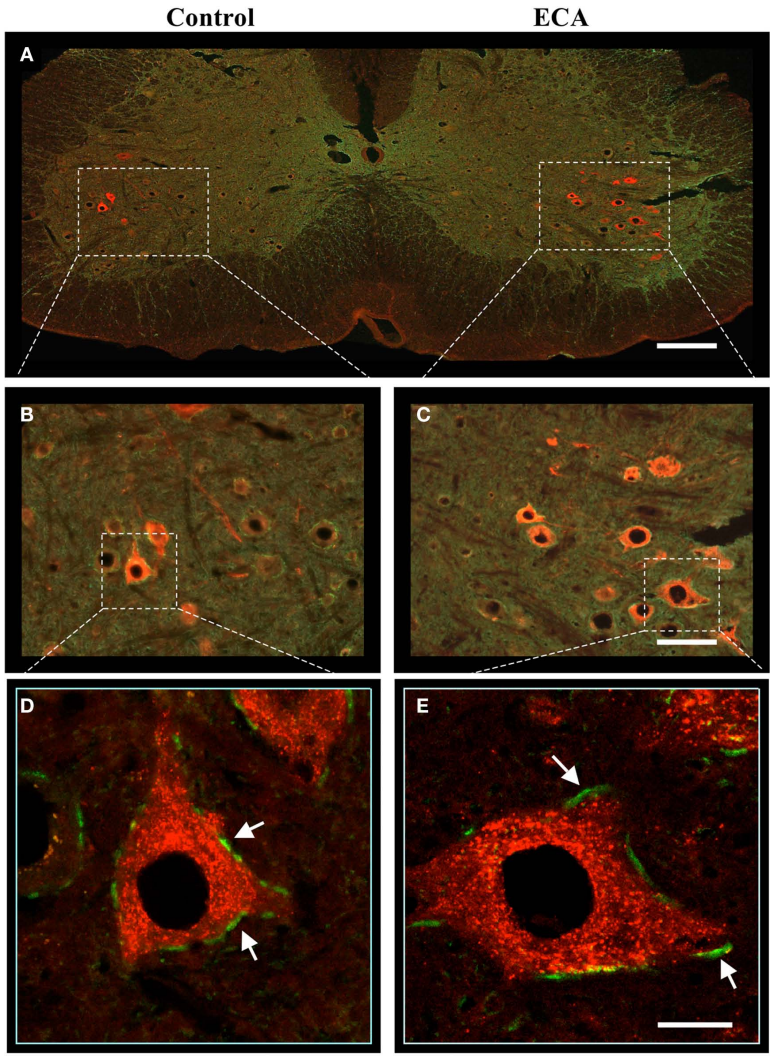

FIGURE 4 | Transverse L5 spinal cord section 6 months after transection and repair of the left rat sciatic nerve with ETC and double-labeling with anti-synaptophysin (green) and anti-CTB (red). Microphotographs showing RLMs in the lateral ventral horn from the ipsilateral ECA-repaired side **(A,C)** and the uninjured contralateral side **(A,B)**. Note the greater number and the scattered distribution of the RLMs on the repaired side. Confocal projection images **(D,E)** showing contacts (arrows) between synaptophysin immuno-labeled structures (displayed in green) along the membrane of the RLMs (displayed in red). Immunoreactivity for synaptophysin in the assessed area was consistently reduced in injured motoneurons but did not reveal any significant difference between the two repair methods. Scale bar **(A)** = 250 μm, **(B,C)** = 100 μm, **(D,E)** = 25 μm.

CONFOCAL MICROSCOPY FOR SYNAPTOPHYSIN-IMMUNOREACTIVE PROFILES

Confocal microscopy further confirmed the apposition of synaptophysin-immunoreactive profiles on α-MNs, on both their cell bodies and proximal dendrites (**Figures 4D,E**). A quantitative estimation indicated some reduction after injury, irrespective of the repair method, when repaired versus control sides was correlated.

Immunoreactivity for synaptophysin over the ECA-repaired motoneuron pool was somewhat lower compared to the corresponding ratio for the suture-repaired motoneuron pool. When ECA and suture repair were compared, no significant difference in synaptophysin expression could be seen (**Table 3**).

Table 3 | Mean (SD) morphometric data on the degree of intensity of synaptophysin-labeled profiles in contact with RLMs in the lateral ventral horn of the L5 spinal cord 6 months after transection and repair of the left rat sciatic nerve with either ECA or epineurial sutures. The ratio occupied by the labeled structure of interest was estimated as the percentage (%) of the repaired versus the control side (*n* = 6 in each group).

	Suture	ECA	*P*-value
Repair	23 (1)	24 (2)	
Control	29 (4)	31 (3)	
Repair/ctrl %	79 (12)	76 (9)	0.47

LATERAL GASTROCNEMIUS MUSCLE WEIGHT

On visual examination, the LGCs on the operated sides demonstrated noticeable atrophy compared to the contralateral normal limbs. This could also be demonstrated by reduced muscle weight on the experimental side, although no statistical difference could be detected between the two repair methods (**Figure 5**).

DISCUSSION

This study demonstrates that the precision in reinnervation of the LGC is far from perfect after repair with ECA. However, compared to conventional microsutures, the results appear to be comparable. Thus, no significant difference was seen with regard to localization in the ventral horn or the number, size or synaptic covering of reinnervating α-MNs between the two repair methods.

In the present study we used retrograde tracing as a tool to assess the accuracy of reinnervation after repair with ECA. The selectivity of reinnervation of the LGC was studied. The response of the LGC is well characterized from animal studies and it is mainly innervated at spinal level L5 (Tredici et al., 1996). The tracer was administered bilaterally to the tibial nerve branch close to the entrance into the LGC in order to detect motoneurons that had innervated this nerve branch and to evaluate the three-dimensional distribution of its spinal cord motor nuclei in order to document the alterations of the spinal myotopy due to peripheral reinnervation after repair using two different methods. There are a few methodological considerations connected with the technique employed, such as leakage or uptake in the soleus nerve branch (Leong and Ling, 1990). It seems more difficult to achieve a complete and reproducible uptake from intramuscular injections, which is probably related to the fact that this muscle is composed of four subdivisions. However, the methodological problems and limitations should be similar in both examined repair methods.

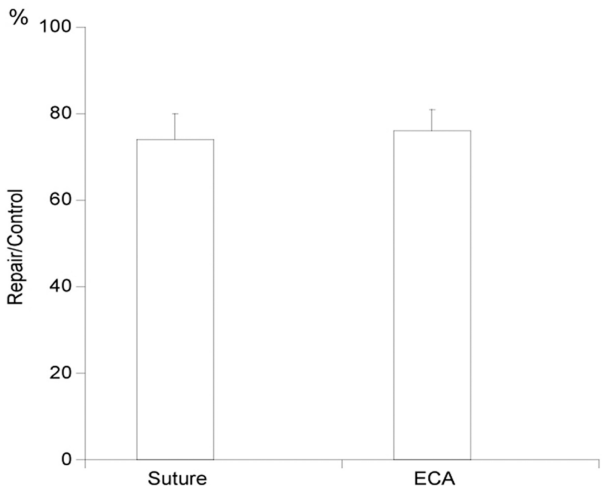

FIGURE 5 | Histogram representing the wet weight, expressed as mean (SD), of the lateral gastrocnemius muscles (LGCs) 6 months after transection and repair of the left sciatic nerve with either ECA or epineurial sutures. Each column shows the weight relationship (%) of the LGCs calculated by dividing the muscle mass of the repaired side by the muscle mass of the control side ($n = 8$ in each group).

The outcome of nerve repair can be assumed to be the result of several factors, such as retrograde degeneration of injured neurons and the effectiveness and accuracy of reinnervation. Synaptic plasticity in the spinal cord is probably also a limiting factor. Most studies indicate that the retrograde loss of motoneurons is very limited in adult animals (Arvidsson and Aldskogius, 1982; Schmalbruch, 1984), whereas sensory, a substantial proportion of the injured dorsal root ganglion neurons may be lost (Aldskogius et al., 1985). Furthermore, return of sensory function can be a limiting factor for the functional outcome. Additionally, in this study we have concentrated on acute repair. The outcome after a delayed repair can be assumed to be worse and could possibly differ between the methods, as an additional resection of the injured nerve stumps is usually necessary.

Two prevailing views have emerged about how nerve sprouts could find the correct route to their original target muscle. One is that the Schwann cell tubes of the respective pathways maintain a specific, interpreted identity that can be recognized by regenerating motor axons. The other opinion is that regenerating motor axons (randomly) assess the relative levels of trophic support in each pathway and preferentially remain in the one that provides the greater amount of support, so-called "pruning" (i.e., the withdrawal of the axon branches that reinnervate the wrong target; see detailed review: Madison et al., 2007). In this study we have assessed, by using retrograde tracing techniques, whether a synthetic adhesive, added to the lesioned nerve ending prior to coaptation, would exert any negative effect on the accuracy of the regrowth. In our present study, motoneurons projecting to a specific muscle were scattered throughout a larger volume of the spinal cord gray matter than in controls and were intermingled within the lumbar ventral horn, suggesting that motoneurons originally belonging to adjacent nuclei aberrantly project to the experimental muscle after regeneration. Valero-Cabre et al. (2004) demonstrated a spreading of the tibialis anterior nucleus to more ventral regions of the spinal cord gray matter, indicating that motoneurons originally projecting to the LGC aberrantly reinnervate the tibialis anterior muscle after nerve cut and repair, and vice versa. Our quantitative results show an increase in the proportion of transversal expansion of the LGC. These results are consistent with Valero-Cabre et al. (2004) who found three motor nuclei from the hind limb significantly enlarged in the transversal perimeter after sciatic nerve transection and suture repair. The most marked increase was in the anterior–posterior axis of the nucleus of the LGC. Our findings of an apparent increase in the number, together with a larger myotopic distribution area, of RLMs, regardless of the repair method, can be seen consistently in previous reports. However, regenerating axons have been shown to form more than one branch (Shawe, 1955) and, as a consequence, polyinnervation, i.e., the attachment endplate of more than one motoneuron to the same endplate (Ijkema-Paassen et al., 2002), hyperinnervation, i.e., the projection of more motoneurons into the same muscle after reinnervation than before lesion (Angelov et al., 1993) and axonal trunk bifurcation, i.e., simultaneous axonal branches to more than one muscle from long collateral branches of the same motoneuron (Hennig and Dietrichs, 1994), all being contributory factors

that might largely explain the increase in number as well as the enlarged and disorganized myotopic distribution of RLMs once reinnervation had been completed.

Within the assumed normal myotopic distribution area we found that the number of RLMs was reduced, regardless of the repair method, by approximately one-fourth on the repair side compared to the control side. The number of labeled neurons is therefore an indication of surviving cells reinnervating the motor targets, and a reduction after repair may be attributed to axonal misdirection to non-labeled targets rather than to neuronal death. In any case, with a more sparse α-MN population in the assumed normal myotopic distribution area connected to the original peripheral target, there follows a presumed decrease in appropriate supraspinal and propriospinal input, resulting in reduced functionality in the muscle.

Retraction of axonal terminals from the surface of injured motoneurons is a well-known phenomenon. A preferential reduction of excitatory synapses could possibly have a neuroprotective role (Linda et al., 1992). Brannstrom and Kellerth (1998) studied the ultrastructural changes in the synaptology of adult cat spinal α-MNs after axotomy of the medial gastrocnemius nerve. At 12 weeks after permanent axotomy, the synaptic covering was reduced by 83% on the cell soma compared to the normal situation. In a parallel study by the same authors, the nerve was allowed to reinnervate its muscle through a nerve graft after 6 weeks of ligation. Two years later, the axotomized and reinnervated motoneurons had not regained their original synaptic covering, which was still reduced by more than 25% as compared to the normal situation (Brannstrom et al., 1992).

Synaptophysin, used in our study, is a presynaptic membrane protein of neurotransmitter-containing synaptic vesicles and is expressed ubiquitously throughout all synapses of the CNS and PNS (Wiedenmann and Franke, 1985). Synaptophysin immunostaining is thus a good marker for presynaptic terminals which has been widely used to estimate the increase or decrease in the number of synapses on identified motoneurons (Zang et al., 2005). In both of our experimental repair groups we found a similar synaptic coverage of labeled motoneurons, although a significant decrease compared to control sides of approximately one-fifth. These findings suggest that the existing reinnervated α-MNs in the LGC nucleus, 6 months after transection and repair of the sciatic nerve, are subjected to an additive reduction (compared to the control side) in synaptic inputs which could result in a further reduction in muscle functionality.

From a clinical perspective, complementary functional tests (i.e., walking pattern, foot withdrawal reflex or toe spreading reflex tests) could be desirable to increase our understanding of the fate of motoneurons after surgical nerve repair with a synthetic adhesive. However, Beer et al. (2008) showed muscle weight to be a more detailed method to evaluate functional recovery than toe spreading reflex testing and thereby justify its use as a functional parameter of motor regeneration. In our present study, an obvious reduction in weight of the LGC, compared to controls, but without any difference between the two repair methods, was observed 6 months after repair. One limitation is that by measuring the muscle weight alone, only the weight, but not the strength, of the muscle is measured.

CONCLUSION

Previous studies have suggested that for peripheral nerve repair in the rat, there is no difference between synthetic adhesive and microsutures with respect to recovery of function or electrophysiological and morphometric indices of recovery in the peripheral nerve (Choi et al., 2004; Pineros-Fernandez et al., 2005; Landegren et al., 2006). These studies have, however not looked upon the morphological selectivity of regeneration. The limited number of animals used in this study shows a tendency to greater labeling of anterior horn cells from the LGC when synthetic adhesives are used, but this finding does not reach statistical significance. A larger study involving more animals might reveal whether this difference is significant.

Moreover, this study has involved immediate repair only. Despite an increasing amount of information showing that delayed repair is inferior to immediate repair (Bignotti et al., 1986), the former is widely used for practical reasons in the clinical situation. It would be of considerable interest to compare the results obtained here with a clinically relevant experimental study in which delayed repair of the peripheral nerve was used. It seems likely, from a speculative point of view, that this avenue will prove to be fruitful in distinguishing the relative values of immediate and late repair of peripheral nerves.

ACKNOWLEDGMENTS

The present study was supported by the Stockholm County Council, the Swedish Defence Research Agency Innovation Foundation, and the Karolinska Institutet, Stockholm, Sweden. The excellent technical assistance given by Ms. Maria Angeria and MS. Birgitta Robertsson is gratefully acknowledged. We thank Peter Rosén, Pixmix, for his indispensable help in the photographic artwork and graphics processing.

REFERENCES

Aldskogius, H., Arvidsson, J., and Grant, G. (1985). The reaction of primary sensory neurons to peripheral nerve injury with particular emphasis on transganglionic changes. *Brain Res.* 357, 27–46.

Angelov, D. N., Gunkel, A., Stennert, E., and Neiss, W. F. (1993). Recovery of original nerve supply after hypoglossal-facial anastomosis causes permanent motor hyperinnervation of the whisker-pad muscles in the rat. *J. Comp. Neurol.* 338, 214–224.

Arvidsson, J., and Aldskogius, H. (1982). Effect of repeated hypoglossal nerve lesions on the number of neurons in the hypoglossal nucleus of adult rats. *Exp. Neurol.* 75, 520–524.

Beer, G. M., Seifert, B., Schneller, M., Iscru, G., and Schmitz, H. C. (2008). Relevance of muscle weight as a functional parameter for the regeneration of the peroneal nerve in rabbits. *J. Reconstr. Microsurg.* 24, 11–19.

Bertelli, J. A., and Mira, J. C. (1993). Nerve repair using freezing and fibrin glue: immediate histologic improvement of axonal coaptation. *Microsurgery* 14, 135–140.

Bignotti, B., Origo, C., Schenone, A., Ratto, S., Mancardi, G. L., and Ferrari, M. L. (1986). Experimental studies on peripheral nerve repair following early or delayed suture. *Ital. J. Orthop. Traumatol.* 12, 259–266.

Brannstrom, T., Havton, L., and Kellerth, J. O. (1992). Restorative effects of reinnervation on the size and dendritic arborization patterns of axotomized cat spinal alpha-motoneurons. *J. Comp. Neurol.* 318, 452–461.

Brannstrom, T., and Kellerth, J. O. (1998). Changes in synaptology of adult cat spinal alpha-motoneurons after axotomy. *Exp. Brain Res.* 118, 1–13.

Brushart, T. M. (1993). Motor axons preferentially reinnervate motor pathways. *J. Neurosci.* 13, 2730–2738.

Brushart, T. M., Tarlov, E. C., and Mesulam, M. M. (1983). Specificity of muscle reinnervation after epineurial and individual fascicular suture of the rat sciatic nerve. *J. Hand. Surg. Am.* 8, 248–253.

Choi, B. H., Kim, B. Y., Huh, J. Y., Lee, S. H., Zhu, S. J., Jung, J. H., and Cho, B. P. (2004). Microneural anastomosis using cyanoacrylate adhesives. *Int. J. Oral Maxillofac. Surg.* 33, 777–780.

Dvali, L., and Mackinnon, S. (2007). The role of microsurgery in nerve repair and nerve grafting. *Hand Clin.* 23, 73–81.

Fu, S. Y., and Gordon, T. (1995a). Contributing factors to poor functional recovery after delayed nerve repair: prolonged denervation. *J. Neurosci.* 15(Pt 2), 3886–3895.

Fu, S. Y., and Gordon, T. (1995b). Contributing factors to poor functional recovery after delayed nerve repair: prolonged axotomy. *J. Neurosci.* 15(Pt 2), 3876–3885.

Galtrey, C. M., and Fawcett, J. W. (2007). Characterization of tests of functional recovery after median and ulnar nerve injury and repair in the rat forelimb. *J. Peripher. Nerv. Syst.* 12, 11–27.

Hennig, R., and Dietrichs, E. (1994). Transient reinnervation of antagonistic muscles by the same motoneuron. *Exp. Neurol.* 130, 331–336.

Hoke, A., Redett, R., Hameed, H., Jari, R., Zhou, C., Li, Z. B., Griffin, J. W., and Brushart, T. M. (2006). Schwann cells express motor and sensory phenotypes that regulate axon regeneration. *J. Neurosci.* 26, 9646–9655.

Ijkema-Paassen, J., Meek, M. F., and Gramsbergen, A. (2002). Reinnervation of muscles after transection of the sciatic nerve in adult rats. *Muscle Nerve* 25, 891–897.

Landegren, T., Risling, M., Brage, A., and Persson, J. K. (2006). Long-term results of peripheral nerve repair: a comparison of nerve anastomosis with ethyl-cyanoacrylate and epineural sutures. *Scand. J. Plast. Reconstr. Surg. Hand. Surg.* 40, 65–72.

Leong, S. K., and Ling, E. A. (1990). Labelling neurons with fluorescent dyes administered via intravenous, subcutaneous or intraperitoneal route. *J. Neurosci. Methods* 32, 15–23.

Linda, H., Cullheim, S., and Risling, M. (1992). A light and electron microscopic study of intracellularly HRP-labeled lumbar motoneurons after intramedullary axotomy in the adult cat. *J. Comp. Neurol.* 318, 188–208.

Madison, R. D., Robinson, G. A., and Chadaram, S. R. (2007). The specificity of motor neurone regeneration (preferential reinnervation). *Acta Physiol. (Oxf.)* 189, 201–206.

Millesi, H. (1973). Microsurgery of peripheral nerves. *Hand* 5, 157–160.

Pineros-Fernandez, A., Rodeheaver, P. F., and Rodeheaver, G. T. (2005). Octyl 2-cyanoacrylate for repair of peripheral nerve. *Ann. Plast. Surg.* 55, 188–195.

Schmalbruch, H. (1984). Motoneuron death after sciatic nerve section in newborn rats. *J. Comp. Neurol.* 224, 252–258.

Shawe, G. D. (1955). On the number of branches formed by regenerating nerve-fibres. *Br. J. Surg.* 42, 474–488.

Siemionow, M., and Brzezicki, G. (2009). Chapter 8: current techniques and concepts in peripheral nerve repair. *Int. Rev. Neurobiol.* 87, 141–172.

Sullivan, D. J. (1985). Results of digital neurorrhaphy in adults. *J. Hand Surg. Br.* 10, 41–44.

Sumner, A. J. (1990). Aberrant reinnervation. *Muscle Nerve* 13, 801–803.

Suri, A., Mehta, V. S., and Sarkar, C. (2002). Microneural anastomosis with fibrin glue: an experimental study. *Neurol. India* 50, 23–26.

Tredici, G., Migliorini, C., Barajon, I., Cavaletti, G., and Cece, R. (1996). Anatomical organization of the spinal paths to the soleus and gastrocnemius muscles of the rat hind limb. *J. Hirnforsch.* 37, 81–89.

Valero-Cabre, A., Tsironis, K., Skouras, E., Navarro, X., and Neiss, W. F. (2004). Peripheral and spinal motor reorganization after nerve injury and repair. *J. Neurotrauma* 21, 95–108.

Verdu, E., Ceballos, D., Vilches, J. J., and Navarro, X. (2000). Influence of aging on peripheral nerve function and regeneration. *J. Peripher. Nerv. Syst.* 5, 191–208.

Vertruyen, M. F., Burgeon, M. A., Dachy, B. S., and Ley, R. E. (1994). Sensory recovery after microsurgical repair of digital nerves. *Acta Chir. Belg.* 94, 325–328.

Wiedenmann, B., and Franke, W. W. (1985). Identification and localization of synaptophysin, an integral membrane glycoprotein of Mr 38,000 characteristic of presynaptic vesicles. *Cell* 41, 1017–1028.

Zang, D. W., Lopes, E. C., and Cheema, S. S. (2005). Loss of synaptophysin-positive boutons on lumbar motor neurons innervating the medial gastrocnemius muscle of the SOD1G93A G1H transgenic mouse model of ALS. *J. Neurosci. Res.* 79, 694–699.

Zhao, Q., Dahlin, L. B., Kanje, M., and Lundborg, G. (1992). Specificity of muscle reinnervation following repair of the transected sciatic nerve. A comparative study of different repair techniques in the rat. *J. Hand Surg. Br.* 17, 257–261.

Conflict of Interest Statement: The authors declare that the research was conducted in the absence of any commercial or financial relationships that could be construed as a potential conflict of interest.

Received: 03 December 2010; paper pending published: 01 February 2011; accepted: 03 April 2011; published online: 27 April 2011.

Citation: Landegren T, Risling M, Hammarberg H and Persson JKE (2011) Selectivity in the reinnervation of the lateral gastrocnemius muscle after nerve repair with ethyl cyanoacrylate in the rat. Front. Neur. ***2****:25. doi: 10.3389/fneur.2011.00025*

This article was submitted to Frontiers in Neurotrauma, a specialty of Frontiers in Neurology.

frontiers in
NEUROLOGY

REVIEW ARTICLE
published: 10 December 2010
doi: 10.3389/fneur.2010.00151

The importance of systemic response in the pathobiology of blast-induced neurotrauma

Ibolja Cernak*

Biomedicine Business Area, National Security Technology Department, Johns Hopkins University Applied Physics Laboratory, Laurel, MD, USA

Edited by:
Marten Risling, Karolinska Institutet, Sweden

Reviewed by:
Marten Risling, Karolinska Institutet, Sweden
Hans Lindå, Karolinska Institutet, Sweden

****Correspondence:***
Ibolja Cernak, Johns Hopkins University Applied Physics Laboratory, 11100 Johns Hopkins Road, Mail Stop MP2 N108, Laurel, MD 20723, USA.
e-mail: ibolja.cernak@jhuapl.edu

Due to complex injurious environment where multiple blast effects interact with the body parallel, blast-induced neurotrauma is a unique clinical entity induced by systemic, local, and cerebral responses. Activation of autonomous nervous system; sudden pressure increase in vital organs such as lungs and liver; and activation of neuroendocrine–immune system are among the most important mechanisms that contribute significantly to molecular changes and cascading injury mechanisms in the brain. It has been hypothesized that vagally mediated cerebral effects play a vital role in the early response to blast: this assumption has been supported by experiments where bilateral vagotomy mitigated bradycardia, hypotension, and apnea, and also prevented excessive metabolic alterations in the brain of animals exposed to blast. Clinical experience suggests specific blast–body–nervous system interactions such as (1) direct interaction with the head either through direct passage of the blast wave through the skull or by causing acceleration and/or rotation of the head; and (2) via hydraulic interaction, when the blast overpressure compresses the abdomen and chest, and transfers its kinetic energy to the body's fluid phase, initiating oscillating waves that traverse the body and reach the brain. Accumulating evidence suggests that inflammation plays important role in the pathogenesis of long-term neurological deficits due to blast. These include memory decline, motor function and balance impairments, and behavioral alterations, among others. Experiments using rigid body- or head protection in animals subjected to blast showed that head protection failed to prevent inflammation in the brain or reduce neurological deficits, whereas body protection was successful in alleviating the blast-induced functional and morphological impairments in the brain.

Keywords: blast, traumatic brain injury, autonomous nervous system, inflammation

INTRODUCTION

The history of blast injuries coincides with the history of explosives and modern warfare. Blast effects from high explosives have been described in the World Wars I and II as well as in the military actions of the twentieth and current centuries. For several reasons, the wars of the twenty-first century brought a new injury pattern: (1) the overwhelming majority of injuries are caused by explosions or blasts by rocket-propelled grenades, improvised explosive devices (IEDs), and land mines (Ritenour et al., 2010); (2) the mortality caused by explosion is relatively low due to improved interceptive properties of body armors, effectiveness of treatments, and promptness of medical evacuation, among others; and (3) due to increased survivability, the rate of severe, long-term deficits shows increasing trend. Based on the U.S. Defense and Veterans Brain Injury Center (DVBIC) analysis, approximately 180,000 U.S. military service members had a diagnosis of traumatic brain injury (TBI) in the period of 2001–2010. The overwhelming distribution of mild TBI (mTBI) was caused by blast. Because many servicemen with potential TBI remain undiagnosed or have delayed diagnosis, this number could be potentially higher (Terrio et al., 2009).

The complexity of the injurious environment generated by an explosion has been long recognized (Zuckerman, 1940). The injuries caused by multiple effects of the blast wave have been identified as: (a) primary blast injury cased by the blast wave itself; (b) secondary injury caused by the fragments of debris propelled by the explosion; (c) tertiary injury due to the acceleration of the body or part of the body by the blast wind and the sudden deceleration when it hits a ground or surrounding object; and (d) flash burns or toxic gas inhalation due to the intense heat of the explosion (Owen-Smith, 1981). It has been long posited that primary blast, e.g., blast overpressure generated during an explosion typically affects gas-containing organs through main mechanisms such as spalling, implosion, inertia, and pressure differences. On the other hand, the possibility of blast-induced neurotrauma (BINT) remained underestimated due to an outdated dogma that neurologic impairments caused by primary blasts are rare since the skull provides excellent protection for the brain (Rossle, 1950). Interestingly, despite several detailed reports published in 1940s portraying neurological symptoms in soldiers exposed to blast and describing underlying clinical findings and morphological changes in the brain not seen before (Stewart and Russel, 1941; Garai, 1944), the medical community ignored the pre-existing knowledge and attributed neurologic impairments due to blast to rare cases of air emboli in cerebral blood vessels (Clemedson, 1956).

While many servicemen with TBI experience remission of their symptoms, over one-third suffers at least one mTBI-related symptom at the post-deployment health assessment (Terrio et al., 2009). Immediately after exposure, individuals exposed to blast

reported memory loss for events before and after explosion, confusion, impaired sense of reality, and reduced decision-making ability (Cernak et al., 1999a,b; Martin et al., 2008; Warden et al., 2009). Later, sometimes months and years after blast exposure, patients with BINT may experience irritability; memory and speech problems (reduced verbal fluency, working memory, and executive functioning; Nelson et al., 2009); headache; dizziness and balance problems (Hoffer et al., 2010); as well as psychological impairments such as depression and post-traumatic stress disorder (Terrio et al., 2009; Peskind et al., 2010). While many question the possibility that primary blast could have damaging effects to the brain, there is a higher-level agreement about the aspects of BINT that sets aside this pathological condition from civilian TBI, including high rates of sensory impairment, increased sensitivity toward pain issues, multiple organ involvement, and strong emotional context in which the injury occurred (French, 2010).

Thus, to be able to develop reliable and accurate diagnostic tools, efficient and timely treatments, and successful preventive measures, we have to identify what makes BINT potentially different from civilian TBI, and specify the main elements involved in the complexity of BINT.

BASIC MECHANISMS OF BINT

Traumatic brain injury of all types and etiologies is caused by mechanical factors interacting with the brain either directly or indirectly. It is a complex process that consists of four overlapping phases: primary injury; evolution of the primary injury; secondary or additional injury; and regeneration (Reilly, 2001; Cernak, 2005). In civilian, non-blast TBI, the primary injury develops as a consequence of a direct interaction between the mechanical force and the head. The predominate injury causes are (1) direct contusion of the brain from the skull as a consequence of a direct hit; (2) brain contusion caused by a movement against rough interior surfaces of the skull, and/or indirect contusion of the brain opposite to the sate of the impact, i.e., coup–contrecoup; (3) shearing and stretching of the brain tissue due to a motion of the brain structures relative to each other or the skull; and (4) vascular consequences of the impact such as subdural hematoma originating from ruptured bridging blood vessels between brain and dura mater; reduced cerebral blood flow caused by intracranial pressure or infarction (Greve and Zink, 2009); and brain edema developing as a consequence of increased permeability of cerebral vasculature.

In BINT, these primary injury categories can be induced by: (a) fragments of the environment generated by explosion (so called "secondary blast effect") and impacting the head causing either blunt or penetrating head trauma; or (b) when explosion propels (i.e., accelerates) the body through the air and the brain is contused either due to the acceleration/deceleration (coup–contrecoup), or a hit from the surrounding objects or ground (so called "tertiary blast effect"). Nevertheless, in addition to these primary injury categories seen in civilian environment, primary blast is a unique injurious factor that is exclusively generated by explosion. The shockwave or blast wave, comprised of a high-pressure front that compresses the surrounding air and is followed by a negative pressure phase, is the major determinant of primary blast-induced injury. It travels with a high velocity, often thousands km/h (Owen-Smith, 1981), and damages its surroundings in few milliseconds. Primary blast envelops the whole body, and interacts with all organs and organ systems, including the brain, simultaneously (Cernak and Noble-Haeusslein, 2010). The main mechanisms by which primary blast may cause brain injury can be direct or indirect. A direct passage of the blast wave through the skull might cause bruising, acceleration, or rotation of the brain. On the other hand, as the front of the blast wave connects with the elastic body wall, it compresses the abdomen and chest transferring its kinetic energy inside the body, to the body's fluid phase (i.e., blood). The resulting "rippling" effect generates oscillating waves in the blood that traverse the body delivering the kinetic energy of the blast wave to organs, including the brain, remote from the initial point of coupling. Once delivered, that kinetic energy initiates functional and morphological alterations in distinct, mainly deep brain structures (Cernak et al., 1999a; Warden et al., 2009; Peskind et al., 2010). This second, indirect interactive pathway is unique for BINT, and underlies its immense complexity as compared to non-blast TBI.

SYSTEMIC EFFECTS OF BINT

Blast-induced neurotrauma is caused by multiple, interwoven mechanisms of systemic, local, and cerebral responses to blast exposure, often interacting with the body simultaneously (Cernak et al., 1991, 1996b; Cernak and Noble-Haeusslein, 2010; **Figure 1**). While the importance of multi-system, multi-organ response to blast exposure is more obvious in moderate-to-severe brain injuries, it is often neglected in the case of mild BINT. Nevertheless, accumulating clinical and experimental evidence show that systemic and local alterations initiated by blast significantly influence the brain's response, thus contribute to the pathobiology of acute and/or chronic deficits due to blast.

IMMEDIATE ACTIVATION OF THE AUTONOMOUS NERVOUS SYSTEM

In the experiments using rabbits, the animals were exposed to a blast overpressure generated by a compressed air-driven shock tube and causing mild-to-moderate blast lung injury. Aiming to analyze the effects of instantaneous activation of parasympathetic nervous system (PSNS) on the early response to blast, one subset of the animals was subjected to pulmonary deafferentation performed by bilateral dissection of the vagus 2 h before a blast exposure. Measured 30 min after blast exposure, brain edema and significant metabolic disturbances were found in the brain including decreased glucose and adenosine-triphosphate (ATP) concentrations (Cernak et al., 1996b); increased calcium and reduced magnesium concentrations as well as reduced magnesium/calcium ratio (Cernak et al., 1995). Bilateral vagotomy successfully mitigated bradycardia, hypotension, and apnea caused by blast; prevented extreme metabolic alterations and brain edema; but failed to eliminate oxidative stress in the brain due to blast (Cernak et al., 1996b).

It was hypothesized that hyperinflation of the lungs caused by blast overpressure stimulates the juxtacapillary J-receptors located in the alveolar interstitium and innervated by vagal fibers, triggering a vago-vagal reflex that leads to apnea followed by tachypnea, bradycardia, and hypotension (Zuckerman, 1940; Cernak et al., 1996b). In addition, hypoxia/ischemia caused by the pulmonary vagal reflex stimulates chemoreceptors in the left ventricle and subsequently activates a cardiovascular decompressor Bezold–Jarish reflex leading to significant parasympathetic efferent discharge to the heart

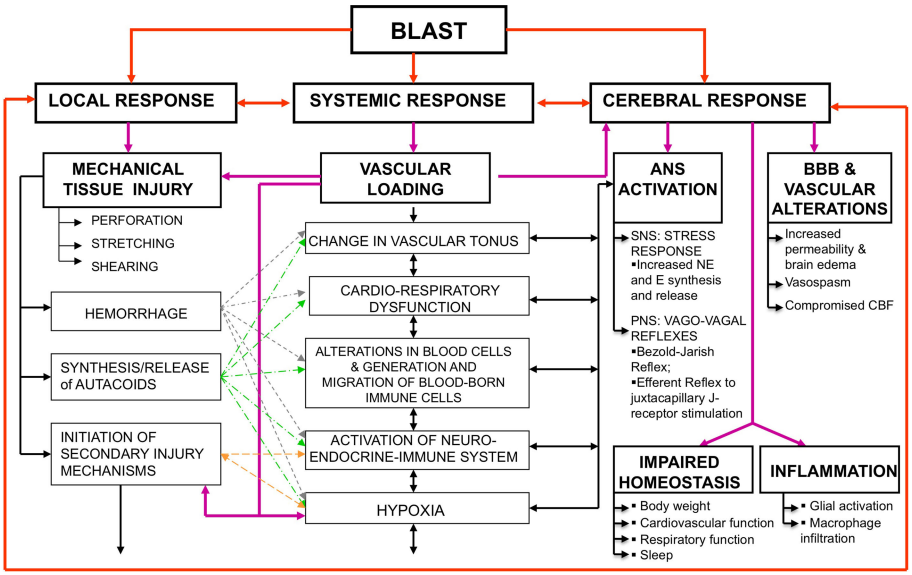

FIGURE 1 | Simultaneous activation of systemic, local, and cerebral responses to blast exposure, and interactive mechanisms causing or contributing to the pathobiology of BINT. Abbreviations: ANS, autonomous nervous system; BBB, blood brain barrier; BINT, blast-induced neurotrauma; CBF, cerebral blood flow; E, epinephrine; NE, norepinephrine; SNS, sympathetic nervous system; PNS, parasympathetic nervous system.

(Zucker, 1986). This, in turn, further deepens heart rate reduction (bradycardia) and peripheral blood vessel dilatation resulting in lowering blood pressure and eventually contributing to cerebral hypoxemia (Cernak et al., 1996a).

NA^+, K^+-ATPASE DURING EARLY POST-TRAUMATIC PHASE

Based on previous studies showing that blast exposure induces distinct pathological alterations in the brain including impaired energy metabolism (Cernak et al., 1995, 1996b), the activity of sodium–potassium ATPase (Na^+, K^+-ATPase; E.C.3.6.1.3.) was measured in the brainstem and erythrocyte membranes of rabbits exposed to blast. The aim was to establish the comparability of the enzyme changes as an indirect measure of systemic-cerebral response interaction during the early post-traumatic period after blast (Cernak et al., 1997). The Na^+, K^+-ATPase, i.e., sodium pump, is a ubiquitous plasma membrane enzyme that catalyzes the movement of K^+ into cells in exchange for Na^+, sustaining a gradient for Na^+ in to and for K^+ out of the cell (Skou and Esmann, 1992). The resulting gradient is used as an energy source for the de- and re-polarization of the membrane potential, regulation of cytoplasmic ionic composition, and for transepithelial transport. The sodium pump is regulated by numerous factors including several circulating hormones (Lopina, 2000; Lima et al., 2008). Since Na^+, K^+-ATPase is very sensitive to free radical reactions (Petrushanko et al., 2007) and impairments of energy metabolism (Silver and Erecinska, 1997), its activity can indicate membrane response to an insult indirectly giving insight into the efficiency of compensatory mechanisms and the level of membrane dysfunction.

Adult male rabbits were randomly assigned to three groups: control, mild-to-moderate, and moderate-to-severe blast injury groups. The blast injury groups were anesthetized and subjected to a blast overpressure generated by a compressed air-driven shock tube. During the early post-traumatic period (i.e., 30 min post-exposure), arterial pressure, electrocardiogram (ECG) and electroencephalogram (EEG) activities were measured. At the end of the 30-min observation period, arterial blood samples were collected, the animals sacrificed, and brain structures harvested. Light-microscopy examinations of brain samples stained with Hematoxylin–Eosin, Trichrom Masson, and van Gieson Elastica were also performed. Erythrocyte plasma membranes (Dodge et al., 1963; Mrsulja et al., 1993) and brainstem homogenates (Enseleit et al., 1984; Cernak et al., 1997) for the Na^+, K^+-ATPase assays were prepared as previously described. Briefly, the reaction mixture for the Na^+, K^+-ATPase assay contained 5.0 mM/L $MgCl_2$, 130.0 mM/L NaCl, 20.0 mM/L KCl, and 45.0 mM/L Tris–HCl buffer, pH 7.4. The reaction was started by the addition of ATP (disodium salt, vanadium free) to a final concentration of 0.1, 0.5, 1.0, 1.5, 3.0, and 5.0 mM, and stopped after a 60 min incubation period with the addition of the ice cold $HClO_4$. The activity obtained in the presence of 2 mM ouabain (without the NaCl and KCl) was attributed to Mg^{2+}-ATPase. Na^+, K^+-ATPase activity was calculated as a difference between the total ATPase activity (Na^+, K^+, Mg^{2+}-dependent) and Mg^{2+}-ATPase activity. Released inorganic phosphate (P_i) was measured by the method of Fiske and Subbarow (1925). Enzyme specific activity was expressed as nmol P_i released per mg of protein per min. All assays were performed in duplicate and the mean was used for statistical analysis. In this experiment, protein was measured by the method of (Lowry et al., 1951), with bovine serum albumin used as standard. The Michaelis–Menten constant (K_m) and the maximum reaction rate (V_{max}) of Na^+, K^+-ATPase were calculated using the Lineweaver–Burk double reciprocal plot.

Blast exposure caused the characteristic fall in mean arterial pressure, bradycardia, fast and shallow respiration, and significant increases in both frequency and amplitude of the EEG activity as

compared to control animals (25 versus 15–18 Hz, and 22 versus 10 μV, respectively). The neuropathology analysis showed no hemorrhages or areas of contused brain tissue. The development of brain edema as well as the sodium pump changes demonstrated a graded response to the shockwave intensity, i.e., more prominent in the moderate-to-severe blast group as compared to the animals subjected to mild-to-moderate intensity blast. In all tested groups Na^+, K^+-ATPase activity in plasma membrane was substrate (ATP) dependent, such that the lowest activity was obtained at 0.1 mM, whereas the highest activity was at 1–1.5 mM concentrations of the substrate, ATP. At these substrate concentrations, the activity of the Na^+, K^+-ATPase was significantly increased in the erythrocyte membranes and the brainstem as compared to control values.

Changes in Na^+, K^+-ATPase have been shown being time-dependent (Sztriha et al., 1987), and in the present study the activity Na^+, K^+-ATPase was measured at the time when significant neuro-endocrine changes occur in the brain with TBI. Indeed, complex alterations such as the over-activation or inhibition of neurotransmitter synthesis, release, or transport have been reported during the early period after TBI (McIntosh et al., 1994). Among the most important neuro-endocrine changes, an increase in norepinephrine (NE) synthesis and metabolism have been reported in animal experiments inducing transient cerebral ischemia (Globus et al., 1989; Bhardwaj et al., 1990), focal cortical lesions (Pappius, 1991), and fluid-percussion TBI (McIntosh et al., 1994) during the first hours after the insult. Several mechanisms have been suggested to explain the NE activation of the enzyme: one involves specific receptors or a non-specific chelating action related to the catechol group that would relieve the inhibition by divalent cations such as Ca^{2+} (Godfraind et al., 1974; Adam-Vizi et al., 1979; Phillis and Wu, 1981), while the other describes a possibility that NE removes an endogenous inhibitory factor present in the cytoplasm (Hernandez, 1992). A dose-dependent response of the Na^+, K^+-ATPase to dopamine and NE concentrations in mouse brain synaptosomes have been confirmed by Desaiah and Ho (1977) reporting that these catecholamines modified the behavior of the enzyme kinetics against ATP, producing an increase in V_{max}. Our previous studies have shown a direct relationship between injury severity and blood concentrations of epinephrine and NE in soldiers with military gunshot or missile (thus explosive) injuries (Savic et al., 1995) as well as in the brain of rats exposed to whole-body blast during the early post-traumatic phase.

Taken together, we hypothesize that the increased activity and V_{max} of the Na^+, K^+-ATPase in our study may be related to the catecholamine surge in the brain. Additionally, the edema formation developed in the brainstem parallel with the increase in the Na^+, K^+-ATPase activity could be explained as a result of Na^+-influx, bearing in mind that abrupt increase of cytoplasmic Na^+ in the brain tissue has been shown after trauma both *in vitro* (Young et al., 1986; Sheldon et al., 2004; Wang et al., 2009) and *in vivo* (Young et al., 1986). Moreover, the role of the Na^+-influx in the pathobiology of acute vasogenic edema was demonstrated by *in vivo* sodium MRI imaging in both clinical and experimental studies of brain edema development compared with signal in health brain tissue (Turski et al., 1986).

IMPORTANCE OF THE INDIRECT BLAST–BRAIN INTERACTING PATHWAY IN LONG-TERM NEUROLOGICAL DEFICITS

In an attempt to link systemic and cerebral inflammation as one of the potential mechanisms leading to long-term neurological deficits caused by blast, we performed real-time, *in vivo* imaging of myeloperoxidase (MPO) activity of activated phagocytes in mice exposed to mild intensity blast, during a 1-month post-injury period. Namely, migration and accumulation of polymorphonuclear leukocytes (PMNs) are among the major hallmarks of the host response to injuries (Maslinska and Gajewski, 1998; Toft et al., 2003; Menezes et al., 2008). Locally, activated PMNs release antimicrobial and inflammatory mediators, such as MPO, among others. MPO is a key inflammatory enzyme secreted by activated PMNs and macrophages/microglia, capable of generating highly reactive oxygen species to cause additional damage in various pathological conditions such as cerebral ischemia (Weston et al., 2007; Breckwoldt et al., 2008); ischemic heart conditions (Loria et al., 2008); inflammatory bowel disease (Naito et al., 2007); and kidney (Malle et al., 2003) and lung (Kinnula, 2005) pathologies, among others. Based on its importance in inflammatory processes and as a reliable indicator of PMN presence in tissues (Arnhold and Flemmig, 2010), MPO has been widely used as an inflammatory marker of both acute and chronic conditions (Werner and Szelenyi, 1992; Breckwoldt et al., 2008; Faith et al., 2008).

Briefly, mice were anesthetized, mounted in supine position to the animal holder secured inside the driven section of the helium-driven shock tube, and exposed to mild intensity shock wave (measured rupture pressure: 183 ± 14 kPa, i.e., 26.5 ± 2.1 psig; measured total pressure: 103 kPa, i.e., 14.9 psig) causing 5% mortality (Cernak et al., 2010). Subsets of animals ($n = 5$) were exposed to: (1) whole-body blast; (2) blast with torso (chest and abdomen) protection using a custom-made rigid Plexiglas "body armor," while the head exposed; or (3) blast with head protection using a custom-made Plexiglas "helmet" covering skull, face, and the neck of the animal while the torso exposed (**Figure 2**). Ten minutes before imaging, mice were injected with XenoLight Rediject Inflammation probe (Caliper Life Sciences; Hopkinton, MA, USA) at 200 mg/kg (150 μL/mouse) intraperitoneally. The XenoLight Rediject Inflammation probe is a chemiluminescent reagent in a ready-to-use format that allows for longitudinal tracking of MPO level and inflammation status, *in vivo*, in a variety of disease models. Bioluminescence imaging (BLI) was performed using the IVIS® Imaging System 3-D Series (Caliper Life Sciences, Hopkinton, MA, USA). During the imaging, the animals were anesthetized with a gas mixture (isoflurane:nitrous oxide:oxygen at 1:66:33% proportions, respectively) using the integrated system for gas anesthesia. The duration of imaging was 5 min. To validate substrate injection quality, fluorescence images were taken right before BLI, using the 745-nm excitation and 800-nm emission filter set, and exposure time between 1 and 5 s. Photons were quantified using Living Image software (Caliper Life Sciences, Hopkinton, MA, USA). Sham control animals did show only low-intensity localized bioluminescence at the injection site (results not shown).

Figure 3 shows the distribution of increased bioluminescence in mice subjected to whole-body blast exposure imaged during the 1-month observation period. One day after blast exposure, the

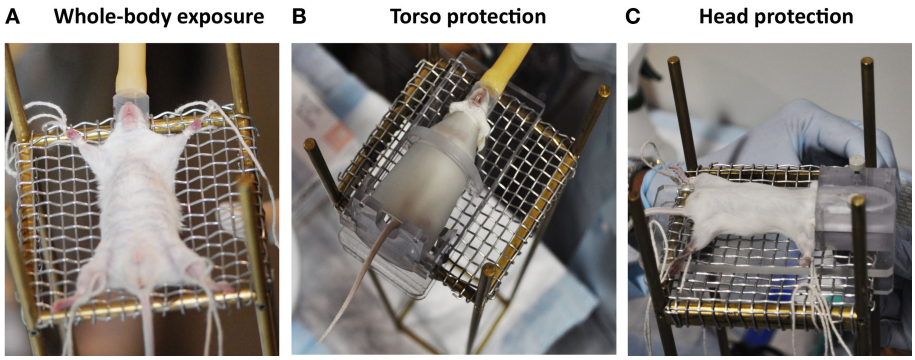

FIGURE 2 | Experimental setting for establishing the importance of blast-head and blast–body interactive pathways in the pathobiology of BINT. **(A)** whole-body blast exposure without protection; **(B)** head blast exposure with torso (chest and abdomen) protection; and **(C)** torso blast exposure with head protection.

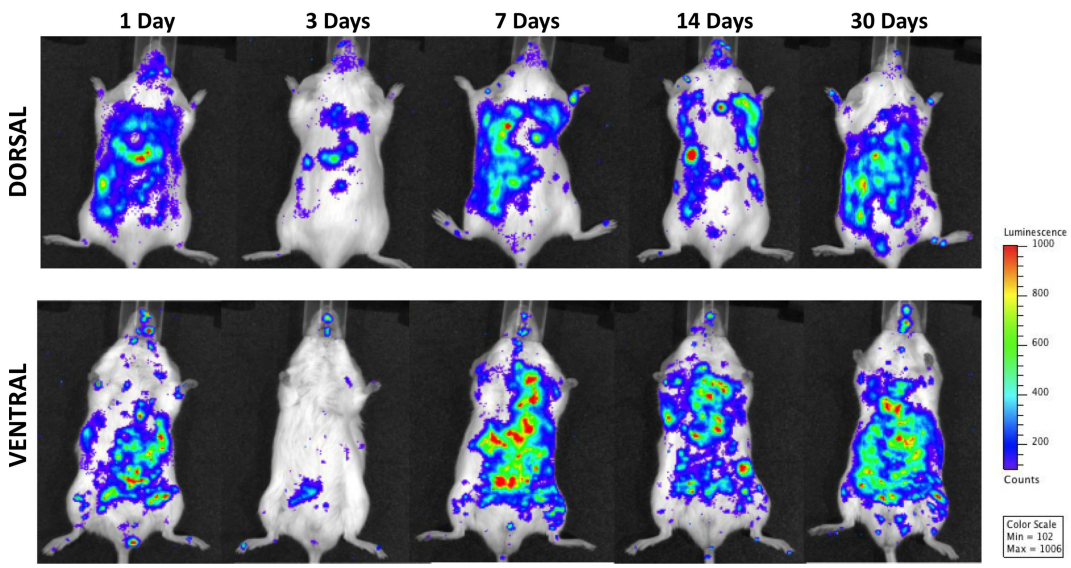

FIGURE 3 | Distribution of increased bioluminescence showing MPO activity in mice subjected to whole-body blast exposure, imaged during the 1-month observation period. The representative photographs show the same animal imaged in both dorsal and ventral positions at the given time point after blast exposure. The intensity of bioluminescence was scaled based on the photon counts. The nose cone that can be discerned on the photos is part of the anesthesia device that is the integral part of the IVIS® imaging system 3-D series, and does not represent a head cover.

highest MPO activity is found in the gastrointestinal tract, with clearly outlined transverse and descending colon. Additionally, enhanced signal is observed bilaterally in diaphragmal mediastinal parts of the lungs as well as in the brain. Interestingly, the PMNs activation showed a declining trend 3 days post-exposure followed by intensified MPO activity in lungs, gastrointestinal tract and the brain measured at 7, 14, and 30 days after blast. It is noteworthy that the most intense bioluminescence signal measured in the brain was found 1 month after injury.

Figure 4 demonstrates MPO activity in animals subjected to blast with head protection. Because the torso was exposed to blast, the finding of the activation of PMNs in lungs and gastrointestinal tract, similar to the changes observed in animals with whole-body blast exposure, is not surprising. The temporal and spatial profiles of MPO activity were also comparable, i.e., a declining trend at 3 days post-trauma followed by progressively increasing signal peaking at 1 month after blast. However, regardless of the head protection, MPO was significantly increased in the brain, with the highest activity at 14 and 30 days post-injury suggesting chronic inflammation. Importantly, the increase in MPO activity observed in mice with head protection was equal to corresponding changes found in the brain of animals exposed to whole-body blast without head protection, suggesting that head protection did not prevent inflammation in the brain and implying the importance of inflammatory cells of systemic origin in the pathobiology of blast-induced inflammatory processes in the brain.

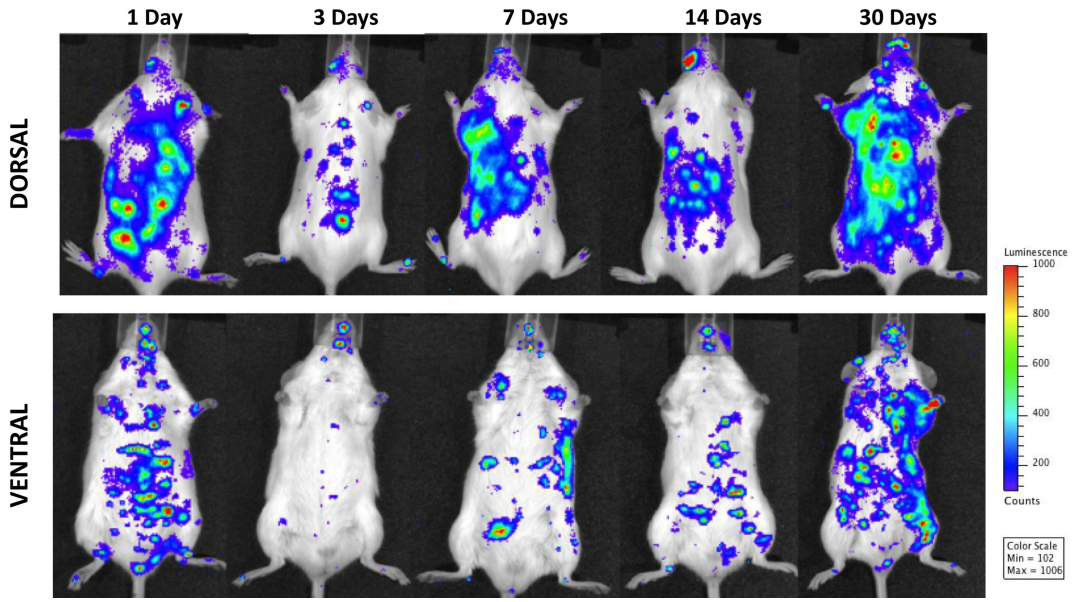

FIGURE 4 | Distribution of increased bioluminescence showing MPO activity in mice subjected to blast with head protection, imaged during the 1-month observation period. The representative photographs show the same animal imaged in both dorsal and ventral positions at the given time point after blast exposure. The intensity of bioluminescence was scaled based on the photon counts. The nose cone that can be discerned on the photos is part of the anesthesia device that is the integral part of the IVIS® imaging system 3-D series, and does not represent a head cover.

It is also noteworthy that while head protection did not prevent inflammation in the brain, it did reduce MPO activity in the gastrointestinal tract. It is well known that vagal afferent neurons play an important role in gut–brain communication (Berthoud and Neuhuber, 2000; Danzer et al., 2004) responding to a variety of physiological stimuli relevant not only to food intake and regulation of digestive activity, but in the response to immunological and noxious stimuli also (Gaykema et al., 2007). Indeed, direct and indirect pathways that originate in the caudal brainstem and propagate immune-related information from the periphery have been shown to play important role in the integration of brain responses to infection and injury (Gaykema et al., 2007). Additionally, it has been suggested that part of the peripheral immune information can be conveyed *via* vagal pathway to the catecholaminergic neurons in the medullary visceral zone from where it is transferred to the central amygdaloid nucleus (Ge et al., 2001). Such an approach suggests a complex interaction of the autonomous nervous system components with immune system elements in the response to injury-induced inflammation. Thus, we hypothesize that protecting the head reduced the susceptibility of the brain toward incoming vagal information and subsequently decreased the intensity of the efferent feedback response to peripheral injury; this in turn led to diminished inflammation in the gastrointestinal tract and lungs after blast as compared to animals with whole-body blast exposure.

Figure 5 shows progressive development of inflammation in both peripheral organs/organ systems and the brain of animals subjected to blast with torso protection. Systemic inflammation and the intensity of MPO activation in the brain were significantly reduced throughout the 1 month post-injury period as compared to mice either with whole-body exposure to blast or those with head protection. Moreover, while the inflammation in the brain was evident at 24 h post-exposure and still present at the end of the observation period, its intensity was significantly less than in animals with whole-body exposure or with head protection.

The fact that there was still MPO activation in the lungs regardless of the torso protection could be explained by pulmonary complications of the head injury such as neurogenic lung edema, seen both experimentally (Baumann et al., 2007; Irwin et al., 2008) and clinically (Dettbarn and Davidson, 1989; Fontes et al., 2003) after TBI. The roles of systemic sympathetic discharge, changes in intracranial pressure, and inflammation in central nervous system trigger zones have been suggested as essential mechanisms underlying the etiopathogenesis of neurogenic pulmonary edema (Sedy et al., 2008).

Taken together, the results of our study clearly demonstrate the importance of the indirect, i.e., blast–body interaction as well as the decisive role of autonomous nervous–neuroendocrine–immune systems interaction in the pathogenesis of BINT.

DISCUSSION AND CONCLUSIONS

Our findings demonstrate a multi-phase and multi-factorial nature of BINT where the mechanisms essential for the injury development and progress show significantly different phase-dependent trends. While acute alterations reflect compensatory attempts (such as increased activation of the sodium pump to potentially compensate for injury-induced impairments in electrolyte milieu or

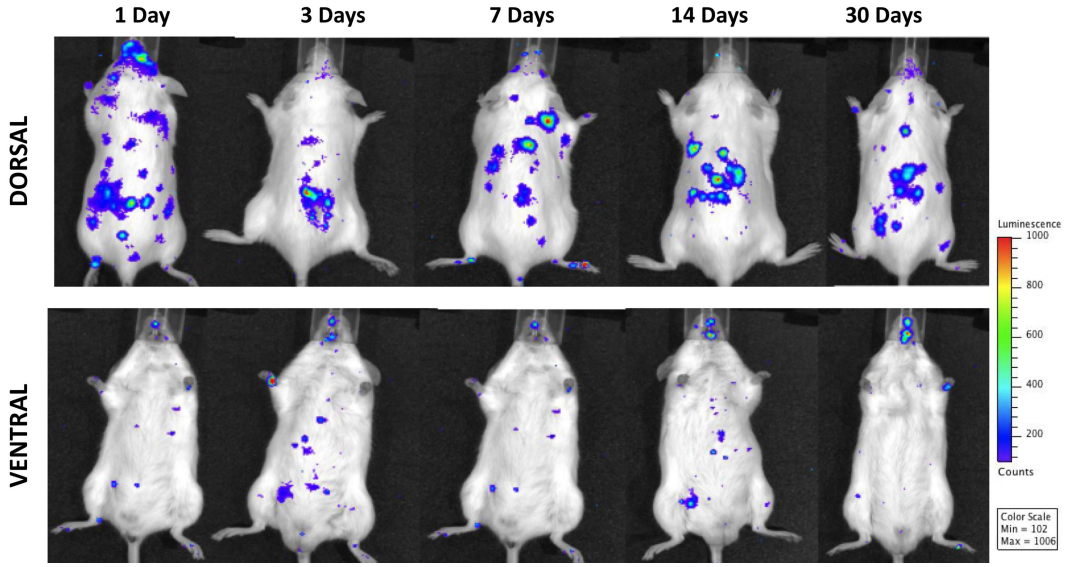

FIGURE 5 | Distribution of increased bioluminescence showing MPO activity in mice subjected to blast with torso protection while the head exposed, imaged during the 1-month observation period. The representative photographs show the same animal imaged in both dorsal and ventral positions at the given time point after blast exposure. The intensity of bioluminescence was scaled based on the photon counts. The nose cone that can be discerned on the photos is part of the anesthesia device that is the integral part of the IVIS® imaging system 3-D series, and does not represent a head cover.

parasympathetic stimulation to counteract the sudden pressure increase in the lungs and heart), chronic changes such as inflammation can lead to irreversible degenerative pathologies. Thus, to establish reliable diagnostic tools capable of identifying BINT and its progress, we should fully understand and characterize the multiple phases of the brain response to blast exposure.

The Na^+, K^+-ATPase activity change is an excellent example demonstrating the duality of response mechanisms to injury where increased and reversible activity after various brain insults in animals during the acute (<3 h) post-injury period (MacMillan, 1982; Goldberg et al., 1984; Sztriha et al., 1987) is followed by reduced activity during the chronic post-injury period (Jovicic et al., 2008; Crema et al., 2010) potentially leading to irreversible neurodegenerative central nervous system disorders (Seddik et al., 1991; Kumar and Kurup, 2002; Lima et al., 2008). While the Na^+, K^+-ATPase activity is not disease specific, its phase-dependent activity change as well as its kinetic profile to ATP might be a useful indicator of the BINT development and progress. The fact that the sodium pump changes correspond well to the changes in the erythrocyte membranes makes measurements of the Na^+, K^+-ATPase even more feasible as diagnostic parameters for BINT. There is a long list of research tasks ahead of us that concerns the importance of the Na^+, K^+-ATPase in the pathobiology of the BINT including establishing temporal and spatial profile characterization of its activity and kinetic pattern in the brain structures parallel with the changes in the erythrocyte membrane, and testing the diagnostic values of identified alterations in predicting functional neurological (memory, cognition, motor, and behavior) deficits, among others.

The results showing that head protection does not prevent chronic inflammation and neurological deficits suggest the vital importance of the blast–body interactive pathway in the etiopathogenesis of BINT. This fact is extremely important in designing effective protective equipment for servicemen that would prevent blast-body coupling, thus prevent the systemically induced mechanisms of BINT, as well as protect the brain from the direct impact caused by blast.

We need well-organized studies that begin in the field and identify the blast environment in relation to immediate and delayed mTBI symptoms in servicemen. Further, those data should be shared with the basic and applied research community to understand the uniqueness of this injury and to develop adequate and sensitive diagnostic tools and successful treatment. Without knowing what and how the blast injury occurred, it will be difficult to develop timely, reliable and specific diagnosis, and treatments for our servicemen. This multifaceted task is extremely challenging, and its successful solution is possible only through highly synchronized multi-institutional and international research efforts.

ACKNOWLEDGMENTS

Dr. Farid A. Ahmed significantly contributed to the Section "Importance of the Indirect Blast–Brain Interacting Pathway in Long-term Neurological Deficits" study. The study described in Section "Importance of the Indirect Blast–Brain Interacting Pathway in Long-term Neurological Deficits" was supported by the Johns Hopkins University Applied Physics Laboratory internal research and development (IR&D) funds. The sponsor did not influence the study design; data collection, analysis and interpretation of data; or the writing of the article.

REFERENCES

Adam-Vizi, V., Vizi, E. S., and Horvath, I. (1979). Stimulation by noradrenaline of Na^+K^+ ATPase in different fractions of rat brain cortex. *J. Neural Transm.* 46, 59–69.

Arnhold, J., and Flemmig, J. (2010). Human myeloperoxidase in innate and acquired immunity. *Arch. Biochem. Biophys.* 500, 92–106.

Baumann, A., Audibert, G., McDonnell, J., and Mertes, P. M. (2007). Neurogenic pulmonary edema. *Acta Anaesthesiol. Scand.* 51, 447–455.

Berthoud, H. R., and Neuhuber, W. L. (2000). Functional and chemical anatomy of the afferent vagal system. *Auton. Neurosci.* 85, 1–17.

Bhardwaj, A., Brannan, T., Martinez-Tica, J., and Weinberger, J. (1990). Ischemia in the dorsal hippocampus is associated with acute extracellular release of dopamine and norepinephrine. *J. Neural Transm. Gen. Sect.* 80, 195–201.

Breckwoldt, M. O., Chen, J. W., Stangenberg, L., Aikawa, E., Rodriguez, E., Qiu, S., Moskowitz, M. A., and Weissleder, R. (2008). Tracking the inflammatory response in stroke in vivo by sensing the enzyme myeloperoxidase. *Proc. Natl. Acad. Sci. U.S.A.* 105, 18584–18589.

Cernak, I. (2005). Animal models of head trauma. *NeuroRx* 2, 410–422.

Cernak, I., Ignjatovic, D., Andelic, G., and Savic, J. (1991). Metabolic changes as part of the general response of the body to the effect of blast waves. *Vojnosanit. Pregl.* 48, 515–522.

Cernak, I., Malicevic, Z., Prokic, V., Zunic, G., Djurdjevic, D., Ilic, S., and Savic, J. (1997). Indirect neurotrauma caused by pulmonary blast injury: development and prognosis. *Int. Rev. Armed Forces Med. Serv.* 52, 114–120.

Cernak, I., Merkle, A. C., Koliatsos, V. E., Bilik, J. M., Luong, Q. T., Mahota, T. M., Xu, L., Slack, N., Windle, D., and Ahmed, F. A. (2010). The pathobiology of blast injuries and blast-induced neurotrauma as identified using a new experimental model of injury in mice. *Neurobiol. Dis.* doi: 10.1016/j.nbd.2010.10.025. [Epub ahead of print].

Cernak, I., and Noble-Haeusslein, L. J. (2010). Traumatic brain injury: an overview of pathobiology with emphasis on military populations. *J. Cereb. Blood Flow Metab.* 30, 255–266.

Cernak, I., Radosevic, P., Malicevic, Z., and Savic, J. (1995). Experimental magnesium depletion in adult rabbits caused by blast overpressure. *Magnes. Res.* 8, 249–259.

Cernak, I., Savic, J., Ignjatovic, D., and Jevtic, M. (1999a). Blast injury from explosive munitions. *J. Trauma.* 47, 96–103; discussion 103–104.

Cernak, I., Savic, J., Zunic, G., Pejnovic, N., Jovanikic, O., and Stepic, V. (1999b). Recognizing, scoring, and predicting blast injuries. *World J. Surg.* 23, 44–53.

Cernak, I., Savic, J., Malicevic, Z., Zunic, G., Radosevic, P., and Ivanovic, I. (1996a). Leukotrienes in the pathogenesis of pulmonary blast injury. *J. Trauma* 40, S148–S151.

Cernak, I., Savic, J., Malicevic, Z., Zunic, G., Radosevic, P., Ivanovic, I., and Davidovic, L. (1996b). Involvement of the central nervous system in the general response to pulmonary blast injury. *J. Trauma* 40, S100–S104.

Clemedson, C. J. (1956). Blast injury. *Physiol. Rev.* 36, 336–354.

Crema, L., Schlabitz, M., Tagliari, B., Cunha, A., Simao, F., Krolow, R., Pettenuzzo, L., Salbego, C., Vendite, D., Wyse, A. T., and Dalmaz, C. (2010). Na^+, K^+ ATPase activity is reduced in amygdala of rats with chronic stress-induced anxiety-like behavior. *Neurochem. Res.* 35, 1787–1795.

Danzer, M., Jocic, M., Samberger, C., Painsipp, E., Bock, E., Pabst, M. A., Crailsheim, K., Schicho, R., Lippe, I. T., and Holzer, P. (2004). Stomach–brain communication by vagal afferents in response to luminal acid backdiffusion, gastrin, and gastric acid secretion. *Am. J. Physiol. Gastrointest. Liver Physiol.* 286, G403–G411.

Desaiah, D., and Ho, I. K. (1977). Kinetics of catecholamine sensitive Na^+-K^+ ATPase activity in mouse brain synaptosomes. *Biochem. Pharmacol.* 26, 2029–2035.

Dettbarn, C. L., and Davidson, L. J. (1989). Pulmonary complications in the patient with acute head injury: neurogenic pulmonary edema. *Heart Lung* 18, 583–589.

Dodge, J. T., Mitchell, C., and Hanahan, D. J. (1963). The preparation and chemical characteristics of hemoglobin-free ghosts of human erythrocytes. *Arch. Biochem. Biophys.* 100, 119–130.

Enseleit, W. H., Domer, F. R., Jarrott, D. M., and Baricos, W. H. (1984). Cerebral phospholipid content and Na^+, K^+-ATPase activity during ischemia and postischemic reperfusion in the mongolian gerbil. *J. Neurochem.* 43, 320–327.

Faith, M., Sukumaran, A., Pulimood, A. B., and Jacob, M. (2008). How reliable an indicator of inflammation is myeloperoxidase activity? *Clin. Chim. Acta* 396, 23–25.

Fiske, C. H., and Subbarow, Y. (1925). The colorimetric determination of phosphorus. *J. Biol. Chem.* 66, 375–400.

Fontes, R. B., Aguiar, P. H., Zanetti, M. V., Andrade, F., Mandel, M., and Teixeira, M. J. (2003). Acute neurogenic pulmonary edema: case reports and literature review. *J. Neurosurg. Anesthesiol.* 15, 144–150.

French, L. M. (2010). Military traumatic brain injury: an examination of important differences. *Ann. N. Y. Acad. Sci.* 1208, 38–45.

Garai, O. (1944). Blast injury: non-fatal case with neurological signs. *Lancet* 1, 788–789.

Gaykema, R. P., Chen, C. C., and Goehler, L. E. (2007). Organization of immune-responsive medullary projections to the bed nucleus of the stria terminalis, central amygdala, and paraventricular nucleus of the hypothalamus: evidence for parallel viscerosensory pathways in the rat brain. *Brain Res.* 1130, 130–145.

Ge, X., Yang, Z., Duan, L., and Rao, Z. (2001). Evidence for involvement of the neural pathway containing the peripheral vagus nerve, medullary visceral zone and central amygdaloid nucleus in neuroimmunomodulation. *Brain Res.* 914, 149–158.

Globus, M. Y., Busto, R., Dietrich, W. D., Martinez, E., Valdes, I., and Ginsberg, M. D. (1989). Direct evidence for acute and massive norepinephrine release in the hippocampus during transient ischemia. *J. Cereb. Blood Flow Metab.* 9, 892–896.

Godfraind, T., Koch, M. C., and Verbeke, N. (1974). The action of EGTA on the catecholamines stimulation of rat brain Na-K-ATPase. *Biochem. Pharmacol.* 23, 3505–3511.

Goldberg, W. J., Watson, B. D., Busto, R., Kurchner, H., Santiso, M., and Ginsberg, M. D. (1984). Concurrent measurement of (Na^+, K^+)-ATPase activity and lipid peroxides in rat brain following reversible global ischemia. *Neurochem. Res.* 9, 1737–1747.

Greve, M. W., and Zink, B. J. (2009). Pathophysiology of traumatic brain injury. *Mt. Sinai J. Med.* 76, 97–104.

Hernandez, R. J. (1992). $Na^+/K^{(+)}$-ATPase regulation by neurotransmitters. *Neurochem. Int.* 20, 1–10.

Hoffer, M. E., Balaban, C., Gottshall, K., Balough, B. J., Maddox, M. R., and Penta, J. R. (2010). Blast exposure: vestibular consequences and associated characteristics. *Otol. Neurotol.* 31, 232–236.

Irwin, D. C., Subudhi, A. W., Klopp, L., Peterson, D., Roach, R., and Monnet, E. (2008). Pulmonary edema induced by cerebral hypoxic insult in a canine model. *Aviat. Space Environ. Med.* 79, 472–478.

Jovicic, M. E., Popovic, M., Nesic, K. J., Popovic, N., Pavlovic, S. J., and Rakic, L. (2008). Aging, aluminium and basal forebrain lesions modify substrate kinetics of erythrocyte membrane Na, K-ATPase in the rat. *J. Alzheimers Dis.* 14, 85–93.

Kinnula, V. L. (2005). Production and degradation of oxygen metabolites during inflammatory states in the human lung. *Curr. Drug Targets Inflamm. Allergy* 4, 465–470.

Kumar, A. R., and Kurup, P. A. (2002). Inhibition of membrane Na^+-K^+ ATPase activity: a common pathway in central nervous system disorders. *J. Assoc. Physicians India* 50, 400–406.

Lima, F. D., Souza, M. A., Furian, A. F., Rambo, L. M., Ribeiro, L. R., Martignoni, F. V., Hoffmann, M. S., Fighera, M. R., Royes, L. F., Oliveira, M. S., and de Mello, C. F. (2008). Na^+, K^+-ATPase activity impairment after experimental traumatic brain injury: relationship to spatial learning deficits and oxidative stress. *Behav. Brain Res.* 193, 306–310.

Lopina, O. D. (2000). Na^+, K^+-ATPase: structure, mechanism, and regulation. *Membr. Cell Biol.* 13, 721–744.

Loria, V., Dato, I., Graziani, F., and Biasucci, L. M. (2008). Myeloperoxidase: a new biomarker of inflammation in ischemic heart disease and acute coronary syndromes. *Mediators Inflamm.* 2008, 135625.

Lowry, O. H., Rosebrough, N. J., Farr, A. L., and Randall, R. J. (1951). Protein measurement with the Folin phenol reagent. *J. Biol. Chem.* 193, 265–275.

MacMillan, V. (1982). Cerebral Na^+, K^+-ATPase activity during exposure to and recovery from acute ischemia. *J. Cereb. Blood Flow Metab.* 2, 457–465.

Malle, E., Buch, T., and Grone, H. J. (2003). Myeloperoxidase in kidney disease. *Kidney Int.* 64, 1956–1967.

Martin, E. M., Lu, W. C., Helmick, K., French, L., and Warden, D. L. (2008). Traumatic brain injuries sustained in the Afghanistan and Iraq wars. *Am. J. Nurs.* 108, 40–47.

Maslinska, D., and Gajewski, M. (1998). Some aspects of the inflammatory process. *Folia Neuropathol.* 36, 199–204.

McIntosh, T. K., Yu, T., and Gennarelli, T. A. (1994). Alterations in regional brain catecholamine concentrations after experimental brain injury in the rat. *J. Neurochem.* 63, 1426–1433.

Menezes, G. B., Rezende, R. M., Pereira-Silva, P. E., Klein, A., Cara, D. C., and Francischi, J. N. (2008). Differential involvement of cyclooxygenase isoforms in neutrophil migration in vivo and in vitro. *Eur. J. Pharmacol.* 598, 118–122.

Mrsulja, B. B., Stojadinovic, N., Maletic-Savatic, M., Stojanovic, T., Cvejic,

V., Nenadovic, M., Paunovic, V. R., Marinkovic, D., and Kostic, V. S. (1993). Substrate erythrocyte membrane Na, K-ATPase: a potentially ubiquitous mechanism reflecting central nervous system pathology. *Iugoslav. Physiol. Pharmacol. Acta* 29, 115–119.

Naito, Y., Takagi, T., and Yoshikawa, T. (2007). Molecular fingerprints of neutrophil-dependent oxidative stress in inflammatory bowel disease. *J. Gastroenterol.* 42, 787–798.

Nelson, L. A., Yoash-Gantz, R. E., Pickett, T. C., and Campbell, T. A. (2009). Relationship between processing speed and executive functioning performance among OEF/OIF veterans: implications for postdeployment rehabilitation. *J. Head Trauma Rehabil.* 24, 32–40.

Owen-Smith, M. S. (1981). Explosive blast injury. *Med. Bull. US Army Eur.* 38, 36–43.

Pappius, H. M. (1991). Brain injury: new insights into neurotransmitter and receptor mechanisms. *Neurochem. Res.* 16, 941–949.

Peskind, E. R., Petrie, E. C., Cross, D. J., Pagulayan, K., McCraw, K., Hoff, D., Hart, K., Yu, C. E., Raskind, M. A., Cook, D. G., and Minoshima, S. (2010). Cerebrocerebellar hypometabolism associated with repetitive blast exposure mild traumatic brain injury in 12 Iraq war Veterans with persistent postconcussive symptoms. *Neuroimage.* doi:10.1016/j.neuroimage.2010.04.008. [Epub ahead of print].

Petrushanko, I. Y., Bogdanov, N. B., Lapina, N., Boldyrev, A. A., Gassmann, M., and Bogdanova, A. Y. (2007). Oxygen-induced regulation of Na/K ATPase in cerebellar granule cells. *J. Gen. Physiol.* 130, 389–398.

Phillis, J. W., and Wu, P. H. (1981). Catecholamines and the sodium pump in excitable cells. *Prog. Neurobiol.* 17, 141–184.

Reilly, P. L. (2001). Brain injury: the pathophysiology of the first hours. "Talk and die revisited". *J. Clin. Neurosci.* 8, 398–403.

Ritenour, A. E., Blackbourne, L. H., Kelly, J. F., McLaughlin, D. F., Pearse, L. A., Holcomb, J. B., and Wade, C. E. (2010). Incidence of primary blast injury in US military overseas contingency operations: a retrospective study. *Ann. Surg.* 251, 1140–1144.

Rossle, R. (1950). "Pathology of blast effects," in *German Aviation Medicine, World War II* ed. USAF School of Aviation Medicine, (Washington, DC: Department of the Air Force), 1260–1273.

Savic, J., Lazarov, A., Malicevic, Z., Nikolic, J., and Vujinov, S. (1995). Relationship between early neuroendocrine response and severity of war injury according to the red cross classification. *Vojnosanit. Pregl.* 52, 107–117.

Seddik, Z., Habib, Y. A., and el Shamy, E. (1991). The prognostic value of the brain sodium–potassium ATPase enzyme concentration in head injury. *Childs Nerv. Syst.* 7, 135–138.

Sedy, J., Zicha, J., Kunes, J., Jendelova, P., and Sykova, E. (2008). Mechanisms of neurogenic pulmonary edema development. *Physiol. Res.* 57, 499–506.

Sheldon, C., Diarra, A., Cheng, Y. M., and Church, J. (2004). Sodium influx pathways during and after anoxia in rat hippocampal neurons. *J. Neurosci.* 24, 11057–11069.

Silver, I. A., and Erecinska, M. (1997). Energetic demands of the Na^+/K^+ ATPase in mammalian astrocytes. *Glia* 21, 35–45.

Skou, J. C., and Esmann, M. (1992). The Na, K-ATPase. *J. Bioenerg. Biomembr.* 24, 249–261.

Stewart, O. W., and Russel, C. K. (1941). Injury to the central nervous system by blast. *Lancet* 1, 172–174.

Sztriha, L., Joo, F., Dux, L., and Boti, Z. (1987). Effects of systemic kainic acid administration on regional Na^+, K^+-ATPase activity in rat brain. *J. Neurochem.* 49, 83–87.

Terrio, H., Brenner, L. A., Ivins, B. J., Cho, J. M., Helmick, K., Schwab, K., Scally, K., Bretthauer, R., and Warden, D. (2009). Traumatic brain injury screening: preliminary findings in a US army brigade combat team. *J. Head Trauma Rehabil.* 24, 14–23.

Toft, P., Andersen, S. K., and Tonnesen, E. K. (2003). The systematic inflammatory response after major trauma. *Ugeskr. Laeg.* 165, 669–672.

Turski, P. A., Perman, W. H., Hald, J. K., Houston, L. W., Strother, C. M., and Sackett, J. F. (1986). Clinical and experimental vasogenic edema: in vivo sodium MR imaging. Work in progress. *Radiology* 160, 821–825.

Wang, J. A., Lin, W., Morris, T., Banderali, U., Juranka, P. F., and Morris, C. E. (2009). Membrane trauma and Na^+ leak from Nav1.6 channels. *Am. J. Physiol., Cell Physiol.* 297, C823–C834.

Warden, D. L., French, L. M., Shupenko, L., Fargus, J., Riedy, G., Erickson, M. E., Jaffee, M. S., and Moore, D. F. (2009). Case report of a soldier with primary blast brain injury. *Neuroimage* 47(Suppl. 2), T152–T153.

Werner, U., and Szelenyi, I. (1992). Measurement of MPO activity as model for detection of granulocyte infiltration in different tissues. *Agents Actions* Spec No. C101–C103.

Weston, R. M., Jones, N. M., Jarrott, B., and Callaway, J. K. (2007). Inflammatory cell infiltration after endothelin-1-induced cerebral ischemia: histochemical and myeloperoxidase correlation with temporal changes in brain injury. *J. Cereb. Blood Flow Metab.* 27, 100–114.

Young, W., DeCrescito, V., Flamm, E. S., Hadani, M., Rappaport, H., and Cornu, P. (1986). Tissue Na, K, and Ca changes in regional cerebral ischemia: their measurement and interpretation. *Cent. Nerv. Syst. Trauma* 3, 215–234.

Zucker, I. H. (1986). Left ventricular receptors: physiological controllers or pathological curiosities? *Basic Res. Cardiol.* 81, 539–557.

Zuckerman, S. (1940). Experimental study of blast injuries to the lungs. *Lancet* 236, 219–224.

Conflict of Interest Statement: The author declares that the research was conducted in the absence of any commercial or financial relationships that could be construed as a potential conflict of interest.

Received: 16 November 2010; accepted: 24 November 2010; published online: 10 December 2010.

*Citation: Cernak I (2010) The importance of systemic response in the pathobiology of blast-induced neurotrauma. Front. Neur. **1**:151. doi: 10.3389/fneur.2010.00151*

This article was submitted to Frontiers in Neurotrauma, a specialty of Frontiers in Neurology.

frontiers in NEUROLOGY

ORIGINAL RESEARCH ARTICLE
published: 04 April 2011
doi: 10.3389/fneur.2011.00019

Low level primary blast injury in rodent brain

Pamela B. L. Pun[1], Enci Mary Kan[1], Agus Salim[2], Zhaohui Li[3], Kian Chye Ng[1], Shabbir M. Moochhala[1], Eng-Ang Ling[4], Mui Hong Tan[1] and Jia Lu[1]*

[1] Combat Care Laboratory, Defence Medical and Environmental Research Institute, DSO National Laboratories, Singapore
[2] Department of Epidemiology and Public Health, Yong Loo Lin School of Medicine, National University of Singapore, Singapore
[3] Bek Chai Heah Laboratory of Cancer Genomics, Cellular and Molecular Research, Humphrey Oei Institute of Cancer Research, National Cancer Centre, Singapore
[4] Department of Anatomy, Yong Loo Lin School of Medicine, National University of Singapore, Singapore

Edited by:
Marten Risling, Karolinska Institutet, Sweden

Reviewed by:
Hans Lindå, Karolinska Institutet, Sweden
Ibolja Cernak, Johns Hopkins University, USA

***Correspondence:**
Jia Lu, Combat Care Laboratory, Defence Medical and Environmental Research Institute, DSO National Laboratories, 27 Medical Drive, Singapore 117510, Singapore.
e-mail: ljia@dso.org.sg

The incidence of blast attacks and resulting traumatic brain injuries has been on the rise in recent years. Primary blast is one of the mechanisms in which the blast wave can cause injury to the brain. The aim of this study was to investigate the effects of a single sub-lethal blast over pressure (BOP) exposure of either 48.9 kPa (7.1 psi) or 77.3 kPa (11.3 psi) to rodents in an open-field setting. Brain tissue from these rats was harvested for microarray and histopathological analyses. Gross histopathology of the brains showed that cortical neurons were "darkened" and shrunken with narrowed vasculature in the cerebral cortex day 1 after blast with signs of recovery at day 4 and day 7 after blast. TUNEL-positive cells were predominant in the white matter of the brain at day 1 after blast and double-labeling of brain tissue showed that these DNA-damaged cells were both oligodendrocytes and astrocytes but were mainly not apoptotic due to the low caspase-3 immunopositivity. There was also an increase in amyloid precursor protein immunoreactive cells in the white matter which suggests acute axonal damage. In contrast, Iba-1 staining for macrophages or microglia was not different from control post-blast. Blast exposure altered the expression of over 5786 genes in the brain which occurred mostly at day 1 and day 4 post-blast. These genes were narrowed down to 10 overlapping genes after time-course evaluation and functional analyses. These genes pointed toward signs of repair at day 4 and day 7 post-blast. Our findings suggest that the BOP levels in the study resulted in mild cellular injury to the brain as evidenced by acute neuronal, cerebrovascular, and white matter perturbations that showed signs of resolution. It is unclear whether these perturbations exist at a milder level or normalize completely and will need more investigation. Specific changes in gene expression may be further evaluated to understand the mechanism of blast-induced neurotrauma.

Keywords: primary blast injury, central nervous system, histopathology, immunohistochemistry, gene expression

INTRODUCTION

Blast attacks involving weapons such as roadside bombs, grenades, and improvised explosive devices (IEDs) are an increasingly common feature of terrorist attacks, with as many as 1513 such attacks recorded in the period of January to November 2007, affecting both civilian and military populations and resulting in over 16,000 casualties (Lawson Terrorism Information Centre, 2009). In particular, blast-induced neurotrauma (BINT) is an increasing problem for which mild traumatic brain injury (MTBI) forms the majority of these injuries (Ling et al., 2009; Cernak and Noble-Haeusslein, 2010). Despite the pressing urgency for accurate and effective diagnostic, prognostic, and therapeutic approaches to blast injuries, there remain significant gaps in our knowledge of this condition (Kochanek et al., 2009).

Primary neurotrauma occurs when the insult delivers a direct blow to the head which may be penetrating or non-penetrating (closed head). In a blast injury, primary injury is a result of the directs effects of the blast wave to the head compared to other forms of blast injuries such as secondary (e.g., victim is hit on head by an object propelled by the blast wave) and tertiary (e.g., victim is flung by the blast wave against an object and injures his head) injuries. The most commonly assessed blast wave parameter for primary blast injury is usually the peak blast over pressure (BOP), duration of the positive phase and impulse. The effects of primary blast injury on air-containing organs such as the lungs have been widely investigated and characterized (Kirkman and Watts, 2011). Blast-induced pulmonary injury thresholds have also been elucidated and refined (Bowen et al., 1968; Rafaels et al., 2010). Advancement in body armor material and protection has been able to mitigate in part, the vulnerability of pulmonary injuries to blast (Phillips et al., 1988) though not totally. Together with improved efficiencies in medical evacuations and advances in medical care which contribute to increased survival rate, incidences of BINT are on the rise in modern warfare.

Given the prevalence of BINT, the mechanism of primary blast injury to the central nervous system (CNS) is less well characterized and especially so for blast-induced MTBI. To date, most primary blast injury rodent CNS research has focused on peak BOPs > 110 kPa. However, it has been reported that BOPs > 110 kPa can also cause concomitant pulmonary injury

in animals with high incidence of mortality (Bauman et al., 1997; Gorbunov et al., 2004; Chavko et al., 2006; Long et al., 2009). Hence, we were particularly interested in the effects of low-intensity blast on the brain at peak BOPS < 110 kPa without causing overt pulmonary damage and mortality.

Previous studies investigating BINT in rodents have reported a wide spectrum of perturbations post-blast that encompass cerebrovascular changes, white matter damage, neuronal changes in the hippocampus, oxidative stress, and increased blood–brain barrier permeability (Bauman et al., 1997; Cernak et al., 2001a,b; Long et al., 2009; Cernak, 2010; Readnower et al., 2010; Risling et al., 2011). Recent literature has also pointed toward the presence of cerebral inflammation that could be mediated by systemic inflammation due to the CNS effects of the primary blast wave through the unprotected torso (Cernak, 2010). Hence, in this low level blast study, we aimed to profile the acute changes post-blast especially with regards to regions vulnerable to apoptotic cell death and inflammation through the activation of microglial cells which are the major inflammatory cells in the CNS.

Furthermore, we also sought to profile changes in gene expression post-blast for the identification of broad functional changes through clustering and to provide a platform for biomarker discovery. Biomarkers should be definitive indicators of pathogenic processes (Biomarkers Definitions Working Group, 2001) which are sorely lacking for MTBI for which better experimental designs into underlying molecular mechanisms are required (Svetlov et al., 2009). A proteomics approach to identifying relevant molecules has previously been suggested (Agoston et al., 2009). We present here, a microarray technique that can be applied to low level primary blast research and also venture to provide a conceptual model of an alternative and complementary genomics-based approach.

MATERIALS AND METHODS

ANIMALS AND BLAST EXPOSURE

Animal experiments were approved by the DSO Institutional Animal Care and Use Committee (DSO IACUC). Male Sprague-Dawley rats (250–350 g) were used for this study. Rats were anesthetized prior to blast exposure with an intraperitoneal injection of 75 mg/kg ketamine and 10 mg/kg xylazine. The animals were then secured with Velcro straps in metal cages that were anchored to the ground at the blast site. The source of BOP was 120 kg of 2,4,6-trinitrotoluene (TNT). Blast sensors (seven side-on pressure gages and three stagnation pressure gages) were used to monitor intensity and duration of BOP exposure during test and actual blast trials. Animals were placed at either 24 or 30 m away from the TNT source and were exposed to different sub-lethal BOP intensities (i.e., low, high). Six to eight animals were strapped loosely using Velcro to a metal mesh cage at the specified distances and doused with water to minimize dehydration and singeing of fur. A 0.4 m × 0.4 m concrete block was placed between the animals and the explosive source at a distance of 1.5 m from the animals. This block served as a shield against debris from the explosion, thus protecting animals against secondary blast injuries due to the projectiles. A schematic of the blast set-up is given in **Figure 1A**. Preliminary trials and simulations revealed no influence of the block on the blast wave at the position of the animals (data not shown). Control animals were transported to the blast

A

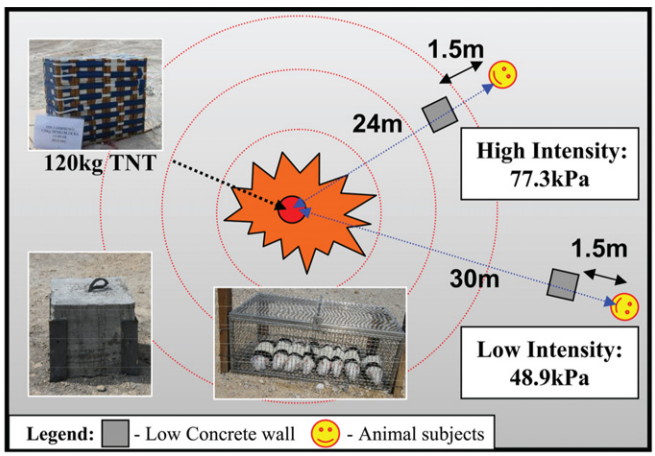

B

Blast condition	Distance (m)	Peak blast over pressure (kPa)	Positive duration (msec)	Mortality (%)
Low	30	48.9	14.5	4.4
High	24	77.3	18.2	8.3

FIGURE 1 | (A) Schematic of blast set-up for six to eight rodents placed in a mesh metal cage at 24 m (high intensity) and 30 m (low intensity) from blast source (120 kg TNT) shielded from debris with a concrete block (0.4 m × 0.4 m) at 1.5 m from the animals. **(B)** Actual blast parameters: pressure (kPa) and duration (milliseconds) and mortality (%) at low and high blast exposure.

site then anesthetized as with the blast-exposed animals, but were not exposed to the actual blast. After blast exposure, the animals were returned to the animal holding facility and allowed to recover from the effects of anesthesia. Access to food and drinks was *ad libitum*. The animals were sacrificed at day 1, day 4, and day 7 after the blast.

HISTOPATHOLOGY AND IMMUNOHISTOCHEMISTRY

By method of transcardial perfusion, the animals were perfused with Ringer's solution until the liver and lungs were cleared of blood followed by 10% buffered paraformaldehyde. The brains were harvested and post-fixed in 10% buffered formalin. The brains were then dehydrated in an ascending series of alcohol, cleared with xylene, and then embedded in paraffin wax. Paraffin sections of 4 μm thickness were then cut and microwaved in citrate buffer for antigen retrieval and blocked with peroxidase blocking reagent (S2023, DAKO UK Ltd, UK). Brain and lung sections were stained for routine histology using hematoxylin and eosin (H&E) for general morphology analysis. For apoptosis staining, brain sections were stained according to the protocol provided in the ApopTag® Peroxidase *In Situ* Apoptosis Detection Kit (S7100, Chemicon International, Inc., MA, USA). For the preparation of double-labeled brain sections, a second antibody of rabbit anti-glial fibrillary acidic protein (GFAP) (AB5804, Chemicon International, Inc., MA, USA) diluted 1:1500 in PBS, biotinylated *Ricinus communis* Agglutinin I (RCA_{120}) anti-lectin (B-1085, Vector Laboratories, Inc., CA, USA) diluted 1:1000 in PBS or rabbit polyclonal anti-myelin basic protein (MBP; AB980, Chemicon International, Inc., MA, USA) diluted 1:200 in PBS was used to detect GFAP, lectin, and MBP respectively. For immunohistochemistry, brain sections were also incubated with rabbit polyclonal anti-caspase-3 (#RB-1197-P, Thermo Fisher Scientific Inc., USA) diluted 1:100 in PBS; rabbit anti-ionized calcium binding adaptor molecule-1 (Iba-1; #019-19741, Wako Pure Chemical) diluted 1:500 in PBS; and rabbit polyclonal amyloid β precursor protein (APP; AB17467, Abcam) diluted 1:100 in PBS; for detection of caspase-3, Iba-1, and APP respectively. Subsequent antibody detection was carried out using either anti-mouse or anti-rabbit IgG (Envision + system-HRP, DAKO UK Ltd, UK) except for lectin which was carried out using horseradish peroxidase streptavidin (SA-5004, Vector Laboratories). All samples were then visualized using 3,3′-diaminobenzidine (DAB) and examined under a light microscope (Olympus, Japan). A cell count of at least three sections at 20× magnification of TUNEL, Iba-1, and APP positive cells in the white matter was carried out and results are expressed as mean ± standard error of the mean (SEM). Statistical comparison between groups was performed by one-way ANOVA with *post hoc* Tukey's HSD test. Significance was accepted at $p < 0.05$.

MICROARRAY

Brain tissue from animals exposed to the lower BOP were harvested, quick frozen in lqN_2 and stored at −80°C for subsequent microarray analyses. RNA was isolated using standard Trizol-based RNA extraction methods. The RNA quality was then determined based on RNA integrity number (RIN) and an electropherogram, both of which were analyzed using the Agilent 2100 Bioanalyzer platform (Agilent Technologies). Only samples with RIN greater than 6 were used (Fleige and Pfaffl, 2006). RNA samples were amplified and labeled with Cy3, hybridized to Agilent Whole Rat Genome Oligo Microarrays 4x44k, and analyzed using a microarray scanner system. All procedures were carried out in duplicates using commercial kits (Agilent Technologies) by a microarray service provider (Miltenyi Biotec GmbH, Germany). Microarray results were analyzed using R/Bioconductor and Partek Genomic Suite (Partek, MO, USA). Two independent analyses were conducted. The first set of analysis compared the expression levels of genes in blast-exposed animals vs. that in controls at each time-point. The second set of analysis investigated the changes in log ratio of blast-exposed vs. control animals [log (blast/control)] over time [e.g., log $(\text{blast/control})_{\text{day 4}}$ vs. log $(\text{blast/control})_{\text{day 1}}$, log $(\text{blast/control})_{\text{day 7}}$ vs. log $(\text{blast/control})_{\text{day 1}}$]. The overall type I error was taken at 0.01, and *p*-values were corrected for multiple testings using false discovery rates.

RESULTS

BLAST EXPOSURE AND SURVIVAL

A total of 58 animals were used in this study, of which 11 were controls, 23 were exposed to BOP at 48.9 kPa (or 7.1 psi) and positive over pressure duration of 14.5 ms at 30 m from TNT source, and 24 were exposed to BOP at 77.3 kPa (or 11.3 psi) and positive over pressure duration of 18.2 ms at 24 m (**Figure 1B**). For the purposes of the current work, we shall refer to the blast exposure conditions employed in simplistic terms as either high (BOP = 77.3 kPa) or low (BOP = 48.9 kPa) intensity. Corresponding mortality rates for the groups (low, high) were 4.4 and 8.3% respectively (**Figure 1B**). All of these animals died within 30 min of blast exposure. Deaths in the blast groups revealed pulmonary hemorrhage post-mortem. Surviving rats were used for subsequent investigation.

HISTOLOGY AND IMMUNOHISTOCHEMISTRY OF BLAST INJURIES

Lung gross histopathology

Rats were sacrificed at day 1, day 4, or day 7 after blast for investigation. Two tissues were examined, namely the brain and lungs. Other tissues were not examined as no external hemorrhage was observed. There was no apparent lung injury in both blast-exposed groups on day 1 post-blast. However, a few petechiae and ecchymoses were observed in the periphery of lung tissue upon harvesting at day 4 and day 7 after blast. H&E staining of the lung sections revealed alveolar lesions with accumulation of red blood corpuscles in lung alveolar space at day 4 and day 7 post high-intensity blast (**Figure 2**).

Brain and lung gross histopathology

No obvious extra- and/or sub-dural hemorrhage was observed in the brains of all blast-exposed animals relative to the untreated controls H&E staining of brain sections from cerebral cortex showed darkened neurons (identified from the presence of projecting dendrites and polygonal shape of cell body) after high-intensity blast mostly at day 1 post-blast which appeared to abate at day 4 and day 7. These darkened neurons were also shrunken as evidenced by the presence of peri-somal spaces. Furthermore, the vasculature appeared to be narrowed at day 1 and day 4 post-blast compared to control (**Figure 3**).

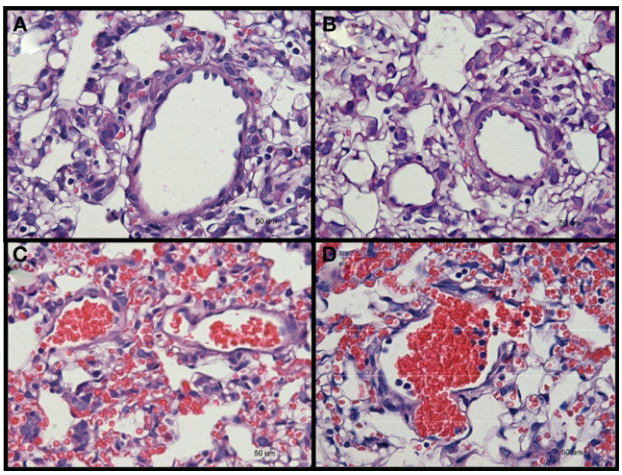

FIGURE 2 | Hematoxylin and eosin stained sections of lung tissues from (A) control, and low-intensity blast-exposed animals at (B) day 1 (C) day 4, and (D) day 7, after blast signs of hemorrhage, macrophage infiltration, and thickening of the alveolar septae, were observed at day 4 and day 7 after blast injury.

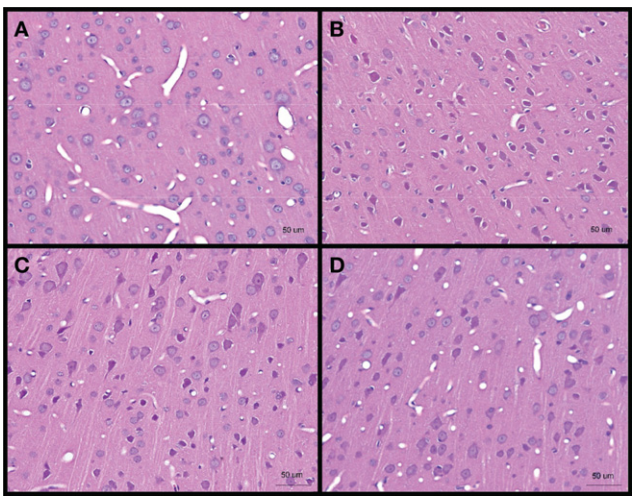

FIGURE 3 | Hematoxylin and eosin stained sections of brain cerebral cortex from (A) control, and low-intensity blast-exposed animals at (B) day 1 (C) day 4, and (D) day 7 after blast. Darkened and shrunken neurons evidenced by the presence of peri-somal spaces at day 1 post-blast compared to control and in lesser quantities at day 4 and day 7 post-blast. Vasculature appears to be narrowed in day 1 and day 4 post-blast compared to control.

White matter damage

To confirm the presence of injury in the brains of rats exposed to high- and low-intensity BOP, TUNEL and caspase-3 staining was carried out to identify apoptotic cells in the brains. There were only a few cells positive for caspase-3 (not shown) compared to TUNEL-positive cells in the white matter. There was significantly more TUNEL-positive cells in the white matter of blast-exposed rats at high- and low-intensity relative to control on day 1 after blast (**Figure 4**). By day 7, however, there appeared to be no major difference between controls and blast-treated rats (data not shown). Double-staining for TUNEL and non-neuronal cells (GFAP, lectin, or MBP) revealed that the cells with DNA fragmentation were mainly oligodendrocytes and astrocytes, but not microglial cells (**Figure 5**). Iba-1 staining for CNS macrophages/microglia also showed no changes in microglia density between control and both blast-groups at day 1 post-blast (**Figure 6**). In addition to the presence of apoptotic astrocytes and oligodendrocytes, APP immunostaining was also significantly increased in both blast conditions compared to control on day 1 after blast (**Figure 7**).

GENE EXPRESSION CHANGES IN MILD TRAUMATIC BRAIN INJURY

Microarray analyses of brain RNA samples from both control and rats exposed to low-intensity blast was carried out to determine gene expression changes. For the purpose of analysis, we hypothesized that functionally relevant genes are likely to include those whose expressions are significantly altered by blast exposure and/or show a significant time evolution after blast.

In our first set of analyses, we found 5786 probe sets which showed significant changes in the blast-exposed group relative to the controls at least one time-point. Most of these probe sets either had no confirmed identities or no known biological functions. Only 676 were established genes with well-defined functions (**Table A1** in Appendix). We grouped these genes according to their functions and the results are shown in **Figure 8**. It appears that most changes took place at day 1 and day 4 after blast, with far fewer alterations observed at day 7. Clustering of the genes whose expressions varied most between arrays revealed high concordance between two replicates under the same condition which cluster together. In particular, day 1 and day 7 replicates clusters seemed similar while day 4 is different (**Figure 9**).

Our second set of analyses revealed 203 probe sets that showed significant time-course evolution, i.e., the log $(\text{blast/control})_{\text{day 4 or day 7}}$ was different relative to that at day 1. Based upon their time-evolution pattern, these 203 probe sets were grouped into eight clusters based on similar evolution (**Figure 10**). The biological functions of genes in each cluster, except clusters 5 and 8 which do not have genes with information, are given in **Table A2** of Appendix. Out of the 203, only 34 are known genes with established functions (**Table 1**). Between our two sets of microarray analyses, there was an overlap of 10 genes (**Table 2**).

DISCUSSION

Blast-induced neurotrauma is the signature of the modern war (Elder et al., 2010). We were particularly interested in mild TBI as it accounts for over 77.8% of all TBI injuries sustained during combat (Defense and Veterans Brain Injury Center, 2010). In our open field blast test, we set out to investigate the effects of two relatively low BOP exposures of 77.3 and 48.9 kPa to cause mild BINT and to determine its effects on pulmonary injury in rodents with no body armor. The low BOP exposure was determined from the Bowen's curve to determine if these BOP values could cause mild BINT without any overt pulmonary damage and also to minimize mortality in the animals. At the time of our study, there was only one report investigating the effects of peak BOP < 100 kPa on the effects in the rodent CNS (Saljo et al., 2009).

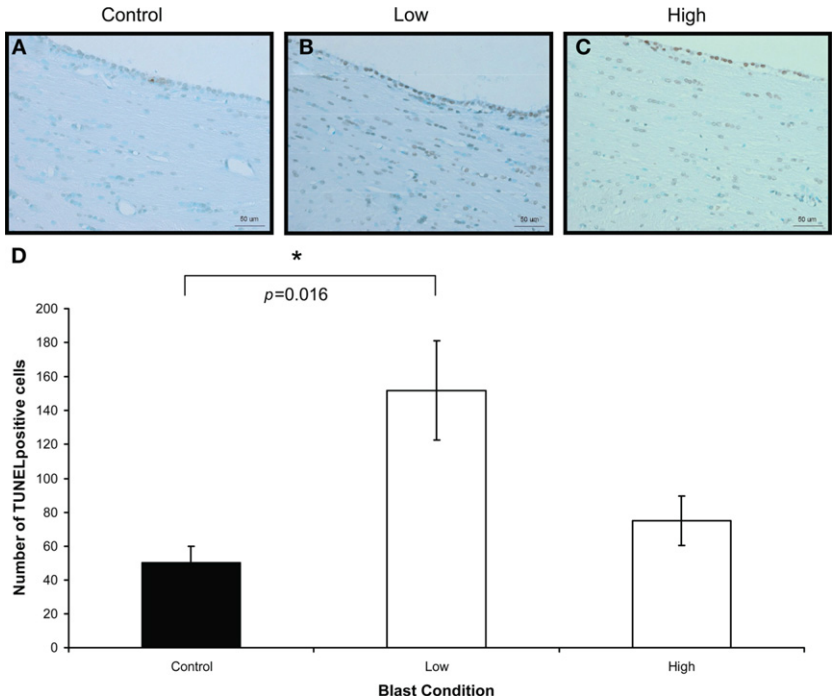

FIGURE 4 | Iba-1 immunostaining (brown) of (A) control (B) low, and (C) high, blast exposure 1 day after blast. Scale bar = 50 μm. **(D)** Mean number of Iba-1 positive cells per field view in the corpus callosum of control, low ($p = 0.26$ vs. control) and high ($p = 0.019$ vs. control) blast-exposed animals 1 day after blast at ×20 magnification. No difference in Iba-1 positive cells was found between blast exposure groups (low and high) and control. *$p < 0.05$.

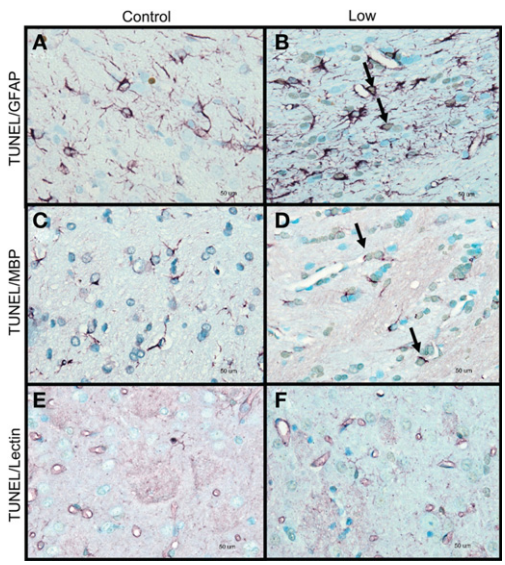

FIGURE 5 | Double-labeling of non-neuronal cells with TUNEL for apoptotic cells (light brown staining, indicated by small arrows) and glia markers (purple staining) for (A,B) apoptotic astrocytes, indicated by thick arrows (TUNEL and GFAP double-labeling). (C,D) Apoptotic oligodendrocytes, indicated by thick arrows (TUNEL and MBP double-labeling). **(E,F)** Lectin-positive microglia and TUNEL-labeled cells (TUNEL and lectin double-labeling). Control animals **(A,C,E)**, low-intensity blast-exposed animals **(B,D,F)**. Note lack of overlapping of labeling in apoptotic cells and microglia in low-intensity blast-exposed animals. Scale bar = 50 μm.

Our findings showed the appearance of hemorrhagic lesions in the lung which is a feature of pulmonary blast injury even at the test levels of BOP of 77.3 and 48.9 kPa compared to previous studies in which lung injury was reported at higher BOP exposure of 118 kPa (Chavko et al., 2006; Gorbunov et al., 2006). The late appearance of lung petechiae and alveolar hemorrhage at day 4 and day 7 after blast suggests a delayed response as opposed to immediate (as early as 2 h) pulmonary injury that could occur at higher BOPs (Gorbunov et al., 2006). Recent evidence investigating a BOP model <110 kPa also demonstrated that a shockwave of 11.5 kPa resulted in no evidence of lung injury but was evident at 66 kPa (Park et al., 2010). Hence, it may be suggested that the BOP range of 48.9–77.3 kPa represents the threshold for blast-induced lung injury in the unprotected rodent. The use of improved protective body armor in combat situations has largely mitigated against pulmonary injury and mortality (Phillips et al., 1988). It is now generally accepted that the threshold for BINT is higher than that of pulmonary injury. Pulmonary blast injury has been reported to be due to the pressure changes at the tissue-density interface (DePalma et al., 2005). The Bowen's curve for which the study's sub-lethal BOP levels were chosen was based on this theory. However, other factors such as the viscoelasticity of the tissue (Stuhmiller, 1997) and internal spalling and implosion (Treadwell, 1989) may also contribute to pulmonary blast injury.

The BOP exposure to animals in our study resulted in the "darkening" or enhanced H&E staining of cortical neurons in the gray matter which may be due to the condensation of the neuronal cytoplasm which has also been previously reported to occur in a global cerebral ischemic condition (Kawai et al., 1992). These

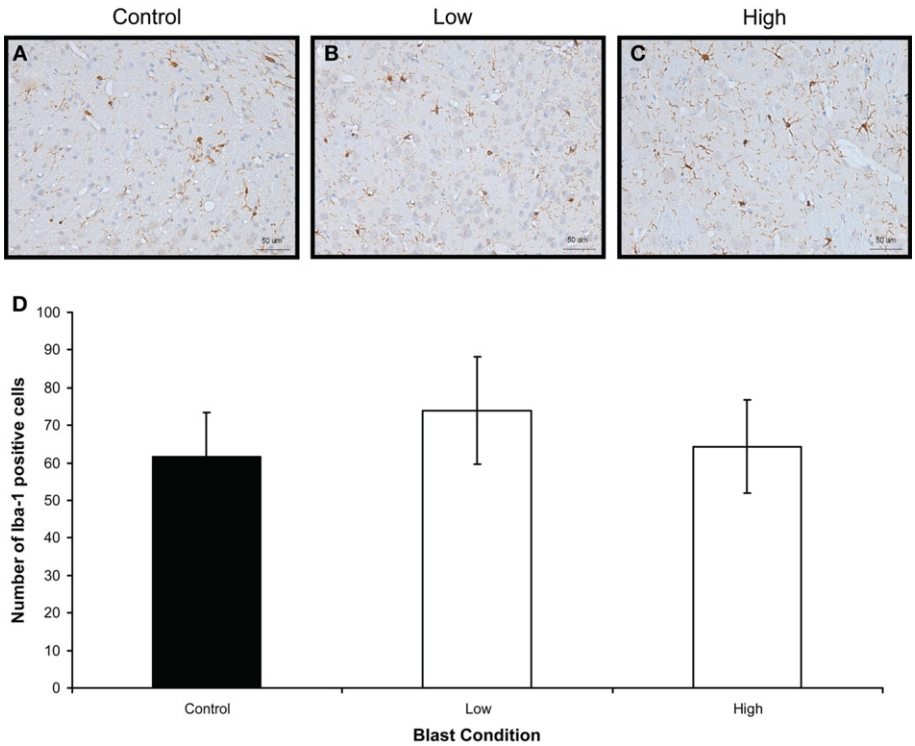

FIGURE 6 | Iba-1 immunostaining (brown) of (A) control (B) low, and (C) high, blast exposure 1 day after blast. Scale bar = 50 μm. **(D)** Mean number of Iba-1 positive cells per field view in the corpus callosum of control, low ($p = 0.26$ vs. control), and high ($p = 0.019$ vs. control) blast-exposed animals 1 day after blast at ×20 magnification. No difference in Iba-1 positive cells was found between blast exposure groups (low and high) and control. *$p < 0.05$.

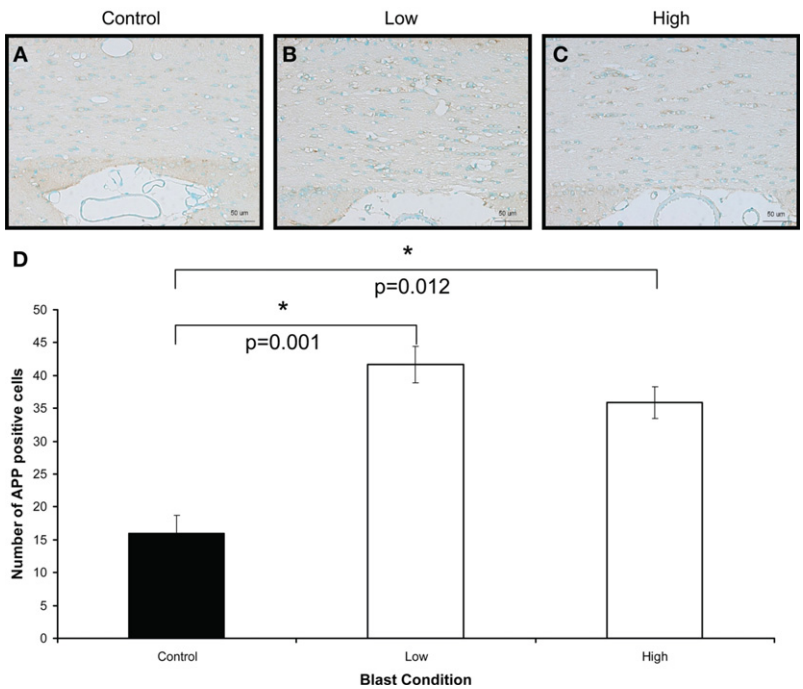

FIGURE 7 | Amyloid β precursor protein immunostaining (brown) of (A) control (B) low, and (C) high, blast exposure 1 day after blast. Scale bar = 50 μm. **(D)** Mean number of APP positive cells per field view in the white matter of control, low ($p = 0.26$ vs. control) and high ($p = 0.019$ vs. control) blast-exposed animals 1 day after blast at ×20 magnification. Both low and high blast exposure animals had significantly higher APP+ cells than control. *$p < 0.05$.

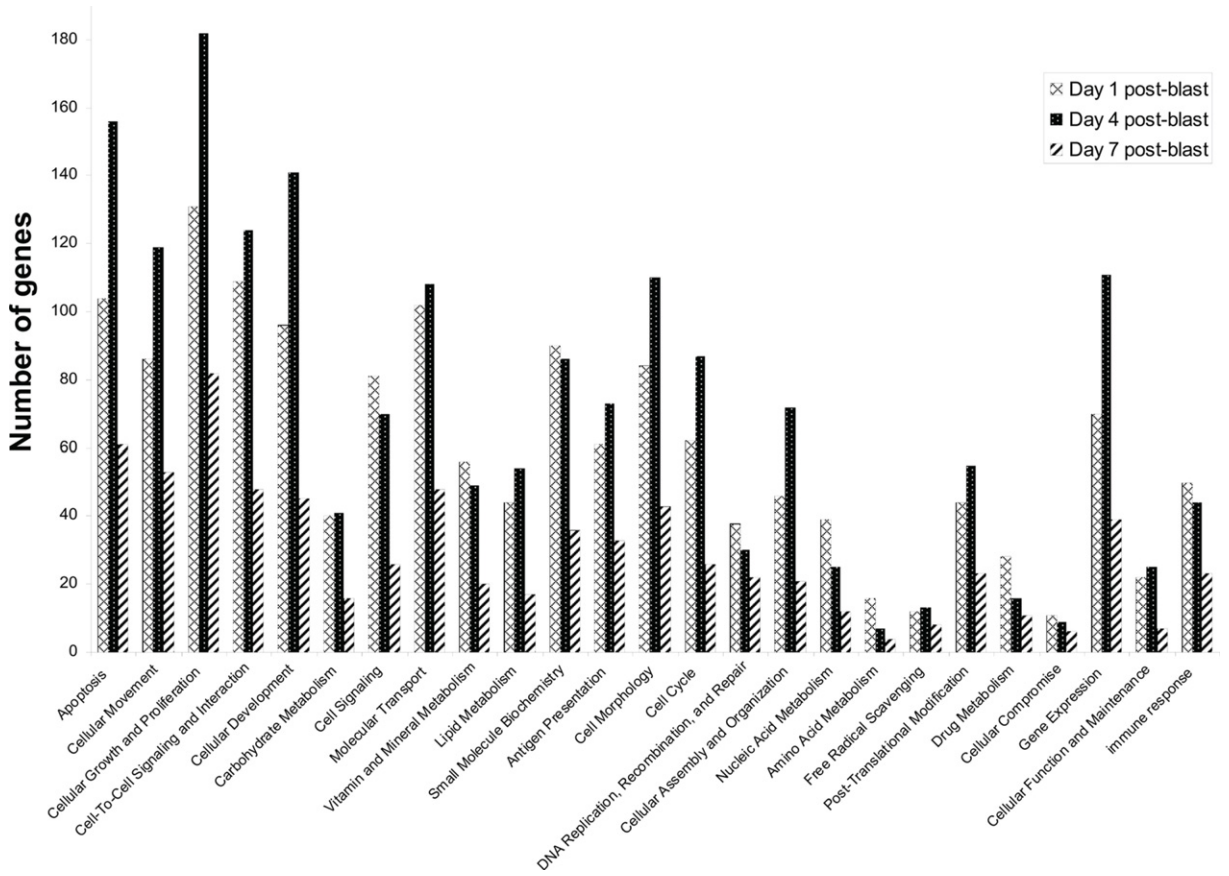

FIGURE 8 | Functional categorization of genes whose expression levels are altered by blast. Genes were categorized based on their biological functions. Probe sets with unknown functions were ignored in this analysis. A total of 1200 functionally characterized genes were identified in our microarray experiments using brain tissue from rats exposed to a BOP of 48.9 kPa. As each gene can have multiple functions, every gene may contribute more than once to the gene count shown here.

cortical changes is also consistent with our previous study investigating BOP of 20 kPa in rodents 1 day post-blast (Moochhala et al., 2004). Furthermore, the changes in vascular profiles post-blast suggest the occurrence of vasospasm which has also been reported as a feature of blast injury (Armonda et al., 2006). The alleviation in darkening at day 4 and day 7 post-blast and a rescue in vascular morphology at day 7 points to the existence of an acute transient ischemic cerebral environment that can recover with time after blast. Interestingly, cerebrovascular changes such as microvascular density and vasospasm have also been reported in studies in blast and impact TBI (Armonda et al., 2006; Park et al., 2010; Svetlov et al., 2010). However, it is unclear whether there is a complete recovery to the original state and whether the mild changes persist. Despite these cortical histopathological changes, TUNEL-staining was not observed in the white matter. This suggests that cortical gray matter and vasculature is affected by the blast wave in a differential manner from white matter.

Our study also showed that low BOP exposures at $<$110 kPa predominantly caused DNA fragmentation in the glial cells of the white matter with corresponding accumulation of APP probably due to axonal damage which is apparent at day 1 post-blast. The presence of white matter damage post-blast is becoming well-documented and the presence of this damage at low BOP levels suggest that primary injury from the shockwave can act to disrupt axonal transport and to cause cell death in oligodendrocytes and astrocytes which play important supportive functions in the white matter. This axonal pathology is further corroborated by findings of early increases in α-II spectrin, an axonal cytoskeletal protein, and sustained expression of NF200, an axonal neurofilament, in a mild BINT rodent model (Park et al., 2010).

Our study was only focused on the head-on exposure of the shockwave to the skull of the animal although it has been suggested that different orientations of the animal can have different pressure transmission, whether direct or reflected off the skull (Chavko et al., 2011), and the effects of different wave propagation on the CNS due to orientation remains to be investigated. Despite reports of blood–brain barrier permeability changes and inflammation post-blast (Bauman et al., 1997; Cernak et al., 2001a,b; Long et al., 2009; Cernak, 2010; Readnower et al., 2010; Risling et al., 2011), we did not find any changes in AQP-4 expression on S100B+ astrocytes (results not shown) as well as changes in Iba-1 immunoreactivity for microglia, the main inflammatory macrophages in the CNS, as well as systemic cytokines (results not shown). These negative findings may be explained by the lower

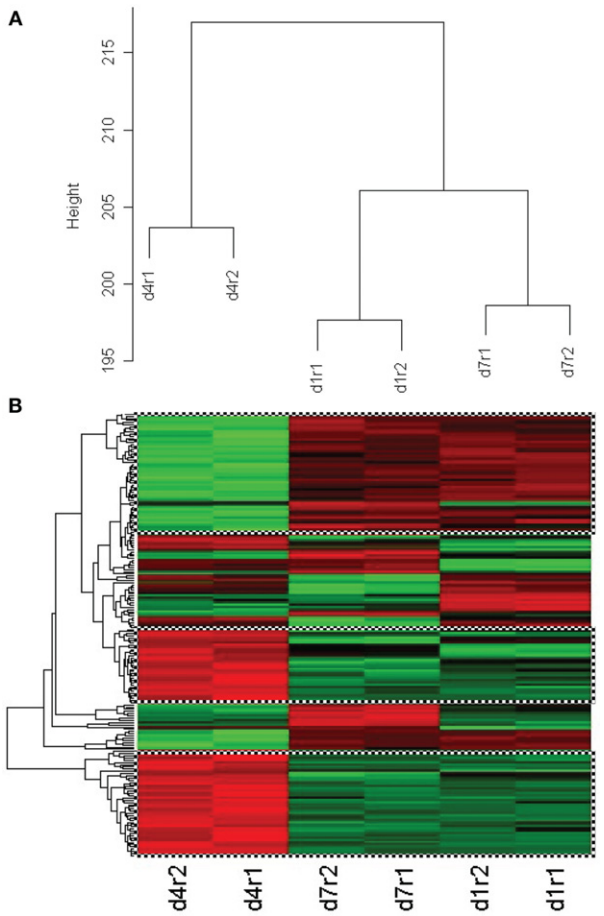

FIGURE 9 | (A) Cluster dendrogram of genes whose expression varied most from control between arrays for two replicates (r1, r2) of the same condition at day 4, day 1, and day 7 after low-intensity blast. Replicates are observed to cluster at the same level whilst clusters for day 4 appear different from day 1 and day 7. **(B)** Clustering of 203 genes that show similar behavior between replicates of day 4 (column 1), day 7 (column 2), and day 1 (column 3) after light intensity blast. Green color represents upregulation whilst red color represents downregulation from control. The topmost cluster (checked box) shows genes that are up-regulated at day 4 but down-regulated at day 1 and day 7, whilst the middle and bottom clusters (checked box) show the opposite trend.

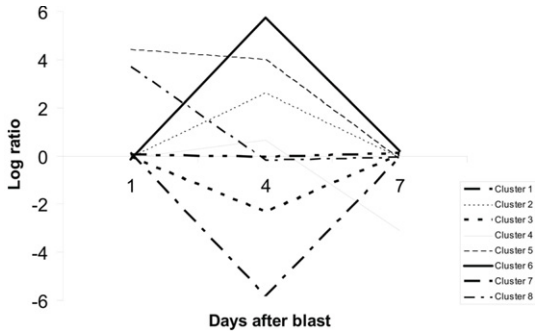

FIGURE 10 | Clustering of probe sets with significant time-course evolution. A total of 203 probe sets showing such evolution were identified, and grouped into eight clusters based on their time-evolution profiles. Probe sets in cluster 1 showed no major variation over time. They are consistently and weakly up-regulated or down-regulated across all time-points. Those in clusters 2 and 6 were up-regulated while those in clusters 3 and 7 were down-regulated at day 4. Probe sets in clusters 4, 5, and 8 were respectively down-regulated at day 7, up-regulated at day 1 and day 4, and up-regulated at day 1 only.

BOPs used in our study or that the animals were not observed for longer periods of time post-blast.

Given that the lethal threshold is lowest for blast lung injury than other organ systems, no significant mortality was expected in our blast model used here. This was confirmed by our findings (4.4% low BOP, 8.3% high BOP). Although two different BOPs were investigated in this study, both lie on the lower limit of the BOP range tested across many experimental blast studies. This may explain the non-significant differences in mortality, histopathological, and immunohistochemical changes between the low and high BOP. However, the blast set-up employed in this study can be used to establish a blast pressure-dependent mortality or morbidity response curve by placing animals at varying distances from the TNT source and by varying the amount of TNT.

Besides the low BOP, the animals were also exposed to a long positive duration of 14.5 and 18.2 ms in the low and high intensity settings respectively due to the distance that the subjects were placed away from the TNT explosive as opposed to other models of blast injury using compressed air, helium, oxyhydrogen or cyclotrimethylenetrinitramine (Reneer et al., 2011). The duration of the overpressure is thought to be of much significance in causing damage (de Candole, 1967) as the length of this positive duration would also affect the impulse at which the animals are subjected to. This longer positive overpressure duration also reflects the increasing use of thermobaric and other novel explosives in the modern war (Rafaels et al., 2010) and could have different mechanisms from other models investigating short positive overpressure durations (Cooper and Jonsson, 1997). However, it is unclear whether the long positive duration in our study had any impact on CNS injury and is a component of the blast wave that will require a more thorough examination and comparison against other blast models of the same BOP but of different duration.

Separately, the blast set-up and exposure in our study also provides a platform for scaling up to other animal species and to allow comparison between species on BINT thresholds and injury presentation. In a separate study investigating effects of sub-lethal BOP on non-human primates (NHPs) in the same blast set-up, increases in TUNEL-positive cells and APP immunoreactivity in white matter, together with the darkening of neurons were also observed in NHPs exposed to 80 kPa BOP as in our rodent study (unpublished). Further investigations with different small and large animal species using the same blast set-up but with additional strain gages in the body and brains will provide useful information in how blast waves of the same pressure transmit differently through skull and brain tissue properties between species.

Our microarray studies focused on brain samples from animals exposed at the lower BOP of 48.9 kPa vs. the controls. We found 676 genes whose expression profiles were significantly altered by blast. A common feature of trauma to the CNS involves

Table 1 | Genes whose expressions show significant time-course evolution after blast in the brains of rats exposed to a BOP of 48.9 kPa.

AR	FCER1A	ITGB5	PPIB	SH3GLB1
ARHGAP4	FLT1	KIF11	PRKACB	SLC40A1
CETN1	FOLR1	KLHL10	PRKCH	TFG
COQ6	GADAY 1	MMP11	PTTG1	TPM1
CRYAB	GHR	NFKBIA	PYY	UCP1
DNAJB11	GTF2F2	PARP1	RALBP1	VEGFA
F2RL3	HMGA1	PLG	RASA3	

Table 2 | List of genes whose expression levels are significantly altered in blast-exposed animals and which also show a time-course evolution pattern between day 1, day 4, and day 7 after blast.

FLT1	GADAY 1	KIF11	PARP1	PRKCH
FOLR1	HMGA1	NFKBIA	PRKACB	SLC40A1

Table 3 | Table of illustrative examples of how genes may be classified into non-target and target groups.

Type of gene	Gene expression ratios			
	Day 1	**Day 4**	**Day 7**	**Linear/ quadratic time trend**
Gene expression is not significantly altered at any time-point and shows no time-course evolution	1.1 ($p > 0.05$)	1.1 ($p > 0.05$)	1.1 ($p > 0.05$)	$p > 0.05$
Gene expression is significantly altered by blast in some or all time points, *but* no significant time-course evolution	1.1 ($p < 0.05$) 1.1 ($p < 0.05$)	1.1 ($p < 0.05$) 1.1 ($p > 0.05$)	1.1 ($p < 0.05$) 1.1 ($p > 0.05$)	$p > 0.05$
Gene expression is not significantly altered by blast *but* overall show significant time-course evolution	1.1 ($p > 0.05$)	1.2 ($p > 0.05$)	2 ($p > 0.05$)	$p < 0.05$
Gene expression is significantly altered at least one time-point, and shows time-course evolution (overlapping genes)	1.1 ($p < 0.05$) 1.1 ($p > 0.05$)	5 ($p < 0.05$) 5 ($p < 0.05$)	1.1 ($p < 0.05$) 1.1 ($p > 0.05$)	$p < 0.05$

p-values represent the statistical significance of comparisons between blast-exposed and control samples at each time-point.

pronounced changes in the expressions of cell proliferation and apoptotic genes (Byrnes and Faden, 2007). Accordingly, we found the highest number of blast-affected genes to belong to these functional groups, suggesting that our model was fundamentally sound in approach. We also observed that the number of genes affected in all functional groups decreased from day 4 to day 7 post-blast. Based on our H&E and TUNEL observations, this corresponds to a period during which there was almost complete recovery of the brain from blast injury, suggesting that recovery from blast injury was associated with a return to baseline of the expression of most genes. However, we did not observe a similar correspondence from day 1 to day 4 post-blast, which suggests that the injury-gene expression association may be time-dependent and differ between the immediate (<day 4) and the short (day 4 to day 7) terms after blast. The difference in the expression levels at day compared to day 1 and day 7 points toward a quadratic expression profile post-blast, i.e., cluster of genes up-regulated or down-regulated at day 4 as opposed to day 1 and day 7 expression. The lack of significance may be due to the small sample size used and the result should be followed up with more extensive sampling and further analysis.

In this study, we also took a multi-pronged approach using a strategy based upon the hypothesis that any gene whose expression is significantly altered by blast exposure is more likely than any other random gene to be critically involved in blast. Likewise, genes whose expression patterns show significant time evolution following blast have higher probability than others to be functionally relevant. Note that genes in the two groups may overlap or be distinct. Based upon our strategy, it follows then that genes in the overlapping group are the more likely genes to influence clinical outcome in blast injuries. The identities of functionally relevant genes will be especially important in the design of novel therapeutics or treatment approaches in blast victims. In terms of diagnostics, however, there could be an additional level of approach besides identifying specific genes. This would involve studying the overall pattern of functional changes in gene expressions based upon the functional categorization of genes whose expressions are modulated following blast exposure. Thus, our model enables the identification of four potential markers for diagnostics and/or treatment design as summarized in **Table 3**.

We separately found 34 genes to show a time-course evolution over time after blast exposure. Ten genes were common to both our analyses (i.e., blast exposure significantly modulated their expression profiles which also changed over time). It is unclear whether

these 10 identified genes and/or their protein products critically affects injury outcome in blast victims and its reliability to form a consistent "fingerprint" of blast-induced mild TBI. Considering the 10 overlapping genes in which the involvement of some such as FLT1 (involved in cell proliferation and angiogenesis) and PARP1 (participates in DNA repair) could be said to be instinctive, that of others such as HMGA1 (commonly found in prostate tumors and thought to be involved in transformation) may be less so. It is possible that genes such as HMGA1 are also involved in injury repair which have yet to be defined. Further studies would be required to determine if this is so. However, the potential for genes and "fingerprints" identified here to be used as biomarkers and therapeutic targets in blast research cannot be denied.

Overall, we have presented a primary blast injury rodent model exposed to low BOP levels in an open-field setting. Pulmonary injury was mild and delayed whilst neuronal and non-neuronal changes were immediate at day 1 and was found to be alleviated at day 4 and day 7 suggesting the ability of the brain to recover from mild BINT on the histopathological level although it is not clear whether there is complete recovery. Acute CNS changes after low BOP exposure suggest that cortical cerebrovascular changes and white matter changes are key features of acute low level BINT. In the first, ischemia may be a resultant effect whilst predominant white matter damage suggests vulnerability to primary blast injury. Furthermore, the concomitant increases in gene expression at day 1 and day 4 suggests a time-dependent injury response and recovery period. Of the 676 genes that were significantly altered, a framework was derived to narrow these to 10 according to the time-course evolution and functional relevance. Some of these up-regulated functional genes such as FLT1 and PARP1 point toward repair after injury and may contribute to the recovery in the histopathological changes seen at day 4 and day 7. Future work will center upon the validation of our model. This would involve efforts to determine if the "fingerprints" identified here are consistent and reproducible across different animal models of blast injury and in different tissues from blast-exposed animals. Most importantly, a time-course profile of the relationship between changes in gene expression patterns, conditions of blast exposure (e.g., BOP), histopathological changes, and blast injury severity should also be evaluated and for a longer time post-blast to observe for sustained changes or the development of secondary pathobiology.

ACKNOWLEDGMENTS

The authors express their gratitude to Leonard Heng, Karen Chong, Rick Tan, Chor Boon Ng from Defence Science and Technology Agency; Julie Yeo, Jian Wu and Melissa Teo from DSO National Laboratories.

REFERENCES

Agoston, D. V., Gyorgy, A., Eidelman, O., and Pollard, H. B. (2009). Proteomic biomarkers for blast neurotrauma: targeting cerebral edema, inflammation, and neuronal death cascades. *J. Neurotrauma* 26, 901–911.

Armonda, R. A., Bell, R. S., Vo, A. H., Ling, G., DeGraba, T. J., Crandall, B., Ecklund, J., and Campbell, W. W. (2006). Wartime traumatic cerebral vasospasm: recent review of combat casualties. *Neurosurgery* 59, 1215–1225; discussion 25.

Bauman, R. A., Elsayed, N., Petras, J. M., and Widholm, J. (1997). Exposure to sublethal blast overpressure reduces the food intake and exercise performance of rats. *Toxicology* 121, 65–79.

Biomarkers Definitions Working Group. (2001). Biomarkers and surrogate endpoints: preferred definitions and conceptual framework. *Clin. Pharmacol. Ther.* 69, 89–95.

Bowen, I. G., Fletcher, E. R., and Richmond, D. R. (1968). *Estimae of Man's Tolerance to the Direct Effects of air Blast*. Albuquerque: Lovelace Foundation for Medical Education and Research.

Byrnes, K. R., and Faden, A. I. (2007). Role of cell cycle proteins in CNS injury. *Neurochem. Res.* 32, 1799–1807.

Cernak, I. (2010). The importance of systemic response in the pathobiology of blast-induced neurotrauma. *Front. Neurol.* 1:151. doi: 10.3389/fneur.2010.00151

Cernak, I., and Noble-Haeusslein, L. J. (2010). Traumatic brain injury: an overview of pathobiology with emphasis on military populations. *J. Cereb. Blood Flow Metab.* 30, 255–266.

Cernak, I., Wang, Z., Jiang, J., Bian, X., and Savic, J. (2001a). Cognitive deficits following blast injury-induced neurotrauma: possible involvement of nitric oxide. *Brain Inj.* 15, 593–612.

Cernak, I., Wang, Z., Jiang, J., Bian, X., and Savic, J. (2001b). Ultrastructural and functional characteristics of blast injury-induced neurotrauma. *J. Trauma* 50, 695–706.

Chavko, M., Prusaczyk, W. K., and McCarron, R. M. (2006). Lung injury and recovery after exposure to blast overpressure. *J. Trauma* 61, 933–942.

Chavko, M., Watanabe, T., Adeeb, S., Lankasky, J., Ahlers, S. T., and McCarron, R. M. (2011). Relationship between orientation to a blast and pressure wave propagation inside the rat brain. *J. Neurosci. Methods* 195, 61–66.

Cooper, G., and Jonsson, A. (1997). *Protection Against Blast Injury*. New York: Butterworth-Heinemann.

de Candole, C. A. (1967). Blast injury. *Can. Med. Assoc. J.* 96, 207–214.

Defense and Veterans Brain Injury Center. (2010). *Department of Defense Numbers for Traumatic Brain Injury*. Accessed January 19, 2010, from http://www.dvbic.org/TBI-Numbers.aspx

DePalma, R. G., Burris, D. G., Champion, H. R., and Hodgson, M. J. (2005). Blast injuries. *N. Engl. J. Med.* 352, 1335–1342.

Elder, G. A., Mitsis, E. M., Ahlers, S. T., and Cristian, A. (2010). Blast-induced mild traumatic brain injury. *Psychiatr. Clin. North Am.* 33, 757–781.

Fleige, S., and Pfaffl, M. W. (2006). RNA integrity and the effect on the real-time qRT-PCR performance. *Mol. Aspects Med.* 27, 126–139.

Gorbunov, N. V., Asher, L. V., Ayyagari, V., and Atkins, J. L. (2006). Inflammatory leukocytes and iron turnover in experimental hemorrhagic lung trauma. *Exp. Mol. Pathol.* 80, 11–25.

Gorbunov, N. V., McFaul, S. J., Van Albert, S., Morrissette, C., Zaucha, G. M., and Nath, J. (2004). Assessment of inflammatory response and sequestration of blood iron transferrin complexes in a rat model of lung injury resulting from exposure to low-frequency shock waves. *Crit. Care Med.* 32, 1028–1034.

Kawai, K., Nitecka, L., Ruetzler, C. A., Nagashima, G., Joo, F., Mies, G., Nowak, T. S. Jr., Saito, N., Lohr, J. M., and Klatzo, I. (1992). Global cerebral ischemia associated with cardiac arrest in the rat: I. Dynamics of early neuronal changes. *J. Cereb. Blood Flow Metab.* 12, 238–249.

Kirkman, E., and Watts, S. (2011). Characterization of the response to primary blast injury. *Philos. Trans. R. Soc. Lond., B, Biol. Sci.* 366, 286–290.

Kochanek, P. M., Bauman, R. A., Long, J. B., Dixon, C. R., and Jenkins, L. W. (2009). A critical problem begging for new insight and new therapies. *J. Neurotrauma* 26, 813–814.

Lawson Terrorism Information Centre. (2009). Terrorism incidents and significant dates calendar. Accessed May 20, 2009, from http://www.terrorisminfo.mipt.org

Ling, G., Bandak, F., Armonda, R., Grant, G., and Ecklund, J. (2009). Explosive blast neurotrauma. *J. Neurotrauma* 26, 815–825.

Long, J. B., Bentley, T. L., Wessner, K. A., Cerone, C., Sweeney, S., and Bauman, R. A. (2009). Blast

overpressure in rats: recreating a battlefield injury in the laboratory. *J. Neurotrauma* 26, 827–840.

Moochhala, S. M., Md, S., Lu, J., Teng, C. H., and Greengrass, C. (2004). Neuroprotective role of aminoguanidine in behavioral changes after blast injury. *J. Trauma* 56, 393–403.

Park, E., Gottlieb, J. J., Cheung, B., Shek, P. N., and Baker, A. J. (2010). A model of low-level primary blast exposure results in cytoskeletal proteolysis and chronic functional impairment in the brain in the absence of lung barotrauma. *J. Neurotrauma.* 28, 343–357.

Phillips, Y. Y., Mundie, T. G., Yelverton, J. T., and Richmond, D. R. (1988). Cloth ballistic vest alters response to blast. *J. Trauma* 28, S149–S152.

Rafaels, K. A., Bass, C. R., Panzer, M. B., and Salzar, R. S. (2010). Pulmonary injury risk assessment for long-duration blasts: a meta-analysis. *J. Trauma* 69, 368–374.

Readnower, R. D., Chavko, M., Adeeb, S., Conroy, M. D., Pauly, J. R., McCarron, R. M., and Sullivan, P. G. (2010). Increase in blood–brain barrier permeability, oxidative stress, and activated microglia in a rat model of blast-induced traumatic brain injury. *J. Neurosci. Res.* 88, 3530–3539.

Reneer, D. V., Hisel, R. D., Hoffman, J. M., Kryscio, R. J., Lusk, B. T., and Geddes, J. W. (2011). A multi-mode shock tube for investigation of blast-induced traumatic brain injury. *J. Neurotrauma* 28, 95–104.

Risling, M., Plantman, S., Angeria, M., Rostami, E., Bellander, B. M., Kirkegaard, M., Arborelius, U., and Davidsson, J. (2011). Mechanisms of blast induced brain injuries, experimental studies in rats. *Neuroimage* 54(Suppl. 1), S89–S97.

Saljo, A., Svensson, B., Mayorga, M., Hamberger, A., and Bolouri, H. (2009). Low-level blasts raise intracranial pressure and impair cognitive function in rats. *J. Neurotrauma* 26, 1345–1352.

Stuhmiller, J. H. (1997). Biological response to blast overpressure: a summary of modeling. *Toxicology* 121, 91–103.

Svetlov, S. I., Larner, S. F., Kirk, D. R., Atkinson, J., Hayes, R. L., and Wang, K. K. (2009). Biomarkers of blast-induced neurotrauma: profiling molecular and cellular mechanisms of blast brain injury. *J. Neurotrauma* 26, 913–921.

Svetlov, S. I., Prima, V., Kirk, D. R., Gutierrez, H., Curley, K. C., Hayes, R. L., and Wang, K. K. (2010). Morphologic and biochemical characterization of brain injury in a model of controlled blast overpressure exposure. *J. Trauma* 69, 795–804.

Treadwell, I. (1989). Effects of blasts on the human body. *Nurs. RSA* 4, 32–36.

Conflict of Interest Statement: The authors declare that the research was conducted in the absence of any commercial or financial relationships that could be construed as a potential conflict of interest.

Received: 16 February 2011; accepted: 15 March 2011; published online: 04 April 2011.

Citation: Pun PBL, Kan EM, Salim A, Li Z, Ng KC, Moochhala SM, Ling E-A, Tan MH and Lu J (2011) Low level primary blast injury in rodent brain. Front. Neur. ***2****:19. doi: 10.3389/fneur.2011.00019*

This article was submitted to Frontiers in Neurotrauma, a specialty of Frontiers in Neurology.

APPENDIX

Table A1 | Genes whose expressions are significantly altered by blast in the brains of rats exposed to a BOP of 48.9 kPa.

ABCA2	CAPZA3	DLK1	GPX3	KIF11	OMP	RAMP2	ST3GAL5
ABCC3	CASR	DNAJA3	GRIN1	KIF1C	ONECUT1	RAP1B	STAG3
ABCG2	CATSPER2	DNAJA4	GRINL1A	KIF2C	OPRL1	RAPGEF1	STC1
ABRA	CBARA1	DNAJB4	GRK1	KIT	OPRM1	RASDAY 1	STK38
ACCN2	CBR1	DNDAY 1	GRM5	KLF15	ORC2L	RASSF2	STX1A
ACHE	CCL2	DNM1L	GRPR	KLF5	OXT	RASSF5	SUFU
ACSL1	CCL3	DNMT3B	GSPT1	KLF6	P2RX2	RB1	SULT1B1
ACTB	CCL4	DPP4	GUCY1A3	KNG1	P2RY2	RBM17	SYNJ1
ADAM10	CCNB2	DPYSL5	GUSB	KRT20	PA2G4	RBP3	SYT1
ADAM9	CCNDAY 1	DR1	GZMA	LHB	PAH	RCOR2	TAAR1
ADCY6	CCNG1	DRD2	GZMB	LITAF	PAQR3	REG3G	TAC1
ADIPOR1	CCR4	DRDAY 4	H1F0	LPIN1	PARG	REST	TACC2
ADM	CCR5	DSP	HAVCR2	LPL	PARP1	RFX3	TAF5L
ADORA2A	CCT6A	DUSP5	HCLS1	LRPAP1	PARVA	RGS10	TAPBP
ADRA2B	CDAY 14	DUSP9	HCRT	LRRK2	PAX4	RGS19	TAX1BP1
AES	CD2	EBF1	HERPUDAY 1	LTB4R	PCDHAC2	RHOA	TBCE
AGRP	CD2AP	ECEL1	HES3	LTBP1	PCNA	RHOH	TBX3
AGT	CD320	ECM1	HINT1	LYPD3	PDCDAY 4	RIPK2	TCEA1
AK2	CD36	EDNRA	HIST1H1T	LZTS1	PDCD6IP	RLN1	TCIRG1
AK3L1	CD38	EGF	HIVEP1	MAEA	PDCL	RNF10	TDG
AKAP13	CD3G	EGFR	HMGA1	MAL	PDE4B	RNF14	TEAD2
AKAP4	CDAY 44	EGR1	HMMR	MAP1B	PDHA2	ROBO4	TERF1
ALB	CDC25A	EGR2	HNF4A	MAP3K10	PDLIM2	RPN2	TGFB1
ALDH2	CDC25B	EHDAY 1	HOMER1	MAPK1	PDYN	RPS15A	TGFB1I1
ALDOA	CDC2L5	EIF4B	HOMER2	MAPK14	PDZK1IP1	RRM1	TGM1
ALG5	CDC42BPB	ELA2	HOXA5	MAPK8	PELO	RTKN	TH
AMDAY 1	CDCA2	ENAH	HOXC6	MAPK9	PELP1	S100A8	THAP1
AMHR2	CDH16	ENTPDAY 1	HP	MAPRE1	PEMT	SAA4	THBD
ANTXR1	CDH22	EP400	HPS1	MAT1A	PHGDH	SATB1	THEM4
ANXA2	CDK10	ERBB2	HPSE	MATK	PIK3C3	SBDS	THPO
AOC3	CDKN1A	ESM1	HSDAY 11B2	MATR3	PIR	SCAMP2	TIAM1
APBA1	CDKN1B	ETS2	HSPA1A	MBL2	PKDAY 1	SCARB1	TK1
APCS	CDKN1C	ETV6	HSPA8	MCF2L	PKNOX1	SCN10A	TLE4
APH1A	CDX2	F12	HSPBP1	MFN2	PLA2G4A	SCN4B	TMOD2
APH1B	CEBPE	F2R	HSPDAY 1	MGAT2	PLAT	SCN9A	TMOD3
APLN	CES1	F2RL2	HTR1B	MINA	PLCG1	SCNN1B	TNF
APOC2	CFH	F5	HTR1D	MLH1	PLD2	SEMA3D	TNFRSF1A
AQP4	CFTR	FABP7	HTR2A	MLL	PLEKHF1	SENP2	TNNI2
AREG	CGA	FADS1	HTR2B	MST1	PLXNA3	SERINC3	TNNT1
ARF6	CHI3L1	FAIM	IBSP	MSX2	PMCH	SERPINB2	TNP2
ARHGEF7	CHMP5	FAU	ICAM1	MTA1	PNLIP	SERPINI1	TNR
ARL11	CHRM4	FCGR3A	ID2	MTPN	POLA1	SFRP2	TOB2
ARL2BP	CHRNA10	FGF13	ID3	MXD3	PON2	SFRS2	TOP2A
ASAH2	CIT	FGF4	IFNG	MXI1	POU2F1	SFTPC	TPH1
ATF3	CITED2	FGFR1	IGF1R	MYCL1	POU2F2	SGTB	TPM3
ATG7	CKAP5	FGG	IGFBP1	MYO5A	POU3F1	SH3BP5	TPST1
ATP1A1	CLDN11	FGL2	IGFBP4	NAP1L1	PPAP2C	SHC1	TPT1
ATP2A3	CLU	FGR	IGHMBP2	NCR3	PPEF1	SHH	TRADD
ATP2C2	CNR1	FHIT	IKBKG	NDFIP1	PPIL2	SHMT1	TRIB3

(Continued)

Table A1 | Continued

ABCA2	CAPZA3	DLK1	GPX3	KIF11	OMP	RAMP2	ST3GAL5
ATP6V1C1	CNTF	FKRP	IL12RB2	NDN	PPM1J	SIP1	TRIM32
ATP6V1F	CNTN3	FLT1	IL13	NDRG1	PPP1R1B	SIX3	TRIM63
ATP7B	CNTN4	FN1	IL13RA1	NEFL	PPP2R2B	SLC16A2	TRPC3
AVP	COL16A1	FOLR1	IL13RA2	NEO1	PPP2R3A	SLC16A4	TRPM6
AZGP1	COL2A1	FOXM1	IL18RAP	NEU1	PPP2R5B	SLC17A3	TRPM7
AZI2	COMT	FSHR	IL1A	NEU3	PPYR1	SLC18A2	TRPV1
B4GALNT1	CORO1B	FTH1	IL1B	NEUROG3	PRDX5	SLC1A3	TTN
BACE1	CREB1	FUBP1	IL22RA2	NFIA	PRIM1	SLC22A2	TTR
BAD	CRKRS	FUT4	IL4	NFKBIA	PRKAB1	SLC24A3	TUBB2C
BAK1	CRTC2	FXYD5	IL8RB	NFKBIB	PRKACB	SLC25A10	TWIST1
BCAN	CRY1	GABBR1	IMPACT	NGFR	PRKCD	SLC25A14	UBC
BCAP31	CSDA	GADAY 1	IMPDH2	NIDAY 1	PRKCH	SLC25A27	UBE2D2
BCL2	CSF3	GADDAY 45GIP1	INHBB	NINJ2	PRKCZ	SLC2A4	UBE2D3
BCL2L10	CSNK1A1	GALNS	INSIG2	NKX3-1	PRLR	SLC34A1	UBTF
BDKRB2	CSNK1G1	GAP43	INSRR	NLGN3	PRM1	SLC36A2	UCHL1
BID	CSPG4	GATA1	IPPK	NMT1	PRPF19	SLC37A4	UCP2
BMP4	CSPG5	GATA6	IRS1	NNT	PRPF8	SLC40A1	UGCG
BNIP3	CTH	GATAD2A	ITGA1	NOS3	PSMB2	SLC6A3	USH2A
BTRC	CTNNB1	GFAP	ITGA2	NOVA1	PSMD2	SLC6A4	USP14
BYSL	CTSB	GGCX	ITGA4	NPDC1	PSMDAY 4	SLC6A5	VNN1
C3AR1	CUGBP1	GHRL	ITGA5	NPEPPS	PSMD9	SLC7A2	VPS4B
C9	CXCL11	GLI1	ITGAL	NPFF	PTGDS	SLC7A5	VTCN1
CA3	CYB5R4	GLIPR1	ITGB2	NPR1	PTGER4	SLC8A1	WEE1
CABP1	CYP1A1	GLP2R	ITPKB	NPY	PTGES	SLC9A1	WNT2
CACNA1B	CYP2E1	GLTSCR2	JAG1	NR1D2	PTGS2	SMAD3	XRCC1
CACNB2	CYR61	GNA14	JAM2	NR1I2	PTHLH	SMO	YBX1
CALCA	DAB2	GNAL	KCNA1	NR2C2	PTK2	SNAPC2	ZBTB10
CALCRL	DBH	GNB2	KCNA6	NR2F2	PTMS	SNCA	ZDHHC2
CALDAY 1	DCC	GNB5	KCNC1	NR4A3	PTPN2	SOD3	ZHX2
CAMK2A	DCLK1	GNG2	KCNC3	NR5A2	PTPN3	SP2	ZIC1
CAMK4	DDR1	GNG4	KCNH1	NRTN	PTPRV	SPG7	ZMYNDAY 11
CAMKK1	DEAF1	GNG5	KCNJ11	NRXN2	PTS	SPP1	ZP2
CAMKK2	DGAT1	GNRH1	KCNMA1	NTRK1	QPRT	SQSTM1	
CAMP	DGAT2	GPC1	KCNMB1	NTRK2	RABGGTA	SREBF2	
CANT1	DKC1	GPR44	KCNN3	NUP98	RAG1	SST	
CAPN2	DLC1	GPS1	KIDINS220	OMG	RALGDS	ST18	

Table A2 | Biological functions of genes in each cluster (clusters 1–4, 6, and 7; except clusters 5 and 8 which do not have genes with information).

Category	Molecules
CLUSTER 1 FUNCTIONS	
Amino acid metabolism	GADAY 1
Antigen presentation	PLG, NFKBIA, VEGFA, ITGB5
Carbohydrate metabolism	GPI, F2RL3
Cell cycle	PLG, CETN1, NFKBIA, VEGFA, KIF11, CLIP1, GPI, CRYAB, GHR
Apoptosis	LPAR1, NFKBIA, VEGFA
Cell morphology	PLG, LPAR1, NFKBIA, VEGFA, CLIP1, ITGB5, GPI, GHR
Cell signaling	PLG, LPAR1, VEGFA, FCER1A, PYY, ARHGAP4, PPIB, F2RL3
Cell-to-cell signaling and interaction	PLG, VEGFA, PRKACB, PYY, ITGB5, GPI, GHR
Cellular assembly and organization	CETN1, LPAR1, SH3GLB1, VEGFA, FCER1A, ITGB5, F2RL3, CRYAB, PLG, KIF11, CLIP1, ARHGAP4, GPI, GHR
Cellular compromise	PLG, VEGFA, KIF11, GPI, GHR
Cellular development	PLG, NFKBIA, VEGFA, FCER1A, GHR
Cellular function and maintenance	PLG, NFKBIA, KIF11, PYY, ITGB5, ARHGAP4, GPI, F2RL3, GHR
Cellular growth and proliferation	LPAR1, VEGFA, C19ORF10, ITGB5, PYY,CRYAB, PLG, TFG, NFKBIA, KIF11, GADAY 1, GPI, WNK1, GHR, SKAP2
Cellular movement	PLG, LPAR1, NFKBIA, VEGFA, PYY, ITGB5, GADAY 1, GPI, PPIB
DNA replication, recombination, and repair	VEGFA, PPIB, WNK1, GHR
Drug metabolism	VEGFA, PPIB, GHR
Energy production	PLG
Gene expression	NFKBIA, VEGFA, GHR
Lipid metabolism	NFKBIA, VEGFA, PYY, GHR
Molecular transport	PLG, LPAR1, NFKBIA, VEGFA, FCER1A, PYY, GPI, PPIB, F2RL3, GHR
Nucleic acid metabolism	PLG, VEGFA, PPIB, WNK1, GHR
Post-translational modification	VEGFA, GADAY 1
Protein folding	VEGFA
Protein synthesis	PLG, VEGFA, PYY
Protein trafficking	NFKBIA
Small molecule biochemistry	PLG, NFKBIA, VEGFA, PYY, GADAY 1, GPI, PPIB, F2RL3, WNK1, GHR
Vitamin and mineral metabolism	PLG, LPAR1, VEGFA, FCER1A, PYY, PPIB, F2RL3
Immune response	PLG, VEGFA, FCER1A, ITGB5
CLUSTER 2 FUNCTIONS	
Amino acid metabolism	HIPK2, PRKCH, PPM1D
Antigen presentation	PPM1D
Carbohydrate metabolism	UCP1
Cell cycle	HIPK2, PRKCH, PPM1D
Apoptosis	HIPK2
Cell morphology	PRKCH, UCP1
Cell signaling	HIPK2
Cellular assembly and organization	HIPK2
Cellular compromise	HIPK2, UCP1
Cellular development	HIPK2, PRKCH
Cellular function and maintenance	UCP1, PPM1D
Cellular growth and proliferation	HIPK2, PRKCH, UCP1
DNA replication, recombination, and repair	PRKCH, UCP1
Drug metabolism	UCP1
Energy production	UCP1
Free radical scavenging	UCP1
Gene expression	PRKCH, UCP1
Lipid metabolism	UCP1
Molecular transport	PRKCH, UCP1
Nucleic acid metabolism	UCP1
Post-translational modification	HIPK2, PRKCH, PPM1D
Small molecule biochemistry	HIPK2, PRKCH, UCP1, PPM1D
Immnue response	PPM1D
CLUSTER 3 FUNCTIONS	
Amino acid metabolism	PARP1
Antigen presentation	FLT1, IRF8
Carbohydrate metabolism	PARP1, FLT1, RALBP1
Cell cycle	DDB1, PARP1, FLT1, TPM1, HMGA1
Apoptosis	PARP1, NDRG1, FLT1, RALBP1, TPM1, COQ6, HMGA1, IRF8
Cell morphology	FLT1, CDAY 151, RALBP1, TPM1, HMGA1
Cell signaling	FLT1
Cell-to-cell signaling and interaction	FLT1, CDAY 151, IRF8
Cellular assembly and organization	PARP1, FLT1, TPM1
Cellular compromise	KLHL10, PARP1, NDRG1, FLT1, TPM1, HMGA1
Cellular development	KLHL10, PARP1, NDRG1, FLT1, VSX2, CDAY 151, RALBP1, TPM1, HMGA1, RASA3, IRF8
Cellular function and maintenance	PARP1, FLT1, TPM1, IRF8
Cellular growth and proliferation	NDRG1, FLT1, VSX2, RALBP1, TPM1, HMGA1, IRF8
Cellular movement	PARP1, FLT1, CDAY 151, RALBP1, TPM1

(Continued)

Table A2 | Continued

Category	Molecules
Cellular response to therapeutics	PARP1
DNA replication, recombination, and repair	DDB1, PARP1, HMGA1
Drug metabolism	PARP1, RALBP1
Energy production	PARP1
Gene expression	DDB1, PARP1, GTF2F2, VSX2, RALBP1, HMGA1, IRF8
Lipid metabolism	FDPS, FLT1
Molecular transport	PARP1, RALBP1
Nucleic acid metabolism	DDB1, PARP1, RALBP1
Post-translational modification	PARP1
RNA post-transcriptional modification	PARP1
Small molecule biochemistry	DDB1, FDPS, PARP1, FLT1, RALBP1
Immune response	FLT1, IRF8
CLUSTER 4 FUNCTIONS	
Amino acid metabolism	FOLR1
Antigen presentation	MMP11
Carbohydrate metabolism	INPP5K
Apoptosis	MMP11
Cellular assembly and organization	INPP5K
Cellular function and maintenance	FOLR1, SLC40A1
Cellular growth and proliferation	MMP11, FOLR1
DNA replication, recombination, and repair	FOLR1
Drug metabolism	FOLR1
Lipid metabolism	INPP5K
Molecular transport	INPP5K, FOLR1, SLC40A1
Nucleic acid metabolism	FOLR1
Post-translational modification	MMP11
Protein synthesis	FOLR1
Protein trafficking	FOLR1
Small molecule biochemistry	INPP5K, FOLR1, SLC40A1
Vitamin and mineral metabolism	FOLR1
Immune response	MMP11
CLUSTER 6 FUNCTIONS	
Cellular assembly and organization	EIF4A1
Gene expression	EIF4A1
Protein synthesis	EIF4A1
RNA post-transcriptional modification	EIF4A1
RNA trafficking	EIF4A1
CLUSTER 7 FUNCTIONS	
Carbohydrate metabolism	PTTG1
Cell cycle	AR, PTTG1
Apoptosis	AR, PTTG1
Cell morphology	AR, PTTG1
Cell signaling	AR
Cell-to-cell signaling and interaction	AR
Cellular assembly and organization	AR, PTTG1
Cellular compromise	AR, PTTG1
Cellular development	AR, PTTG1
Cellular function and maintenance	AR
Cellular growth and proliferation	AR, PTTG1
Cellular movement	AR
DNA replication, recombination, and repair	AR, PTTG1
Drug metabolism	AR, PTTG1
Gene expression	AR, PTTG1
Lipid metabolism	AR, PTTG1
Molecular transport	AR, PTTG1
Nucleic acid metabolism	AR
RNA damage and repair	DNAJB11
RNA post-transcriptional modification	DNAJB11
Small molecule biochemistry	AR, PTTG1
Immune response	AR, PTTG1

frontiers in NEUROLOGY

ORIGINAL RESEARCH ARTICLE
published: 07 March 2011
doi: 10.3389/fneur.2011.00012

Stress and traumatic brain injury: a behavioral, proteomics, and histological study

Sook-Kyung C. Kwon[1†], Erzsebet Kovesdi[1†], Andrea B. Gyorgy[1], Daniel Wingo[1], Alaa Kamnaksh[1], John Walker[1], Joseph B. Long[2] and Denes V. Agoston[1]*

[1] *Department of Anatomy, Physiology and Genetics, School of Medicine, Uniformed Services University, Bethesda, MD, USA*
[2] *Division of Military Casualty Research, Walter Reed Army Institute of Research, Silver Spring, MD, USA*

Edited by:
Marten Risling, Karolinska Institutet, Sweden

Reviewed by:
Linda Noble, University of California at San Francisco, USA
Robert Vink, University of Adelaide, Australia

****Correspondence:***
Denes V. Agoston, Department of Anatomy, Physiology and Genetics, School of Medicine, Uniformed Services University, 4301 Jones Bridge Road, Bethesda, MD 20814, USA.
e-mail: vagoston@usuhs.edu

[†]Sook-Kyung C. Kwon and Erzsebet Kovesdi have contributed equally.

Psychological stress and traumatic brain injury (TBI) can both result in lasting neurobehavioral abnormalities. Post-traumatic stress disorder and blast induced TBI (bTBI) have become the most significant health issues in current military conflicts. Importantly, military bTBI virtually never occurs without stress. In this experiment, we assessed anxiety and spatial memory of rats at different time points after repeated exposure to stress alone or in combination with a single mild blast. At 2 months after injury or sham we analyzed the serum, prefrontal cortex (PFC), and hippocampus (HC) of all animals by proteomics and immunohistochemistry. Stressed sham animals showed an early increase in anxiety but no memory impairment at any measured time point. They had elevated levels of serum corticosterone (CORT) and hippocampal IL-6 but no other cellular or protein changes. Stressed injured animals had increased anxiety that returned to normal at 2 months and significant spatial memory impairment that lasted up to 2 months. They had elevated serum levels of CORT, CK-BB, NF-H, NSE, GFAP, and VEGF. Moreover, all of the measured protein markers were elevated in the HC and the PFC; rats had an increased number of TUNEL-positive cells in the HC and elevated GFAP and Iba1 immunoreactivity in the HC and the PFC. Our findings suggest that exposure to repeated stress alone causes a transient increase in anxiety and no significant memory impairment or cellular and molecular changes. In contrast, repeated stress and blast results in lasting behavioral, molecular, and cellular abnormalities characterized by memory impairment, neuronal and glial cell loss, inflammation, and gliosis. These findings may have implications in the development of diagnostic and therapeutic measures for conditions caused by stress or a combination of stress and bTBI.

Keywords: stress, blast traumatic brain injury, anxiety, memory, gliosis, inflammation, neurogenesis

INTRODUCTION

Traumatic brain injury (TBI) is one of the leading causes of death and chronic disability worldwide (Bruns and Hauser, 2003; Tagliaferri et al., 2006). Blast induced TBI (bTBI) caused by explosive devices is especially frequent in recent conflicts in Iraq and in Afghanistan (Warden and French, 2005; Taber et al., 2006; Warden, 2006). Epidemiological studies have shown that mild bTBI (mbTBI) can result in chronic neurobehavioral changes such as increased anxiety and memory impairment (Ryan and Warden, 2003; Okie, 2005). Importantly, virtually no bTBI occurs on the battlefield without the exposure to psychological stress. Exposure to stress alone (i.e., traumatic and/or life-threatening events) without physical injury can lead to a chronic condition called post-traumatic stress disorder (PTSD) in some but not all affected individuals (Breslau and Kessler, 2001). PTSD is especially frequent among soldiers; about 14% of soldiers suffer from PTSD-like symptoms compared to 4% of the US adult population (Keane et al., 2006; Richardson et al., 2010).

Although bTBI shares some of the clinical features of the closed head and the penetrating TBIs, bTBI appears to be a fundamentally different form of neurotrauma (Ling et al., 2009). Several factors are responsible for the uniqueness of bTBI; explosive blast rapidly dissipates very high levels of energy in the form of supersonic pressure waves (Mayorga, 1997; Okie, 2005). Within the brain parenchyma, the high-energy high-velocity blast waves can cause substantial damage to blood vessels, neuronal and glial cell bodies and their processes (Kaur et al., 1997; Cernak et al., 2001). Clinical hallmarks of severe bTBI include an unusually early onset (hours after injury) and rapid development of diffuse malignant cerebral edema, and delayed (10–14 days post-injury) vasoconstriction (Armonda et al., 2006; Ling et al., 2009; Ling and Ecklund, 2011). Given that blast almost always affects the whole body, subclinical thoracic or abdominal injuries can also contribute to the pathophysiology of bTBI (Cernak et al., 2010). It has been thought that the secondary injury process in bTBI includes vascular changes, neuroinflammation, and gliosis (Kaur et al., 1997; Mayorga, 1997; Cernak et al., 2001; Taber et al., 2006).

Exposure to mild blast poses especially difficult challenges. Even though there are no life-threatening injuries in mbTBI and soldiers do not lose consciousness, 6–9 months later many soldiers develop neurobehavioral abnormalities that include memory impairment, anxiety, and mood disorders (Belanger et al., 2007; Brenner et al., 2009). These symptoms indicate damage to the hippocampus (HC) and the prefrontal cortex (PFC), brain structures that are also indicated as the neuroanatomical substrates of PTSD (Jaffee and Meyer, 2009). Stress is a constant factor on the battlefield

(Warden et al., 1997; Brenner et al., 2009); soldiers are repeatedly exposed to various life-threatening situations and to the visual and audible cues of blasts without necessarily suffering from any visible physical injury.

In order to better understand the long-term consequences of stress with and without the exposure to blast, we used a rodent model of stress and mbTBI and assessed the behavior of animals at various time points after sham or injury and analyzed their sera and brains for cellular and molecular changes. Due to our experimental setup, we were unable to determine the effect of blast injury alone. During our pilot studies we learned that handling and transporting animals (associated with the exposure to blast) resulted in a significant amount of stress as indicated by substantially elevated serum CORT levels of animals.

MATERIALS AND METHODS

ANIMALS, HOUSING CONDITIONS, AND EXPERIMENTAL SCHEDULE

Sprague-Dawley male rats (245–265 g; Charles River Laboratories, Wilmington, MA, USA) were housed in cages with free access to food and water in a reverse 12/12 h light/dark cycle. The experimental schedule is depicted in **Figure 1**. After 7 days of acclimation and handling in our animal facility, control animals (C) were housed two per cage; stressed sham injured (SS) and stressed injured animals (SI) were housed individually. All animals were handled according to protocol approved by the Institutional Animal Care and Use Committee (IACUC) at the Uniformed Services University of the Health Sciences. All behavioral tests were conducted during animals' dark cycle.

INJURY

On the day of the exposure, animals in the SS and SI groups were transported from USU (Bethesda, MD, USA) to Walter Reed Army Institute of Research (Silver Spring, MD, USA) for injury. Blast TBI was generated using a compression-driven shock tube as described earlier (Long et al., 2009). Before injury, rats in the SI group were anesthetized with 4% isoflurane (Forane, Baxter Healthcare Corporation, Deerfield, IL, USA), placed in an animal holder in a transverse prone position and then transferred to the shock tube where they were exposed to whole body blast overpressure (20.6 ± 3 psi). Immediately after exposure, the duration of apnea was measured and rats were moved back to their home cages. Animals in the SS group received the same amount of anesthesia and underwent the same procedure but were not exposed to blast overpressure. However, SS as well as SI animals were exposed to the sounds of the blast, which is likely an additional stressor. Following exposures (or sham), animals were transported back to USU.

CHRONIC STRESS

Rats in the SI and SS groups were exposed to a combination of predator and unpredictable stressors for 1 week prior to and 1 week after the first behavioral testing session (**Figure 1**). Unpredictable stress is a face-valid model of human stress that has been shown to reliably elevate stress hormone levels in rodents (Fride et al., 1986; Weinstock et al., 1992).

A combination of fox urine and unpredictable stress (Campbell et al., 2003) was performed with modifications (Berger and Grunberg, in preparation). Rats were exposed to fox urine for 10 min/day (Red fox urine, Buck Stop Lure Company, Stanton, MI, USA) as a predator stress, and loud noises and sudden cage movements at irregular times as an unpredictable stressor. During the stress routine, rats were moved to the animal facility's procedure room. Each rat was transferred to a clean empty cage with a cotton ball containing 15 ml of fox urine; each day the position of the cotton ball was changed. Within the 10 min stress period, rats were exposed to loud noises and irregular cage movement. After stress, the rats were immediately moved back to their home cages and transferred back to the animal housing room. Control rats were neither transferred to the procedure room nor exposed to any of the stressors.

SCHEDULE OF BEHAVIORAL TESTS

Before chronic stress and injury all animals underwent a baseline open field (OF) measurement (**Figure 1**). Horizontal activity results were used to create three groups with no statistical significance among them. After the first stress phase and blast (or sham) injury, rats underwent a series of behavioral evaluations. In each behavioral session OF was conducted first to ascertain whether animals had any motor problems, which can confound other behavioral tests. One day after OF, elevated plus maze (EPM) was performed to measure anxiety levels. Barnes maze (BM) was performed last to measure spatial learning and memory. The three behavioral assessments were performed on separate days starting at 24 h, 1, and 2 months after injury (**Figure 1**).

Open field

The OF test is an indicator of potential motor deficits but can also reflect fluctuations in anxiety levels based on changes in exploratory behavior (Heath and Vink, 1999). Several studies have shown this test to reliably measure anxiety and depression in rodents (von Horsten et al., 1998) including after TBI (Vink et al., 2003). OF tests were performed using Omnitech Electronics' Digiscan infrared photocell system (test box model RXYZCM, Omnitech Electronics, Columbus, OH; Elliott and Grunberg, 2005). The OF system is a

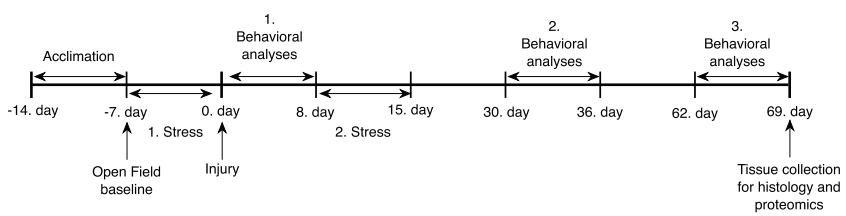

FIGURE 1 | Outline of the experimental schedule.

40 × 40 × 30 (*L* × *W* × *H*) cm clear Plexiglas arena with a perforated lid. During the 60 min testing period, we measured horizontal activity (locomotor activity), time spent in the margins (anxiety), and in the center. Data were automatically gathered and transmitted to a computer via an Omnitech Model DCM-BBU analyzer.

Elevated plus maze

The EPM is a widely used, ethologically relevant test that assesses anxiety states in rodents (Carobrez and Bertoglio, 2005; Salzberg et al., 2007; Walf and Frye, 2007). The maze is an elevated structure (1 m above ground) consisting of four intersecting arms. The arms of the maze are 50 cm long and 10 cm wide; the closed arms have walls on three sides that are 40 cm high while the open arms have none. The lighting in the middle of the maze was set at 90 lux. On testing days rats were placed one by one in the center of the maze facing one of the open arms; each animal was allowed to explore freely for 5 min while its movement was video-tracked. Total distance traveled, number of entries made, and time spent (duration) in each arm was recorded using ANY-maze 4.2 Software (Stoelting Company, Wood Dale, IL, USA).

Barnes maze

Barnes maze was used to assess spatial learning and memory (Barnes, 1979; Maegele et al., 2005; Doll et al., 2009). BM represents a widely used, validated, and less stressful alternative to the commonly used water maze test (Harrison et al., 2009). The maze is a circular platform (1.2 m in diameter) with 18 evenly spaced holes around the periphery. One of the holes is the entrance to a darkened escape box that is not visible from the surface of the board. Each rat was tested twice per day for six consecutive days to find the escape box (only day 1 of the first BM session had three trials). In each trial, latency to locate and enter the escape box was measured (ANY-maze 4.2 Software, Stoelting Company, Wood Dale, IL, USA).

During the first (teaching) trial of the first BM session, all animals were trained to locate the escape chamber. Each animal was placed in the escape box and covered for 30 s. The escape box was then removed with the animal inside and moved to the center of the maze. The rat was removed from the box and allowed to explore the maze for a few seconds, after which the rat was returned to its home cage. No latency times were recorded for the teaching trials. The escape box and the maze were cleaned with 30% ethanol solution between each trial. In the second trial the same rat was placed under a start box in the center of the maze for 30 s; the start box was then removed and the rat was allowed to explore freely to find the escape chamber. Training sessions ended after the animal had entered the escape box or when a pre-determined time (240 s) had elapsed. If the animal had not found the escape box during the given time period, it was placed in the escape box for 1 min at the end of the trial.

TISSUE COLLECTION AND PROCESSING

On day 67 post-injury (or sham; **Figure 1**) all animals were deeply anesthetized with isoflurane until a tail pinch produced no reflex movement. Anesthesia was maintained using a mask/nose cone attached to the anesthetic vaporizer, and blood was collected (1.5 ml) from a tail vein. For proteomics and ELISA assays, rats were decapitated under deep anesthesia. Brains were immediately removed and placed on ice. The PFC and HC were dissected, frozen, and stored at −80°C. For histology, rats were transcardially perfused with cold phosphate-buffered saline (PBS) followed by 4% buffered paraformaldehyde solution under deep isoflurane anesthesia. Following overnight post-fixation in 4% buffered paraformaldehyde solution brains were consecutively immersed in cold 15 and 30% sucrose solutions in 1× PBS for cryoprotection and then frozen on dry ice. Frozen brains were sectioned coronally at a 20-μm thickness using a cryostat (Cryocut 1800; Leica Microsystems, Bannockburn, IL, USA) and sections were kept at −80°C until use.

PROTEOMICS

Preparation of samples

Sample preparation, printing, scanning, and data analysis were performed as described later in detail (Gyorgy et al., 2010). Flash-frozen tissues were briefly pulverized in liquid nitrogen; 200 mg of the frozen powder was transferred into 1 ml of T-per lysis buffer (Thermo Fisher, Waltham, MA, USA) with protease and phosphatase inhibitors (Thermo Fisher) and then sonicated. Samples were centrifuged for 15 min at 4°C; the supernatants were aliquoted and stored at −80°C. Protein concentrations were measured by using a BCA assay (Thermo Fisher). Blood samples were promptly centrifuged after removal at 10,000×*g* for 15 min at 4°C; the supernatants were aliquoted, flash-frozen, and stored at −80°C. Tissue samples were diluted in print buffer (10% glycerol, 0.05% SDS, 50 mM DTT in 1× TBS) to a final protein concentration of 1 mg/ml, while serum samples were diluted 1:10. Samples were then subjected to an 11-point serial 1:2 dilution and transferred into Genetix 384-well plates (X7022, Fisher Scientific, Pittsburgh, PA, USA) as described (Gyorgy et al., 2010). Plates were transferred into an Aushon 2470 Arrayer (Aushon Biosystems, Billerica, MA, USA) and samples were printed on ONCYTE Avid (tissue samples) or ONCYTE Nova (serum samples) single-pad nitrocellulose coated glass slides (Grace Bio-Labs, Bend, OR, USA).

Printing parameters

The Aushon Arrayer was programmed to use 16 pins (4 × 4 pattern). Each sample was printed in 12 dilutions (12 rows) and in triplicate (3 columns), resulting in a block of 3 × 12 dots per sample. The Spot Diameter was set to 250 nm with a spacing of 500 nm between dots on the *x*-axis and 375 nm on the *y*-axis. Wash time was set at 2 s without delays. The printer was programmed for a single deposition per dot for printing serum and tissue extracts.

Immunochemical detection

Primary antibodies were diluted to 10× the optimal Western analysis concentration in antibody incubation buffer (0.1% bovine serum albumin (BSA), protease inhibitors (EDTA-free Halt protease and phosphatase inhibitor cocktail, Thermo Fisher, Waltham, MA, USA; 1× TBS, 0.5% Tween 20) as described (Gyorgy et al., 2010). Primary antibodies were used in the following dilutions: VEGF 1:100 (Abcam ab-53465), s100b 1:50 (Abcam ab-41548), GFAP 1:500 (Abcam ab-7260), Tau-protein 1:20 (Santa Cruz sc-1995), CK-BB 1:20 (Santa Cruz sc-15157), NSE 1: 100 (Abcam, Cat# ab53025), NF-H 1:20 (Sigma N4142). Slides were incubated with the primary antibody solution overnight at 4°C covered by a cover slip (Nunc* mSeries LifterSlips, Fisher Scientific, Pittsburg, PA).

The following day slides were washed and then incubated with an Alexa Fluor® 635 goat anti-mouse (Cat# A-31574), goat anti-rabbit (Cat# A-31576), or rabbit anti-goat IgG (H + L; Cat# A-21086) secondary antibodies from Invitrogen at 1:6000 dilution in antibody incubation buffer for 1 h at room temperature (RT). After washing and drying, the fluorescent signals were measured in a Scan Array Express HT microarray scanner (Perkin Elmer, Waltham, MA, USA) using a 633 nm wavelength laser and a 647 nm filter. Data from the scanned images were imported into a Microsoft Excel-based bioinformatics program developed in house for analysis (Gyorgy et al., 2010).

Data analysis and bioinformatics

The program calculates total net intensity after local background subtraction for each spot. The intensity data from the dilution series of each sample are then plotted against dilution on a log–log graph. The linear regression of the log–log data was calculated after the removal of flagged data, which include signal to noise ratios of less than 2, spot intensities in the saturation range or noise range, or high variability between duplicate spots (>10–15%). The total amount of antigen is determined by the *y*-axis intercept (Gyorgy et al., 2010).

CORTICOSTERONE ASSAY

Serum corticosterone (CORT) levels were measured using Cayman's Corticosterone EIA Kit according to the manufacturer's instructions (Cayman Chemical, Ann Arbor, MI, USA). Each sample was diluted 1:500 and measured in triplicate.

IL-6 AND INFγ ASSAYS

INFγ and IL-6 levels were measured from brain tissues using the rat Interferon gamma ELISA and the Rat IL-6 ELISA kits (both are from Thermo Fisher, Waltham, MA, USA). The IL-6 ELISA kit required a 1:5 dilution using the supplied dilution buffer in order to avoid saturation in the wells. After the dilution of brain samples, the assay was performed according to the manufacturer's instructions.

HISTOLOGY

Immunohistochemistry

Every first and tenth coronal section containing either the PFC, the dorsal HC (DHC), or the ventral HC (VHC) were mounted on positively charged glass slides with two sections per slide. Three slides per animal, containing sections with identical *z*-axes, were selected per brain region for each immunostaining. Slides containing the frozen sections were equilibrated at RT and hydrated with 1× PBS for 30 min. Antigen retrieval was performed by incubating the sections in 10 mM citrate buffer (pH 6.0) at 80°C for 30 min followed by cooling down to RT. After rehydration with 1× PBS, sections were permeabilized with 0.5% Triton X-100 in PBS for 1 h and blocked in 1× PBS containing 5% normal goat serum (NGS), 5% BSA, 0.1% sodium azide, and 0.5% Triton X-100 for 1 h. The same solution minus NGS was used to dilute primary antibodies. The following primary antibodies were used: mouse anti-GFAP (Millipore, Temecula, CA, USA; 1:400) rabbit anti-doublecortin (DCX; Cell Signaling Technology, Beverly, MA, USA; 1:1000), and goat anti-Iba1 (Abcam, Cambridge, MA, USA; 1:1000). Sections were incubated with the primary antibodies overnight at 4°C. After washing with 1× PBS, they were incubated with appropriate secondary antibodies (Alexa Fluor 555 goat anti-mouse IgG, 488 goat anti-rabbit IgG, or 488 donkey anti-goat IgG (Invitrogen, Carlsbad, CA) was applied for 1 h at RT 1:100), Hoechst 33342 (Molecular Probes, Eugene, OR, USA) at 1 μg/ml was applied for 2 min, sections washed and coverslipped using anti-fading media (Vectashield, Vector Laboratories, Burlingame, CA, USA).

TUNEL assay

Apoptotic cell death marked by DNA fragmentation was determined using a TUNEL *in situ* cell death detection kit, POD (Roche, Indianapolis, IN, USA) according to the manufacturer's instructions. Sections were hydrated with PBS and endogenous peroxidase activity was quenched by 3% H_2O_2 in methanol for 10 min at RT. Sections were permeabilized by 0.1 M sodium citrate buffer (pH 6.0) at 70°C for 30 min followed by PBST for 30 min at RT. TUNEL reaction was performed for 1 h at 37°C and the signal was converted using converter-POD. TUNEL-positive cells were visualized by DAB substrate. Dark brown TUNEL-positive cells were counted from four sections per animal.

Histological data acquisition

Histological sections were visualized in an Olympus IX-71 microscope using the appropriate filters and images were collected using a SPOT digital camera (Diagnostic Instruments Inc., Sterling Heights, MI, USA). The collected images were colored using TIFFany Caffeine Software.

STATISTICAL ANALYSIS AND COMPARISON OF DATA

Behavioral test results were analyzed with ANOVA and Tukey *post hoc* tests. Differences with a p-value of <0.05 were considered significant. Statistical analyses were performed using GraphPad InStat software. Proteomics and ELISA results were analyzed with Student's t-test. Data are reported as the average ± standard error of the mean. Proteomics data results were followed up with a one-way ANOVA. For each of our numerical measurements, we determined statistical significance among experimental groups by ($p < 0.05$ depicted by one star; $p < 0.01$ by two and $p < 0.001$ by three).

RESULTS

BEHAVIORAL EFFECTS

Locomotor activity

Twenty-four hours after exposure to blast (or sham), rats in the SI group showed a decrease in horizontal activity compared to rats in the SS and C groups (**Figure 2A**) but the difference was statistically insignificant. Animals in the SI group spent significantly more time in the periphery and significantly less time in the center (**Figures 2B,C**) compared to C and SS animals. SS animals showed no significant difference compared to C animals.

At 1 and 2 months after injury (or sham), we found no significant differences in any of the measured parameters between animals in all experimental groups (**Figures 2A–C**).

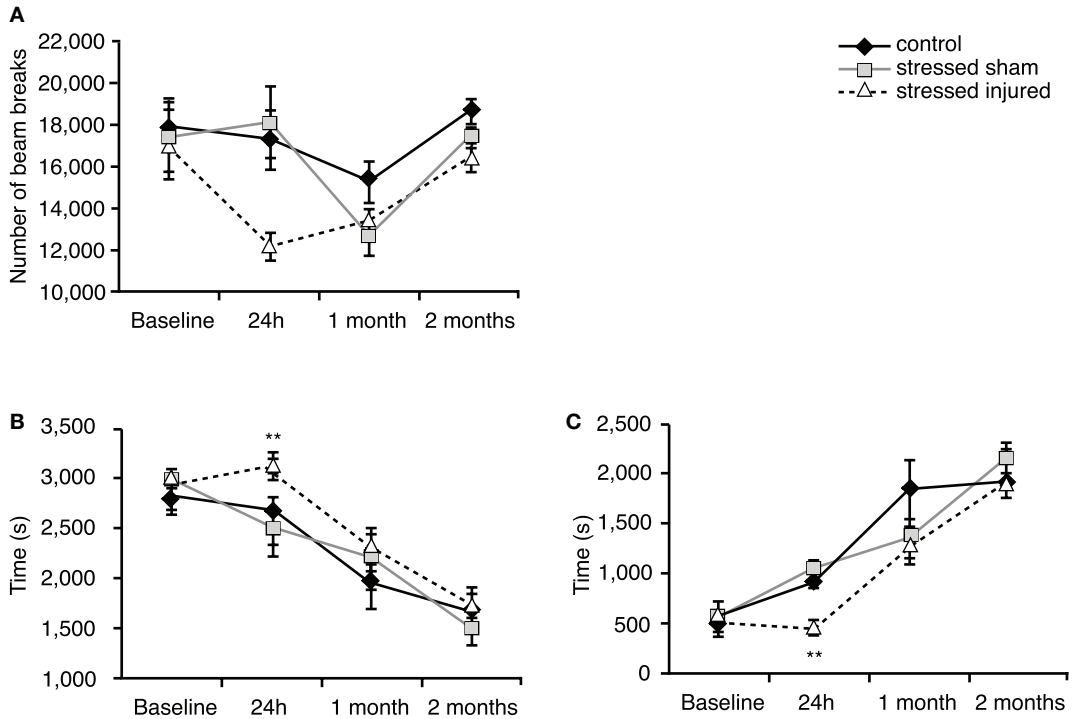

FIGURE 2 | Locomotor activity of animals in the various experimental groups. Open field was used to assess **(A)** horizontal activity (number of beam breaks), **(B)** time spent in the peripheral zone (seconds) and **(C)** time spent in the central zone (seconds). $^{**}p < 0.01$ SI compared to C rats. Data are presented in mean ± SEM. (C: $n = 4$; SS: $n = 6$; and SI: $n = 6$).

Anxiety

Forty-eight hours after blast (or sham) injury, we found that SI rats traveled significantly shorter distances than C animals (**Figure 3A**). Animals in the SS group also traveled shorter distances but the differences were not statistically significant. Animals in both SS and SI groups spent significantly less time in the open arms and more time in the closed arms (**Figures 3B,C**).

At 1 month both SS and SI groups traveled shorter distances compared to C animals (**Figure 3A**). Among the stressed groups only SI animals exhibited raised anxiety by spending less time in the open arms and more time in the closed arms (**Figures 3B,C**). Animals in the SS group did not show significant differences in the time spent in the open arms vs. closed arms compared to the controls.

Two months after blast or sham injury, all animals performed similarly with no significant differences in total distance traveled or time spent in the open and the closed arms.

Spatial learning and memory

During the first BM session, performed between days 3 and 8 post-blast (or sham; see **Figure 1** for schedule) we observed significant differences in the performance of animals on the last testing day only (day 8). SS rats needed significantly more time to find the escape box compared to C rats. SI rats spent less time finding the escape box than SS rats, but more time compared to C rats; the difference was not statistically significant (**Figure 4A**).

During the second BM session, performed between days 32 and 36 post-blast (or sham), we found no difference in the latency times of animals in the SS and the C groups. However, SI animals required significantly longer times to find the escape box on day 33 through 36 (**Figure 4B**).

The last BM session was performed between days 64 and 69 post-injury (or sham). Again, the performance of SS animals was not statistically different from animal in the control group (**Figure 4C**). In contrast, SI rats performed very poorly in the BM on day 64. These animals had increased latency times similar to those measured during the first BM session (**Figures 4C,D**) showing significant memory problems on days 65 and 68, indicating lasting memory impairment caused by blast.

EFFECTS ON PROTEIN MARKERS

Serum changes

At the end of the last behavioral session (69 days post-injury or sham), we obtained serum from each animal and compared NF-H, CK-BB, GFAP, VEGF, and NSE levels across all experimental groups. We found that serum levels of all protein markers listed above were significantly elevated at this late time point in SI animals (**Figure 5**). As expected, serum CORT levels were significantly elevated in both SS and SI groups. However, the difference in serum CORT levels between the two groups was statistically insignificant.

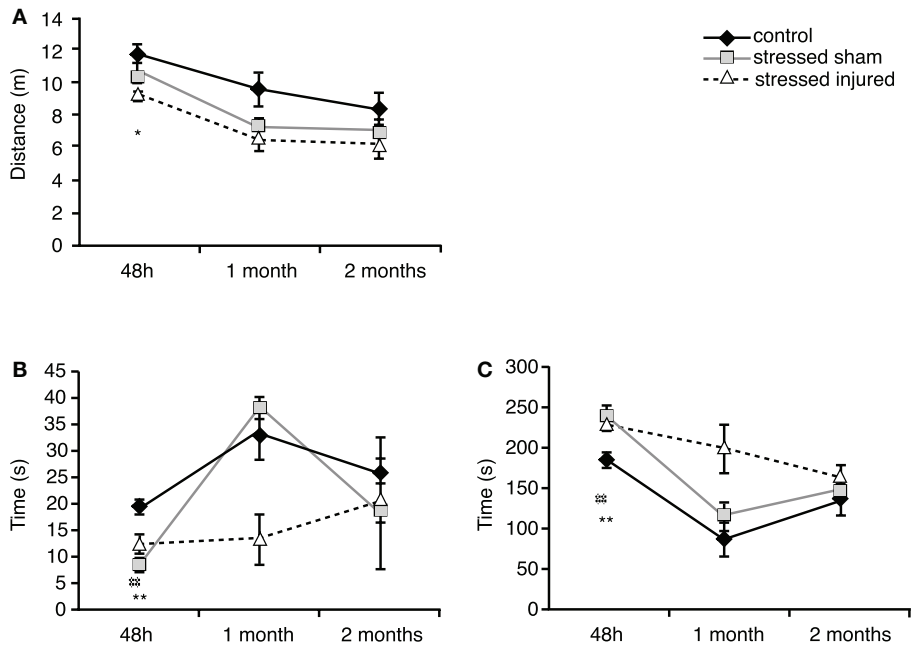

FIGURE 3 | Anxiety of animals in the various experimental groups. Elevated plus maze was used to assess **(A)** total distance traveled (meter), **(B)** time spent in the open arms (seconds) and **(C)** time spent in the closed arms (seconds). $*p < 0.05$ and $**p < 0.01$ SI compared to C rats, $^{\#\#}p < 0.01$ SS to C rats. Data are presented in mean ± SEM. (C: $n = 4$; SS: $n = 6$; and SI: $n = 6$).

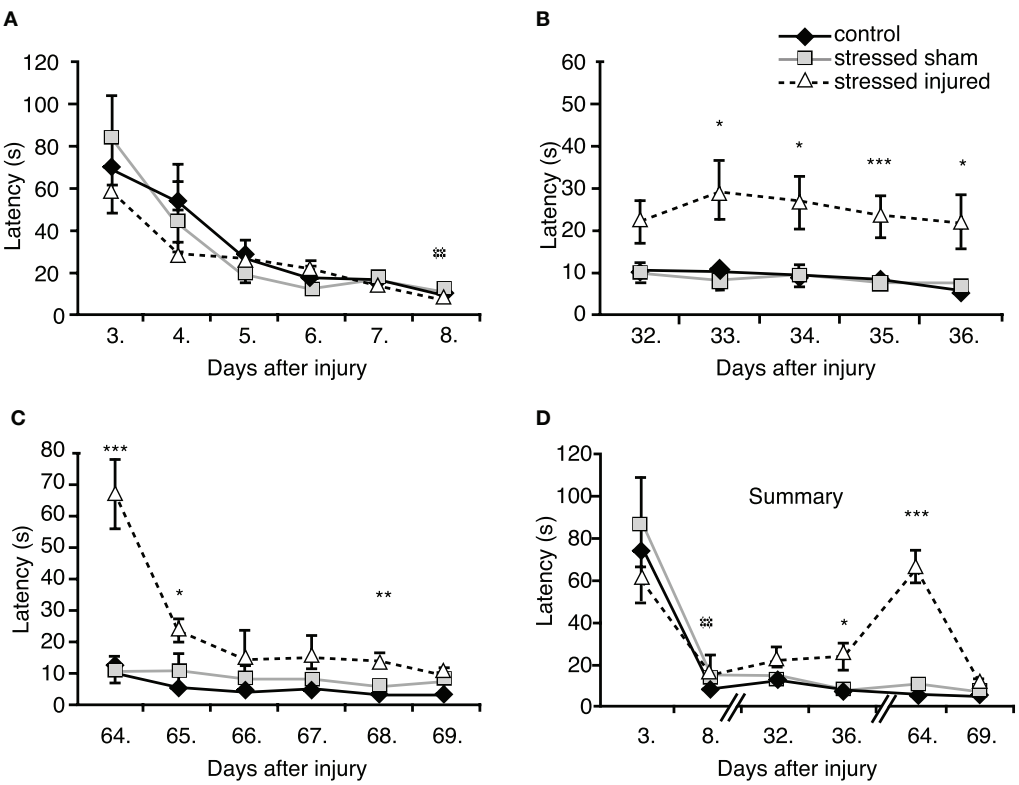

FIGURE 4 | Spatial learning and memory of animals in the various experimental groups. Barnes maze was used to determine latencies to find the escape box **(A)** 3–8 days post-injury, **(B)** 32–36 days post-injury, **(C)** 64–69 days post-injury. **(D)** Summarized time-line of latencies of the three sets of Barnes maze test. $*p < 0.05$, $**p < 0.01$, and $***p < 0.01$ SI compared to C rats, $^{\#\#}p < 0.01$ SS to C rats. Data are presented in mean ± SEM (C: $n = 4$; SS: $n = 6$; and SI: $n = 6$).

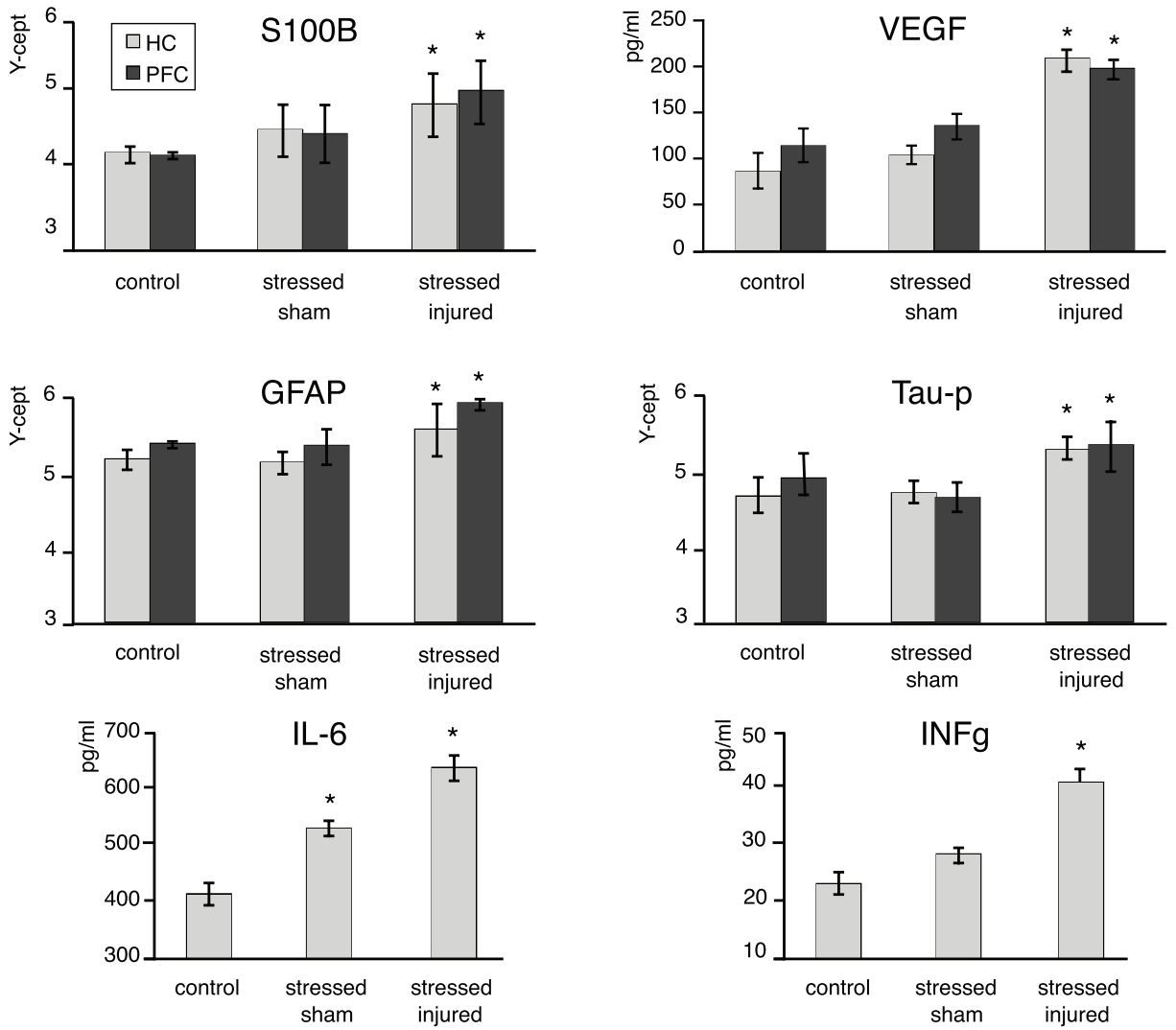

FIGURE 5 | Protein markers in the PFC and the HC of animals in the various experimental groups. Tissue extracts were prepared from dissected PFC and HC regions of C, SS, and SI rat brains. The tissue levels of the selected marker proteins were assayed using either RPPM or ELISA. The *y*-axis intercept (Y-cept) and pg/ml (IL-6 and IFNg) indicate the measured protein levels. $*p < 0.05$, $**p < 0.01$ compared to C rats, error bars are ± SEM. (C: $n = 2$; SS: $n = 3$; and SI: $n = 3$).

Changes in the brain

At the end of the last behavioral session we analyzed changes in the expression of S100β, VEGF, GFAP, Tau-protein, IL-6, and INFγ in the PFC and the HC of all animals. We found significantly elevated levels of all markers (except IL-6) in the PFC and the HC of SI animals only (**Figure 6**). Interestingly, we found that IL-6 levels were significantly increased in the HC of SS animals while no such effect of stress alone was seen on hippocampal INFγ levels.

CELLULAR CHANGES

Astrogliosis

To identify the cellular changes underlying the observed behavioral abnormalities, we analyzed the HC and the PFC for GFAP expression at 2 months post-blast (or sham). Consistent with our proteomics data, we found that exposure to stress alone (SS) had no observable effect on GFAP expression in the PFC or the HC (**Figure 7**). However, in SI animals we detected a noticeable increase in GFAP immunoreactivity in the PFC and the VHC.

Importantly, an increase in GFAP+ cells displaying a stellar morphology characteristic of reactive astrocytes was observed in the PFC and the VHC of SI animals (**Figure 7C**, and insert).

Inflammation

Similar to the gliotic response above, exposure to stress alone had no significant effect on Iba1 immunoreactivity in the PFC or the HC (**Figure 8**). While increased Iba1 immunoreactivity was observed in the SI group, there was a noticeable increase in Iba1 immunoreactivity (albeit to a lesser degree) in the PFC of SS animals. No significant differences were observed in Iba1 immunoreactivity in the DHC of any of the experimental groups.

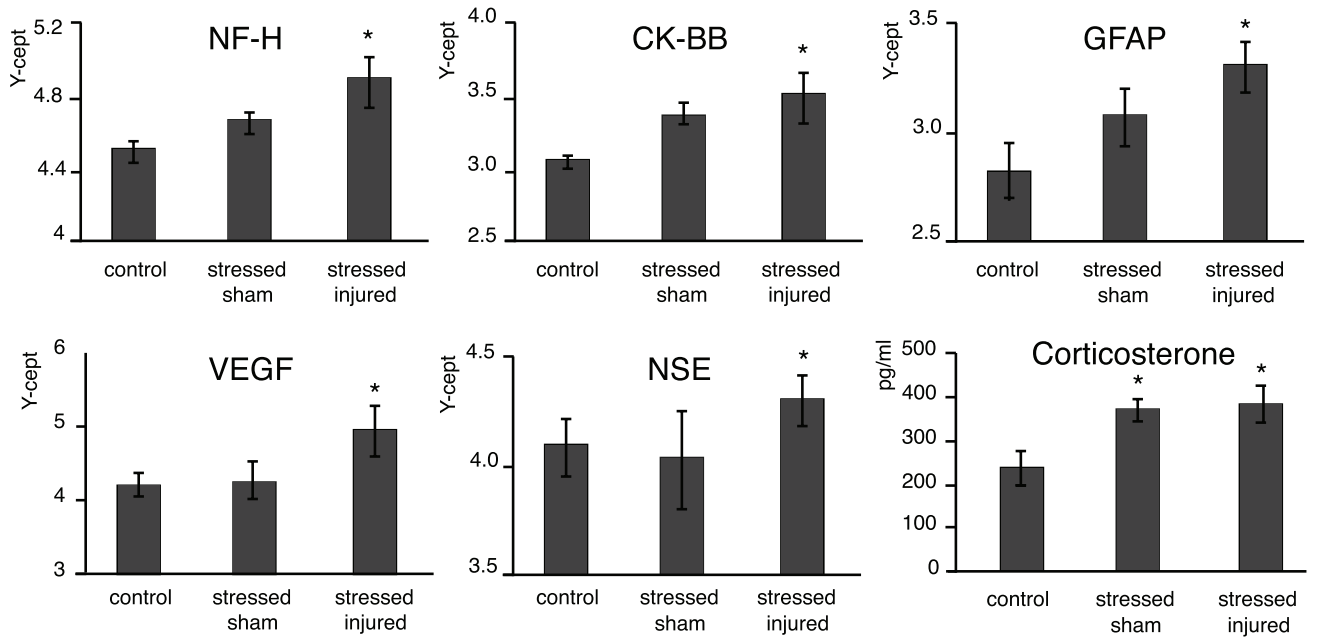

FIGURE 6 | Serum markers of animals in the various experimental groups. Blood was drawn and sera were prepared from the C, SS, and SI rats. The levels of the selected marker proteins were assayed using either RPPM or ELISA, and corticosterone levels were assayed using ELISA. The *y*-axis intercept (Y-cept) and pg/ml (corticosterone) indicate the measured protein levels. $*p < 0.05$, $**p < 0.01$ compared to C rats, error bars are ± SEM (C: $n = 4$; SS: $n = 6$; and SI: $n = 6$).

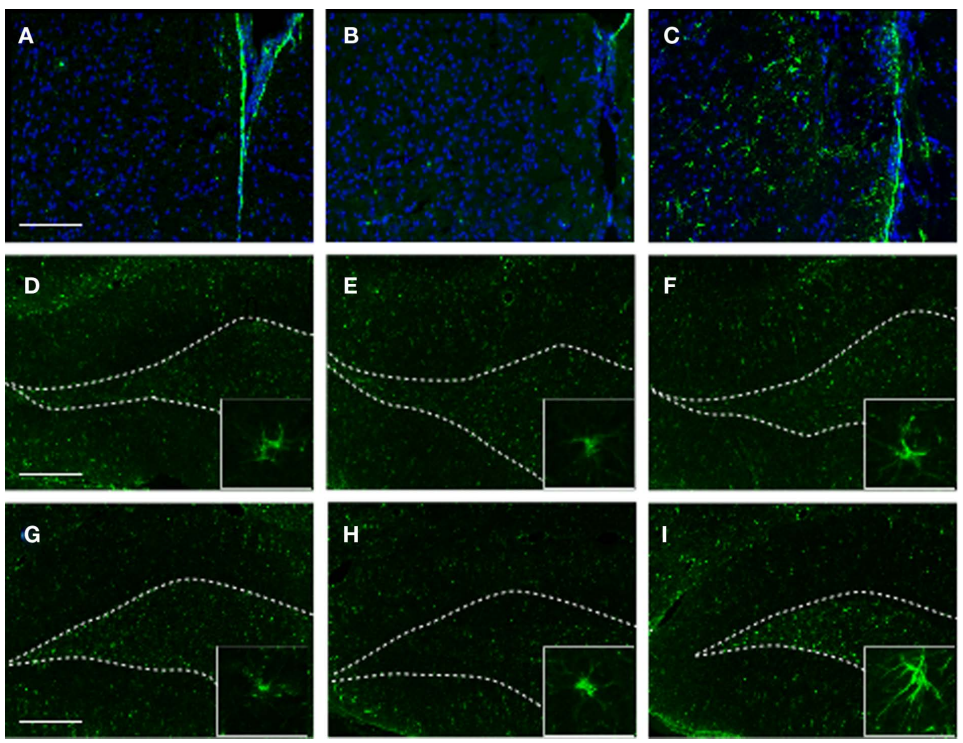

FIGURE 7 | GFAP immunoreactivity in selected brain regions of animals in the various experimental groups. Frozen coronal sections containing the PFC, DHC, and VHC were cut and processed for immunohistochemistry using a GFAP antibody. Sections were stained with Hoechst 33342 to mark cellular nuclei. PFC of **(A)** C, **(B)** SS, and **(C)** SI rats; DHC of **(D)** C, **(E)** SS, and **(F)** SI rats; VHC of **(G)** C, **(H)** SS, and **(I)** SI rats. Inlays display morphological extension of stellar-like processes in VHC of SI rats. White-dotted line outlines DG layer of hippocampus.

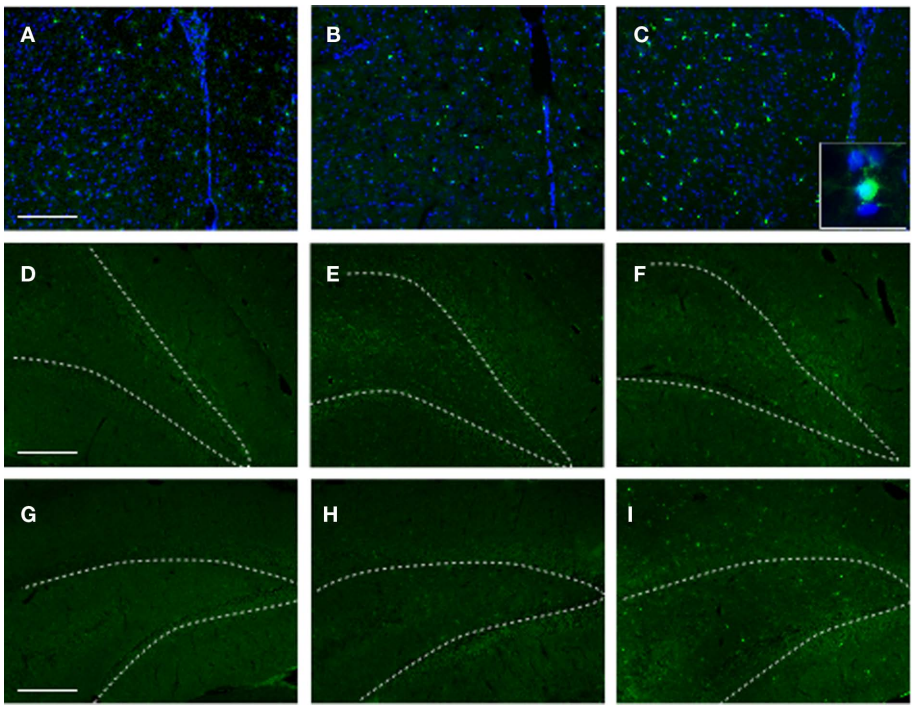

FIGURE 8 | Iba1 immunoreactivity in selected brain regions of animals in the various experimental groups. Frozen coronal sections containing the PFC, DHC, and VHC were cut and processed for immunohistochemistry using an Iba1 antibody. Sections were stained with Hoechst 33342 to mark cellular nuclei. PFC of **(A)** C, **(B)** SS, and **(C)** SI rats; DHC of **(D)** C, **(E)** SS, and **(F)** SI rats; VHC of **(G)** C, **(H)** SS, and **(I)** SI rats. White-dotted line outlines DG layer of hippocampus.

Apoptotic cell death

TUNEL histology was used to determine the extent of apoptotic cell death in the PFC, VHC, and DHC across all experimental groups. The number of TUNEL-positive cells was significantly increased in the hilus of the VHC and the DHC of the SI group (**Figure 9**). Interestingly, there was no increase in the number of TUNEL-positive cells in the PFC of animals in any of the experimental groups (**Figure A1** in Appendix). The exposure to stress alone resulted in no increase in the number of TUNEL-positive cells in any of the SS brain regions investigated.

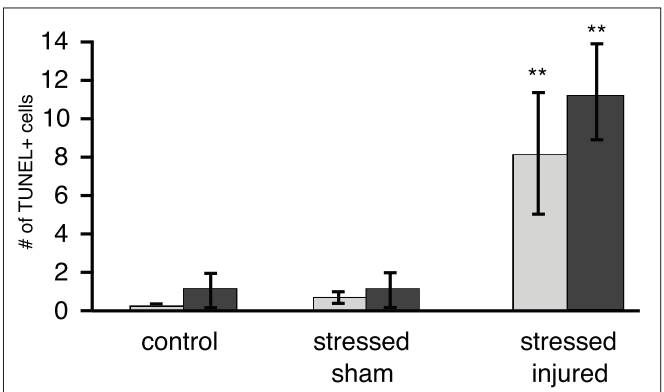

FIGURE 9 | TUNEL-positive cells in selected brain regions of animals in the various experimental groups. Frozen coronal sections containing the hilus of the DHC and VHC of C, SS, and SI rats were cut and processed for TUNEL histology. The number of TUNEL-positive cells were counted and expressed as positive cells per unit area ± SEM. $*p < 0.05$ and $**p < 0.01$ compared to C rats.

Neurogenesis

To gain insight into the potential effects of stress (with or without injury) on hippocampal *de novo* neurogenesis, we performed DCX immunohistochemistry. We observed a noticeable increase in DCX expression in the VHC of SI animals; DCX immunoreactive cells displayed specific morphologies with elaborate processes reaching well into the DG (**Figure 10F** and insert). Stress alone caused an apparent increase in DCX positive cells in the VHC compared to the controls (**Figure 10**). However, the DCX+ cells in SS animals lacked the elaborate processes seen in SI animals.

DISCUSSION

The main finding of this study is that repeated stress alone caused a transient increase in anxiety and no major cellular and molecular abnormalities, while the exposure to stress and a single mild blast resulted in a transient (but longer lasting) increase in anxiety and chronic memory impairment. These behavioral changes are associated with neuroinflammation, vascular changes, and neuronal and glial cell loss.

Repetitive stress alone resulted in an early (48 h) increase in anxiety that dissipated at later time points. Our finding is consistent with previous studies where the exposure of rats to a fear-provoking environment resulted in a short-term increase in anxiety

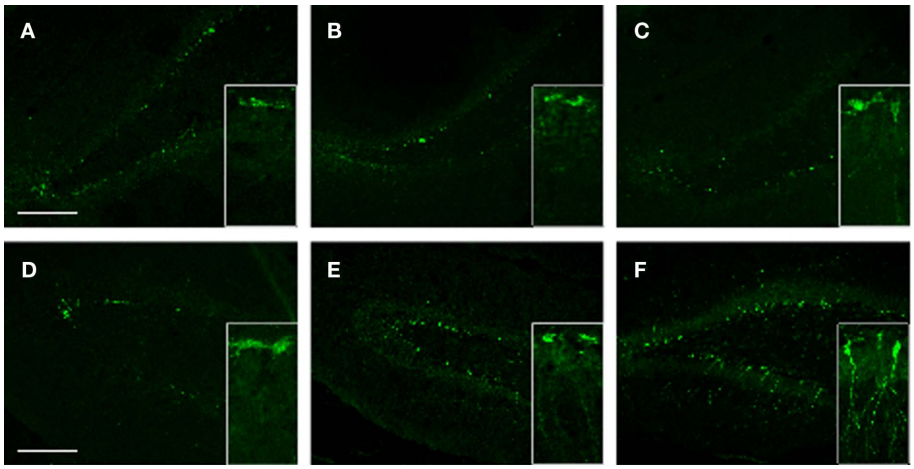

FIGURE 10 | DCX immunoreactivity in selected brain regions of animals in the various experimental groups. Frozen coronal sections containing the PFC, DHC, and VHC were cut. Immunohistochemistry was performed using a DCX antibody. Sections were stained with Hoechst 33342 to mark cellular nuclei. DHC of **(A)** C, **(B)** SS, and **(C)** SI rats; VHC of **(D)** C, **(E)** SS, and **(F)** SI rats. Inlays show the finer details of the cell bodies and processes of DCX cells within the DG of the VHC.

(Pynoos et al., 1996). Other studies also reported increased anxiety that lasted up to 7 days after daily exposure to predator odor (Adamec and Shallow, 1993; Cohen et al., 1996, 2000, 2003; Adamec et al., 1997, 1999). On the other hand, exposure of stressed animals to blast appears to prolong the period of increased anxiety, as these animals had elevated anxiety levels up to 1 month after injury. Importantly, anxiety levels of even these animals returned to normal at 2 months post-injury (or sham).

These findings suggest that the long-term effects of stress and injury can dissipate. However, epidemiological studies show that traumatic event(s) or repeated stress can result in PTSD, a chronic condition (Woon et al., 2010), although not all individuals exposed to traumatic events develop PTSD (Gross and Hen, 2004; Yehuda and LeDoux, 2007). The neuroanatomical substrates mediating symptom formation in PTSD include the medial PFC, amygdala, and HC (Bremner, 2007; Liberzon and Sripada, 2008). Within the HC, the VHC is predominantly involved in mediating anxiety-related functions while the DHC is involved in learning and memory-associated functions (Henke, 1990; Moser et al., 1995). *In vivo* imaging studies have found correlation between hippocampal volume and susceptibility to PTSD development (Karl et al., 2006). A recent meta-analytic study concluded that hippocampal volume reduction is associated with the exposure to trauma independent of PTSD diagnosis, but additional hippocampal reduction is associated with the development of PTSD compared to the trauma-exposed group without PTSD (Woon et al., 2010). A recent comprehensive *in vivo* imaging study showed that the volume of CA3/DG fields of the HC was significantly reduced in veterans with combat-related PTSD (Wang et al., 2010).

Both genetic and epigenetic factors are suspected in individuals' susceptibility to developing PTSD. These include an abnormal serotonin system and an altered response to CORT (Gross and Hen, 2004). Stress can alter the function of the hypothalamus–pituitary–adrenal axis (HPA), which in turn leads to abnormally elevated levels of CORT (Yehuda, 2006). Chronically elevated levels of CORT, as we observed, can adversely affect the architecture of the HC. However, a recent study found that chronically elevated CORT levels did not reduce cell number but caused a pronounced loss of synapses, suggesting that volume measures can substantially underestimate the effects of CORT on hippocampal structure and importantly on function (Tata et al., 2006; Tata and Anderson, 2010).

The HC, specifically the DHC, is also a critical neuroanatomical substrate of learning and memory (Henke, 1990; Moser and Humpel, 2005); elevated CORT levels can adversely affect memory (Bannerman et al., 2004). Although we found that CORT levels remained elevated even after 2 months in both SS and SI groups, we found that SS animals did not display memory deficits. Previous studies showed that following daily (foot-shock) stress for 14 days, CORT levels were elevated during the first 7 days post-stress, but returned to control levels by day 14 (Kant et al., 1987). However, there have been no studies to our knowledge that measure the long-term (e.g., 2 months) effects of stress on CORT levels.

In contrast to the transient increase in anxiety, we found that memory impairment was both specific to blast injury and also appeared to be a "chronic" condition. In BM, the performance of SS animals was not significantly different from C animals at any given time point, except on day 8 post-injury. Previous behavioral paradigms, in which rats were exposed to another form of predator stress (Diamond et al., 2006) have indicated that stress can have different effects on memory formation and consolidation depending on the time of exposure. Importantly, our data showed that memory impairment was at its highest at 2 months post-injury. These findings suggest that blast injury predominantly affects the DHC as evidenced by impaired spatial memory.

We found an increased number of TUNEL-positive cells in the hilus of the HC but not in the PFC of animals in the SI group at 2 months post-injury. This apparent lasting apoptotic processes after TBI is quite unusual. The limited information available indicates that in other models of TBI apoptotic activity returned to control levels 2 months after injury (Luo et al., 2002). There were no significant differences in the number of TUNEL-positive cells

of animals that were exposed to chronic stress only. As discussed above, SS animals had elevated serum CORT levels but showed no increase in the number of TUNEL-positive cells in their HC or PFC. These findings suggest that in addition to elevated CORT levels, other factors like inflammation may be required to sustain the increase in apoptotic cell death.

Our immunohistochemical data showed an increase in Iba1 immunoreactivity in the PFC as well as the HC of SI animals. Within the HC of SI animals, Iba1 immunoreactivity appeared to be higher in the VHC than in the DHC. However, we also found that exposure to stress alone resulted in an increase in hippocampal IL-6 (but not INFγ) levels 2 month after injury (or sham). IL-6 and INFγ are inflammatory cytokines produced by activated microglia and astroglia and are involved in mediating various responses to injury (Morganti-Kossmann et al., 2001, 2002; Nimmo et al., 2004). Depending on the cellular and molecular context, IL-6 can be neurotoxic or can act as a neuroprotectant (Toulmond et al., 1992).

IL-6 can act as a potent inhibitor of *de novo* hippocampal neurogenesis; one of several innate regenerative processes triggered by TBI (Vallieres et al., 2002). After a latency period following TBI, the rate of *de novo* hippocampal neurogenesis increases (Dash et al., 2001; Chirumamilla et al., 2002; Lee and Agoston, 2010). Newborn neurons, marked by DCX expression, migrate from the SGL to the granule cell layer (GCL) where many of the surviving neurons differentiate into granule cells (Altman and Das, 1965; Cameron et al., 1993). We found an apparent increase in DCX positive cells at 2 months after injury in the VHC but not in the DHC of SI rats. Additionally, these cells showed elaborate processes extending well into the DG. Animals in the SS group also showed an increase in DCX immunoreactivity in the VHC but the cells lacked the elaborate processes observed in SI rats. These findings suggest an increase in *de novo* neurogenesis in the VHC in response to stress, but particularly to the combination of stress and blast. This may indicate that increased *de novo* neurogenesis in the VHC is partly responsible for the normalization of anxiety observed at 2 months.

The apparent increase in DCX+ cells in the VHC of SI animals contradict what the Iba1 immunohistochemistry and the IL-6 ELISA data would imply. In addition to chronically elevated CORT levels, elevated hippocampal IL-6 levels and the presence of Iba1+ cells in the HC would imply a decrease or repression in neurogenetic activity as neuroinflammation and elevated CORT levels are known inhibitors of hippocampal *de novo* neurogenesis (Cameron and Gould, 1994; Yu et al., 2004; Montaron et al., 2006); with males showing a greater vulnerability to elevated CORT (Brummelte and Galea, 2010). However, the regulation of *de novo* hippocampal neurogenesis is rather complex; large numbers of molecules are involved and the exact nature of the regulatory process is currently not fully understood (Kempermann and Gage, 2000; Kempermann, 2002). Even though it has been accepted that an increase in DCX+ cells indicates increased *de novo* neurogenesis, DCX is only transiently expressed by *de novo* neurons. Thus, a more detailed BrdU/Prox1 double immunohistochemical and stereological quantification of the histology results is required to determine changes in *de novo* neurogenesis after stress and blast.

One of the positive regulators of *de novo* neurogenesis is VEGF; we and others have found that VEGF is significantly upregulated in various forms of TBI (Jin et al., 2002; Lee and Agoston, 2010) increased VEGF level promotes survival of *de novo* hippocampal neurons by blocking apoptotic cell death (Lee and Agoston, 2010). Consistent with the previous observation, we found that injury and stress, but not stress alone, increases VEGF levels in the HC and also in the PFC. Consistent with the previous observation, we found that injury and stress, but not stress alone, increases VEGF levels in the HC and also in the PFC. Previous studies have demonstrated that an increase in VEGF concentration can also increase vascular permeability as indicated by the breach of the BBB (Dvorak et al., 1995). Interestingly, a recent clinical study has shown that increased serum level of VEGF is indicative of good outcome after ischemic stroke (Sobrino et al., 2009).

We found increased serum levels of several neuronal and glia-specific proteins including NF-H, NSE, CK-BB, and GFAP 2 months post-injury. These molecules have previously been used to assess the extent and the outcome of TBI (Berger, 2006; Korfias et al., 2009). For example, NF-H has been used as a biomarker of neuronal loss and BBB damage and predicting outcome (Anderson et al., 2008). That serum levels of these proteins remain elevated at 2 month after injury suggest ongoing neuronal and glial cell loss as well as a chronically increased BBB permeability in which elevated levels of VEGF may play a role (Ay et al., 2008; Gerstner et al., 2009).

We also found significantly elevated levels of S100β and GFAP in the HC and in the PFC of SI animals. Elevated tissue levels of S100β may indicate astroglial proliferation and overall glial response to injury (Kleindienst et al., 2005). Elevated expression of GFAP by astrocytes, combined with morphological changes (reactive astrogliosis), is a hallmark of CNS neurotrauma (Eng and Ghirnikar, 1994; Fitch and Silver, 2008). We found that the VHC and the DHC appear to have differential expression of stellar GFAP astroglia following exposure to stress only and to the combination stress and injury. The role of increased GFAP immunoreactivity and stellar astroglia in CNS injury is complex. Astrocytic responses can lead to either reparative or detrimental outcomes depending on the type and time after injury (Eng and Ghirnikar, 1994; Fitch and Silver, 2008). However, increasing evidence also indicates a protective role of astrogliosis in reducing the toxic effects of extracellular glutamate and enabling barrier reconstruction after TBI (Buffo et al., 2010). In light of our behavioral findings, showing normalized anxiety levels of SI animals at 2 months post-injury, we speculate that the apparent increase in GFAP positive cells in the VHC may contribute to reparative pathomechanisms and the restoration of normal anxiety levels. Chronic stress has been shown to significantly reduce both the number and somal volume of astroglia in the HC (Czeh et al., 2006). Interestingly, we did see a differential effect of stress alone and stress and injury in the DHC and VHC. While the VHC displayed an apparent increase in GFAP+ cells with stellar processes, the same was not observed in the DHC and memory impairment remained significant 2 months post-injury. A possible explanation for the lasting memory deficits occurring in SI animals is that stress may selectively impair the restorative and/or regenerative action of reactive astrocytes in the DHC. While compelling, the results obtained require further exploration.

In summary, we found that when stressed animals are exposed to a single mild blast overpressure, there are lasting behavioral, molecular, and cellular abnormalities characterized by memory

impairment, neuronal and glial cell losses, inflammation, and gliosis. In contrast, stress alone resulted only in a transient increase in anxiety, no memory deficit and no detectable tissue damage. If our findings are independently verified, the potential ramifications can be significant in developing tools to assess the severity and to predict the outcome of psychological and physical traumas.

ACKNOWLEDGMENTS

We thank the Neurotrauma Team (WRAIR) for their technical help during the exposures; Ms. Cara Olsen (USU) for her help in statistical analysis; Drs. Grunberg and Wu (USU) for their input in designing and interpreting the behavioral experiments. The work was supported by CDMRP, grant# W81XWH-08-2-0176.

REFERENCES

Adamec, R. E., Burton, P., Shallow, T., and Budgell, J. (1999). NMDA receptors mediate lasting increases in anxiety-like behavior produced by the stress of predator exposure – implications for anxiety associated with posttraumatic stress disorder. *Physiol. Behav.* 65, 723–737.

Adamec, R. E., and Shallow, T. (1993). Lasting effects on rodent anxiety of a single exposure to a cat. *Physiol. Behav.* 54, 101–109.

Adamec, R. E., Shallow, T., and Budgell, J. (1997). Blockade of CCK(B) but not CCK(A) receptors before and after the stress of predator exposure prevents lasting increases in anxiety-like behavior: implications for anxiety associated with posttraumatic stress disorder. *Behav. Neurosci.* 111, 435–449.

Altman, J., and Das, G. D. (1965). Autoradiographic and histological evidence of postnatal hippocampal neurogenesis in rats. *J. Comp. Neurol.* 124, 319–335.

Anderson, K. J., Scheff, S. W., Miller, K. M., Roberts, K. N., Gilmer, L. K., Yang, C., and Shaw, G. (2008). The phosphorylated axonal form of the neurofilament subunit NF-H (pNF-H) as a blood biomarker of traumatic brain injury. *J. Neurotrauma* 25, 1079–1085.

Armonda, R. A., Bell, R. S., Vo, A. H., Ling, G., Degraba, T. J., Crandall, B., Ecklund, J., and Campbell, W. W. (2006). Wartime traumatic cerebral vasospasm: recent review of combat casualties. *Neurosurgery* 59, 1215–1225; discussion 1225.

Ay, I., Francis, J. W., and Brown, R. H. Jr. (2008). VEGF increases blood–brain barrier permeability to Evans blue dye and tetanus toxin fragment C but not adeno-associated virus in ALS mice. *Brain Res.* 1234, 198–205.

Bannerman, D. M., Rawlins, J. N., Mchugh, S. B., Deacon, R. M., Yee, B. K., Bast, T., Zhang, W. N., Pothuizen, H. H., and Feldon, J. (2004). Regional dissociations within the hippocampus – memory and anxiety. *Neurosci. Biobehav. Rev.* 28, 273–283.

Barnes, C. A. (1979). Memory deficits associated with senescence: a neurophysiological and behavioral study in the rat. *J. Comp. Physiol. Psychol.* 93, 74–104.

Belanger, H. G., Vanderploeg, R. D., Curtiss, G., and Warden, D. L. (2007). Recent neuroimaging techniques in mild traumatic brain injury. *J. Neuropsychiatry Clin. Neurosci.* 19, 5–20.

Berger, R. P. (2006). The use of serum biomarkers to predict outcome after traumatic brain injury in adults and children. *J. Head Trauma Rehabil.* 21, 315–333.

Bremner, J. D. (2007). Functional neuroimaging in post-traumatic stress disorder. *Expert Rev. Neurother.* 7, 393–405.

Brenner, L. A., Vanderploeg, R. D., and Terrio, H. (2009). Assessment and diagnosis of mild traumatic brain injury, posttraumatic stress disorder, and other polytrauma conditions: burden of adversity hypothesis. *Rehabil. Psychol.* 54, 239–246.

Breslau, N., and Kessler, R. C. (2001). The stressor criterion in DSM-IV posttraumatic stress disorder: an empirical investigation. *Biol. Psychiatry* 50, 699–704.

Brummelte, S., and Galea, L. A. (2010). Chronic high corticosterone reduces neurogenesis in the dentate gyrus of adult male and female rats. *Neuroscience* 168, 680–690.

Bruns, J., and Hauser, W. A. (2003). The epidemiology of traumatic brain injury: a review. *Epilepsia* 44(Suppl.), 2.

Buffo, A., Rolando, C., and Ceruti, S. (2010). Astrocytes in the damaged brain: molecular and cellular insights into their reactive response and healing potential. *Biochem. Pharmacol.* 79, 77–89.

Cameron, H. A., and Gould, E. (1994). Adult neurogenesis is regulated by adrenal steroids in the dentate gyrus. *Neuroscience* 61, 203–209.

Cameron, H. A., Woolley, C. S., Mcewen, B. S., and Gould, E. (1993). Differentiation of newly born neurons and glia in the dentate gyrus of the adult rat. *Neuroscience* 56, 337–344.

Campbell, T., Lin, S., Devries, C., and Lambert, K. (2003). Coping strategies in male and female rats exposed to multiple stressors. *Physiol. Behav.* 78, 495–504.

Carobrez, A. P., and Bertoglio, L. J. (2005). Ethological and temporal analyses of anxiety-like behavior: the elevated plus-maze model 20 years on. *Neurosci. Biobehav. Rev.* 29, 1193–1205.

Cernak, I., Merkle, A. C., Koliatsos, V. E., Bilik, J. M., Luong, Q. T., Mahota, T. M., Xu, L., Slack, N., Windle, D., and Ahmed, F. A. (2010). The pathobiology of blast injuries and blast-induced neurotrauma as identified using a new experimental model of injury in mice. *Neurobiol. Dis.* 41, 538–551.

Cernak, I., Wang, Z., Jiang, J., Bian, X., and Savic, J. (2001). Ultrastructural and functional characteristics of blast injury-induced neurotrauma. *J. Trauma.* 50, 695–706.

Chirumamilla, S., Sun, D., Bullock, M. R., and Colello, R. J. (2002). Traumatic brain injury induced cell proliferation in the adult mammalian central nervous system. *J. Neurotrauma* 19, 693–703.

Cohen, H., Benjamin, J., Kaplan, Z., and Kotler, M. (2000). Administration of high-dose ketoconazole, an inhibitor of steroid synthesis, prevents posttraumatic anxiety in an animal model. *Eur. Neuropsychopharmacol.* 10, 429–435.

Cohen, H., Friedberg, S., Michael, M., Kotler, M., and Zeev, K. (1996). Interaction of CCK-4 induced anxiety and post-cat exposure anxiety in rats. *Depress. Anxiety* 4, 144–145.

Cohen, H., Zohar, J., and Matar, M. (2003). The relevance of differential response to trauma in an animal model of posttraumatic stress disorder. *Biol. Psychiatry* 53, 463–473.

Czeh, B., Simon, M., Schmelting, B., Hiemke, C., and Fuchs, E. (2006). Astroglial plasticity in the hippocampus is affected by chronic psychosocial stress and concomitant fluoxetine treatment. *Neuropsychopharmacology* 31, 1616–1626.

Dash, P. K., Mach, S. A., and Moore, A. N. (2001). Enhanced neurogenesis in the rodent hippocampus following traumatic brain injury. *J. Neurosci. Res.* 63, 313–319.

Diamond, D. M., Campbell, A. M., Park, C. R., Woodson, J. C., Conrad, C. D., Bachstetter, A. D., and Mervis, R. F. (2006). Influence of predator stress on the consolidation versus retrieval of long-term spatial memory and hippocampal spinogenesis. *Hippocampus* 16, 571–576.

Doll, H., Truebel, H., Kipfmueller, F., Schaefer, U., Neugebauer, E. A., Wirth, S., and Maegele, M. (2009). Pharyngeal selective brain cooling improves neurofunctional and neurocognitive outcome after fluid percussion brain injury in rats. *J. Neurotrauma* 26, 235–242.

Dvorak, H. F., Brown, L. F., Detmar, M., and Dvorak, A. M. (1995). Vascular permeability factor/vascular endothelial growth factor, microvascular hyperpermeability, and angiogenesis. *Am. J. Pathol.* 146, 1029–1039.

Elliott, B. M., and Grunberg, N. E. (2005). Effects of social and physical enrichment on open field activity differ in male and female Sprague-Dawley rats. *Behav. Brain Res.* 165, 187–196.

Eng, L. F., and Ghirnikar, R. S. (1994). GFAP and astrogliosis. *Brain Pathol.* 4, 229–237.

Fitch, M. T., and Silver, J. (2008). CNS injury, glial scars, and inflammation: inhibitory extracellular matrices and regeneration failure. *Exp. Neurol.* 209, 294–301.

Fride, E., Dan, Y., Feldon, J., Halevy, G., and Weinstock, M. (1986). Effects of prenatal stress on vulnerability to stress in prepubertal and adult rats. *Physiol. Behav.* 37, 681–687.

Gerstner, E. R., Duda, D. G., Di Tomaso, E., Ryg, P. A., Loeffler, J. S., Sorensen, A. G., Ivy, P., Jain, R. K., and Batchelor, T. T. (2009). VEGF inhibitors in the treatment of cerebral edema in patients with brain cancer. *Nat. Rev. Clin. Oncol.* 6, 229–236.

Gross, C., and Hen, R. (2004). Genetic and environmental factors interact to influence anxiety. *Neurotox. Res.* 6, 493–501.

Gyorgy, A. B., Walker, J., Wingo, D., Eidelman, O., Pollard, H. B., Molnar, A., and Agoston, D. V. (2010). Reverse phase protein microarray technology in traumatic brain injury. *J. Neurosci. Methods.* 192, 96–101.

Harrison, F. E., Hosseini, A. H., and Mcdonald, M. P. (2009). Endogenous anxiety and stress responses in water maze and Barnes maze spatial memory tasks. *Behav. Brain Res.* 198, 247–251.

Heath, D. L., and Vink, R. (1999). Optimization of magnesium therapy after severe diffuse axonal brain injury in rats. *J. Pharmacol. Exp. Ther.* 288, 1311–1316.

Henke, P. G. (1990). Hippocampal pathway to the amygdala and stress ulcer development. *Brain Res. Bull.* 25, 691–695.

Jaffee, M. S., and Meyer, K. S. (2009). A brief overview of traumatic brain injury (TBI) and post-traumatic stress disorder (PTSD) within the Department of Defense. *Clin. Neuropsychol.* 23, 1291–1298.

Jin, K., Zhu, Y., Sun, Y., Mao, X. O., Xie, L., and Greenberg, D. A. (2002). Vascular endothelial growth factor (VEGF) stimulates neurogenesis in vitro and in vivo. *Proc. Natl. Acad. Sci. U.S.A.* 99, 11946–11950.

Kant, G. J., Leu, J. R., Anderson, S. M., and Mougey, E. H. (1987). Effects of chronic stress on plasma corticosterone, ACTH and prolactin. *Physiol. Behav.* 40, 775–779.

Karl, A., Schaefer, M., Malta, L. S., Dorfel, D., Rohleder, N., and Werner, A. (2006). A meta-analysis of structural brain abnormalities in PTSD. *Neurosci. Biobehav. Rev.* 30, 1004–1031.

Kaur, C., Singh, J., Lim, M. K., Ng, B. L., Yap, E. P., and Ling, E. A. (1997). Ultrastructural changes of macroglial cells in the rat brain following an exposure to a non-penetrative blast. *Ann. Acad. Med. Singap.* 26, 27–29.

Keane, T. M., Marshall, A. D., and Taft, C. T. (2006). Posttraumatic stress disorder: etiology, epidemiology, and treatment outcome. *Annu. Rev. Clin. Psychol.* 2, 161–197.

Kempermann, G. (2002). Regulation of adult hippocampal neurogenesis – implications for novel theories of major depression. *Bipolar Disord.* 4, 17–33.

Kempermann, G., and Gage, F. H. (2000). Neurogenesis in the adult hippocampus. *Novartis Found. Symp.* 231, 220–235; discussion 235–241, 302–226.

Kleindienst, A., Mcginn, M. J., Harvey, H. B., Colello, R. J., Hamm, R. J., and Bullock, M. R. (2005). Enhanced hippocampal neurogenesis by intraventricular S100B infusion is associated with improved cognitive recovery after traumatic brain injury. *J. Neurotrauma* 22, 645–655.

Korfias, S., Papadimitriou, A., Stranjalis, G., Bakoula, C., Daskalakis, G., Antsaklis, A., and Sakas, D. E. (2009). Serum biochemical markers of brain injury. *Mini Rev. Med. Chem.* 9, 227–234.

Lee, C., and Agoston, D. V. (2010). Vascular endothelial growth factor is involved in mediating increased de novo hippocampal neurogenesis in response to traumatic brain injury. *J. Neurotrauma* 27, 541–553.

Liberzon, I., and Sripada, C. S. (2008). The functional neuroanatomy of PTSD: a critical review. *Prog. Brain Res.* 167, 151–169.

Ling, G., Bandak, F., Armonda, R., Grant, G., and Ecklund, J. (2009). Explosive blast neurotrauma. *J. Neurotrauma* 26, 815–825.

Ling, G. S., and Ecklund, J. M. (2011). Traumatic brain injury in modern war. *Curr. Opin. Anaesthesiol.* doi: 10.1097/ACO.0b013e32834458da. [Epub ahead of print].

Long, J. B., Bentley, T. L., Wessner, K. A., Cerone, C., Sweeney, S., and Bauman, R. A. (2009). Blast overpressure in rats: recreating a battlefield injury in the laboratory. *J. Neurotrauma* 26, 827–840.

Luo, C., Jiang, J., Lu, Y., and Zhu, C. (2002). Spatial and temporal profile of apoptosis following lateral fluid percussion brain injury. *Chin. J. Traumatol.* 5, 24–27.

Maegele, M., Lippert-Gruener, M., Ester-Bode, T., Sauerland, S., Schafer, U., Molcany, M., Lefering, R., Bouillon, B., Neiss, W. F., Angelov, D. N., Klug, N., Mcintosh, T. K., and Neugebauer, E. A. (2005). Reversal of neuromotor and cognitive dysfunction in an enriched environment combined with multimodal early onset stimulation after traumatic brain injury in rats. *J. Neurotrauma* 22, 772–782.

Mayorga, M. A. (1997). The pathology of primary blast overpressure injury. *Toxicology* 121, 17–28.

Montaron, M. F., Drapeau, E., Dupret, D., Kitchener, P., Aurousseau, C., Le Moal, M., Piazza, P. V., and Abrous, D. N. (2006). Lifelong corticosterone level determines age-related decline in neurogenesis and memory. *Neurobiol. Aging* 27, 645–654.

Morganti-Kossmann, M. C., Rancan, M., Otto, V. I., Stahel, P. F., and Kossmann, T. (2001). Role of cerebral inflammation after traumatic brain injury: a revisited concept. *Shock* 16, 165–177.

Morganti-Kossmann, M. C., Rancan, M., Stahel, P. F., and Kossmann, T. (2002). Inflammatory response in acute traumatic brain injury: a double-edged sword. *Curr. Opin. Crit. Care* 8, 101–105.

Moser, K. V., and Humpel, C. (2005). Vascular endothelial growth factor counteracts NMDA-induced cell death of adult cholinergic neurons in rat basal nucleus of Meynert. *Brain Res. Bull.* 65, 125–131.

Moser, M. B., Moser, E. I., Forrest, E., Andersen, P., and Morris, R. G. (1995). Spatial learning with a minislab in the dorsal hippocampus. *Proc. Natl. Acad. Sci. U.S.A.* 92, 9697–9701.

Nimmo, A. J., Cernak, I., Heath, D. L., Hu, X., Bennett, C. J., and Vink, R. (2004). Neurogenic inflammation is associated with development of edema and functional deficits following traumatic brain injury in rats. *Neuropeptides* 38, 40–47.

Okie, S. (2005). Traumatic brain injury in the war zone. *N. Engl. J. Med.* 352, 2043–2047.

Pynoos, R. S., Ritzmann, R. F., Steinberg, A. M., Goenjian, A., and Prisecaru, I. (1996). A behavioral animal model of posttraumatic stress disorder featuring repeated exposure to situational reminders. *Biol. Psychiatry* 39, 129–134.

Richardson, L. K., Frueh, B. C., and Acierno, R. (2010). Prevalence estimates of combat-related post-traumatic stress disorder: critical review. *Aust. N. Z. J. Psychiatry* 44, 4–19.

Ryan, L. M., and Warden, D. L. (2003). Post concussion syndrome. *Int. Rev. Psychiatry* 15, 310–316.

Salzberg, M., Kumar, G., Supit, L., Jones, N. C., Morris, M. J., Rees, S., and O'brien, T. J. (2007). Early postnatal stress confers enduring vulnerability to limbic epileptogenesis. *Epilepsia* 48, 2079–2085.

Sobrino, T., Arias, S., Rodriguez-Gonzalez, R., Brea, D., Silva, Y., De La Ossa, N. P., Agulla, J., Blanco, M., Pumar, J. M., Serena, J., Davalos, A., and Castillo, J. (2009). High serum levels of growth factors are associated with good outcome in intracerebral hemorrhage. *J. Cereb. Blood Flow Metab.* 29, 1968–1974.

Taber, K. H., Warden, D. L., and Hurley, R. A. (2006). Blast-related traumatic brain injury: what is known? *J. Neuropsychiatry Clin. Neurosci.* 18, 141–145.

Tagliaferri, F., Compagnone, C., Korsic, M., Servadei, F., and Kraus, J. (2006). A systematic review of brain injury epidemiology in Europe. *Acta Neurochir. (Wien)* 148, 255–268.

Tata, D. A., and Anderson, B. J. (2010). The effects of chronic glucocorticoid exposure on dendritic length, synapse numbers and glial volume in animal models: implications for hippocampal volume reductions in depression. *Physiol. Behav.* 99, 186–193.

Tata, D. A., Marciano, V. A., and Anderson, B. J. (2006). Synapse loss from chronically elevated glucocorticoids: relationship to neuropil volume and cell number in hippocampal area CA3. *J. Comp. Neurol.* 498, 363–374.

Toulmond, S., Vige, X., Fage, D., and Benavides, J. (1992). Local infusion of interleukin-6 attenuates the neurotoxic effects of NMDA on rat striatal cholinergic neurons. *Neurosci. Lett.* 144, 49–52.

Vallieres, L., Campbell, I. L., Gage, F. H., and Sawchenko, P. E. (2002). Reduced hippocampal neurogenesis in adult transgenic mice with chronic astrocytic production of interleukin-6. *J. Neurosci.* 22, 486–492.

Vink, R., O'Connor, C. A., Nimmo, A. J., and Heath, D. L. (2003). Magnesium attenuates persistent functional deficits following diffuse traumatic brain injury in rats. *Neurosci. Lett.* 336, 41–44.

von Horsten, S., Exton, M. S., Voge, J., Schult, M., Nagel, E., Schmidt, R. E., Westermann, J., and Schedlowski, M. (1998). Cyclosporine A affects open field behavior in DA rats. *Pharmacol. Biochem. Behav.* 60, 71–76.

Walf, A. A., and Frye, C. A. (2007). The use of the elevated plus maze as an assay of anxiety-related behavior in rodents. *Nat. Protoc.* 2, 322–328.

Wang, Z., Neylan, T. C., Mueller, S. G., Lenoci, M., Truran, D., Marmar, C. R., Weiner, M. W., and Schuff, N. (2010). Magnetic resonance imaging of hippocampal subfields in posttraumatic stress disorder. *Arch. Gen. Psychiatry* 67, 296–303.

Warden, D. (2006). Military TBI during the Iraq and Afghanistan wars. *J. Head Trauma Rehabil.* 21, 398–402.

Warden, D. L., and French, L. (2005). Traumatic brain injury in the war zone. *N. Engl. J. Med.* 353, 633–634.

Warden, D. L., Labbate, L. A., Salazar, A. M., Nelson, R., Sheley, E., Staudenmeier, J., and Martin, E. (1997). Posttraumatic stress disorder in patients with traumatic brain injury and amnesia for the event? *J. Neuropsychiatry Clin. Neurosci.* 9, 18–22.

Weinstock, M., Matlina, E., Maor, G. I., Rosen, H., and Mcewen, B. S. (1992). Prenatal stress selectively alters the reactivity of the hypothalamic-pituitary adrenal system in the female rat. *Brain Res.* 595, 195–200.

Woon, F. L., Sood, S., and Hedges, D. W. (2010). Hippocampal volume deficits associated with exposure to psychological trauma and posttraumatic stress disorder in adults: a meta-analysis. *Prog. Neuropsychopharmacol. Biol. Psychiatry* 34, 1181–1188.

Yehuda, R. (2006). Advances in understanding neuroendocrine alterations in PTSD and their therapeutic implications. *Ann. N. Y. Acad. Sci.* 1071, 137–166.

Yehuda, R., and LeDoux, J. (2007). Response variation following trauma: a translational neuroscience approach to understanding PTSD. *Neuron* 56, 19–32.

Yu, I. T., Lee, S. H., Lee, Y. S., and Son, H. (2004). Differential effects of corticosterone and dexamethasone on hippocampal neurogenesis in vitro. *Biochem. Biophys. Res. Commun.* 317, 484–490.

Conflict of Interest Statement: The authors declare that the research was conducted in the absence of any commercial or financial relationships that could be construed as a potential conflict of interest.

Received: 11 December 2010; accepted: 19 February 2011; published online: 07 March 2011.

Citation: Kwon S-KC, Kovesdi E, Gyorgy AB, Wingo D, Kamnaksh A, Walker J, Long JB and Agoston DV (2011) Stress and traumatic brain injury: a behavioral, proteomics, and histological study. Front. Neur. ***2****:12. doi: 10.3389/fneur.2011.00012*

This article was submitted to Frontiers in Neurotrauma, a specialty of Frontiers in Neurology.

APPENDIX

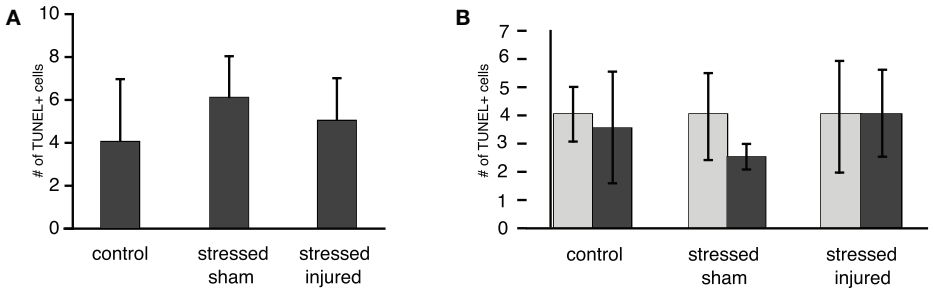

FIGURE A1 | TUNEL-positive cells in selected brain regions of animals in the various experimental groups. Frozen coronal sections containing the **(A)** PFC and **(B)** DG of the DHC and VHC of C, SS, and SI rats were counted and expressed as positive cells per unit area ± SEM. $*p < 0.05$ and $**p < 0.01$ compared to C rats.

frontiers in
NEUROLOGY

METHODS ARTICLE
published: 17 June 2011
doi: 10.3389/fneur.2011.00041

A new model to produce sagittal plane rotational induced diffuse axonal injuries

Johan Davidsson[1] and Marten Risling[2]*

[1] *Vehicle Safety Division, Department of Applied Mechanics, Chalmers University of Technology, Göteborg, Sweden*
[2] *Experimental Traumatology, Department of Neuroscience, Karolinska Institutet, Stockholm, Sweden*

Edited by:
Mattias Sköld, Uppsala University, Sweden

Reviewed by:
Niklas Marklund, University of Uppsala, Sweden
Bridgette D. Semple, University of California San Francisco, USA

***Correspondence:**
Marten Risling, Department of Neuroscience, Karolinska Institutet, Retzius väg 8, 171 77 Stockholm, Sweden.
e-mail: marten.risling@ki.se

A new *in vivo* animal model that produces diffuse brain injuries in sagittal plane rearward rotational acceleration has been developed. In this model, the skull of an anesthetized adult rat is tightly secured to a rotating bar. During trauma, the bar is impacted by a striker that causes the bar and the animal head to rotate rearward; the acceleration phase last 0.4 ms and is followed by a rotation at constant speed and a gentle deceleration when the bar makes contact with a padded stop. The total head angle change is less than 30°. By adjusting the air pressure in the rifle used to accelerate the striker, resulting rotational acceleration between 0.3 and 2.1 Mrad/s^2 can be produced. Numerous combinations of trauma levels, post-trauma survival times, brain and serum retrieval, and tissue preparation techniques were adopted to characterize this new model. The trauma caused subdural bleedings in animals exposed to severe trauma. Staining brain tissue with β-Amyloid Precursor Protein antibodies and FD Neurosilver that detect degenerating axons revealed wide spread axonal injuries (AI) in the corpus callosum, the border between the corpus callosum and cortex and in tracts in the brain stem. The observed AIs were apparent only when the rotational acceleration level was moderate and above. On the contrary, only limited signs of contusion injuries were observed following trauma. Macrophage invasions, glial fibrillary acidic protein redistribution or hypertrophy, and blood brain barrier (BBB) changes were unusual. S100 serum analyses indicate that blood vessel and glia cell injuries occur following moderate levels of trauma despite the absence of obvious BBB injuries. We conclude that this rotational trauma model is capable of producing graded axonal injury, is repeatable and produces limited other types of traumatic brain injuries and as such is useful in the study of injury biomechanics, diagnostics, and treatment strategies following diffuse axonal injury.

Keywords: brain, animal model, diffuse axonal injury

INTRODUCTION

Traumatic brain injuries (TBI) represent approximately 60% of all deaths in hospitals among children and young adults in the western world (Melvin et al., 1993). Among survivors these injuries are often irreversible, causing long term pain, and disability. Although TBI can be associated with skull fractures, it commonly occurs without fractures (Gennarelli and Thibault, 1982). About 40% of all TBI patients admitted to hospitals are non-focal injuries (Wismans et al., 2000) and are usually referred to as distributed brain injuries (DBI).

At least four categories of DBI can be identified: diffuse axonal injury (DAI); diffuse hypoxic, anoxic, or ischemic injury; diffuse swelling; and diffuse vascular injury. DAI is the most common type of DBI and commonly results in unconsciousness or death (Gennarelli et al., 1982; Melvin et al., 1993). The DAI pathology, which is characterized by perturbations to the axoplasmic transport along the length of axons (Povlishock and Jenkins, 1995), is likely to cause axonal swelling or degeneration which can reduce the functionality or disconnect the axons from their existing networks (Povlishock, 1992). It has been reported that DAI commonly are localized in the subcortical white matter, gray–white matter interface, and corpus callosum (Gennarelli et al., 1982; Ommaya, 1984; Smith and Meaney, 2000) as well as at points of attachment, such as cranial nerves (Viano, 1997).

Distributed brain injuries is commonly a result of inertial induced loads; intracranial motions arise when the skull is accelerated and the brain mass, due to its inertia, lags behind or continues its motion relative to the skull. These inertia induced loads are most common in rapid head rotations (Holbourn, 1943) which often occur in fall accidents, traffic accidents, and military assaults. It has been hypothesized that these inertia induced loads produce strains in the brain tissue and that these strains cause neurological deficiencies (Strich, 1961; Adams et al., 1989; Margulies et al., 1990; Margulies and Thibault, 1992; Povlishock, 1992; Zhang et al., 2004). Meaney et al. (1993) used numerical simulations to reconstruct experiments with miniature pigs (Ross et al., 1994) to determine the DAI-tolerance level on tissue level. For grade 1 and grade 2 DAI a maximum strain of 0.1 and 0.25, respectively, was suggested. Using animal models, it has been suggested that the severity of DBI correlates with the amplitude of the angular acceleration (Abel et al., 1978; Ono et al., 1980; Margulies and Thibault, 1992). The use of detailed mathematical models of the

head and brain, however, has indicated that injury correlates with the resulting angular velocity (Kleiven, 2007). In addition, duration of the impact has been reported to affect the injury type; short duration impacts result in a larger extent of focal injury, while long duration impacts mainly result in DBI (Margulies and Thibault, 1992). It has also been shown, in experiments with monkeys, that the incidence and degree of DBI correlated, although indirectly, with the direction of the head acceleration: coronal plane angular acceleration was the direction that caused the longest lasting coma, while sagittal plane angular accelerations and oblique accelerations produced coma for a shorter period (Gennarelli et al., 1982).

An attractive approach to studying DBI pathology and its associated injury mechanism and threshold would be to reconstruct well documented accident cases in which the patient is slightly injured. The real life accidents are however commonly rather complex and the patients suffer from a multitude of injuries. Therefore anesthetized animals have been used in the past to study DBI and DAI.

Primates were extensively used in the past but currently smaller animals such as miniature swine, rabbits, and rats are used (**Table 1**). In a model described by Marmarou et al. (1994), a cap the size of a dime is cemented to the denuded bone on top of the rat skull. During trauma this plate is impacted by a drop weight which causes the head to accelerate linearly and rotate forward in the sagittal plane. The initial purpose with the model was not to assess the threshold for DAI in rotational head trauma but rather to study the pathology and treatment of TBI in general. For head rotations in the coronal plane, Xiao-Sheng et al. (2000) exposed rats to 2 ms long rotational accelerations, after which they observed axonal swelling and bulblike protrusions on the axons in the medulla oblongata, midbrain, and corpus callosum. In two other studies by Ellingson et al. (2005) and by Fijalkowski et al. (2007), rats were exposed to higher rotational accelerations than in the study by Xiao-Sheng et al. (2000); 368 krad/s^2) for approximately 2 ms in the coronal plane. Despite the higher accelerations, the rats suffered from classical concussion injuries with minimal histological abnormalities. A series of publications have presented a model in which rabbits are exposed to rotational acceleration in the sagittal plane (Gutierrez et al., 2001; Runnerstam et al., 2001; Hamberger et al., 2003; Hansson et al., 2003; Krave et al., 2005, 2011). Due to the size of the rabbit brain as compared to the rat brain, the rabbit has become the preferred choice. However, the rabbit brain is rather elongated as compared to the human brain.

Table 1 | Studies which exposed animal brains to rotational acceleration to improve the understanding of pathologenesis, injury mechanisms, and suggest injury threshold.

Plane of motion	Subject used	Method to assess injury and type of injury produced	Concluding result	Reference
Sagittal plane lin. and rot. acc.	Rat	Histology etc.	Developed to study TBI	Marmarou et al. (1994) and Foda and Marmarou (1994)
	Rabbit	Astrogliosis in hippocampus and cerebral cortex, hemorrhages, focal bleeding, reactive astrocytosis, and axonal injury	Development of test rig, and rot. trauma involves edema and neuronal environment that leads to apoptosis	Gutierrez et al. (2001) and Runnerstam et al. (2001)
	Rabbit	Neurofilament redistribution and beta-amyloid	Effect of trauma on the neuronal cytoskeleton	Hamberger et al. (2003)
Coronal plane rot. acc.	Miniature swine	Histology (NF), retraction bulbs in the cerebral hemispheres		Meaney et al. (1995) and Ross et al. (1994)
	Miniature swine	Histology (NF, GFAP, IgG, Nissel) retraction bulbs in the cerebral hemispheres	DAI occur due to the viscoelastic properties and highly organized structure of the axons	Smith et al. (1997)
	Rat	Silver staining, significant damage to the brainstem	Development of test rig	Xiao-Sheng et al. (2000)
	Rat	Limited macroscopic brain damage, no evidence of axonal swellings	Transient unconsciousness	Ellingson et al. (2005) and Fijalkowski et al. (2007)
Transverse plane rot. acc.	–	–	–	–
Oblique head rot. acc. and contact injury	Sheep	β-APP histology, contusions, and axonal injury	Axonal injury was related to impact severity	Andersson, 2000

To conclude, the number of models in which small animals are used and in which DAI is developed without large quantities of contusion type or hemorrhage injuries are limited. Therefore a new model in which the heads of rats are exposed to sagittal plane rotational accelerations resulting in graded levels of DAI has been developed and is presented here. This new model is intended for studies of inertial loading brain injuries to simulate forehead to hard structure impacts.

MATERIALS AND METHODS

The materials and methods used in this study are presented below. This paper is focused on the presentation of the test rig and its capabilities. The experimental data included were produced for studies with a special purpose and for this reason there is variability in the animal numbers used for different experiments. Additional information is available in Davidsson (2008) and in Risling et al. (2011).

ANIMALS

In total 110 male Sprague-Dawley rats were included in this study. Nineteen animals could not be included in the analysis due to various reasons. In five experiments the skull cap came loose during trauma. Eight additional animals died as a consequence of the anesthesia and six died either from the trauma or the anesthetics. The animals that died from the trauma likely suffered from acute brain stem injury which resulted in severe arrhythmia and respiratory arrest.

Out of the 110 animals, 91 male Sprague-Dawley rats weighing between 0.352 and 0.518 kg (with an average weight of 0.415 kg) were either successfully exposed to rotational injury or served as sham exposed controls in this study (**Table 2**). In addition four animals were not operated on and served as normal controls. All animals were deeply anesthetized by a 2.4-ml/kg intra-abdominal injections of a mixture of 1 ml Dormicum® (5 mg/ml Midazolam, Roche), 1 ml Hypnorm® (Janssen), and 2 ml of distilled water. Thereafter the subjects were given 0.2 ml/kg intra-muscular injections every 0.5 h until the surgery and trauma was carried out. The work was performed in accordance with the Swedish National Guidelines for Animal Experiments, which was approved by the Animal Care and Use Ethics Committee in either Umeå or Stockholm.

A midline incision was made through the skin and periosteum on the skull vault, and parts of the frontal, nose, and parietal bones were freed from adherent tissue. The exposed bone was treated with 15% phosphate acid for 3 min to clean and roughen the surfaces of the bone, thoroughly rinsed with tempered distilled water and dried for 3 min with an air drier providing air that was 37°C in the proximity of the skull bone. The exposed bone was then gently sanded, left to dry for at least an additional 10 min prior to gluing of an aluminum plate, denominated the skull cap (**Figure 1**) and shaped to match the contour of the exposed skull. The dental glue (Super-Bond C and B; Sun Medical Co., Shiga, Japan) was allowed to harden for a minimum of 15 min. During the first 3 min the temperature was kept at 37°C after which it was adjusted to below but close to 37°C.

EXPERIMENTAL SETUP

Prior to experiments, an attachment plate, that had a temperature close to 37°C, was fastened by means of two screws to the skull cap previously glued to the rat skull bone (**Figure 1**). Then

Table 2 | Number of animals included in the various groups in this study (the numbers in the boxes refer to the total number of animals included in the group whereas the numbers in brackets refer to the number of sham exposed animals).

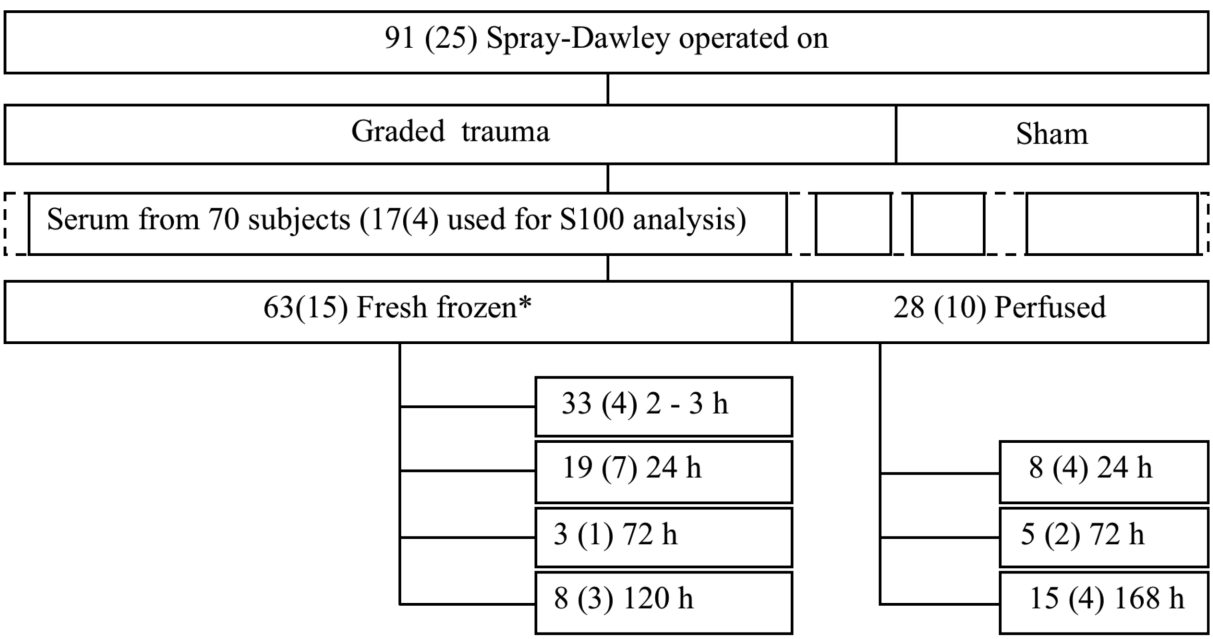

*63 animals used for β-APP analysis of which 31 was used for COX2 analysis.

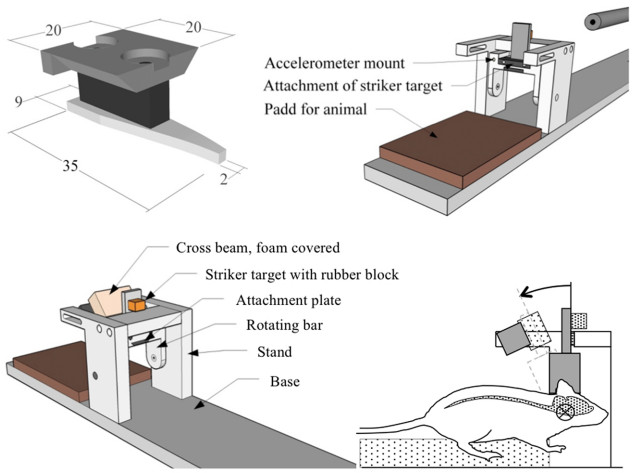

FIGURE 1 | Diagrams. Top row; skull cap and attachment plate and oblique view of test device (crossbeam removed for visibility). Bottom row; oblique view of test device and side view of the head with central nervous system schematically depicted (screws and accelerometer not depicted).

the *attachment plate* was inserted and secured to a *rotating bar* that can rotate freely around a horizontal axis. The resulting pre-trauma position of the head was consistently slightly flexed and the brain center of gravity located about 6.5 mm above the center of rotation. This is equivalent to a center of rotation located 1 mm below the head base and 5 mm forward of the front of the foramina magnum.

Twenty-five animals served as sham exposed controls, thus 66 animals were traumatized. During trauma a weight, denominated the *striker* (brass, diameter 6.3 mm, weight 0.010 kg), was accelerated in a specially designed air driven *accelerator* (CNC-Process AB, Hova, Sweden) and was made to hit a *rubber block* (Polyurethane, Shore A 60, 10 mm thick, 13 mm wide, 10 mm high) that was glued onto a *striker target* (SS4212, aluminum plate 6 mm thick and 15 mm wide). The impulse produced subjected the *rotating bar* and the animal head to a short sagittal plane rearward rotational acceleration. The *striker* hit the rubber block at a height of 57 mm from the center of rotation of the *rotating bar*. This acceleration phase was followed by a rearward rotation at near constant velocity. Finally, the *striker target* made contact with the *crossbeam* (steel, 16 mm square profile) which was covered with high density Tempur foam (20 mm thick and 20 mm high). The trauma represents a forehead impact to the steering wheel in a frontal car collision or to the ground in a fall accident. The rotational acceleration magnitude was selected by modifying the *striker* speed which was varied by means of modifying the air pressure in a specially designed air driven *accelerator*.

After trauma the attachment plate was removed, the skin was made to cover the skull cap and 8–10 sutures closed the incision.

INSTRUMENTATION, DATA ACQUISITION, AND ANALYSIS

An Endeveco Isotron 2255B-01 piezoelectric accelerometer, with integrated electronics and resonance frequency above 300 kHz, was mounted on the *rotating bar* at a radius of 36.5 mm from the center of rotation and connected to an Endeveco 4416B signal conditioner. The signal conditioner gain was set at one with an upper frequency cut off at 40 kHz (−3 dB) which served as anti-aliasing filter. The analog signal was digitized and captured by means of a National Instrument DAQ Card 6062 at 200 kHz. Thereafter the obtained rotational acceleration data was filtered using SAE J211 CFC3000 (5000 Hz).

A chronograph (SKAN PRO1 Series 3) was used to capture the velocity of the striker.

In four experiments, side views of the head trauma were recorded by a Redlake video at 20 000 f/s with a resolution of 120 × 68 pixels. Oblique frontal views of the trauma were also recorded to monitor the rigidity of the head-to-test rig attachment.

Angular velocity and displacement were numerically integrated from the unfiltered acceleration data and compared with the high speed data for accuracy.

DISSECTION, IMMUNOHISTOLOGY, *IN SITU* HYBRIDIZATION, AND SERUM ANALYSIS

Post-trauma survival times were varied from 2 h to 7 days. The short survival times were preferred to assess the axonal injury as soon as possible after trauma to limit detection of secondary effects associated with the trauma or preparation of the animal; the longer survival time was required to detect contusion injuries and degenerative axons.

In case serum was to be collected prior to the sacrifice, the animals were anesthetized for at least 2 h. Thereafter 5–7 ml of blood were retrieved from the right ventricle of the heart with a Safety-Lock needle and SST II blood collection system containers (BD Vacutainer®). The blood containers were filled and treated according to the instructions provided with the system. Serum was frozen immediately after centrifugation and stored at −20°C until the analysis. In case no serum was to be collected, the animals were anesthetized for 15 min prior to being sacrificed.

After possible serum collection, 63 of the animals were killed, the brains were removed and split into three units at 0.6 mm and −3.0 relative to the bregma. The units were fresh frozen on dry ice. The three units are referred to as frontal, middle, and occipital. In total 28 animals were subjected to transcardial perfusion with phosphate buffered saline containing heparin and then fixed with formaldehyde in PBS after which the brain was subsequently removed. The brains were thereafter immersed in buffered formalin for at least a day and transferred for cold storage in sodium azide and sucrose solution in PBS.

Coronal 14 μm cryostat sections from the three regions of the 63 fresh frozen encephalon sections were cut and thawed onto chromealum–gelatine treated slides. For a few animals also the brain stem was sectioned and thawed on slides. The frontal sections were from 1.5 to 0.5 mm relative to the bregma, the middle sections from 0 to −1.0 mm relative to the bregma and occipital sections from 3.0 to 6.0 mm relative to the bregma. The sections were soaked in 0.01 M PBS buffer for 10 min and incubated over night in a humid chamber at 4°C with different antibodies. For detection of injured axons, sections were incubated with rabbit polyclonal β-APP antibodies (51-2700, Invitrogen, Corporation, CA, USA; dilution 1:100). For studies of other brain injuries, sections were incubated with mouse monoclonal antibodies against blood brain barrier (BBB; SM-71, Sternberger Monoclonals Inc., Baltimore,

MD, USA; dilution 1:200) and goat polyclonal antibodies against glial fibrillary acidic proteins (GFAP; 6170, Santa Cruz Biotechnology Inc., Santa Cruz, CA, USA; dilution 1:100). For studies of proliferation of macrophages, sections were incubated with mouse monoclonal anti-rat ED1 (MCA431R, AbD Serotec, Dusseldorf, Germany; dilution 1:1000). All antibodies were diluted in 0.01 M PBS containing 5% donkey serum, 5% Bovine serum albumin, 0.3% triton, and 0.1% sodium azide. The sections were then rinsed in 0.01 M PMS and incubated for 45 min at 20˚C with 0.01 M PBS containing 0.1% sodium azide and 0.3% Triton and either Cy3-conjugated donkey anti-rabbit IgG, Cy3-conjugated donkey antimouse (Jackson Immuno Research Inc., PA, USA; diluted 1:500), Cy2-conjugated donkey anti-rabbit IgG, or Cy2-conjugated donkey antigoat IgG (Jackson; diluted 1:500). After the sections were rinsed in PBS, they were mounted in a mixture of glycerol and PBS and cover slipped.

Similarly, perfused tissue was processed for detection of damage to neuronal processes with FD Neurosilver™ Kit I (PK301, FD Neurotechnologies Inc., Baltimore, MD, USA) according to the provided instructions.

In addition, sections from fresh frozen tissue from the frontal regions of nine animals that had been subjected to maximum rotational accelerations between 0.84 to 1.92 rad/s^2, were fixated in ice cold 100% acetone for 10 min and rinsed in PBS buffer. Thereafter, they were incubated with the same β-APP antibody as above but this was diluted 1:100 in 0.01 M PBS buffer containing 5% BSA, 0.3% Triton and 5% normal horse serum. Sections were incubated over night at 4˚C, rinsed in 0.01 M PBS buffer and then incubated with biotinylated anti-rabbit IgG (BA-1000, Vector Laboratories Inc., CA, USA) followed by biotinylated enzyme complex (VECTASTAIN Elite Kit, PK-6100, Vector Laboratories). Finally, the binding of the APP antibody was localized by incubation with DAB substrate (Vector, SK-4100). The sections were dehydrated and coverslipped with Entellan and examined using the 40× lens in a Nikon E600 microscope. Images were captured with a Nikon Digital Sight DS-U1 (5 megapixel) camera, controlled with Nikon EclipseNet software. A total of 279 APP-positive profiles at the border between the corpus callosum and the subcortical white matter were identified and outlined at a final magnification of 1240× with the polygonal marker. The area was recorded for each of these profiles. The results were analyzed with Graphpad Prism® 5 software for Macintosh using Kruskal–Wallis one-way ANOVA and Dunn's multiple comparison test.

Cyclooxygenase 2 (COX2) is an enzyme responsible for formation of important biological mediators. It has been reported to be abundant in cells at sites of inflammation and has been suggested to correlate with cell death. For this analysis coronal sections from 31 animals were cut in an RNase free environment and thawed onto SuperFrost Plus® (MENZEL-GLÄSER, Germany) object-slides and stored in sealed boxes at −70˚C until used. Thereafter, a 48-mer Synthetic oligonucleotide COX2 probe was synthesized (CyberGene AB, Huddinge, Sweden). The probe was labeled at the 3′-end with deoxyadeno-sine-alpha-(thio)triphosphate, (α-33P)-3000 Ci/mmol, 10 mCi/ml (PerkinElmer, MA, USA) by using terminal deoxynucleotidyl-transferase (Fermentas AB, Sweden) and hybridized to the sections for 16–18 h at 42˚C. The sections were first rinsed in SSC and then in distilled water. Subsequently, dehydration in ethanol was performed. The sections were then counterstained with cresyl violet and mounted.

In the main part of the histological analysis brain sections from each of the three regions in the brain, frontal, middle, and occipital, were chosen arbitrarily and antibody reactivity was assessed with a NIKON E600 microscope equipped with a confocal C1 unit or using dark field microscopy. For β-APP and COX2, the analysis also included scoring according to a grading scheme (**Table 3**). In addition, sections from the brain stem were prepared and antibody reactivity assessed.

Two of the S100 proteins, S100A1B, and S100BB, found in the central nervous system glial cells, are known to be released into body fluids following trauma (Ingebrigtsen et al., 2000). In the current study multiple serum S100BB levels and the total S100B (S100A1B and S100B) levels were assessed using serum from 17 animals using two immunoassays (S100 EIA and S100B EIA, Can Ag Diagnostics AB, Gothenburg, Sweden).

RESULTS

PERFORMANCE OF THE NEW TEST DEVICE

The skull cap was larger in the first 17 experiments and had a size similar to the denuded nasal bone. As a consequence of this close match in size, the location of the skull cap relative to the head varied slightly in the first 17 experiments since the nasal shape of the animal varied. As a consequence, the center of rotation varied slightly in the first few experiments than in the rest of the series. No difference in histological outcome between the first 17 animals and the remaining animals could, however, be detected and the results obtained were included in the analysis.

Table 3 | Grading of β-APP and COX2.

Grade	Number of β-APP-positive axons per section	Shape and dimension of β-APP-positive axons	Intensity of COX2 silver staining per section	Localization of the COX2 positive cells
0	Only slight β-APP stains in cell body	–	Sometimes visible	Distributed regardless of tissue type
1	50–100	Small but asymmetric	Visible in 10× microscope	Localized to cell bodies
2	100–200	Large and asymmetric	Visible in 1× microscope, bright contrast underlying tissue	Localized to cell bodies
3	>200	Large and some extended along the axon	Visible macroscopically and overshadowing tissue behind	Localized to cell bodies

ROTATIONAL AND LINEAR ACCELERATION AND VELOCITY CHANGE

The charge pressure in the accelerator influenced the striker target speed which in turn influenced the rotational acceleration of the rotating bar and animal head unit. The duration of this angular acceleration was about 0.4 ms and was independent of striker velocity. As a consequence, the resulting angular velocity correlated closely with the peak angular acceleration ($r^2 = 0.86$). After 10° of head rotation, the striker target made contact with the foam covered crossbeam and the rotating bar and attached head came to a halt after about 2 ms at an angle of 20°–30° (**Figure 2**). Maximum deceleration was approximately 25% of initial peak acceleration (**Figure 2**). Thereafter the bar and the animal head slowly rotated forward to the position it had prior to trauma.

In this study the pressure in the accelerator was varied between 8 to 30 bar which resulted in striker velocities between 33 to 63 m/s and maximum rotational accelerations between 0.3 to 2.1 rad/s^2 (**Figure 2**).

In the experiments, the center of rotation was not perfectly in the center of gravity of the brain; hence the brain was exposed to a combination of rotational and linear accelerations. As an example, the maximum linear acceleration in the brain center of gravity ranged from 3600 to 7400 m/s^2 for the three experiments included in **Figure 2**.

Images of the rotating bar during trauma were recording using a high speed video for the purpose of evaluating the recorded linear acceleration and subsequent calculation of the rotational acceleration. The time from start to stop of the angulations of the head, obtained from video analysis, matched that of the accelerometer data. Resulting peak angulations of the rotating bar during the trauma, as estimated by double integration of the rotational acceleration, were also consistently about 20° and matched those of the video data (**Figure 2**).

DIFFUSE AXONAL INJURY

Bands of β-APP-positive axons, i.e., axons with reduced axoplasmic transport and accumulation of β-APP, were seen in frontal sections and in the borders between the cortex and the corpus callosum (also forceps minor) in nearly all animals exposed to head rotational trauma of 1.0 Mrad/s^2 or above (**Figures 3** and **8**). No β-APP reactivity was found in the sham exposed animals (**Figure 3**).

These bands were present independent of survival times, however the number of β-APP-positive axons appeared to increase when the survival time was 24 h compared with 3 and 2 h. In animals that were exposed to rotational trauma at 1.3 Mrad/s^2 or higher, bands of β-APP-positive axons were also seen in these borders in the middle and rear sections. This observation was not as consistent as for the frontal sections; animals that were allowed to survive for 5 days exhibited less positive axons in the middle and rear sections. Most animals displayed similar numbers of and intensity of β-APP-positive axons on the right and left hemispheres. The extensions of the β-APP-positive axons in the lateral direction varied from one animal to another.

For approximately 40% of the animals in which β-APP was found in the borders between the cortex and the corpus callosum,

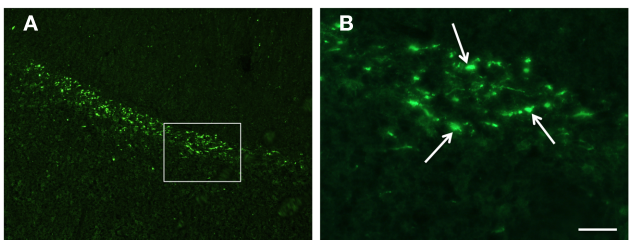

FIGURE 3 | Confocal images of β-APP stained tissue, coronal plane, frontal sections. In **(A)** a low magnification image shows the border between the corpus callosum (lower part) and subcortical white matter. A larger number of β-APP-positive profiles are visible at the border between the corpus callosum and the subcortical white matter, 24 h after high acceleration trauma. The box in **(A)** indicates the area that is shown in higher magnification in **(B)**, in which β-APP-positive profiles have been indicated by arrows (scale bar = 25 μm).

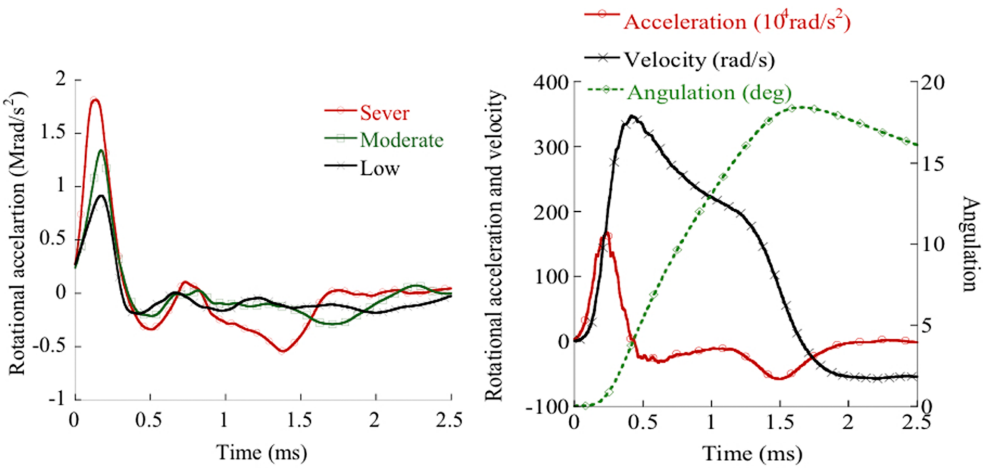

FIGURE 2 | Left: Rotating bar accelerations obtained in experiments that exhibited widespread, slight or no β-APP reactivity. Right: Rotational acceleration and integrated rotational acceleration (velocity).

β-APP was also found in the thalamus, on the lower edges of the corpus callosum, in the corpus callosum, the caudate putamen and the commissure. In the middle brain sections, small diameter β-APP-positive axons were found in animals in the hippocampus region and in the vicinity of the lateral ventricle.

Seven brain stems were dissected and stained for β-APP analysis. Widespread areas with β-APP-positive axons were observed (**Figure 4**). As compared to the bands seen in the upper border of the corpus callosum, the numbers of positive axons were fewer. OBS! The highest concentration was found in the pyramid tracts.

In nine animals β-APP-positive profiles were analyzed with regard to size (area). No significant difference ($p < 0.05$) in size of the profiles could be detected, using the Kruskal–Wallis and Dunn's multiple comparison test. A straight line fitted to the mean values for the analyzed animals had a slope that did not significantly deviate from zero ($r^2 = 0.0008$), suggesting that above the threshold for injury there is not a linear relationship between acceleration and mean size of the β-APP-positive profiles (**Figure 5**). Thus, increased acceleration does not seem to increase the size of the profiles.

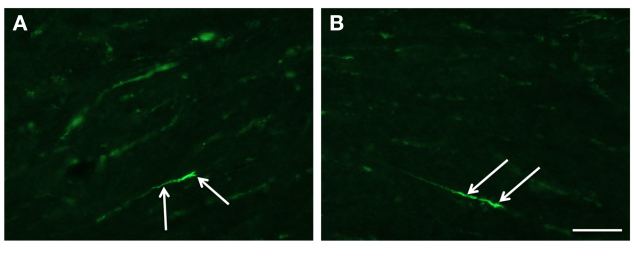

FIGURE 4 | Fluorescence micrographs of sagittal plane sections from the pyramidal tract in brain stem incubated with β-APP (scale bar = 50 μm; magnification in (A) = (B)). Twenty-four hours after high acceleration trauma a number of β-APP-positive axons are present (arrows).

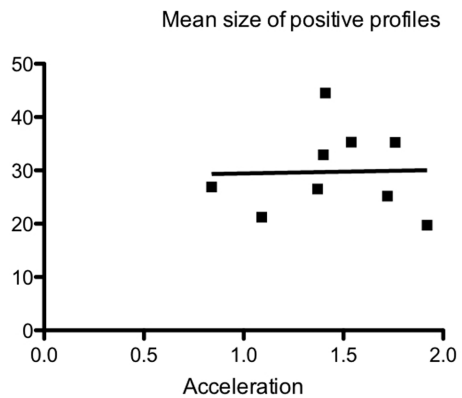

FIGURE 5 | Relationship between maximum acceleration and mean size of β-APP-positive profiles at the border between corpus callosum and subcortical white matter, using the ABC method and image analysis, in nine animals 24 h after trauma. The mean size (μm²) of the analyzed profiles has been plotted against the acceleration. No correlation between size and acceleration was found.

The acceleration trauma also resulted in axonal FD silver labeling in the pyramid tracts in the brainstem (**Figure 6**). This was detected 7 days after severe trauma. It is most likely that silver labeled axons were present in other locations of the brain as well and perhaps at slightly shorter survival times. The silver labeling has not been analyzed in detail at present.

For the average levels of β-APP-positive axons, as determined according to the grading scheme previously presented (**Table 3**), a clear dose-response pattern can be observed; for β-APP-positive axons the increase starts at 1.1 Mrad/s^2 (**Figure 9**).

INFLAMMATORY RESPONSE

An intense induction of COX2 mRNA following trauma was observed in the dentate gyrus within 3 h after trauma (**Figure 7**). A less intensive induction could be detected in some regions of the cortex and the basilar region. This was in contrast to what could be observed in the sham operated animals in which few or no cells were labeled. In the frontal sections, the COX2 was found mainly in the cingulated cortex and in the lateral regions of the cortex. In the middle sections, reactivity was found in the dentate gyrus, putamen/hippocampus region, and lateral regions of the cortex. In the occipital sections mainly the lateral regions of the cortex exhibited COX2 positive cells. The average levels of COX2 intensity, as subjectively determined according to the grading scheme

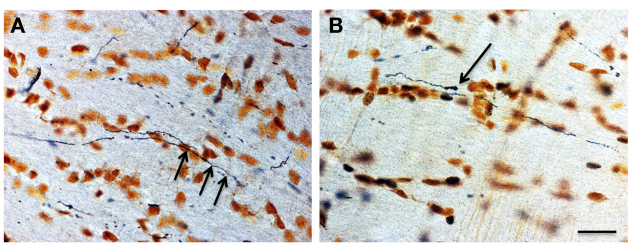

FIGURE 6 | Sections from the pyramidal tract. The micrographs show degenerating axons [**(A)** arrows] in the pyramidal tract 5 days after high level trauma, as revealed with the FD silver method. The axon in **(B)** had the appearance of an endbulb (scale bar = 25 μm; magnification in A = B).

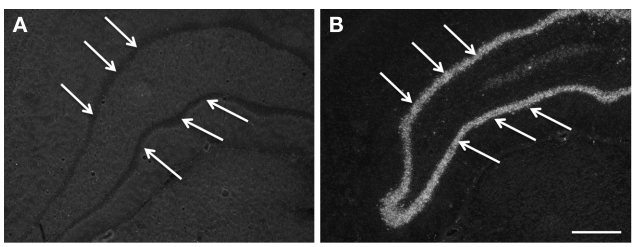

FIGURE 7 | Images, captured in darkfield microscopy, of coronal plane occipital sections of the dentate gyrus (arrows) after *in situ* hybridization for COX2 mRNA. (A) is a section from an animal exposed to a 0.7-Mrad/s^2 rotational acceleration, whereas **(B)** shows a section from an animal exposed to a severe rotational trauma (scale bar = 500 μm; A = B). Note the absence of a signal in **(A)** and the intense signal in the dentate gyrus in **(B)**.

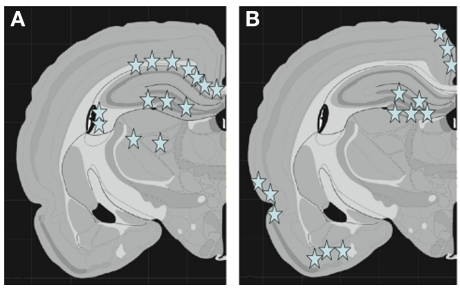

FIGURE 8 | Schematic graphs showing the middle coronal section of the rat brain. In **(A)** the stars indicate the localization of β-APP-positive axons. Note the distribution of positive profiles in corpus callosum, hippocampus, and thalamus. In **(B)** stars indicate the localization of cells with high expression of of COX2 mRNA. Note the high expression in dentate gyrus, cingulate cortex, as well as lateral and basal cortex.

previously presented (**Table 3**), increase with rotational acceleration (**Figure 9**). A clear dose-response pattern can be observed; for COX2 intensity the increase starts at around 0.9 Mrad/s^2.

OTHER INJURIES

During sacrifice, hemorrhages were visible in the foramen magnum region; subdural and subarachnoid hemorrhages were observed on the superior cortex surface in slightly less than half of the exposed animals. A few animals suffered from hemorrhages in the vicinity of the olfactory bulb.

No invasions of ED1 positive macrophages or BBB changes could be observed. Macrophages were only very sparsely observed in the basal region of the brain and in a limited number of animals that had been exposed to high rotational acceleration.

Two repeated analyses of the total S100B levels revealed an increase when the maximum head acceleration was above 0.8 Mrad/s^2 (**Figure 9**) whereas three repeated analyses of S100BB serum levels showed an increase when the acceleration was above 0.9 Mrad/s^2.

DISCUSSION

The experimental data reveal that the new model produces graded injury. β-APP-positive axons and COX2 positive neurons were observed in the brain tissue and an increase of S100B in serum was detected when the rearward rotational acceleration was above 1.0 Mrad/s^2 and the pulse duration was 0.4 ms (**Figure 9**). Increasing the trauma level resulted in prominent levels of β-APP, COX2, and S100B (**Figure 9**).

DIFFUSE AXONAL INJURY

Loads to an axon may cause an immediate axotomy, where the axons and myelin are simultaneously and directly damaged at the site of lesion, or a delayed disruptive injury to the axons. The latter is the most common type of injury to axons in animal models (Maxwell et al., 1993) and is commonly associated with axonal swelling whereas the former is associated with axonal bulbs. These swellings are a consequence of a sequence of events that includes perturbation to the axolemma, formation of nodal blebs, changes to the neurofilament structures and separation of the axolemma from the myelin sheath. Swelling occurs when the axonal transport system is affected which leads to the accumulation of transport material such as proteins and enzymes along the axons. The sequence may end with axonal disconnection and formation of axonal bulbs. Delayed or secondary axotomy is an important feature of TBI and DAI. This axonal injury is now known to be a complex array of responses to injuries of varying severity. In some cases, only the axonal cytoskeleton is injured and in other cases the adjacent axolemma show alterations in permeability, which may contribute to the disconnection of the affected axons. The timetable for such events is varying but can be assumed to continue for days (Farkas and Povlishock, 2007). We have not established the timetable for secondary axotomy in the present experiments. The presence of β-APP-positive profiles is assumed to be a good indicator of disrupted axonal transport, whereas the silver staining represents a marker for disconnected axons following the secondary axotomy.

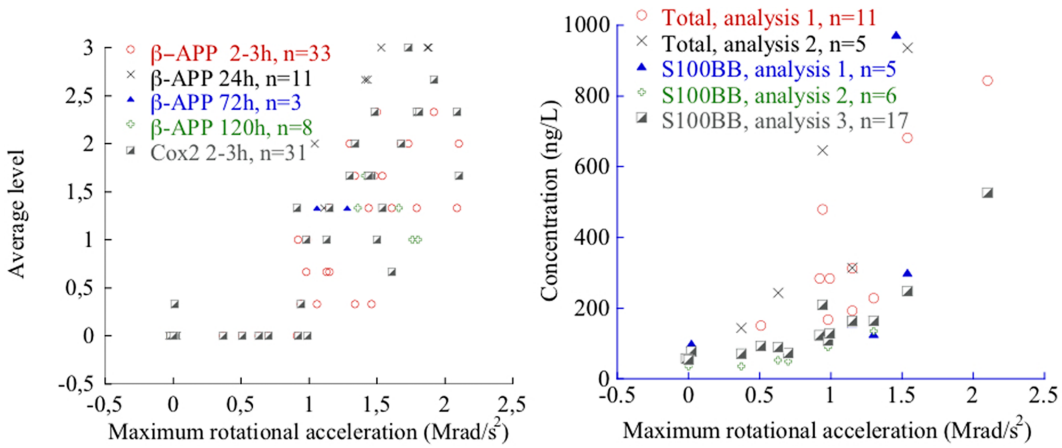

FIGURE 9 | β-APP and COX2 levels (left) and total S100B and S100BB levels after 2–3 h survival time (right) as a function of maximum rotational acceleration. Note that in the left plot, 12 sham exposed controls are included that all exhibited zero level β-APP and three sham exposed controls are included that all exhibited zero level of COX2. For one animal extremely high total S100B and S100 BB values were measured and are not depicted for clarity.

In this study mainly three types of β-APP accumulations were present. These were used to assess risk of axonal injuries (AI) in the brain tissue following rotational trauma. In coronal sections dot like β-APP spots were found on the border between the corpus callosum and the cortex. Furthermore, axons that appeared swollen could be found in the corpus callosum (**Figure 3**). The dot like appearance was evidently a result of the fact that most of the effected axons were cut (**Figure 3**). In sagittal sections of the brain stem, axons with swollen appearance were found in abundance (**Figure 4**). There is no doubt that the new trauma model produces AI. Numerous studies have shown that β-APP is produced in neurons. The β-APP is transported distally in the axon and following an AI it accumulates at the site of injury (Gentleman et al., 1993; Blumbergs et al., 1994). However, due to the fact that most sections studied were coronal, the β-APP analysis alone is not enough to determine whether the new model mainly gave rise to secondary axotomy as a result of perturbation to the axolemma or also produced immediate axotomy.

To shed some light on this, tissue from a limited number of animals was stained using FD silver. The results confirmed the observations found after staining for β-APP and indicate that many of the injured axons degenerate after 7 days survival time. Future studies using stains to study filament changes (e.g., neurofilament and tubulin), as well as electron microscopy will be adopted to validate the method used to detect injury and to further assess the distribution of primary and secondary axotomy.

β-APP-positive axons were found in the edges of and inside the corpus callosum. The largest numbers were found in the superior edges of the frontal region of the corpus callosum. The distribution of injured axons may be an effect of the induced shearing and straining of the tissue during the trauma or/and may reflect an uneven distribution of axons as well as axons of different sizes. An overall density decline from the anterior to the posterior region of the corpus callosum was observed in a study by Riise and Pakkenberg (2011). These authors also found an inverse relationship between the distribution of large and small fibers.

The β-APP-positive profiles could be detected at a lower magnification in animals subjected to a higher acceleration injury. In fluorescence microscopy these profiles appeared larger. However, using ABC for β-APP and image analysis it was observed that there was no difference in mean size of β-APP-positive profiles between animals subjected to different levels of acceleration. This would imply that an intensity difference rather than a size difference can explain why the profiles can be detected by fluorescence microscopy at a lower magnification in animals that have sustained a higher acceleration. Unfortunately, we have no reliable method to measure the intensity in the fluorescence signal, but the possibility that a larger acceleration injury might induce a more drastic accumulation of β-APP that could lead to a higher concentration of the protein cannot be ignored.

The localization of the affected axons in this study partly resembles those commonly reported in the literature following DAI Grade I: characterized by microscopical AI mainly in the corpus callosum and the parasagittal white matter (Adams et al., 1989). The near absence of positive axons in the white matter of the cerebral hemispheres in this study may reflect species differences. Alternatively, they do not appear after the type of trauma used in this study. It has also been reported that DAI is associated with lesions in the brain stem and cerebellum (DAI Grade 3). Preliminary findings, including β-APP-positive axons, FD silver labeled axons, and GFAP changes in the upper brainstem region as studied in about 10 animals suggest that the model also produces DAI grade 3.

Based on the histological findings in this study we are confident that the model used in this study produces DAI since distributed AI are produced in representative regions of the brain and brainstem. Future studies will further categorize the extent of the axonal injury produced by this trauma model.

INFLAMMATORY RESPONSE

Cyclooxygenase converts arachidonic acid to prostaglandin H2, a precursor of the prostanoids, which is a subclass of eicosanoids that includes prostaglandins, thromboxane and prostacyclin. Different COX isoenzymes are known. COX1 is a constitutive enzyme in most mammalian cell types, whereas COX2 is an enzyme that can be induced in macrophages and other cells at sites of inflammation or injury. Our observation of an upregulation of COX2 mRNA in areas such as the dentate gyrus after rotational TBI is compatible with our previous observation that gene clusters relating to inflammation show a significantly changed expression in the hippocampus after this type of injury (Risling et al., 2011). Future behavioral studies tailored to study memory deficiencies and anxiety reactions, e.g., radial maze and elevated plus, will be adopted to assess the effects of the observed inflammation in the hippocampus region following rotational trauma.

OTHER INJURIES

Some previous studies classify brain injury according to the presence of neuropathological changes and the frequency and duration of unconsciousness following trauma (Ono et al., 1980; Gennarelli et al., 1982). In this study the severity of the concussion was not assessed and as such makes a direct comparison difficult.

Contusions have been present following rotational trauma in studies in the past. In this study tissue stained to study astrocyte changes, macrophage invasions, and permeability of BBB indicated that there were no contusions related to the trauma.

Preliminary results from a behavioral study, in which changes to the balance was assessed using a beam walk test, indicate that no major neck muscle injuries or inner ear injuries occurred during the rotational trauma (manuscript in preparation Risling et al., 2011).

Hemorrhages were observed in the foramen magnum region in a large proportion of the animals after the very first few tests using this model. To reduce these injuries, head rearward rotation was limited to approximately 20° during the trauma. Also, the mounting position of the skull cap had an effect on these injuries; when the head center of rotation was shifted forward there were more hemorrhages in the meninges in the brainstem region and also an increased number of deaths immediately after trauma. In a limited number of cases, hemorrhages were also found in the meninges surrounding the olfactory bulbs and on the top of the hemispheres. The incidence rate of hemorrhages did not appear to correlate to the head angle or the position of the center of rotation. Similarly,

only an insignificant correlation between the extent of hemorrhages and rotational acceleration was observed: no hemorrhages were found in unexposed control animals, but they were observed in some of the animals when exposed to rotational trauma above 0.6 Mrad/s^2.

Following moderate level of rotational head trauma we recorded elevated S100B and S100BB levels in serum despite the absence of obvious BBB injuries. The trauma could result in minor BBB injuries, which was not detectable using traditional histology, responsible for the S100B leakage. Future studies using MRI may shed some light on this discrepancy.

In this study, we have shown that the developed model produces axonal injury as detected by β-APP-positive axons and a possible inflammatory response as we have seen an intense induction of COX2 stained nerve cells. In addition we have measured a steady increase in concentrations of S100B and S100BB in serum following rotational acceleration trauma. Since the three markers become apparent and abundant in a rather narrow trauma severity interval, it may be suggested that the three markers indicate one single type of brain tissue injury. This injury would most likely be injuries to the axons, but could also be a combination of AI and contusion injuries to the surface of the brain. However, as mentioned earlier, no macrophage invasion or BBB changes could be observed and COX2 stained nerve cells along the periphery of the brain were only observed sparsely in the basal regions of the brain. These observations indicate that the model produces AI with only minor contusion injuries.

CONCLUSION

We conclude that the developed animal model is capable of producing graded DAI with limited contusion injury. We also conclude that the model is inexpensive to use and produces a reproducible injury panorama. The animal model produces AI mainly in the corpus callosum, on the upper and lower boundaries of the corpus callosum, and in the brain stem, which commonly has been reported in studies of DAI.

ACKNOWLEDGMENTS

The study was funded by Karolinska Institutet, APROSYS 6th Frame Work, The Swedish Armed Forces and Vinnova, Sweden. We thank Mrs. Maria Angeria for excellent technical assistance and Viktoria Hammarstedt for editorial help.

REFERENCES

Abel, J. M., Gennarelli, T. A., and Segawa, H. (1978). "Incidence and severity of cerebral concussion in the rhesus monkey following sagittal plane angular acceleration," in *Proceedings of the 22nd Stapp Car Crash Conference*, Ann Arbor: MI, 780886, 35–53.

Adams, J. H., Doyle, D., and Ford, I. (1989). Diffuse axonal injury in head injury: definition, diagnosis and grading. *Histopathology* 15, 49–59.

Andersson, R. W. G. (2000). *A Study on the Biomechanics of Axonal Injury*. Thesis, University of Adelaide.

Blumbergs, P. C., Scott, G., Manavis, J., Wainwright, H., Simpson, D. A., and McLean, A. J. (1994). Staining of amyloid precursor protein to study axonal damage in mild head injury. *Lancet* 344, 1055–1056.

Davidsson, J. (2008). *A New Model, Experiments and Injury Threshold for Sagittal Plane Rotational Induced Diffuse Brain Injuries*. Report No. AP-SP51-0045, Generated in Project The 6th Frame Work EU-project APROSYS. Available at: http://www.aprosys.com/

Ellingson, B. M., Fijalkowski, R. J., Pintar, F. A., Yoganandan, N., and Gennarelli, T. A. (2005). New mechanism for inducing closed head injury in the rat. *Biomed. Sci. Instrum.* 41, 86–91. PMID: 15850087.

Farkas, O., and Povlishock, J. T. (2007). Cellular and subcellular change evoked by diffuse traumatic brain injury: a complex web of change extending far beyond focal damage. *Prog. Brain Res.* 161, 43–59.

Fijalkowski, R. J., Stemper, B. D., Pintar, F. A., Yoganandan, N., Crowe, M. J., and Gennarelli, T. A. (2007). New rat model for diffuse brain injury using coronal plane angular acceleration. *J. Neurotrauma* 24, 1387–1398.

Foda, M. A., and Marmarou, A. (1994). A new model of diffuse brain injury in rats. Part II: morphological characterization. *J. Neurosurg.* 80, 301–313.

Gennarelli, T. A., and Thibault, L. E. (1982). Biomechanics of subdural hematoma. *J. Trauma* 22, 680–686.

Gennarelli, T. A., Thibault, L. E., Adams, J. H., Graham, D. I., Thompson, C. J., and Marcincin, R. P. (1982). Diffuse axonal injury and traumatic coma in the primate. *Ann. Neurol.* 12, 564–574.

Gentleman, S. M., Nash, M. J., Sweeting, C. J., Graham, D. I., and Roberts, G. W. (1993). Beta-amyloid precursor protein (beta APP) as a marker for axonal injury after head injury. *Neurosci. Lett.* 160, 139–144.

Gutierrez, E., Huang, Y., Haglid, K., Bao, F., Hansson, H. A., Hamberger, A., and Viano, D. (2001). A new model for diffuse brain injury by rotational acceleration. *J. Neurotrauma* 18, 247–257.

Hamberger, A., Huang, Y. L., Zhu, H., Bao, F., Ding, M., Blennow, K., Olsson, A., Hansson, H. A., Viano, D., and Haglid, K. G. (2003). Redistribution of neurofilaments and accumulation of beta-amyloid protein after brain injury by rotational acceleration of the head. *J. Neurotrauma* 20, 169–178.

Hansson, H. A., Höjer, S., and Krave, U. (2003). "Increased neurogenesis and diffuse brain damage after rotational acceleration of the head," in *The 21st Annual National Neurotrauma Society Symposium*, Biloxi, MS.

Holbourn, A. H. (1943). Mechanics of head injuries. *Lancet* 2, 438–441.

Ingebrigtsen, T., Romner, B., Marup-Jensen, S., Dons, M., Lundqvist, C., Bellner, J., Alling, C., and Børgesen, S. E. (2000). The clinical value of serum S-100 protein measurements in minor head injury: a Scandinavian multicentre study. *Brain Inj.* 14, 1047–1055.

Kleiven, S. (2007). "Predictors for traumatic brain injuries evaluated through accident reconstructions," in *Proceedings of the 51st Stapp Car Crash Conference*, San Diego: CA, Vol. 51, 07S–27S.

Krave, U., Al-Olama, M., and Hansson, H. A. (2011). Rotational acceleration closed head flexion trauma generates more extensive diffuse brain injury than extension trauma. *J. Neurotrauma* 28, 57–70.

Krave, U., Höjer, S., and Hansson, H. A. (2005). Transient, powerful pressures are generated in the brain by a rotational acceleration impulse to the head. *Eur. J. Neurosci.* 21, 2876–2882.

Margulies, S. S., and Thibault, L. E. (1992). A proposed tolerance criterion for diffuse axonal injury in man. *J. Biomech.* 25, 917–923.

Margulies, S. S., Thibault, L. E., and Gennarelli, T. A. (1990). Physical model simulations of brain injury in the primate. *J. Biomech.* 23, 823–836.

Marmarou, A., Foda, M. A., van den Brink, W., Campbell, J., Kita, H., Demetriadou, K., Maxwell, W. L., Watt, C., Graham, D. I., and Gennarelli, T. A. (1994). A new model of diffuse brain injury in rats. Part I: pathophysiology and biomechanics. *J. Neurosurg.* 80, 291–300.

Maxwell, W. L., Watt, C., Graham, D. I., and Gennarelli, T. A. (1993). Ultrastructural evidence of axonal shearing as a result of lateral acceleration of the head in non-human primates. *Acta Neuropathol.* 86, 136–144.

Meaney, D. F., Smith, D., Ross, D. T., and Gennarelli, T. A. (1993). "Diffuse axonal injury in the miniature pig: biomechanical development and injury threshold," in *Crashworthiness and Occupant Protection in Transportation Systems*, Eds J. D. Reid and K. H. Yang (NewYork: American Society of Mechanical Engineers), AMD-Vol. 169/BED-Vol. 25 (ASME), 169175.

Meaney, D. F., Smith, D. H., and Shreiber, D. I. (1995). Biomechanical analysis of experimental diffuse axonal injury. *J. Neurotrauma* 12, 689–694.

Melvin, J., Lighthall, W. J., and Ueno, K. (1993).*Accidental Injury, Biomechanics and Prevention*. New York: Springer-Verlag.

Ommaya, A. K. (1984). "The head: kinematics and brain injury mechanisms," in *The Biomechanics and Impact Trauma*, eds B. Aldman and A. Chapon (Amsterdam: Elsevier), 117–125.

Ono, K., Kikuchi, A., Nakamura, M., Kobayashi, H., and Nakamura, N. (1980). "Human head tolerance to sagittal impact reliable estimation deduced from experimental head injury using subhuman primates and human cadaver skulls," in *Proceedings of the 24th STAPP Car Crash Conference*, Troy: MI, 801303, 101–160.

Povlishock, J. T. (1992). Traumatically induced axonal injury: pathogenesis and pathobiological implications. *Brain Pathol.* 2, 1–12.

Povlishock, J. T., and Jenkins, L. W. (1995). Are the pathobiological changes evoked by traumatic brain injury immediate and irreversible? *Brain Pathol.*5, 415–426.

Riise, J., and Pakkenberg, B. (2011). Stereological estimation of the total number of myelinated callosal fibers in human subjects. *J. Anat.* 218, 277–284.

Risling, M., Planman, S., Angeria, M., Rostami, E., Bellander, Kirkegaard, M., Arborelius, U., and Davidsson, J. (2011). Mechanisms of blast induced brain injuries, experimental studies in rats. *Neuroimage* 54S1, S89–S97.

Ross, D. T., Meaney, D. F., Sabol, M. K., Smith, D. H., and Gennarelli, T. A. (1994). Distribution of forebrain diffuse axonal injury following inertial closed head injury in miniature swine. *Exp. Neurol.* 126, 291–299.

Runnerstam, M., Bao, F., Huang, Y., Shi, J., Gutierrez, E., Hamberger, A., Hansson, H. A., Viano, D., and Haglid, K. (2001). A new model for diffuse brain injury by rotational acceleration: II. Effects on extracellular glutamate, intracranial pressure, and neuronal apoptosis. *J. Neurotrauma* 18, 259–273.

Smith, D. H., Chen, X. H., Xu, B. N., McIntosh, T. K., Gennarelli, T. A., and Meaney, D. F. (1997). Characterization of diffuse axonal pathology and selective hippocampal damage following inertial brain trauma in the pig. *J. Neuropathol. Exp. Neurol.* 56, 822–834.

Smith, D. H., and Meaney, D. F. (2000). Axonal damage in traumatic brain injury. *Neuroscientist* 6, 483–495.

Strich, S. J. (1961). Shearing of nerve fibres as a cause of brain damage due to head injury. *Lancet* 2, 443.

Viano, D. C. (1997). *Brain Injury Biomechanics in Closed-Head Impact.* Ph.D. thesis, Karolinska Institute, Solna.

Wismans, J., Janssen, E., Beusenberg, M., and Bovendeerd, P. (2000). *Injury Bio-Mechanics.* Course Book w5-pp3-4.3, Eindhoven: Eindhoven Technical University.

Xiao-Sheng, H., Sheng-Yu, Y., Xiang, Z., Zhou, F., and Jian-ning, Z. (2000). Diffuse axonal injury due to lateral head rotation in a rat model. *J. Neurosurg.* 93, 626–633.

Zhang, L., Yang, K. H., and King, A. I. (2004). A proposed new injury tolerance for mild traumatic brain injury. *J. Biomech. Eng.* 126, 226–236.

Conflict of Interest Statement: The authors declare that the research was conducted in the absence of any commercial or financial relationships that could be construed as a potential conflict of interest.

Received: 01 February 2011; paper pending published: 18 February 2011; accepted: 08 June 2011; published online: 17 June 2011.

Citation: Davidsson J and Risling M (2011) A new model to produce sagittal plane rotational induced diffuse axonal injuries. Front. Neur. ***2****:41. doi: 10.3389/fneur.2011.00041*

This article was submitted to Frontiers in Neurotrauma, a specialty of Frontiers in Neurology.

frontiers in
NEUROLOGY

REVIEW ARTICLE
published: 28 March 2011
doi: 10.3389/fneur.2011.00015

"Studying injured minds" – the Vietnam head injury study and 40 years of brain injury research

Vanessa Raymont[1,2,3], Andres M. Salazar[2], Frank Krueger[2] and Jordan Grafman[2,4]*

[1] *Vietnam Head Injury Study, Henry M. Jackson Foundation, National Naval Medical Center, Bethesda, MD, USA*
[2] *Cognitive Neuroscience Section, National Institute of Neurological Disorders and Stroke, National Institutes of Health, Bethesda, MD, USA*
[3] *Department of Radiology, Johns Hopkins University, Baltimore, MD, USA*
[4] *Traumatic Brain Injury Research Laboratory, Kessler Foundation, West Orange, NJ, USA*

Edited by:
Ibolja Cernak, Johns Hopkins University, USA

Reviewed by:
Jeffrey J. Bazarian, University of Rochester, USA
Vassilis E. Koliatsos, Johns Hopkins University School of Medicine, USA
Harvey S. Levin, Baylor College of Medicine, USA

***Correspondence:**
Jordan Grafman, Traumatic Brain Injury Research Laboratory, Kessler Foundation, 1199 Pleasant Valley Road, West Orange, NJ 07052, USA. e-mail: jgrafman@kesslerfoundation.org

The study of those who have sustained traumatic brain injuries (TBI) during military conflicts has greatly facilitated research in the fields of neuropsychology, neurosurgery, psychiatry, neurology, and neuroimaging. The Vietnam Head Injury Study (VHIS) is a prospective, long-term follow-up study of a cohort of 1,221 Vietnam veterans with mostly penetrating brain injuries, which has stretched over more than 40 years. The scope of this study, both in terms of the types of injury and fields of examination, has been extremely broad. It has been instrumental in extending the field of TBI research and in exposing pressing medical and social issues that affect those who suffer such injuries. This review summarizes the history of conflict-related TBI research and the VHIS to date, as well as the vast range of important findings the VHIS has established.

Keywords: brain imaging, brain injury, brain lesion, neuropsychology

THE RECENT HISTORY OF COMBAT-RELATED TBI RESEARCH

Traumatic brain injury (TBI) is the principal cause of death and disability in those under 35 in the USA. Each year TBI leads to approximately 55,000 deaths, as well as 50,000 cases of associated physical, cognitive, behavioral, and social deficits (Kraus and McArthur, 1996). TBI remains extremely prevalent in combat situations, with nearly two-thirds of injured US soldiers sent from Iraq to Walter Reed Army Medical Center sustaining TBI (Warden, 2006). As recently as 2009, it was quoted that "Head injury has always been, and remains, an unpopular subject with British neurologists, presumably because they tend to see it as a surgical rather than a medical disorder." (van Gijn, 2009). Fortunately this has not been the case for all neurologists. Much of what is known about TBI (e.g., the clinical course, cognitive changes, incidence of post-traumatic epilepsy, PTE) is in fact as a result of neurological studies in military populations. The First World War was the first conflict that led to a major move forward in the study of TBI because of the sheer quantity of casualties, the extent of trench warfare (and so vulnerability to head injuries), the unprecedented use of artillery, and a change to small, low velocity ammunition, which tended to create focal injuries. In addition, advances in the field of neurosurgery meant penetrating head wounds were no longer inevitably fatal. Gordon Holmes, a London neurologist described several groups of First World War veterans, including 23 cases of occipital lesions (Lepore, 1994). This led to what became the standard illustration of the cortical map of the retina (Holmes and Lister, 1916). Henry Head, another English neurologist, had conducted pioneering work into the somatosensory system prior to the First World War, and he expanded this work with George Riddoch by testing reflex activities of isolated portions of the spine subjected to gunshot wounds (Holmes, 1941). Across the channel, brain injury rehabilitation units in Frankfurt and Cologne were responsible for major innovations in neuropsychological assessments and rehabilitation techniques (Boake and Diller, 2005).

During the Second World War, the Russian psychologist Aleksandr Luria examined psychological dysfunctions in patients with brain lesions, and his work gave impetus to the emerging field of neuropsychology. Luria's early work with Zazetsky (Luria, 1972), an ex-soldier who tried to make sense of his "shattered world" predated interest by others in the personal experience of those with TBI. Hans-Lukas Teuber and Morris Bender focused on visual deficits (Bender and Teuber, 1948) and long-term outcome from TBI (Teuber, 1975). Teuber was the first to report on the role of preinjury intelligence in cognition post-TBI (Weinstein and Teuber, 1957), and he also introduced was that of double dissociation of function, which has since become essential to functional localization (Lackner, 2009). Suzanne Corkin started assessing Second World War veterans while working for Teuber. She subsequently commented on the long-term prognosis of TBI, and developed the concept of exacerbated decline in intelligence post-TBI (Corkin et al., 1984, 1989). Her work with conflict-associated TBI was continued by Newcombe and Marshall in Second World War veterans, and later, in Korean War veterans. They focused on language difficulties post-TBI (Newcombe et al., 1971), long-term outcome, and rehabilitation (Newcombe et al., 1980). Their research helped develop a new classification for acquired alexias and lead to the conceptualization of the dual routes of visual processing that Ungerleiter and Mishkin later formalized in their

theory (Mishkin, 1972). The neuropsychiatrist, Lishman (1992), was another early proponent of TBI research, and was amongst the first who examined social behavior changes following TBI.

HISTORY OF THE VIETNAM HEAD INJURY STUDY

SET UP AND PHASE 1

The Vietnam Head Injury Study (VHIS) was set up by William F. Caveness, a neurologist and retired Naval Reserve captain who had served in the Korean War, who was chief of the Laboratory of Experimental Neurology at the National Institute of Neurological and Communicative Disorders and Stroke from 1965. He designed the VHIS registry, which gathered information on 1,221 Vietnam veterans who sustained a TBI between 1967 and 1970 (Caveness et al., 1979). Of the 58,000 US combat fatalities in the Vietnam War, about 40% were due to head and neck wounds. The Vietnam conflict was the first that involved large scale helicopter evacuations and early treatment by neurosurgical teams close to the battlefield, so that most patients received definitive treatment with hours of their injuries, allowing a much higher rate of survival than in previous conflicts (Carey et al., 1982; Rish et al., 1983). In addition, the low velocity penetrating fragment wounds typically sustained resulted in relatively focal defects, and so these subjects provided a particularly large and informative group for study. It should be noted, therefore, that the data from this cohort addresses issues predominantly affecting those with penetrating TBI. This may contrast with closed injuries, which are considerably commoner in the civilian population and especially in mild cases lack some of the frequent, significant sequelae of penetrating TBI, such as impaired consciousness. Caveness requested that field neurosurgeons complete registry forms on those they anticipated would survive, detailing wound characteristics and neurological status immediately post-injury. Although he received around 2,000 registry forms, addresses could only be found for 1,221. Phase 1 (PH1) of the VHIS was a retrospective review of those subjects' military and veterans affairs (VA) medical records from the 5-years post-injury (e.g., Caveness et al., 1979; Weiss et al., 1983, 1986). Patients were excluded if they had a spinal cord injury or if insufficient medical records were available. Caveness set up the VHIS to primarily study the causes of PTE but unfortunately died before the beginning of Phase 2 (PH2; e.g., Caveness et al., 1979; Rish et al., 1979, 1980, 1981; Mohr et al., 1980). The team of investigators that inherited the VHIS subsequently expanded the scope of the study well beyond his original focus.

PHASE 2 – 15 YEARS ON

Phase 2 evaluated 520 head-injured subjects from the original registry who responded to mailings, as well as 85 uninjured Vietnam veteran control subjects, matched by age. Of those who did not come to PH2, some had died, some declined, and some did not respond; 92% had penetrating head injuries (e.g., Grafman et al., 1986a, 1988, 1992; Salazar et al., 1987). Analysis of subjects who did and did not participate in PH2 showed no significant differences in terms of demographics or lesion type (Jonas et al., 1987). Subjects attended Walter Reed Army Medical Center, Washington, DC, USA for a 1-week evaluation, which consisted of neuropsychological, neurological, language, and brain imaging assessments. Specific subgroups and individual patients have returned more often for selected studies between each phase following PH2.

PHASE 3 – 35 YEARS POST-TBI

Of the 520 head-injured subjects assessed at PH2, 484 were still alive, and 182 attended Phase 3 (PH3). Additionally, 17 head-injured subjects identified in PH1 that did not attend PH2 were assessed. Of the original 80 control subjects recruited in PH2, 32 attended and a further 23 were recruited. Subjects were assessed at the National Naval Medical Center, Bethesda, MD, USA, with a broad battery of neuropsychological, neurological, psychiatric, and imaging assessments. Brain lesions were identified by CT scan, and the data were reconstructed with a 3-mm overlapping slice thickness and a 1-mm interval. MRI scans were not used as a large number of the subjects had retained metal in their brains. Lesions were processed using "analysis of brain lesions" software (ABLe; Makale et al., 2002; Solomon et al., 2007). Within ABLe, the lesions were drawn manually in native space on each 1 mm thick slice by Vanessa Raymont (a psychiatrist with clinical experience of reading CT scans), and reviewed by Jordan Grafman, enabling a consensus decision to be reached regarding the limits of each lesion. Normalized lesion volume was calculated, and the percentage of brain lobes and regions involved determined. This methodology is explained further in our earlier paper (Raymont et al., 2008). However, this meant that the assessment of these lesions was to some extent dependent on subjective measurements.

PHASE 4 – 40+ YEARS LATER

Subjects from PH3 were invited to attend for Phase 4 (PH4) of the VHIS, approximately 40–45 years post-injury. PH4 is currently in progress at the National Institute of Neurological Disorders and Stroke in Bethesda, MD, USA, and contains a core set of tasks that are similar to those previously administered in PH2 and PH3, so longitudinal assessments can be completed. In addition, further molecular genetic studies are planned that examine the role of genetic polymorphisms in recovery of function from TBI and in predicting various kinds of outcomes. Experimental cognitive neuroscience studies in PH4 will expand upon previous work in social neuroscience, examining the brain areas associated with certain forms of economic decision-making, human belief systems and moral thinking, social status, and aggression. In addition, PH4 will examine the role of caregiver personality in outcome after combat-related TBI. We hope that these studies contribute to the emerging fields of social neuroscience and behavioral genetics, and lead to improved management and outcome of the patient with a TBI. Although there was no evidence of Alzheimer's disease (AD) in this cohort at PH3, given the evidence of links between AD and TBI (Lindsay et al., 2002), Ann McKee, a neuropathologist from Boston University has also agreed to conduct autopsies on the brains of all VHIS subjects who consent. This will provide yet another dimension to the study by examining the causes and effects of long-term pathological changes following TBI, including the development of abnormal Tau deposits.

The advantages of studying this population have included their uniformity of age, gender, and education at time of injury, as well as the availability of preinjury intelligence data, making this a unique population for longitudinal assessment.

SELECTED FINDINGS FROM THE VHIS

One great advantage of the VHIS is that it has allowed the collection of a vast amount of data from a large cohort, which can subsequently be used to help answer basic neuropsychological questions (e.g., Rueckert and Grafman, 1996, 1998; Dimitrov et al., 1999; Lee et al., 1999). Over 80 papers have been published using VHIS data to date, and many more are expected. Here we describe some selected findings from each phase in order to give the reader a sense of the breadth and depth of our findings.

NEUROSURGICAL FINDINGS

A number of clinical questions regarding acute neurosurgical management were addressed at PH1, and are reviewed elsewhere (Grafman and Salazar, 1999). These include the use of improved protocols for evacuation and triage of large numbers of casualties, aggressive procedures for definitive surgical debridement close to the front, the issues of dural closure, retained metal and bone fragments, incidence and management of brain abscesses, use of antibiotics and anticonvulsants, and the timing of cranioplasty, among others. For example, it was reported that 491 cranioplasties were performed in 1,030 subjects from the registry, with a morbidity rate of 5.5% and a mortality rate was 0.2%, largely associated with surgical outcome (Rish et al., 1979). From these findings it was suggested that cranioplasty after penetrating TBI should be deferred for a minimum of 1 year, to control morbidity. Skull defects or cranioplasty were not found to predict tendency to post-traumatic seizures. In summary, the neurosurgical experience of the Vietnam War marked a turning point in the approach to emergency evacuation and management of severe TBI.

Research at PH2 further investigated the associations of traumatic unconsciousness post-TBI. Surprisingly, only 15% of the 342 subjects who survived severe penetrating TBI had prolonged loss of consciousness. Over half had no or only momentary unconsciousness after injury, and some even remained in battle and received citations for bravery. Over 40% had good recollection of injury events and were also alert at first examination, sometimes in spite of large lesions, further illustrating the largely focal nature of these wounds. The areas most associated with traumatic unconsciousness post-TBI in this cohort included the posterior limb of the left internal capsule, left basal forebrain, midbrain, and hypothalamus (Salazar et al., 1986).

EPILEPSY

Previous studies of World War Two (Walker and Jablon, 1961) and Korean War veterans (Weiss and Caveness, 1972) had confirmed the association between post-traumatic seizures and penetrating TBI. At PH2, of the 421 veterans who had sustained a TBI, 53% had a history of PTE, which had started within a year of TBI in the majority of cases (Salazar et al., 1985). About one-half of the group were still experiencing seizures 15 years after injury. The relative risk of developing PTE dropped from about 580 times higher than the general age-matched population in the first year, to 25 times higher after 10 years, and the frequency of seizures in the first year predicted subsequent severity of seizures. Anticonvulsant therapy with phenytoin in the first year after injury did not prevent later seizures. Patients with focal neurological signs or large lesions had an increased risk of developing PTE. PTE was also associated with the presence of hematoma or retained metal fragments (Weiss et al., 1986). Only five affected brain areas significantly predicted seizure occurrence: right vertex gray matter, left convexity cortex, left temporal gray matter, right frontal white matter, and right corona radiate. Lesions in the left hippocampus correlated with increased seizure frequency, whereas insula and splenium lesions correlated with lower seizure frequency. Lesions of the posterior callosum and caudate nucleus were associated with less persistent seizures. From these data, the authors were able to develop a predictive formula (incorporating data from previous, shorter term studies of risk factors for seizures, all of which suggested that the time between injury and onset of PTE is independent of injury characteristics) for the time between injury and first seizure (**Figure 1**).

$$Q_n = 0.7304 \exp(-0.0915n) + 0.2359 \exp(-0.0001n^2)$$

(Where Q_n=probability of surviving n months after a TBI without developing PTE)

FIGURE 1 | Predictive formula for the risk of developing PTE.

At PH3, the prevalence of seizures in the 199 TBI veterans who attended was 43.7%, similar to that 20 years earlier (Raymont et al., 2010). Remarkably 12.6% reported initial onset of PTE more than 14 years post-injury. These subjects were not different from earlier onset PTE subjects in any of the clinical measures examined. Within this cohort, the most common seizure type last experienced was complex partial seizures (31.0%), with increasing frequency post-injury. Eighty-eight percentage of subjects with PTE were receiving anticonvulsants. Left parietal lobe lesions and retained ferric metal fragments were associated with PTE and total brain volume loss predicted seizure frequency, although it should be emphasized that there is not substantial evidence in the general literature for lesion location being predictive of PTE.

MOTOR DISORDERS

Motor impairments following TBI are a common problem, which are very limiting to patient functioning. Within the first few months following a unilateral brain lesion affecting the motor cortex, therapeutic efforts are aimed primarily at the restoration of motor function on the hemiplegic side. Following on from the localization work conducted at the time of World War One, research carried out at PH1 reported that parietal wounds were particularly associated with hemiparesis, and that regardless of the features of the hemiparesis initially, the severity of the final syndrome was greatest in the hand and arm and least in the face (Mohr et al., 1980). At PH2, 90 subjects were found to have hemiparesis (Schwab et al., 1993), and in 32% of these subjects this prevented them from working. The relationship of preinjury left-hand dominance to post-injury distal motor skills was examined at PH2 (Grafman et al., 1985a). No persistent deficits were seen on distal motor tasks in left-handed adults who suffered a penetrating TBI, compatible with the previously reported

relative sparing of persistent neuropsychological deficits in left-handed subjects following brain damage. In addition, other results indicated similar long-term functional outcome in right and left hemisphere-damaged subjects, despite more severe contralateral functional motor deficits following lesions of the left hemisphere. These results demonstrated that unilateral TBI involving the motor areas of either hemisphere has detrimental effects on ipsilateral upper extremity motor function, suggesting that the left hemisphere has greater neuronal representation for bilateral motor processes (Smutok et al., 1989).

FATIGUE

Fatigue is a common and disabling symptom following TBI, and studies have suggested that the ventromedial prefrontal cortex (vmPFC) could play a significant role in fatigue pathophysiology. At PH3 it was found that individuals with vmPFC lesions were significantly more fatigued than individuals with dorsolateral prefrontal cortex (dlPFC) lesions, individuals with non-frontal lesions, or healthy controls (Pardini et al., 2010). The larger the lesion volume, the higher the fatigue score. This demonstrated that the vmPFC plays a critical role in penetrating brain injury-related fatigue, and possibly provides a rationale to link fatigue to different vmPFC functions, such as effort and reward perception. In contrast, also at PH3, insomnia was found to be associated with left dorsomedial PFC lesions, presumably due to a disruption of the brain systems sustaining the sleep control mechanisms that are associated with brain stem and other midline structures (Koenigs et al., 2010).

NEUROPSYCHOLOGICAL ASSOCIATIONS

One vital issue that was examined at PH2 was the link between preinjury intelligence (as measured by the Armed Forces Qualification Test, AFQT-7A, 1960; DoD) and lesion characteristics, as well as preservation of cognitive function long-term post-TBI. Grafman et al. (1986a, 1988) reported that post-injury overall intelligence was most predicted by preinjury intelligence, followed by size of lesion, with some controls and a few TBI subjects showing an increase in AFQT score from preinjury to PH2 (**Figure 2**), probably secondary to maturation of the educational abilities tested in the AFQT. Lesion location was least important in predicting overall intelligence 15 years post-injury. For subtest scores of intelligence, lesion location assumed much greater predictive value. Specifically, left temporal and occipital lesions impaired performance on subtests assessing vocabulary and object-function matching ability.

Both cognitive change and return to work at PH2 were significantly related to total brain volume loss, third ventricle width, and septum caudate distance (Groswasser et al., 2002), with volume loss and third ventricle width being the most predictive. This suggests that quantity of brain disruption post-TBI influences long-term recovery of day-to-day functioning.

The same issues were revisited at PH3, via examination of past and current performance on the AFQT and current performance on the Wechsler Adult Intelligence Scale (WAIS-III). Raymont et al. (2008) reported that those with TBI showed a greater degree of overall cognitive decline overall during the years following injury compared with controls, which became increasingly significant

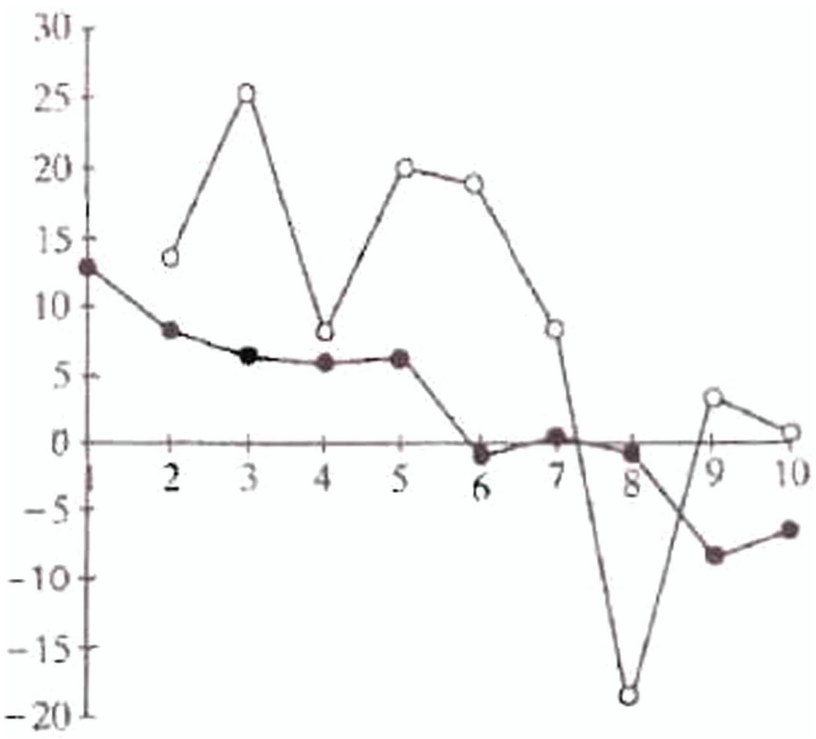

FIGURE 2 | Pre- and PH2 Armed Forces Qualification Test (AFQT) scores in head injured subject (filled circles, $r = -0.32$) and controls (open circles, $r = -0.44$). Plot of pre- to PH2 AFQT differences (D-AFQT) by preinjury AFQT deciles.

later in life. Preinjury intelligence was the most consistent predictor of cognitive outcome and while laterality of lesion was not a factor, there were some predictable associations between atrophy and specific regions of tissue loss and long-term cognitive functioning (see **Figure 3**, which represents the change in intelligence seen in subjects with TBI only).

The VHIS has thus produced some important contributions in terms of theories of neuroplasticity following TBI (Romero et al., 2002). Recent research has emphasized that this takes place via both local restitution, as well as reorganization and compensatory reassignment; processes which may vary at different points in the lifespan. The VHIS has been important in terms of highlighting how these changes may alter with aging, and how they may be impacted by a variety of factors, such as genetic make up (Raymont and Grafman, 2006).

Phase 2 included a review of the long-term outcome of post-TBI aphasia. At PH2, it was reported that aphasia occurred in 244 of the 1,030 patients with TBI, correlating with cause of injury and initial loss of consciousness. The aphasia disappeared within 10 years in 34% of cases. Sensorimotor aphasia usually changed to motor aphasia; motor aphasia disappeared; and sensory aphasia persisted. These improvements continued years after any accompanying hemiparesis stabilized, and were not related to wound site, depth, or whether the wound was caused by gunshot or fragment (Mohr et al., 1980). Chronic non-fluent aphasics demonstrated syntactic processing deficits in all language modalities, with greater posterior extension of their lesions in Wernicke's area, with some involvement of the underlying white matter and basal ganglia in the left hemisphere (Ludlow et al., 1986). This paper also highlighted that that deeper lesions involving the white matter may be the key factor associated with lack of recovery and persistence of language deficits. One PH2 case study also reflected on the localization of calculation knowledge (Grafman et al., 1989). Despite an almost totally destroyed left hemisphere and a severe linguistic disorder, the subject retained the ability to read and write single and two-place digits, perform simple addition and subtraction, accurately judge magnitudes and quantities, and recognize arithmetic operational symbols. This supported the hypothesis of right hemisphere participation in selected aspects of number processing.

Besides more descriptive findings, detailed experiments on the functions of suppression of context-inappropriate meanings

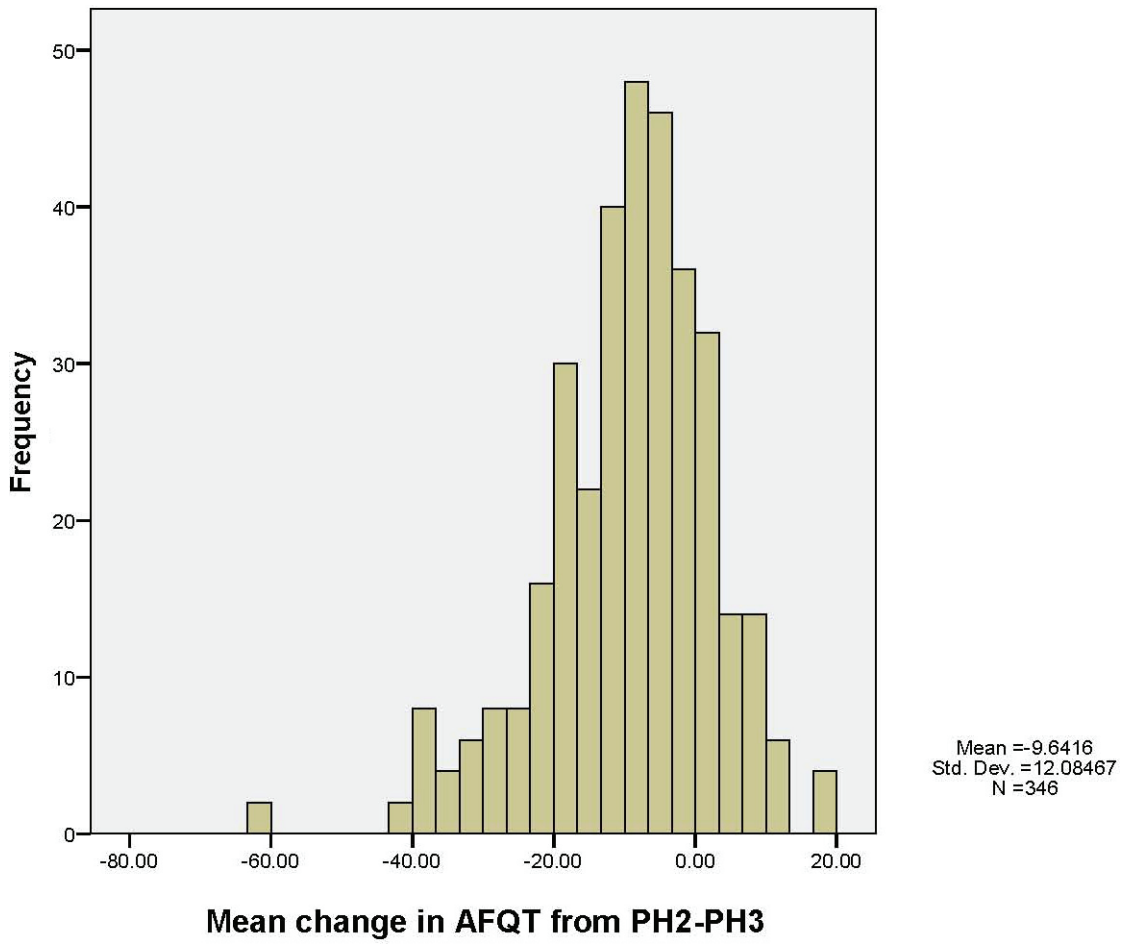

FIGURE 3 | Mean change in AFQT scores from Phase 2 to Phase 3 in subjects with TBI.

during lexical ambiguity resolution were conducted in PH3. Those with prefrontal lesions were found to have significantly lower accuracy rates for context-inappropriate conditions, suggesting a loss of the control aspects of inhibitory processes in lexical ambiguity resolution following prefrontal cortex damage (Frattali et al., 2007).

MEMORY DISORDERS

At PH2, deficits in semantic memory, verbal episodic memory, and visual episodic memory were found to be associated with lesion location, in a manner roughly consistent with the existing neuropsychological literature (Salazar et al., 1986). The advantage of being able to examine isolated brain lesions was vital in enabling the VHIS to identify possible site-specific sources of memory impairment. One case study demonstrated that the fornix cerebri has a role in the maintenance of information accessibility to both encoding and recall during post-working memory processing, as well as in the organization of verbal information (Grafman et al., 1985b). Another explored the basis of facial recognition memory, finding that impairment on tests of face memory was most associated with bilateral lesions and with unilateral lesions of the temporal lobe (Grafman et al., 1986b).

Schooler et al. (2008) used a specific modeling technique; mixture modeling (Muthén and Muthén, 1998–2004), to classify VHIS lesion groups and explore associations with subtypes of memory performance. One striking finding was that marked short term memory deficits were found in all classes of individuals with TBI, regardless of lesion location, and any concomitant effects of depressive symptomatology and substance dependence.

Theories of posterior parietal lobe involvement in memory have evolved over the years. However, definitive neuropsychological evidence supporting the superior parietal lobe's purported role in working memory has been lacking. At PH3, subjects with superior parietal lesions were compared to those with no damage in this region and with control subjects with no history of TBI. Superior parietal damage was associated with deficits on tests involving the manipulation and rearrangement of information in working memory, but not on working memory tests requiring only rehearsal and retrieval processes, nor on tests of long-term memory. These results indicated that the superior parietal cortex is critically important for the manipulation of information in working memory (Koenigs et al., 2009a).

REASONING, DECISION-MAKING, MOOD, AND SOCIAL BEHAVIORAL PLANNING

The large number of subjects with circumscribed frontal lobe lesions in the VHIS enabled both PH2 and PH3 to investigate altered performance on standardized tests of higher cognition. One study of patients with lesions in the prefrontal cortex utilizing the Tower of Hanoi task (Goel and Grafman, 1995) suggested that both subjects with frontal lesions and controls use the same general strategy to solve problems, and that patients' difficulties have little to do with planning deficits (as is generally assumed in the neuropsychology literature). Patient performance was rather explained in terms of an inability to see or resolve a goal–subgoal conflict, which is compatible with several other accounts of frontal lobe dysfunction. In a study of subjects with frontal lobe damage, their performance on the Tower of London task suggested impairment in execution-related processes (Carlin et al., 2000). Such analyses of data collected as part of the VHIS led to further conclusions on the regional contribution of planning and representations, which ultimately lead to novel theories of how the brain represents knowledge and responds to complex events (Goel and Grafman, 2000; Goel et al., 2001; Rattermann et al., 2001; Wood and Grafman, 2003; Wood et al., 2003).

Reasoning

While the role of left prefrontal cortex in reasoning tasks has long been recognized, the role of right prefrontal cortex remains unclear. One study undertaken at PH2 (Goel et al., 2007) found that the right prefrontal cortex plays an essential role in resolving indeterminate relations with no belief-bias cues, a fact that was later confirmed by a fMRI study in healthy control subjects (Goel et al., 2009). In addition, studies of decision-making and social behavior at PH2 provided new insight into these deficits, and helped define appropriate modes of assessing such difficulties in subjects with frontal lesions.

Many VHIS subjects had been previously dishonorably discharged from the military, when personality changes seen after frontal lobe injuries were less recognized. Thus, the VHIS was vital in establishing improvements in the assessment of those with frontal lobe syndrome. It was found that there may be subgroups of patients with specific social deficits even within groups whose lesion encompasses a larger region, e.g., vmPFC lesions (Sanfey et al., 2003; Goel et al., 2004; Mah et al., 2004, 2005). Administration of the Everyday Problem Solving Inventory (EPSI) suggested that some patients with prefrontal lobe lesions may have impaired social judgment that can be directly revealed only through the use of such relatively novel neuropsychological tests (Dimitrov et al., 1996).

Mood disorders

As well as examining the impact of TBI on executive functioning, the VHIS reported on effects in terms of mood and other psychological disorders. At PH2, subjects with TBI were compared with controls in terms of anxiety and aggressive symptoms, to explore the hypotheses regarding the regulation of anxiety by frontal cortical mechanisms (Grafman et al., 1986c). Results indicated that patients with right orbitofrontal lesions were prone to abnormally increased anxiety and depressive symptoms, whereas patients with left dorsofrontal lesions were prone to abnormally increased anger and hostility. These data suggested that mood symptoms are subject to influence by locality of brain damage. These theories were expanded during PH3, when the correlates of depressive disorder were studied in greater detail, in particular whether damage to either the vmPFC or dlPFC is related to the pathogenesis of depression. Bilateral vmPFC lesions were associated with low levels of depression, whereas bilateral dorsal PFC lesions (involving dorsomedial and dorsolateral areas in both hemispheres) were associated with substantially higher levels of depression. These findings suggested both the vmPFC and dorsal PFC are critical to depression, with vmPFC damage offering some resistance to depression, and dorsal PFC damage conferring vulnerability (Koenigs et al., 2008).

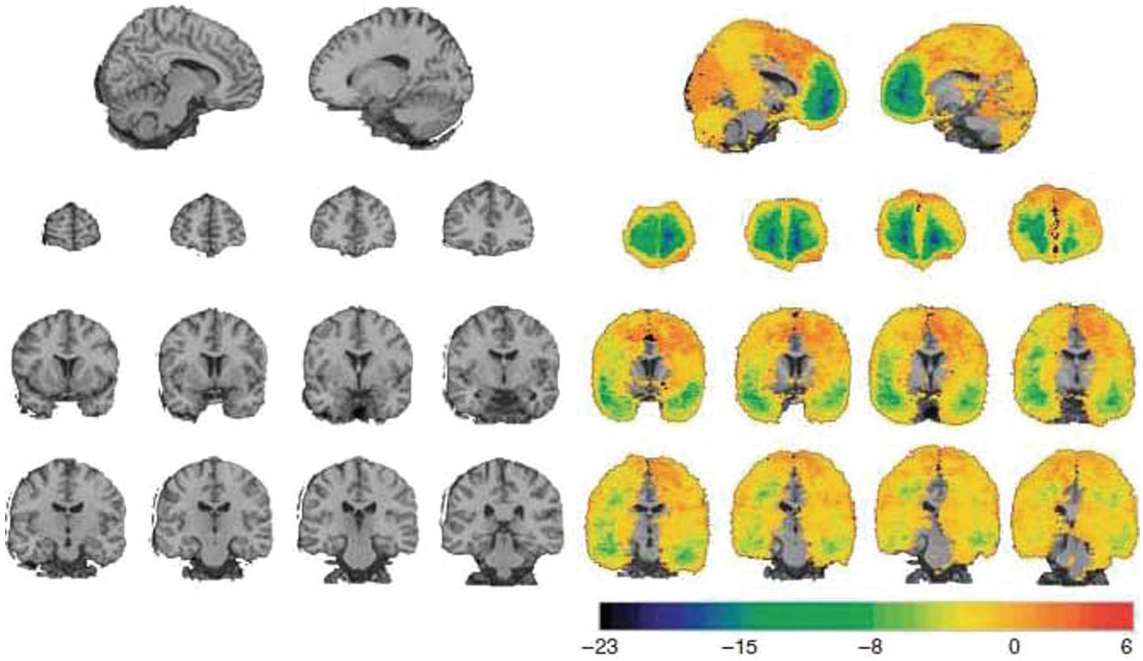

FIGURE 4 | Lesion difference analysis. A healthy adult brain is shown on the left. The lesion difference analysis for the corresponding slices is shown on the right. The color of each voxel indicates the difference between the number of veterans with damage to that voxel that developed PTSD and did not develop PTSD. The colors blue and green indicate the most negative values – areas where damage was relatively infrequently associated with PTSD. Top row, sagittal views of negative value clusters in prefrontal cortex. The left hemisphere ($x = -10$) is on the left and the right hemisphere ($x = 16$) is on the right. Second row, coronal views of negative value clusters in bilateral prefrontal cortex. Slices are arranged with the anterior most slice on the left ($y = 66$, $y = 56$, $y = 36$, respectively). In each coronal slice, the right hemisphere is on the reader's left (radiological convention). Third row, coronal views of negative value clusters in bilateral anterior temporal lobe ($y = 14$, $y = 8$, $y = 2$, $y = -4$, respectively). Fourth row, coronal views of posterior temporal lobe ($y = -10$, $y = -16$, $y = -22$, $y = -28$, respectively).

Post-traumatic stress disorder (PTSD) was specifically assessed at PH3, in particular the causal contribution of specific brain areas to PTSD symptoms. There was a substantially reduced occurrence of PTSD among those individuals with damage to one of two regions of the brain: the vmPFC and an anterior temporal area (that included the amygdala; **Figure 4**). The decreased prevalence of PTSD following vmPFC or amygdala damage appeared to be related to an overall reduction of symptom intensity or number, rather than a complete abolishment of all symptoms, suggesting that treatments aimed at selectively inhibiting vmPFC and/or amygdala function could be used to treat PTSD (Koenigs et al., 2009b).

Personality

Phase 2 investigators sought to establish more concrete evidence for the postulated associations between interictal personality traits and complex partial epilepsy (Swanson et al., 1995). An association between interictal psychopathology and complex partial, partial generalized, and generalized seizures was found, but there were no significant between group differences.

Social cognition

In 1999, PH2 reported a single VHIS case very similar to the famous nineteenth-century patient Phineas Gage (Dimitrov et al., 1999). Phineas Gage's case was described by his physician (Harlow, 1848, 1868), after he sustained a discrete but severe prefrontal cortex lesion during a railroad accident. Not only did Gage regain full consciousness and survive the incident, but he also demonstrated intact speech, learning, memory, and intelligence. However, his personality was profoundly changed, and he lost his "sense of responsibility" and respect for social conventions (Dimitrov et al., 1999). The subject described at PH2 was a 50-year-old male patient with a right frontal ventromedial lesion who showed preserved general cognitive, abstract thinking, and problem-solving abilities, in contrast to gross impairment in his social competence, social decision-making, and social conduct. He also demonstrated diminished sensitivity to socially relevant stimuli and situational nuances, impairment in sexual behavior, lost sense of responsibility, and disinhibition. This was cited as evidence for the regulation of emotion and social conduct by the vmPFC.

It is well reported that those with frontal lobe lesions may present with aggressive behavior. At PH2 family observations and self-reports were collected using scales and questionnaires that assessed a range of aggressive attitudes and behavior (Grafman et al., 1996). Patients with vmPFC lesions consistently demonstrated aggression scores significantly higher than controls and patients with lesions in other brain areas. However, the presence of aggressive and violent behavior was not associated with lesion size or history of seizures. The genotyping that was carried out as

part of PH3 demonstrated an association between prefrontal cortex lesions and MAO-A in modulating aggression (Pardini et al., in press).

Results from a wealth of imaging and lesion studies have highlighted the involvement of the PFC in social cognition. Accumulating evidence demonstrates that representations within the lateral PFC enable people to coordinate their thoughts and actions with their intentions to support goal-directed social behavior. Despite the importance of this region in guiding social interactions, remarkably little is known about the functional organization and forms of social inference processed by the lateral PFC. Evidence from PH2 introduced a framework for understanding the inferential architecture of the PFC; "structured event complex theory" (Barbey et al., 2009). Data from both PH2 and PH3 have subsequently added to the evidence that regions of the PFC that are critical for both implicit and explicit social cognitive, as well as moral judgment processing. It seems there is considerable overlap between regions utilized when individuals engage in social cognition or assess moral appropriateness of behaviors, underscoring the similarity between social cognitive and moral judgment processes. The structured event complex theory emphasizes the dynamic flexibility in neural circuits involved in both implicit and explicit processing, and the likelihood that neural regions thought to uniquely underlie both processes in fact heavily interact (Forbes and Grafman, 2010).

Emotional intelligence (EI) has been referred to a set of competencies that are essential features of human social behavior (Krueger et al., 2009). At PH3 two components of this were assessed; (1) Strategic EI – the competency to understand emotional information and to apply it to management of yourself and others and, (2) Experiential EI – the competency to perceive emotional information and to integrate it into thinking. It was found that vmPFC damage diminishes strategic EI and dlPFC damage diminished experiential EI in subjects with frontal lobe damage.

An aspect of normal social cognition development is the development of stereotypical attitudes. At PH2, subjects with PFC lesions and controls were administered the Implicit Association Task (IAT) that measured the degree of association between male and female names and their stereotypical attributes of strength and weakness. Patients with dlPFC lesions and controls showed a strong association, whereas patients with vmPFC lesions had a significantly lower association, between the stereotypical attributes of men and women and their concepts of gender. This finding provided support for the hypothesis that patients with vmPFC lesions have a deficit in automatically accessing certain aspects of overlearned associated social knowledge (Milne and Grafman, 2001). At PH3, clinical observations of patients with ventral frontal and anterior temporal lesions revealed marked abnormalities in social attitudes. Gozzi et al. (2009) used the IAT to determine the differential effects of the vmPFC, ventrolateral prefrontal (vlPFC), and superior anterior temporal lobe (aTL) cortical lesions on attitudes. It was found that larger lesions in either the vmPFC or the superior aTL were associated with increased stereotypical attitudes, whereas larger lesions in the vlPFC were associated with decreased stereotypical attitudes.

FUNCTIONAL OUTCOME

In PH2, the relationship between neurological, neuropsychological, and social interaction impairments to work status was examined (e.g., Schwab et al., 1993; Salazar et al., 1995). Only 56% of the subjects with TBI were working at PH2, compared to 82% of the uninjured controls. Seven impairments correlated with work status; PTE, paresis, visual field loss, verbal memory loss, visual memory loss, psychological problems, and violent behavior. These disabilities had a cumulative and surprisingly equipotent affect upon the likelihood of work, suggesting that patients find it harder to compensate for increasing amounts of disabilities, whatever the disability. The authors suggested that a simple summed score of the number of these seven disabilities can yield a residual "disability score" which may prove to be a practical tool for assessing the likelihood of return to work post-TBI (**Figures 5** and **6**).

Additionally, 82% had used VA educational benefits to return to school (Kraft et al., 1993), and 64% had achieved associate or bachelor's degrees. Return to work was strongly related to level of educational achievement, particularly among the most severely disabled. Though only 56% of the TBI group were employed at PH2, the occupational distribution of those who were working differed little from uninjured controls, or the male labor force (Kraft et al., 1993). Thus severity of injury appears to affect educational achievement and return to work, but not the occupational distribution of those who do manage to return, implying some level of plasticity may occur which can overcome loss or brain tissue, but may still be restrained by other psychological or social factors.

GENETICS

It has been established that that recovery of function after brain damage results from complex interactions between both environmental effects and genetic factors (Lindsay et al., 2002). In recent years, there has also been increasing evidence of links of between-specific genotypes and risk for accelerated cognitive decline or dementia following TBI. Any associations found between genetic information and outcome following TBI may also aid the acute triage of brain-injured patients as well as help to target future treatments.

One of the major advances at PH3 was the assessment of a large number of the genetic markers and their relation to various outcome measures. Raymont et al. (2008) reported the links with cognition. All subjects were both healthy and physically fit before their injury, yet preinjury intelligence was found to be significantly predicted by the following genotypes; GRIN2C rs689730, GAD2 rs2839670, and DBH444. It was suggested that the presence of all of these markers could account for 15.5% of the variability in preinjury intelligence. However, only GRIN2A rs968301 was found to be able to predict current intelligence and change in intelligence from preinjury to PH3. Experimental animal studies have revealed impaired plasticity following TBI, even in the absence of significant anatomical damage (Giza et al., 2006), evidenced by examining *N*-methyl-D-aspartate (NMDA). NMDA consists of a number of subunits, including the GRIN glutamate receptor, which seems to be specifically involved in the pathophysiology of CHI, including acting as a marker of neuronal death (Parton et al., 2005). There was a trend for dominant homozygotes to have a greater level of decline in intelligence from PH2 to PH3.

	R	Model chi square	Degree of freedom	*p*
Model 1 Work = preinjury intelligence	0.17	21.50	1 *df*	0.001
Model 2 Work = preinjury intelligence + volume loss	0.39	99.66	2 *df*	0.001
Model 3 Work = postinjury intelligence	0.38	90.44	1 *df*	0.001
Model 4 Work = postinjury intelligence + volume loss	0.48	141.58	2 *df*	0.001
Model 5 Work = postinjury intelligence + volume loss + disability score*	0.50	111.43	3 *df*	0.001
Model 6 Work = disability score	0.42	83.68	1 *df*	0.001
* Residual disability score: Number of residual impairments (1-7)				

FIGURE 5 | Logistic regression analysis outcomes for predictive factors of variation in work status.

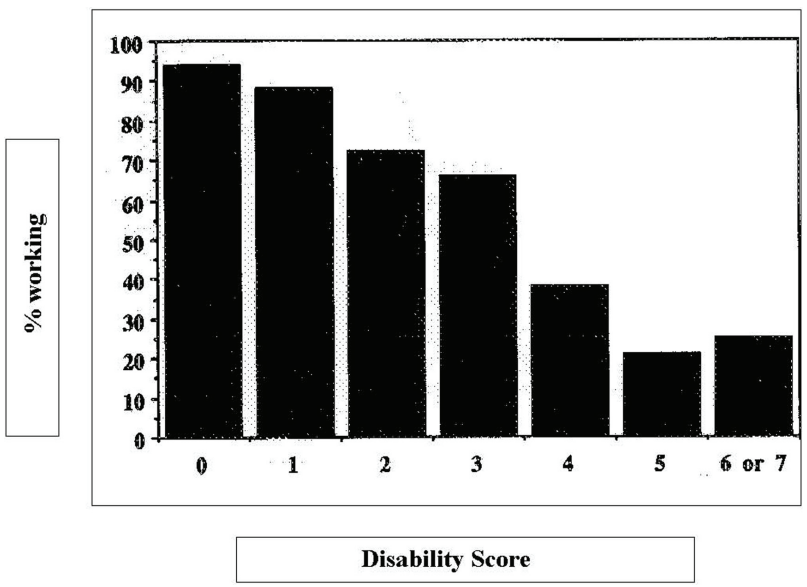

FIGURE 6 | Vietnam Head Injury Study, percent working by disability score. The disability score represents the number of disabilities present (1–7).

Neurotrophins such as brain-derived neurotrophic factor (BDNF) have an impact on neuronal function and synaptic plasticity in the brain (Varon et al., 1991). Recent evidence has shown functional differences between the proteins coded for by the val66 and met66 BDNF alleles in healthy subjects and patients with neurological or psychiatric disorders (Krueger et al., 2011). PH3 reported a functional relationship between the BDNF val66met genotype and recovery of executive function in subjects with

frontal lobe lesions. Individuals carrying one or two copies of the BDNF met allele performed significantly better on cognitive tests measuring executive functions of the frontal cortex compared with individuals carrying the val/val homozygotes, suggesting that the val66met BDNF polymorphism may act differently in the injured and healthy brain.

OVERALL SIGNIFICANCE AND CONSEQUENCES OF THE VHIS

The US military population offers a number of advantages for the study of the effects of TBI; its size, relative uniformity, the fact that all subjects are initially healthy, and the potential for long-term follow-up. Additionally, preinjury intelligence and aptitude testing is available on most military recruits, and the VA medical system allows them to be tracked over a long follow-up period. Given this, and the timing of its initiation coinciding with greater survival from conflict-related TBI, means the VHIS has been and continues to be instrumental in gathering long-term data about subjects with TBI. Results from the VHIS have suggested that penetrating TBI carries a high risk of long-term sequelae, such as PTE and cognitive impairment, which may occur decades after injury, so has provided solid evidence that such patients may require long-term medical follow up. It should be emphasized, however, that these results may not always be generalizable to closed TBI, and therefore the type of injuries seen in the civilian population. Our findings are probably compatible with focal lesions secondary to a variety of causes (e.g., stroke, tumor, etc.), but closed TBI may have additional white matter shearing and pathology that is more extensive than that seen in penetrating TBI. Penetrating TBI also crosses traditional vascular boundaries and does not generally respect different neuronal susceptibilities to disease, so does have a unique signature or profile of impairments in any individual patient, but by interpreting our results by lesion site, we have tried to make our results generalizable by location. However, the ability to maintain a longitudinal assessment of a large sample of subjects from preinjury, through acute injury and many years of follow up is fraught with difficulties. The VHIS has only been able to review the long-term clinical, neuropsychological, and genetic characteristics in a subset of the original cohort, and we may well have seen differing results if we had been able to examine the entire sample throughout the length of the study.

Besides a core clinical evaluation, each phase of the VHIS has tried to address emerging issues within cognitive neuroscience, neurology, and psychiatry. For instance, the need for an accurate assessment of the brain lesions in PH3 lead to the development of the ABLe software program (Makale et al., 2002; Solomon et al., 2007), which characterizes lesions in terms of volume and intersection with Brodmann areas and allows for correlations between subjects with overlapping lesions and behavioral deficit.

In addition, PH2 of the VHIS led directly to the establishment of the Defense and Veterans Head Injury Program (DVHIP). Such TBI units and programs at major Military and VA Hospitals continue to operate to this day, now as Defense and Veterans Brain Injury Centers (DVBIC). Until the creation of the DVHIP, there had been no national systematic program providing TBI-specific care and rehabilitation within the VA (Salazar et al., 2000). The DVHIP was created initially as an interagency clinical program oriented to treatment, rehabilitation, and care management. It was formed by collaboration between the Department of Defense, the Department of Veteran Affairs, the Brain Injury Association (BIA), and the International Brain Injury Association (IBIA). The principal goals of the program now are to ensure that military and veteran TBI patients receive standardized TBI-specific evaluation, treatment, and follow-up, while at the same time helping to define optimal acute and chronic care for victims of TBI nationwide, as well as conducting rehabilitation and clinical treatment trials. The DVHIP also included a simple, updated Head and Spinal Combat Injury Registry form similar to that used by in the original VHIS registry, which is now used within the military and VA via the DVBIC. This has been approved by the Joint Committee of Military Neurosurgeons of the American Association of Neurological Surgeons (AANS) and Congress of Neurological Surgeons (CNS) for deployment in time of war. Thus not only has the VHIS been vital in its contribution to our understanding of TBI and neuropsychology, it has helped produce a system that will facilitate the early identification of future injured soldiers and their long-term management – a worthy legacy for Dr. Caveness and the many victims of TBI studied in the last 40 years. The unique breadth and length of follow up of this cohort makes the future prospects

Table 1 | Five key findings of the VHIS.

PHASE 1
Predictors of brain infection.
Defer cranioplasty until 1 year post-TBI.
Incidence of motor deficits – parietal wounds associated with hemiparesis.
Aphasia occurred in about 25%, correlating with gunshot cause and initial loss of consciousness.
Skull defects and cranioplasty did not predict tendency to PTE.
PHASE 2
Greatest predictor of cognitive decline is premorbid IQ.
Incidence of PTE can be predicted by and left hippocampus lesions correlate with seizure frequency.
Deficits in semantic memory, verbal episodic memory, and visual episodic memory were found to be associated with lesion location.
Right orbitofrontal lesions were prone to anxiety and depression, whereas patients with left dorsofrontal lesions were prone to anger and hostility. Such studies lead to further conclusions on the regional contribution of planning and representations, which ultimately lead to theories of how the brain represents knowledge and responds to complex events.
Seven impairments correlated with work status; PTE, paresis, visual field loss, verbal memory loss, visual memory loss, psychological problems, and violent behavior.
PHASE 3
Greatest predictor of cognitive decline is premorbid IQ.
GRIN2A rs968301 may predict current intelligence and change in change in intelligence after TBI.
Short term memory deficits were found in all classes of brain-injured individuals, regardless of lesion location pattern.
Bilateral ventromedial PFC lesions were associated with low levels of depression, whereas bilateral dorsal PFC lesions (involving dorsomedial and dorsolateral areas in both hemispheres) were associated with substantially higher levels of depression.
Left parietal lobe lesions and retained ferric metal fragments were associated with PTE and total brain volume loss predicted seizure frequency.

Table 2 | Possible future goals for studies of military TBI patients.

1. Further longitudinal studies to explore long-term cognitive impairment post-TBI, and its interaction with normal aging, dementias and other diseases.
2. Comparison of current blast injuries with prior data on closed and penetrating injuries.
3. Combine functional and structural studies to compare functional and connectivity changes, to improve research and clinical imaging of penetrating and closed TBI.
4. Extend genotyping and proteomic research to assess inheritable factors for brain damage response and neuroplasticity, and using such knowledge to help triage types of TBI acutely and target future treatments.
5. Further examination of the role of psychological and psychiatric pathology in cognitive outcome.
6. Additional pathological and imaging correlates of clinical outcome.
7. Addressing emerging cognitive neuroscience issues.
8. Development of neuroprotection as well as cell-based rehabilitation strategies to enhance plasticity.

for information to be collected from PH4 very exciting, and the VHIS has provided a model for subsequent longitudinal studies of TBI (**Tables 1** and **2**). Given the increasing numbers of both civilian patients and military casualties suffering TBI, which will certainly require care in the future, expanding such research seems long overdue.

ACKNOWLEDGMENTS

We are grateful to our research participants whose dedicated, selfless, long-term commitment to the Vietnam Head Injury Study enabled us to carry out our research and change the way the United States military diagnoses and treats traumatic brain injury. We also thank all of the associated principal investigators and collaborators who have helped insure the success of our research program. In particular we want to single out Herbert Brown, Max Hoyt, Karen Schwab, and William F. Caveness for their efforts in helping establish and sustain the Vietnam Head Injury Study. Finally, one of us (Jordan Grafman) benefited from the wise consul of Freda Newcombe, Charles G. Matthews, Herbert Weingartner, and Alwyn Lishman in the early stages of the Vietnam Head Injury Study.

REFERENCES

AFQT-7A. (1960). Department of Defense Form 1293. March 1.

Barbey, A. K., Krueger, F., and Grafman, J. (2009). An evolutionarily adaptive neural architecture for social reasoning. *Trends Neurosci.* 32, 603–610.

Bender, M. B., and Teuber, H. L. (1948). Spatial organization of visual perception following injury to the brain. *Arch. Neurol. Psychiatry* 59, 39–62.

Boake, C., and Diller, L. (2005). "History of rehabilitation for traumatic brain injury," in *Rehabilitation for Traumatic Brain Injury*, eds W. M. High, A. M. Sander, M. A. Struchen, and K. A. Hart (Oxford: Oxford University Press), 3–13.

Carey, M. E., Sacco, W., and Merkler, J. (1982). An analysis of fatal and nonfatal head wounds incurred during combat in Vietnam by U.S. forces. *Acta Chir. Scand. Suppl.* 508, 351–356.

Carlin, D., Bonerba, J., Phipps, M., Alexander, G., Shapiro, M., and Grafman, J. (2000). Planning impairments in frontal lobe dementia and frontal lobe lesion patients. *Neuropsychologia* 38, 655–665.

Caveness, W. F., Meirowsky, A. M., Rish, B. L., Mohr, J. P., Kistler, J. P., Dillon, D., and Weiss, G. H. (1979). The nature of posttraumatic epilepsy. *J. Neurosurg.* 50, 545–553.

Corkin, S., Rosen, T. J., Sullivan, E. V., and Clegg, R. A. (1989). Penetrating head injury in young adulthood exacerbates cognitive decline in later years. *J. Neurosci.* 9, 3876–3883.

Corkin, S., Sullivan, E. V., and Carr, F. A. (1984). Prognostic factors for life expectancy after penetrating head injury. *Arch. Neurol.* 41, 975–977.

Dimitrov, M., Grafman, J., and Hollnagel, C. (1996). The effects of frontal lobe damage on everyday problem solving. *Cortex* 32, 357–366.

Dimitrov, M., Phipps, M., Zahnl, T. P., and Grafman, J. (1999). A thoroughly modern gage. *Neurocase* 5, 345–354.

Forbes, C. E., and Grafman, J. (2010). The role of the human prefrontal cortex in social cognition and moral judgment. *Annu. Rev. Neurosci.* 33, 299–324.

Frattali, C., Hanna, R., McGinty, A. S., Gerber, L., Wesley, R., Grafman, J., and Coelho, C. (2007). Effect of prefrontal cortex damage on resolving lexical ambiguity in text. *Brain Lang.* 102, 99–113.

Giza, C. C., Maria, N. S., and Hovda, D. A. (2006). N-methyl-D-aspartate receptor subunit changes after traumatic brain injury to the developing brain. *J. Neurotrauma* 23, 950–961.

Goel, V., and Grafman, J. (1995). Are the frontal lobes implicated in "planning" functions? Re-interpreting data from the tower of Hanoi. *Neuropsychologia* 33, 623–642.

Goel, V., and Grafman, J. (2000). Role of the right prefrontal cortex in Ill-structured planning. *Cogn. Neuropsychol.* 17, 415–436.

Goel, V., Pullara, S. D., and Grafman, J. (2001). A computational model of frontal lobe dysfunction: working memory and the tower of Hanoi task. *Cogn. Sci.* 25, 287–313.

Goel, V., Shuren, J., Sheesley, L., and Grafman, J. (2004). Asymmetrical involvement of frontal lobes in social reasoning. *Brain* 127, 783–790.

Goel, V., Stollstorff, M., Nakic, M., Knutson, K., and Grafman, J. (2009). A Role for right ventromedial prefrontal cortex in reasoning about indeterminate relations. *Neuropsychologia* 47, 2790–2797.

Goel, V., Tierney, M., Sheesley, L., Bartolo, A., Vartanian, O., and Grafman, J. (2007). Hemispheric specialization in human prefrontal cortex for resolving certain and uncertain inferences. *Cereb. Cortex* 17, 2245–2250.

Gozzi, M., Raymont, V., Solomon, J., Koenigs, M., and Grafman, J. (2009). Dissociable effects of prefrontal and anterior temporal cortical lesions on stereotypical gender attitudes. *Neurology* 74, 749–754.

Grafman, J., Jonas, B., and Salazar, A. (1992). Epilepsy following penetrating head injury to the frontal lobes. Effects on cognition. *Adv. Neurol.* 57, 369–378.

Grafman, J., Jonas, B. S., Martin, A., Salazar, A. M., Weingartner, H., Ludlow, C., Smutok, M. A., and Vance, S. C. (1988). Intellectual function following penetrating head injury in Vietnam veterans. *Brain* 111(Pt 1), 169–184.

Grafman, J., Kampen, D., Rosenberg, J., Salazar, A., and Boller, F. (1989). Calculation abilities in a patient with a virtual left hemispherectomy. *Behav. Neurol.* 2, 183–194.

Grafman, J., and Salazar, A. (1999). The William Fields Caveness Vietnam head injury study: past and future. *Brain Inj. Source* 3, 12–14.

Grafman, J., Salazar, A., Weingartner, H., Vance, S., and Amin, D. (1986a). The relationship of brain-tissue loss volume and lesion location to cognitive deficit. *J. Neurosci.* 6, 301–307.

Grafman, J., Salazar, A. M., Weingartner, H., and Amin, D. (1986b). Face memory and discrimination: a preliminary analysis of the persistent effects of penetrating brain wounds. *Int. J. Neurosci.* 29, 125–139.

Grafman, J., Vance, S. C., Weingartner, H., Salazar, A. M, and Amin, D. (1986c). The effects of lateralized frontal lesions on mood regulation. *Brain* 109(Pt 6), 1127–1148.

Grafman, J., Smutok, M., Sweeney, J., Vance, S. C., Salazar, A. M., and Weingartner, H. (1985a). Effects of left-hand preference on postinjury measures of distal motor ability. *Percept. Mot. Skills* 61, 615–624.

Grafman, J., Salazar, A. M., Weingartner, H., Vance, S. C., and Ludlow, C. (1985b). Isolated impairment of memory following a penetrating lesion of the fornix. *Arch. Neurol.* 42, 1162–1168.

Grafman, J., Schwab, K., Warden, D., Pridgen, A., Brown, H. R., and Salazar, A. M. (1996). Frontal lobe

injuries, violence, and aggression: a report of the Vietnam head injury study. *Neurology* 46, 1231–1238.

Groswasser, Z., Reider-Groswasser, I. I., Schwab, K., Ommaya, A. K., Pridgen, A., Brown, H. R., Cole, R., and Salazar, A. M. (2002). Quantitative imaging in late TBI. Part II: cognition and work after closed and penetrating head injury: a report of the Vietnam head injury study. *Brain Inj.* 16, 681–690.

Harlow, J. M. (1848). Passage of an iron rod through the head. *Boston Med. Surg. J.* 39, 389–393.

Harlow, J. M. (1868). *Recovery After Severe Injury to the Head.* Boston: Massachusetts Medical Society.

Holmes, G. (1941). Henry Head. *Obit. Not. Fell. R. Soc.* 3, 665–689.

Holmes, G., and Lister, W. T. (1916). Disturbances of vision from cerebral lesions, with special reference to the cortical representation of the macula. *Brain* 39, 34.

Jonas, B. S., Schwab, K., and Salazar, A. M. (1987). "Factors influencing participation in a multi-stage study of head injury: potential biases in the Vietnam head injury study," in *Proceedings of the Section on Survey Research Methods of the Association for Statistical Analysis.*

Koenigs, M., Barbey, A., Postle, B. R., and Grafman, J. (2009a). Superior parietal cortex is critical for the manipulation of information in working memory. *J. Neurosci.* 29, 14980–14986.

Koenigs, M., Huey, E. D., Raymont, V., Cheon, B., Solomon, J., Wassermann, E. M., and Grafman, J. (2009b). Focal brain damage protects against post-traumatic stress disorder in combat veterans. *Proc. Natl. Acad. Sci. U.S.A.* 106, 22486–22491.

Koenigs, M., Holliday, J., Solomon, J., and Grafman, J. (2010). Left dorsomedial frontal brain damage is associated with insomnia. *J. Neurosci.* 30, 16041–16043.

Koenigs, M., Huey, E. D., Calamia, M., Raymont, V., Tranel, D., and Grafman, J. (2008). Distinct regions of prefrontal cortex mediate resistance and vulnerability to depression. *Nat. Neurosci.* 11, 232–237.

Kraft, J. F., Schwab, K. A., Salazar, A. M., and Brown, H. R. (1993). Occupational and educational achievements of head injured Vietnam veterans at 15-year follow-up. *Arch. Phys. Med. Rehabil.* 74, 596–601.

Kraus, J. F., and McArthur, D. L. (1996). Epidemiologic aspects of brain injury. *Neurol. Clin.* 14, 435–450.

Krueger, F., Barbey, A. K., McCabe, K., Strenziok, M., Zamboni, G., Solomon, J., Raymont, V., and Grafman, J. (2009). The neural bases of key competencies of emotional intelligence. *Proc. Natl. Acad. Sci. U.S.A.* 106, 22486–22491.

Krueger, F., Pardini, M., Huey, E. D., Raymont, V., Solomon, J., Lipsky, R. H., Hodgkinson, C. A., Goldman, D., and Grafman, J. (2011). The role of the Met66 brain-derived neurotrophic factor allele in the recovery of executive functioning after combat-related traumatic brain injury. *J. Neurosci.* 31, 598–606.

Lackner, J. R. (2009). Hans-Lukas Teuber: a remembrance. *Neuropsychol. Rev.* 19, 4–7.

Lee, S. S., Wild, K., Hollnagel, C., and Grafman, J. (1999). Selective visual attention in patients with frontal lobe lesions or Parkinson's disease. *Neuropsychologia* 37, 595–604.

Lepore, F. E. (1994). Harvey Cushing, Gordon Holmes, and the neurological lessons of World War I. *Arch. Neurol.* 51, 711–722.

Lindsay, J., Laurin, D., Verreault, R., Hebert, R., Helliwell, B., Hill, G. B., and McDowell, I. (2002). Risk factors for Alzheimer's disease: a prospective analysis from the Canadian study of health and aging. *Am. J. Epidemiol.* 156, 445–453.

Lishman, W. A. (1992). What is neuropsychiatry? *J. Neurol. Neurosurg. Psychiatr.* 55, 983–985.

Ludlow, C. L., Rosenberg, J., Fair, C., Buck, D., Schesselman, S., and Salazar, A. (1986). Brain lesions associated with nonfluent aphasia fifteen years following penetrating head injury. *Brain* 109(Pt 1), 55–80.

Luria, A. R. (1972). *The Man with a Shattered World: The History of a Brain Wound.* New York: Basic Books.

Mah, L., Arnold, M. C., and Grafman, J. (2004). Lesions of prefrontal cortex impair social perception. *Am. J. Psychiatry* 161, 1247–1255.

Mah, L. W. Y., Arnold, M. C., and Grafman, J. (2005). Deficits in social knowledge following lesions of ventromedial prefrontal cortex. *J. Neuropsychiatry Clin. Neurosci.* 17, 66–74.

Makale, M., Solomon, J., Patronas, N. J., Danek, A., Butman, J. A., and Grafman, J. (2002). Quantification of brain lesions using interactive automated software. *Behav. Res. Methods Instrum. Comput.* 34, 6–18.

Milne, E., and Grafman, J. (2001). Ventromedial prefrontal cortex lesions in humans eliminate implicit gender stereotyping. *J. Neurosci.* 21, 1–6.

Mishkin, M. (1972). "Cortical visual areas and their interactions," in *Brain and Human Behavior*, eds G. Karczmar and J. C. Eccles (Berlin: Springer), 178–208.

Mohr, J. P., Weiss, G. H., Caveness, W. F., Dillon, J. D., Kistler, J. P., Meirowsky, A. M., and Rish, B. L. (1980). Language and motor disorders after penetrating head injury in Vietnam. *Neurology* 30, 1273–1279.

Muthén, L. K., and Muthén, B. O. (1998–2004). Mplus User's Guide, 3rd Edn. Los Angeles: Muthén & Muthén.

Newcombe, F., Brooks, N., and Baddeley, A. (1980). Rehabilitation after brain damage: an overview. *Int. Rehabil. Med.* 2, 133–137.

Newcombe, F., Oldfield, R. C., Ratcliff, G. G., and Wingfield, A. (1971). Recognition and naming of object-drawings by men with focal brain wounds. *J. Neurol. Neurosurg. Psychiatr.* 34, 329–340.

Pardini, M., Krueger, F., Hodgkinson, C., Raymont, V., Ferrier, C., Goldman, D., Strenziok, M., Guida, S., and Grafman, J. (in press). Prefrontal cortex lesions and MAO-A modulate aggression in penetrating traumatic brain injury.

Pardini, M., Krueger, F., Raymont, V., and Grafman, J. (2010). Ventromedial prefrontal cortex modulates fatigue after penetrating traumatic brain injury. *Neurology* 74, 749–754.

Parton, A., Coulthard, E., and Husain, M. (2005). Neuropharmacological modulation of cognitive deficits after brain damage. *Curr. Opin. Neurol.* 18, 675–680.

Rattermann, M. J., Spector, L., Grafman, J., Levin, H., and Howard, H. (2001). Partial and total-order planning: evidence from normal and prefrontally damaged populations. *Cogn. Sci.* 25, 941–975.

Raymont, V., and Grafman, J. (2006). Cognitive neural plasticity during learning and recovery from brain damage. *Prog. Brain Res.* 157, 199–206.

Raymont, V., Greathouse, A., Reding, K., Lipsky, R., Salazar, A., and Grafman, J. (2008). Demographic, structural and genetic predictors of late cognitive decline after penetrating head injury. *Brain* 131(Pt 2), 543–558.

Raymont, V., Salazar, A. M., Lipsky, R., Goldman, D., Tasick, G., and Grafman, J. (2010). Correlates of post-traumatic epilepsy 35 years following combat brain injury. *Neurology* 75, 224–229.

Rish, B. L., Caveness, W. F., Dillon, J. D., Kistler, J. P., Mohr, J. P., and Weiss, G. H. (1981). Analysis of brain abscess after penetrating craniocerebral injuries in Vietnam. *Neurosurgery* 9, 535–541.

Rish, B. L., Dillon, J. D., Caveness, W. F., Mohr, J. P., Kistler, J. P., and Weiss, G. H. (1980). Evolution of craniotomy as a debridement technique for penetrating craniocerebral injuries. *J. Neurosurg.* 53, 772–775.

Rish, B. L., Dillon, J. D., Meirowsky, A. M., Caveness, W. F., Mohr, J. P., Kistler, J. P., and Weiss, G. H. (1979). Cranioplasty: a review of 1030 cases of penetrating head injury. *Neurosurgery* 4, 381–385.

Rish, B. L., Dillon, J. D., and Weiss, G. H. (1983). Mortality following penetrating craniocerebral injuries. An analysis of the deaths in the Vietnam head injury registry population. *J. Neurosurg.* 59, 775–780.

Romero, S. G., Manly, C. F., and Grafman, J. (2002). Investigating cognitive neuroplasticity in single cases: Lessons learned from applying functional neuroimaging techniques to the traditional neuropsychological case study framework. *Neurocase* 8, 355–368.

Rueckert, L., and Grafman, J. (1996). Sustained attention deficits in patients with right frontal lesions. *Neuropsychologia* 34, 953–963.

Rueckert, L., and Grafman, J. (1998). Sustained attention deficits in patients with lesions of posterior cortex. *Neuropsychologia* 36, 653–660.

Salazar, A., Grafman, J., Jabbari, B., Vance, S. C., and Amin, D. (1987). "Epilepsy and cognitive loss after penetrating head injury," in *Advances in Epileptology*, eds P. Wolf, W. Dam, M. Janz and F. Dreifuss (New York: Raven Press), 627–631.

Salazar, A. M., Grafman, J., Vance, S. C., Weingartner, H., Dillon, J. D., and Ludlow, C. (1986). Consciousness and amnesia following penetrating head injury. *Neurology* 36, 178–187.

Salazar, A. M., Jabbari, B., Vance, S. C., Grafman, J., Amin, D., and Dillon, J. D. (1985). Epilepsy after penetrating head injury. I. Clinical correlates: a report of the Vietnam head injury study. *Neurology* 35, 1406–1414.

Salazar, A. M., Schwab, K., and Grafman, J. H. (1995). Penetrating injuries in the Vietnam war. Traumatic unconsciousness, epilepsy, and psychosocial outcome. *Neurosurg. Clin. N. Am.* 6, 715–726.

Salazar, A. M., Zitnay, G. A., Warden, D. L., and Schwab, K. A. (2000). Defense and Veterans Head Injury Program: background and overview. *J. Head Trauma Rehabil.* 15, 1081–1091.

Sanfey, A. G., Hastie, R., Colvin, M. K., and Grafman, J. (2003). Phineas Gauged: decision-making and the human prefrontal cortex. *Neuropsychologia* 41, 1218–1229.

Schooler, C., Caplan, L. J., Revell, A. J., Salazar, A. M., and Grafman, J. (2008). Brain lesion and memory

functioning: short-term memory deficit is independent of lesion location. *Psychon. Bull. Rev.* 15, 521–527.

Schwab, K., Grafman, J., Salazar, A. M., and Kraft, J. (1993). Residual impairments and work status 15 years after penetrating head injury: report from the Vietnam head injury study. *Neurology* 43, 95–103.

Smutok, M. A., Grafman, J., Salazar, A. M., Sweeney, J. K., Jonas, B. S., and DiRocco, P. J. (1989). Effects of unilateral brain damage on contralateral and ipsilateral upper extremity function in hemiplegia. *Phys. Ther.* 69, 195–203.

Solomon, J., Raymont, V., Braun, A., Butman, J. A., and Grafman, J. (2007). User-friendly software for the analysis of brain lesions (ABLe). *Comput. Methods Programs Biomed.* 86, 245–254.

Swanson, S. J., Rao, S. M., Grafman, J., Salazar, A. M., and Kraft, J. (1995). The relationship between seizure subtype and interictal personality. Results from the Vietnam head injury study. *Brain* 118(Pt 1), 91–103.

Teuber, H. L. (1975). Recovery of function after brain injury in man. *Ciba Found. Symp.* 34, 159–190.

van Gijn, J. (2009). From the archives. Cerebral involvement in head injury. A study based on the examination of two hundred cases. By W. Ritchie Russell, MD. 1932; 55: 549–603. *Brain* 132, 565–567.

Varon, S., Hagg, T., and Manthorpe, M. (1991). Nerve growth factor in CNS repair and regeneration. *Adv. Exp. Med. Biol.* 296, 267–276.

Warden, D. J. (2006). Military TBI during the Iraq and Afghanistan wars. *Head Trauma Rehabil.* 21, 398–402.

Weinstein, S., and Teuber, H. L. (1957). The role of pre-injury education and intelligence level in intellectual loss after brain injury. *J. Comp. Physiol. Psychol.* 50, 535–539.

Weiss, G. H., and Caveness, W. F. (1972). Prognostic factors in the persistence of posttraumatic epilepsy. *J. Neurosurg.* 37, 164–169.

Weiss, G. H., Feeney, D. M., Caveness, W. F., Dillon, D., Kistler, J. P., Mohr, J. P., and Rish, B. L. (1983). Prognostic factors for the occurrence of posttraumatic epilepsy. *Arch. Neurol.* 40, 7–10.

Weiss, G. H., Salazar, A. M., Vance, S. C., Grafman, J., and Jabbari, B. (1986). Predicting posttraumatic epilepsy in penetrating head injury. *Arch. Neurol.* 43, 771–773.

Walker, A. E., and Jablon, S. (1961). *A Follow up Study of Head Wounds in World War II*. Washington, DC: Veterans Administration.

Wood, J. N., and Grafman, J. (2003). Human prefrontal cortex: processing and representational perspectives. *Nat. Rev. Neurosci.* 4, 139–147.

Wood, J. N., Romero, S. G., Makale, M., and Grafman, J. (2003). Category-specific representations of social and non-social knowledge in the human prefrontal cortex. *J. Cogn. Neurosci.* 15, 236–248.

Conflict of Interest Statement: The authors declare that the research was conducted in the absence of any commercial or financial relationships that could be construed as a potential conflict of interest.

Received: 06 December 2010; accepted: 03 March 2011; published online: 28 March 2011.

Citation: Raymont V, Salazar AM, Krueger F and Grafman J (2011) "Studying injured minds" – the Vietnam head injury study and 40 years of brain injury research. Front. Neur. ***2****:15. doi: 10.3389/fneur.2011.00015*

This article was submitted to Frontiers in Neurotrauma, a specialty of Frontiers in Neurology.

frontiers in NEUROLOGY

ORIGINAL RESEARCH ARTICLE
published: 19 September 2011
doi: 10.3389/fneur.2011.00058

Physics of IED blast shock tube simulations for mTBI research

Jesus Mediavilla Varas*, M. Philippens, S. R. Meijer, A. C. van den Berg, P. C. Sibma, J. L. M. J. van Bree and D. V. W. M. de Vries

Physical Protection and Survivability, Netherlands Organization for Applied Scientific Research, Rijswijk, Netherlands

Edited by:
Marten Risling, Karolinska Institutet, Sweden

Reviewed by:
Johan Davidsson, Chalmers University of Technology, Sweden
Svein Kleiven, Kungl Tekniska Högskolan, Sweden

****Correspondence:***
Jesus Mediavilla Varas, TNO, Lange Kleiweg 137, Rijswijk, The Netherlands.
e-mail: jesus.mediavillavaras@tno.nl

Shock tube experiments and simulations are conducted with a spherical gelatin filled skull–brain surrogate, in order to study the mechanisms leading to blast induced mild traumatic brain injury. A shock tube including sensor system is optimized to simulate realistic improvised explosive device blast profiles obtained from full scale field tests. The response of the skull–brain surrogate is monitored using pressure and strain measurements. Fluid–structure interaction is modeled using a combination of computational fluid dynamics (CFD) simulations for the air blast, and a finite element model for the structural response. The results help to understand the physics of wave propagation, from air blast into the skull–brain. The presence of openings on the skull and its orientation does have a strong effect on the internal pressure. A parameter study reveals that when there is an opening in the skull, the skull gives little protection and the internal pressure is fairly independent on the skull stiffness; the gelatin shear stiffness has little effect on the internal pressure. Simulations show that the presence of pressure sensors in the gelatin hardly disturbs the pressure field.

Keywords: mTBI, traumatic brain injury, finite element, blast, shock tube, surrogate, IED, CFD

1. INTRODUCTION

Blasts or explosions are the most common mechanisms of injury in modern warfare (Cernak and Noble-Haeusslein, 2009). The incidence of blast induced mild traumatic brain injury (mTBI) has increased dramatically in recent wars, mainly due to the increase use of improvised explosive devices (IED's) and the improvements in protective equipment, which have decreased the mortality rate. Typical symptoms of troops exposed to blast induced mTBI are memory and cognitive deficits, as irritability, anxiety, fatigue, and headaches. The mechanisms responsible for blast induced mTBI are very complex (Säljö et al., 2011), including direct interaction with the head through the skull and/or head rotation; and interaction between chest and central nervous system through large blood vessels (Cernak and Noble-Haeusslein, 2009; Scherer and Schubert, 2009). The transfer of external blast through the skull into the brain is not known in such detail to develop injury criteria which will allow quantification of the risk on brain injury resulting from blast, and eventually design protective measures (e.g., helmets), as well as improve diagnostics.

To investigate the causes leading to blast induced mTBI, blast experiments on animals have been conducted, either using shock tubes (Long et al., 2009; Alley et al., 2011), explosives (Axelsson et al., 2000), or weapons (Säljö et al., 2008). Testing living animals is controversial due to ethical issues. The mechanical properties of living brain tissue decay very quickly with time (Garo et al., 2007), and hence testing cadavers is not representing reality correctly. As an alternative, blast tests on biofidelic surrogates can be performed (Alley et al., 2011; Zhu et al., 2011), with the limitations that they tend to be too simplistic, and the mechanical properties may differ from the actual head/body they represent. To investigate the complex wave propagation mechanisms leading to mTBI, a combination of experiments and numerical modeling is highly recommended. This enables to: (i) avoid a trial-and-error approach, involving large-scale use of laboratory animals, head surrogates, shock tube experiments, etc; (ii) study a spectrum of blast wave conditions that lead to the onset of mTBI; (iii) understand the brain response related to geometry, skull openings, through different structures of skull, brain, etc; (iv) analyze experimental data. The blast air flow around a human head (helmet) has been studied using Computational Fluid Dynamics (CFD) models (Mott et al., 2008). Fluid–structure interaction (FSI) between blast explosion and human head has been modeled using a combination of Eulerian and Lagrangian models (Chafi et al., 2009; Moore et al., 2009; Moss et al., 2009; Taylor and Ford Corey, 2009; Grujicic et al., 2010). In (Zhu et al., 2011), FSI simulations of shock tube blast experiments on a small surrogate were modeled using a combination of multimaterial arbitrary Lagrangian Eulerian (MMALE) for the air and Lagrangian model for the surrogate, coupled by means of a penalty formulation.

The goal of this investigation is to understand the interaction (reflection/transmission) between a blast wave and the human head. Similar to (Zhu et al., 2011), shock tube blast experiments and simulations are combined. A simplified spherical human head size skull–brain surrogate is used, which is exposed to a typical IED blast load. FSI is modeled using an uncoupled approach, a CFD model for the blast in the shock tube, and a Lagrangian finite element (FE) model for the surrogate response. The structure of this study is as follows: Section 2 discusses the experiments and

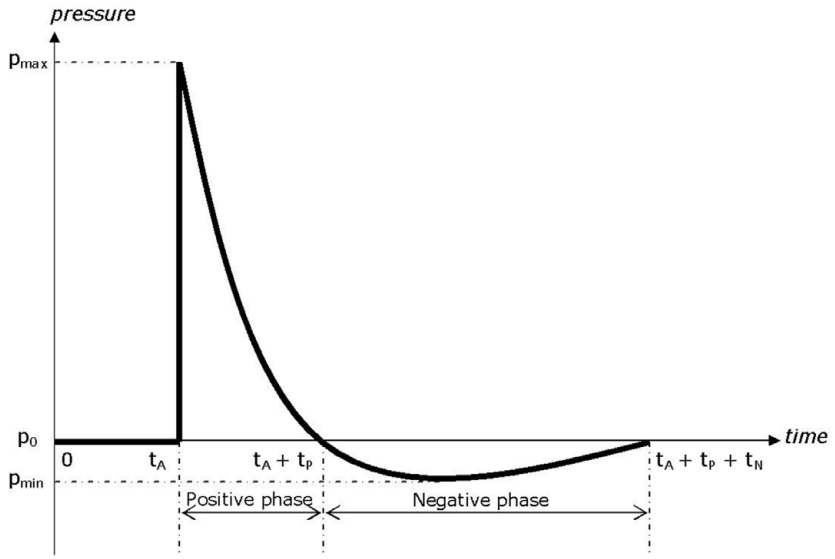

FIGURE 1 | Typical blast pressure-time curve (Friedlander curve).

simulations; the results are presented in Section 3, followed by a discussion and conclusions in Section 4.

2. MATERIALS AND METHODS

The shock tube and the design of the IED blast is discussed in Section 2.1, followed by a description of the surrogate and the measurement devices 2.2, and the numerical model in Section 2.3.

2.1. REPRODUCING AN IED BLAST PROFILE

Far field explosions can be reproduced by means of shock tube experiments, which allow testing living (sedated) animals or surrogates. Shock tubes have the advantage over explosives that the blast profile is more reproducible, and allow to more easily perform measurements. The two most critical components of the wave pressure profile which describe the potential of a wave to cause injury to personnel, or damage to structures, are the maximum overpressure and the duration of the positive phase, **Figure 1**. In a biological material (e.g., brain tissue), the negative phase under pressure could potentially lead to cavitation. The effect of a blast explosion on the human head is a FSI problem, where part of the air shock wave is reflected against the skull, and part is transmitted through the brain internal structures, causing mTBI.

A shock tube consists of a driver section and a driven section. The driver section is pressurized and is separated from the driven section by means of a membrane. When the membrane is perforated, it triggers a shock wave, which moves away from the driver section. The original blast tube used at TNO for this experiments has a cross section of 0.4 m × 0.4 m and a total length of 17.6 m, **Figure 2A**. The shock tube has a transparent section for high speed photography, **Figure 2B**. It is able to generate a blast wave with a maximum peak pressure of 70 kPa, with a positive phase duration of about 40 ms. This phase duration is much too long for an IED. Data with IED experiments are collected and translated in a lethality model, which represents Bass' lethality model (Bass et al., 2008) and an auditory injury model (Richmond and Axelsson, 1990). **Figure 3** presents in what range the IED data are to be expected. A representative IED pressure profile should have a peak pressure in the range of 10–200 kPa and a positive phase duration

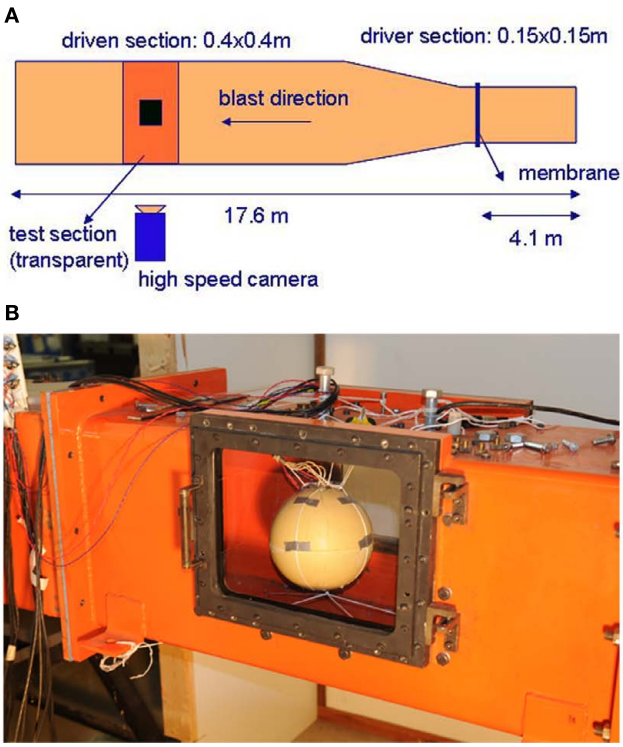

FIGURE 2 | Shock tube. (A) Sketch and dimensions; **(B)** transparent section with surrogate.

in the range of 4–10 ms. The pressure-time blast profile depends on the tube dimensions and driver unit, the gas type, and is highly sensitive to the exact location in the tube. Hence, to obtain such a short phase duration, the original shock tube design was modified, by replacing the original driver section by a smaller driver section (1.2 l) and placing the object closer to the membrane (6 m). The result is a peak pressure and positive phase duration of 40 kPa and 6 ms, which has been used throughout the experimental campaign reported in this study.

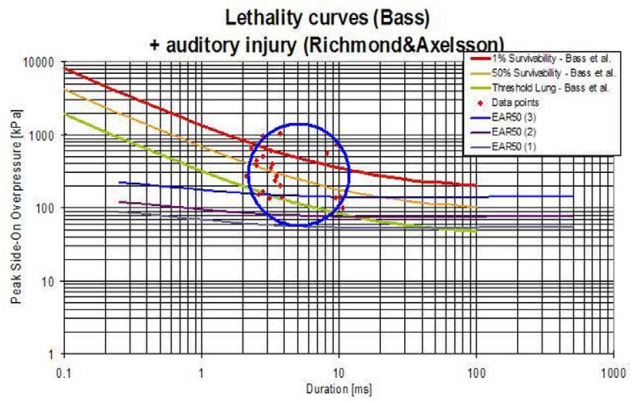

FIGURE 3 | Representative IED and lethality curve. Data from IED experiments presented in a lethality model (Bass et al., 2008) and an eardrum rupture model (Richmond and Axelsson, 1990). The IED data points are presented by the red dots (in the circle).

2.2. SIMPLIFIED SKULL–BRAIN SURROGATE: MEASUREMENTS

A spherical human head size skull–brain surrogate is exposed to a representative IED shock tube generated blast. The sphere ("skull") is made of modified bone-like Synbone[1] polyurethane (PR0110 Generic hollow sphere), 7 mm thick, with a 0.19-m external diameter, and a 0.04-m diameter opening. The sphere is filled up with 10% mass ballistic three gelatin (brain stimulant). It is suspended inside the shock tube by means of strings, which keep it in place, **Figure 2B**. Endevco 8530B-200[2] pressure gages (see detail in **Figure 17**), with an eigen frequency of 750 kHz, are used to measure the air pressure, P1, and P8; and gelatin pressure, P2, P3, and P4. P1 is situated on the skull, opposite to the opening; P8 is placed inside the shock tube, on one of the shock tube walls, at 0.1 m in front of the skull; P3, P2, and P4 are placed in the gelatin, aligned with a 0.03-m spacing, and perpendicular to the blast direction (side-on). See gages' locations in **Figure 4**. Four strain gages TML YFLA-10[3] (length 10 mm, resistance 120 Ω, gage factor 2.1) are placed on the skull in orthogonal directions, as

[1] www.synbone.ch
[2] www.endevco.com
[3] www.tml.jp

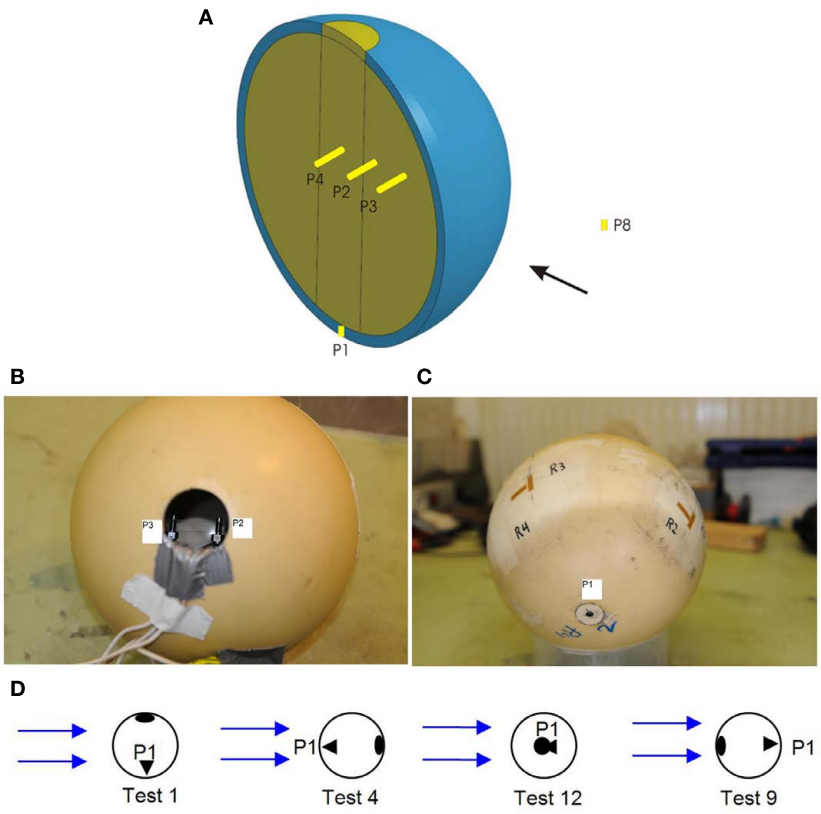

FIGURE 4 | (A) Sketch of sphere section and pressure gages in gelatin: P2, P3, and P4 and air: P1, P8; **(B)** skull with pressure gages: P3 and P2; **(C)** strain gages: R1–R4; **(D)** opening orientation with respect blast direction in different tests: top(test 1), rear (test 4), front (test 9), side (test 12).

shown in **Figure 4**. A Pacific 5800[4] data acquisition system is used (2 MHz sample speed; 350 kHz anti-aliasing filter).

The influence of the opening is studied, and compared with a skull where the opening is closed. To measure the influence of the opening orientation with respect to the blast direction in the gelatin, the sphere is rotated, so that the opening is on top (test 1), at the rear (test 4), in front (test 9), and sideways (test 12).

From the blast experiments, the following observations have been made:

- The pressure and impulse (area under pressure-time curve) in the gelatin is higher when there is an opening in the skull, **Figure 5A**.
- The pressure in the gelatin depends on the opening orientation. The pressure is maximum when the opening faces the blast (test 9), and it is minimum when the opening is opposite to the blast (test 4), **Figure 5B**.
- The pressure wave speed is $c_p = \frac{\Delta x}{\Delta t} = 1463$ m/s, calculated from the time the pressure wave takes to travel between two consecutive pressure gages ($\Delta t = 2.05 \cdot 10^{-5}$ s) and their spacing ($\Delta x = 0.03$ m), **Figure 5C**.

[4]www.pacificinstruments.com

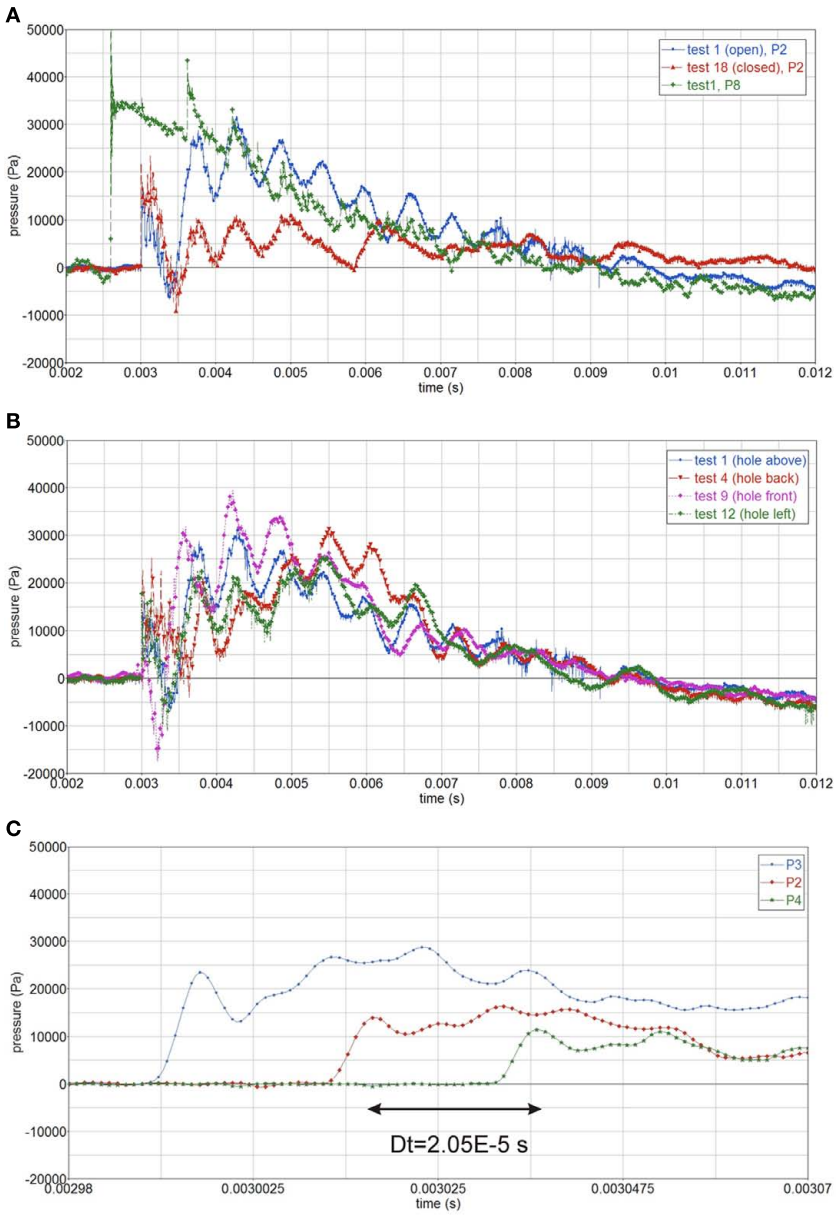

FIGURE 5 | (A) Pressure in gelatin for open and closed skull, P2, and air pressure, P8; **(B)** influence of opening orientation on internal pressure, P2, open skull; **(C)** calculating the pressure wave speed, $c_p = 1463$ m/s.

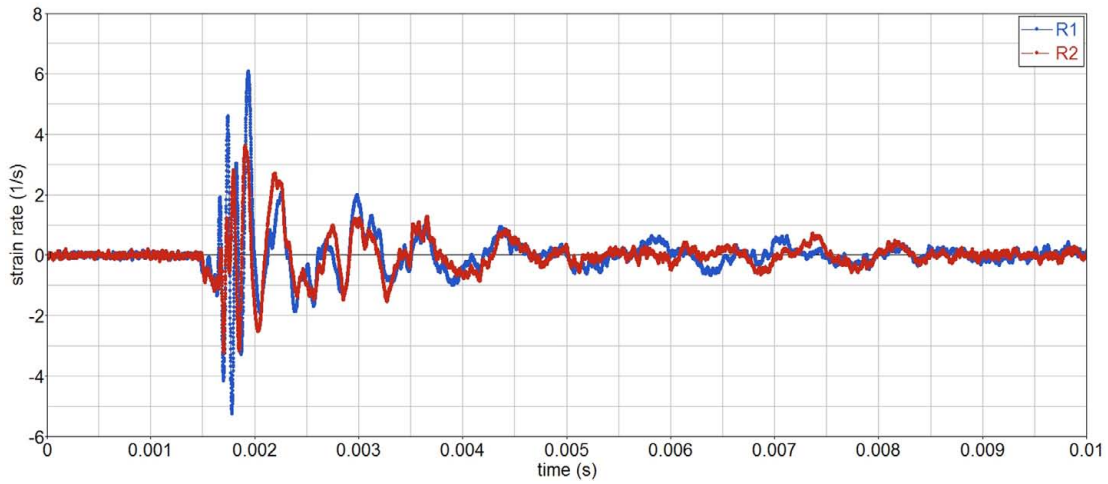

FIGURE 6 | Strain rate history on the skull.

- Surprisingly, the initial pressure in the gelatin becomes negative (in the first 0.5 ms); after which it follows the surrounding air pressure within the tube. The reason for this pressure drop might be due to the experimental setup, since a new series of experiments did not show this effect.
- The strain rate on the skull is moderate, less than $10\,s^{-1}$, **Figure 6**. Hence strain rate dependent behavior should be moderate.
- Closed skull experiments have shown that the internal pressure depends on the blast orientation. This indicates that the skull might not be fully closed or that there might be air trapped inside. Indeed, the skull is closed by sealing off the opening of an originally open skull using a Synbone cap. Although great care is exercised when gluing the cap, there must be a certain amount of leakage penetrating in the gelatin.
- Experiments have shown little influence of the pressure gage direction, side-on, or face-on.

2.3. NUMERICAL MODEL

Simulations of the above described shock tube experiments have been performed. FSI between air blast and surrogate is modeled in an uncoupled manner. The air blast is modeled by means of Eulerian CFD model, and the surrogate's structural response is modeled using a Lagrangian FE model. This uncoupling is reasonable due to the small deformations and displacements of the surrogate during the blast loading. As reference case, the skull with the opening on top is investigated, test 1.

The air blast is simulated using the TNO BLAST code (van den Berg, 2009). Compressible inviscid flow of an ideal gas is described by the Euler conservation equations for mass, momentum, and energy. Due to symmetries, only one quarter of the tube is modeled. The computational domain has dimensions $5\,m \times 0.2\,m \times 0.2\,m^3$, discretized as a uniform grid of 0.005 m grid spacing. The sphere is modeled as a fixed boundary. Appropriate initial boundary conditions have been applied to describe the incident blast.

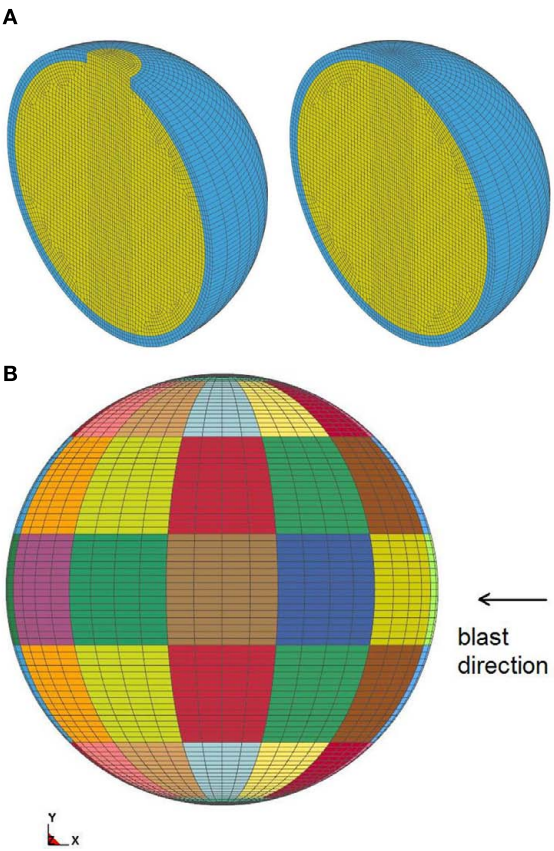

FIGURE 7 | (A) FE mesh of open and closed skull; **(B)** element faces where pressure is applied, each color is a group, corresponding to the same output point of the CFD model.

The structural response is modeled using the FE code LS-DYNA. Only one half of the sphere is modeled due to symmetry using appropriate boundary conditions, **Figure 7A**. The geometry

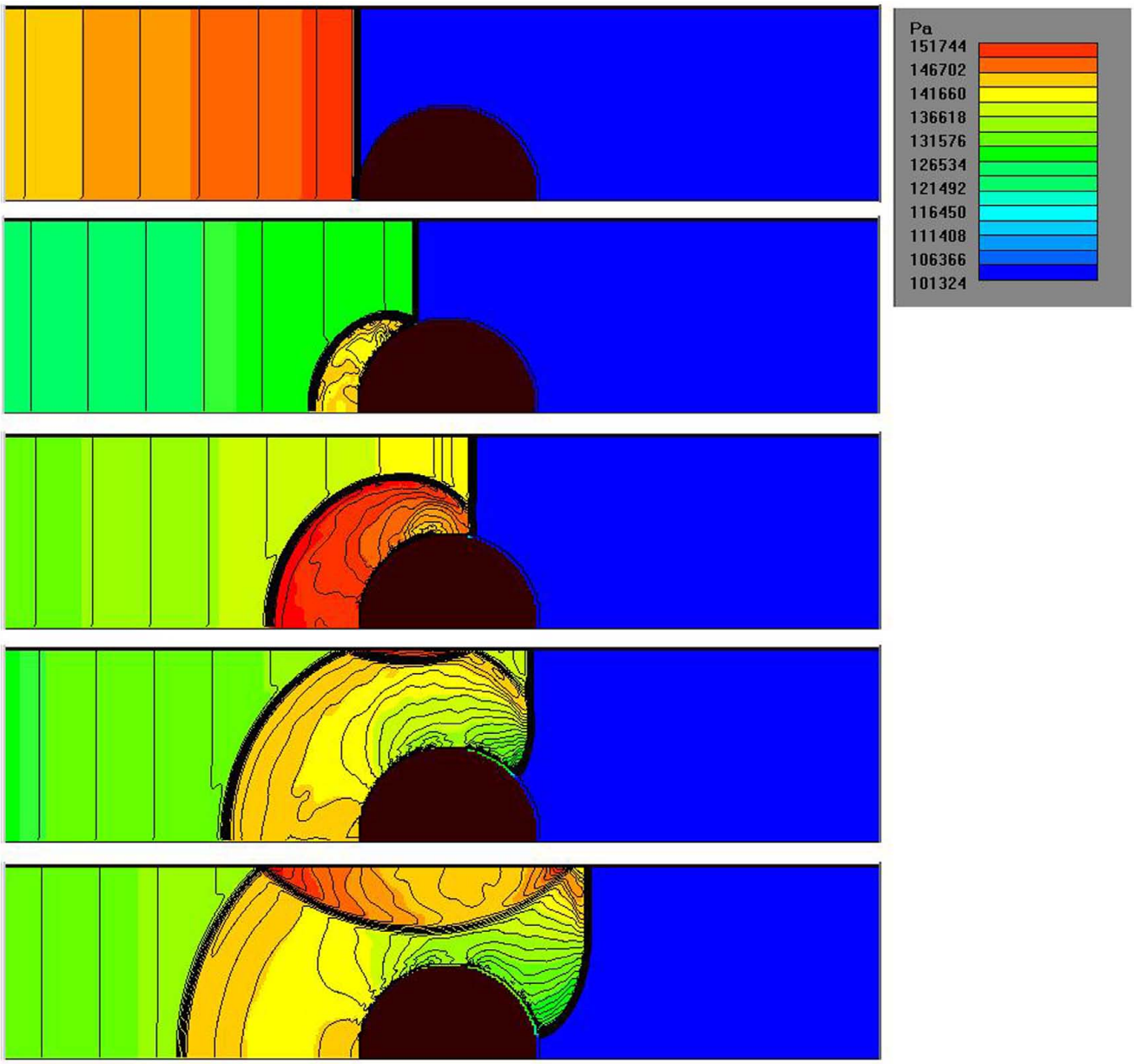

FIGURE 8 | Sequence of contour plots during the passage of the air shock wave. Snapshot interval $\Delta t = 0.00015$ s.

is modeled using roughly 43500 eight-node reduced integrated solid elements. The maximum element dimensions range from $l_e = 0.002$ m at the center, to $l_e = 0.012$ m outside, which is sufficient to describe the wave propagation. A minimum of six elements are needed within the wave propagation length λ, which is the case, i.e., $6l_e = 0.07\,\text{m} < \lambda = 0.19\,\text{m}$ (see Section 3). Three elements are used through the skull thickness. The simulated CFD pressure around the sphere is applied as boundary conditions at the perimeter element faces, **Figure 7B**.

The gelatin is modeled as an elastic material with a density of 960 kg/m^3. The compression wave speed has been calculated, $c_p = 1463$ m/s (see Section 2.2). A shear wave speed $c_s = 40$ m/s has been adopted from literature (Papazoglou et al., 2006). From c_p and c_s the elastic constants have been worked out using Eq. 1, which yield $G = 1.552\text{E}4$ *Pa*, $K = 2.076\text{E}9$ *Pa*, $E = 4.656\text{E}4$ *Pa*, and $\nu = 0.4999963$. The static stiffness of the Synbone skull has been measured from uniaxial tensile tests, $E = 1.4\text{E}9$ *Pa*, which is in agreement with values reported in literature (Cronin et al., 2000); $\nu = 0.469$, and the density is 700 kg/m^3. The compression wave speed and shear wave speed of the Synbone material is $c_p = 3415$ m/s and $c_s = 825$ m/s respectively.

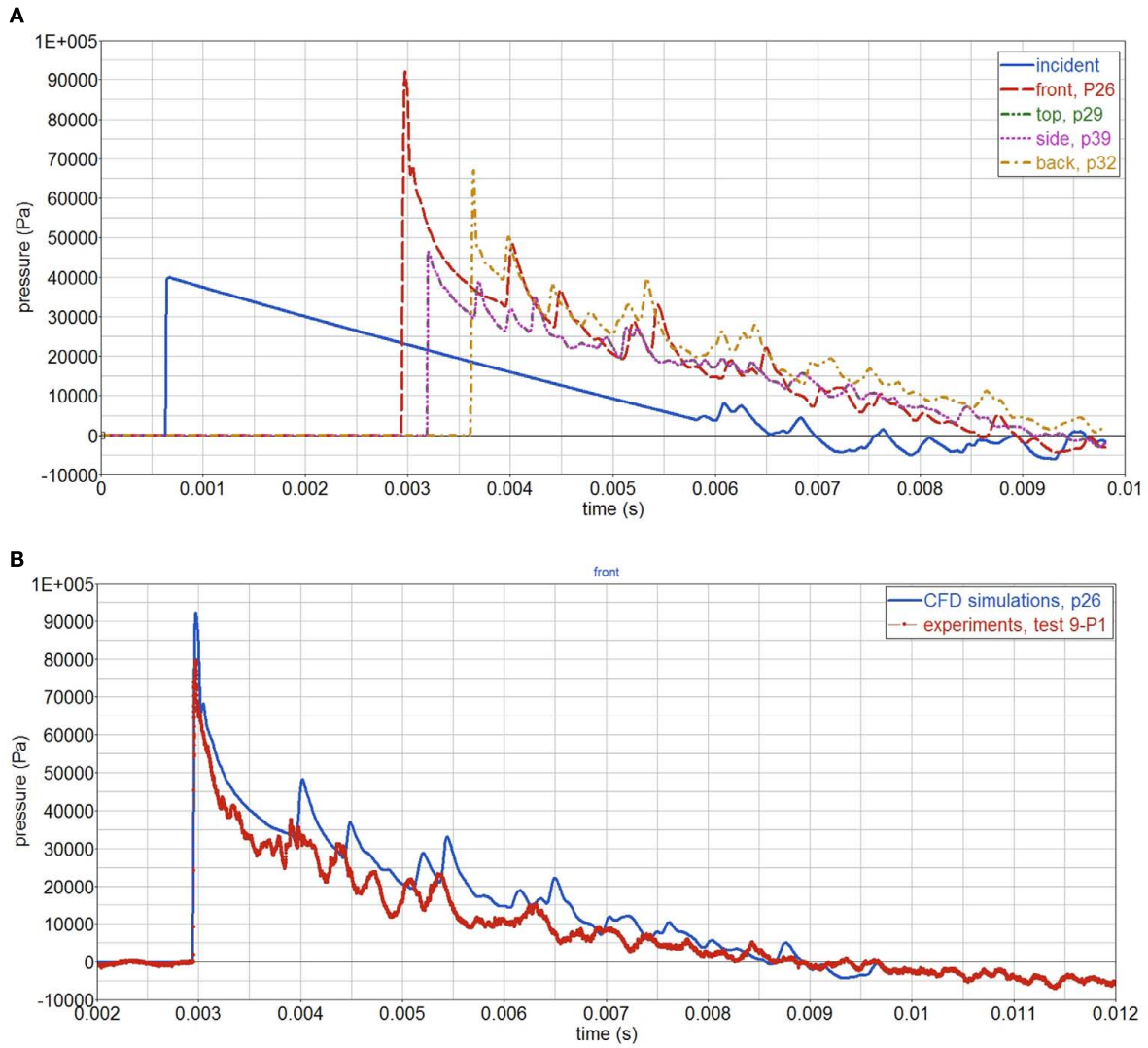

FIGURE 9 | (A) CFD simulated pressure around the sphere; **(B)** CFD simulations and experiments of air pressure at sphere's front face.

$$
\begin{aligned}
c_s &= \sqrt{\frac{G}{\rho}} \\
c_p &= \sqrt{\frac{(K + 4/3G)}{\rho}} \\
G &= \frac{E}{2\,(1+\nu)} \\
K &= \frac{E}{3\,(1-2\nu)}
\end{aligned}
\qquad (1)
$$

3. RESULTS

CFD simulations of the shock tube blast tests show the complex interaction, between the air shock wave (traveling at roughly 400 m/s), the sphere, and the shock tube, **Figure 8**. The pressure-time curves at different locations around the sphere are shown in **Figure 9A**. The highest peak reflected pressure and impulse occurs at the sphere's front face. Compared with the experiments, the simulations slightly overpredict the impulse, **Figure 9B**.

As indicated above, the test case considered is with the top opening, test 1. The reflected pressure of the CFD simulations, is applied as boundary conditions of the FE model. **Figure 10** shows pressure contour plots of the open and closed skull at the same time ($t = 0.008$ s). Experiments and simulations show that when there is an opening, a larger impulse is transferred inside the gelatin, compared with the case with no opening, **Figure 11**. Yet, the simulations do not show the initial pressure drop, which is observed in the experiments. After this initial drop, both measured and simulated gelatin pressure follow the surrounding air pressure in the shock tube, decaying gradually to the atmospheric pressure after 7 ms.

Simulations show a high frequency component, $f = \frac{1}{T} = 7.7$ kHz, which corresponds to the time the pressure wave takes to travel across the sphere, $T = D/c_p = 0.19/1463 = 0.00013$ s. The

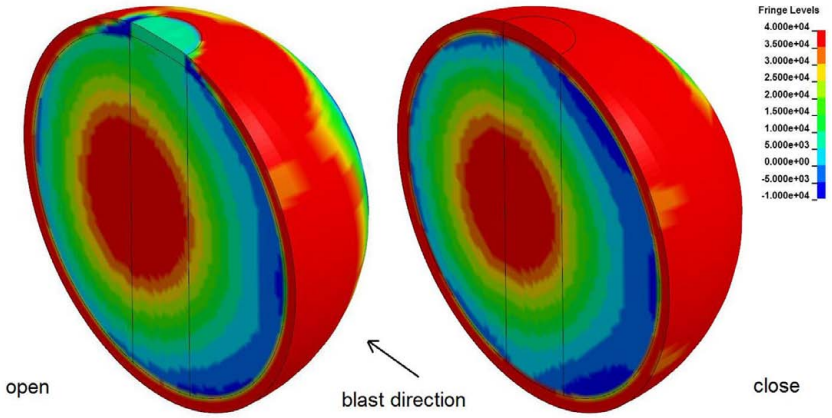

FIGURE 10 | Pressure contour plots for open (left) and closed skull (right), at $t = 0.008$ s.

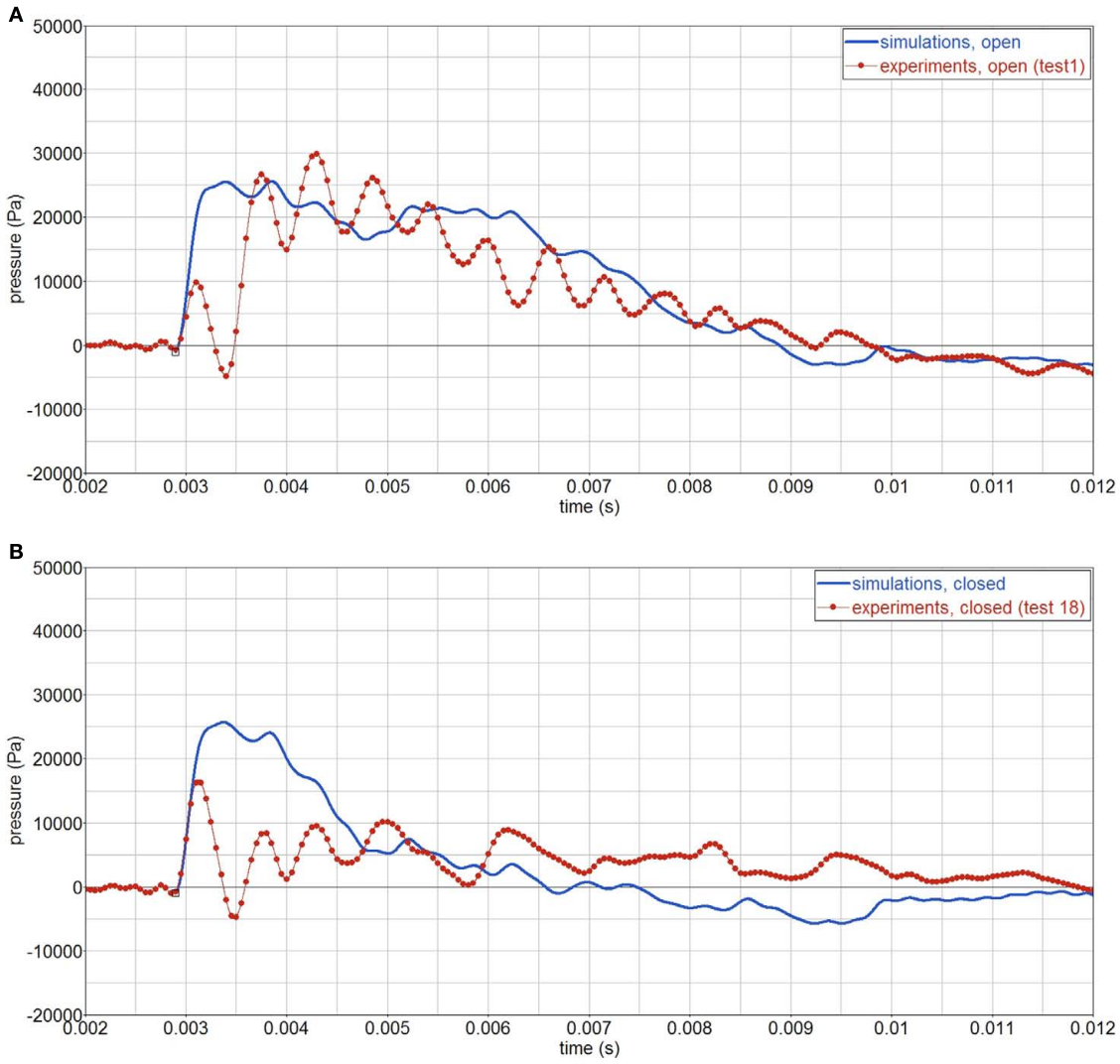

FIGURE 11 | Experimental and simulated pressure history in the gelatin, P2. Signals are filtered using a 4-kHz filter. **(A)** open skull; **(B)** closed skull.

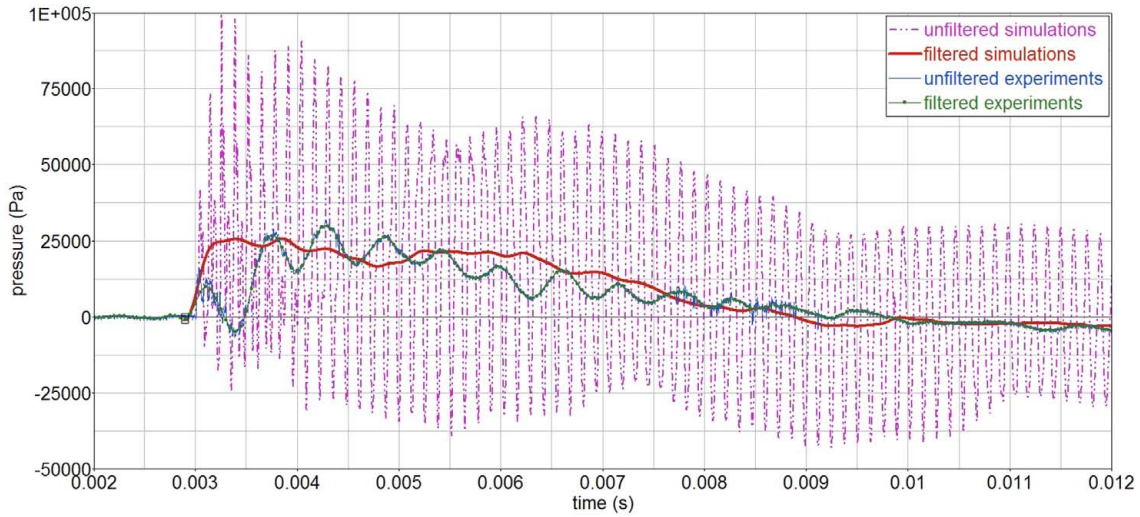

FIGURE 12 | Filtered (4 kHz filter) and unfiltered pressure-time curves in the gelatin, P2.

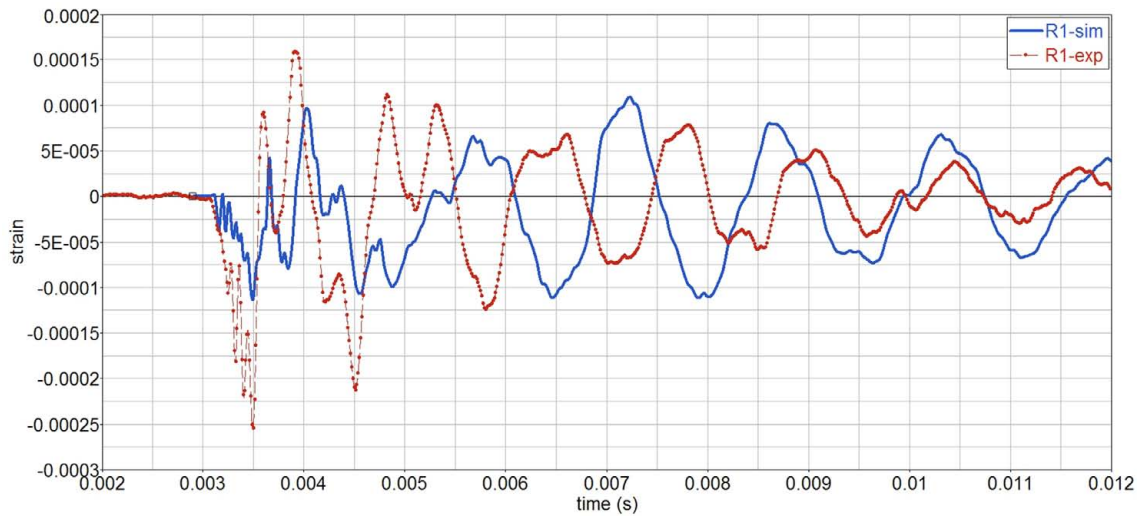

FIGURE 13 | Filtered and unfiltered pressure signals in the gelatin, P2.

wave length is equal to sphere diameter, $\lambda = c_p \cdot T = D = 0.19$ m. For clarity, this high frequency component has been eliminated throughout the analysis using a 4-kHz filter, **Figure 12**. The reason why this high frequency component is not seen in the experiments is not yet understood.

As far as the strains on the skull, **Figure 13**, the amplitudes of simulations and experiments are similar, although the vibration period of the simulations is slightly longer, which indicates an overly soft behavior.

3.1. PARAMETER STUDY

To study the influence of the material properties on the surrogate's response, a parameter study is performed. Firstly, the influence of the gelatin shear stiffness investigated, by varying the shear wave speed c_s, while keeping the pressure wave speed c_p constant. The corresponding elastic constants are given in **Table 1**. The simulations, **Figure 14**, show that the gelatin pressure varies little with c_s, in the range of study, 4–30 m/s.

Table 1 | Pressure and shear wave speeds, and elastic constants of gelatin.

c_p (m/s)	c_s (m/s)	G (*Pa*)	K (*Pa*)	E (*Pa*)	ν
1463	4	1.552E + 04	2.076E + 09	4.655E + 04	4.9999626E-01
1463	10	9.700E + 04	2.076E + 09	2.909E + 05	4.9997664E-01
1463	30	8.730E + 05	2,075E + 09	2.619E + 06	4.9978967E-01

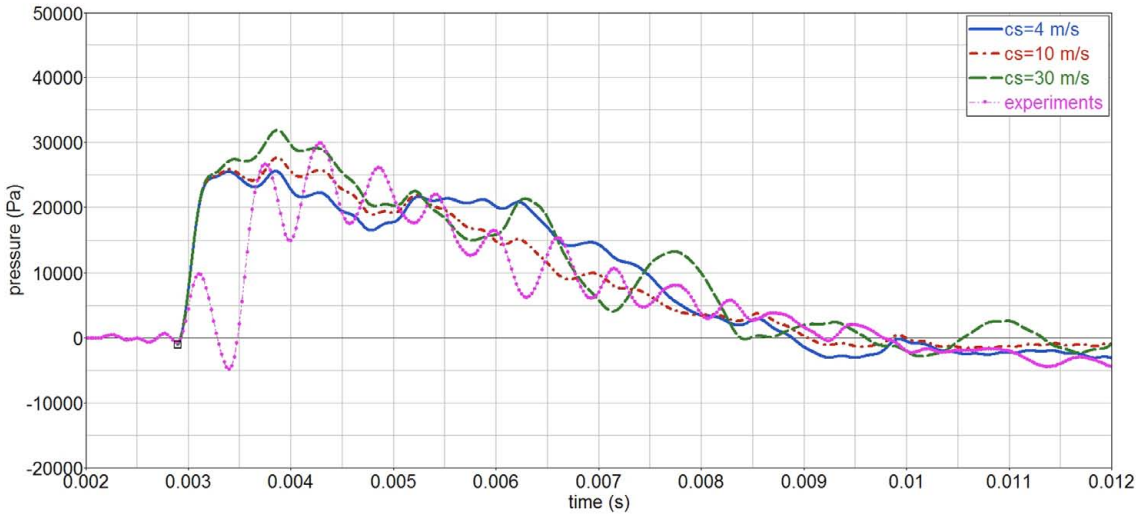

FIGURE 14 | Influence of gelatin shear wave speed c_s on the gelatin pressure, *P2*.

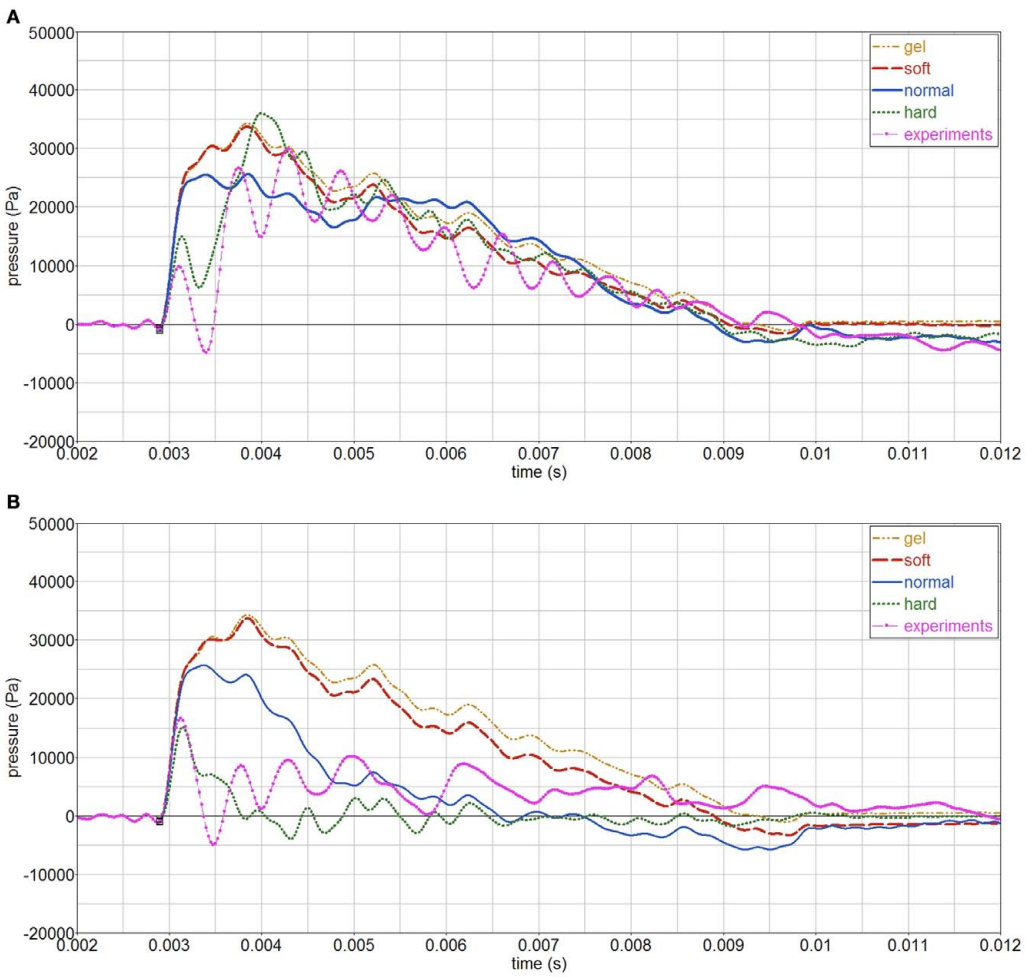

FIGURE 15 | Influence of skull stiffness on gelatin pressure, P2. (A) open skull; **(B)** closed skull.

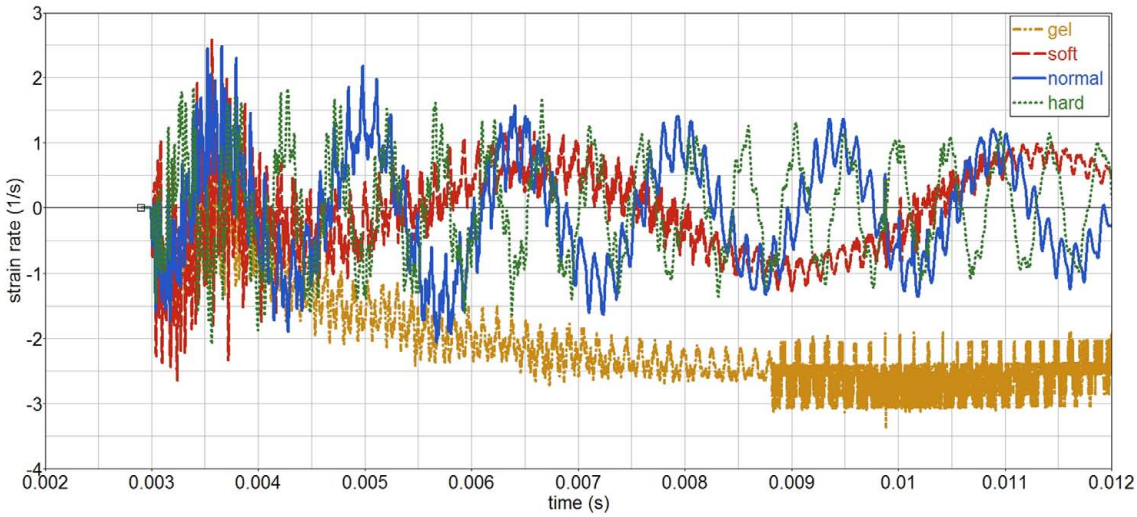

FIGURE 16 | Influence of skull stiffness on gelatin strain rate (open skull).

Secondly, the influence of the skull stiffness E is analyzed for an open and a closed skull. The normal Young's modulus $E_o = 1.4E9$ *Pa* is varied between $E = 0.1E_o$ (soft skull), to $E = 10E_o$ (hard skull), and it is also compared with the case without skull (only gelatin). The open skull simulations show that the skull gives little protection, as the pressure in the gelatin is similar regardless of the skull stiffness, **Figure 15**. The skull stiffness mainly affects the initial part of the pressure-time curve. On the contrary, a closed skull does protect the gelatin inside, since the internal pressure is more sensitive to the skull stiffness. In the closed case, the skull is the only pathway of the stress waves into the gelatin; whereas in the open case, stress waves can also be transmitted through the opening. Hence the larger stiffness sensitivity for the closed skull.

Strain rates in the gelatin are smaller than 3, 1/s, and maximum values are independent of the skull stiffness, **Figure 16**. Frequency does increase with increasing skull stiffness. Since the strain rates are moderate, no special measurement techniques, e.g., split hopkinson bar (SPB), are needed in order to characterize its strain rate behavior.

3.2. INFLUENCE OF PRESSURE GAGES

It has been argued that gages may distort the surrounding pressure field because of their different impedance with respect the medium in which they are embedded (i.e., gelatin). Hence, the measured pressure may be different than the actual pressure, i.e., without gage interference. To study this effect, an Endevco pressure gage, **Figure 17**, has been modeled inside the surrogate. The gage has a mass of 2.3 g, a volume of 5 cc, and is made of stainless steel. Due to the gage, a full 3D model is used, made by mirroring the existing half symmetric model. The pressure gage is modeled by assigning appropriate material properties to a number of elements, which occupy roughly the same volume as the actual gage. The simulated gage has an equivalent density $\rho = 4500\ \text{kg/m}^3$ and steel elastic constants $E = 2.1E11$ *Pa*, $\nu = 0.3$. Hence, $c_p = 7925$ m/s and $c_s = 4237$ m/s. The results show almost no influence of the gage when using a 4-kHz filter, **Figure 18**; a change in amplitude is visible when a 8-kHz filter is used.

4. DISCUSSION AND CONCLUSION

To understand the causes leading to blast induced mTBI, and eventually develop protective measures, the mechanisms of wave propagation in the human head must be investigated. As shown in this paper, shock tube blast tests on simple skull/brain surrogates, complemented with simple numerical models, can be very useful to find trends, and serve as basis upon which more advance surrogates-models can be devised. In the future, to be able to predict mTBI, animal testing, and simulations thereof must be done.

From this study, it can be concluded that:

- The presence of an opening in the skull and its orientation has a large influence on the results. Experiments and simulations show that the pressure and impulse transmitted to the gelatin increases with an opening. The maximum internal pressure occurs when the opening faces the blast. The internal pressure in the gelatin follow the outside air pressure. Experiments, however, show an initial pressure drop in the gelatin, not seen in the simulations, which must be caused by the experimental setup, since more recent measurements did not show this phenomenon. The presence of air bubbles near the pressure gages have not been checked, and these could affect the measurements.
- Simulations show that the effect of the skull stiffness is small if there is an opening in the skull, contrary to what happens with a closed skull. If the skull is closed, the blast pressure can only by transmitted to the gelatin through the skull; there is no alternative path through the opening.
- The gelatin shear wave speed has a small effect on the gelatin pressure, indicating a predominant bulk behavior. Hence, using

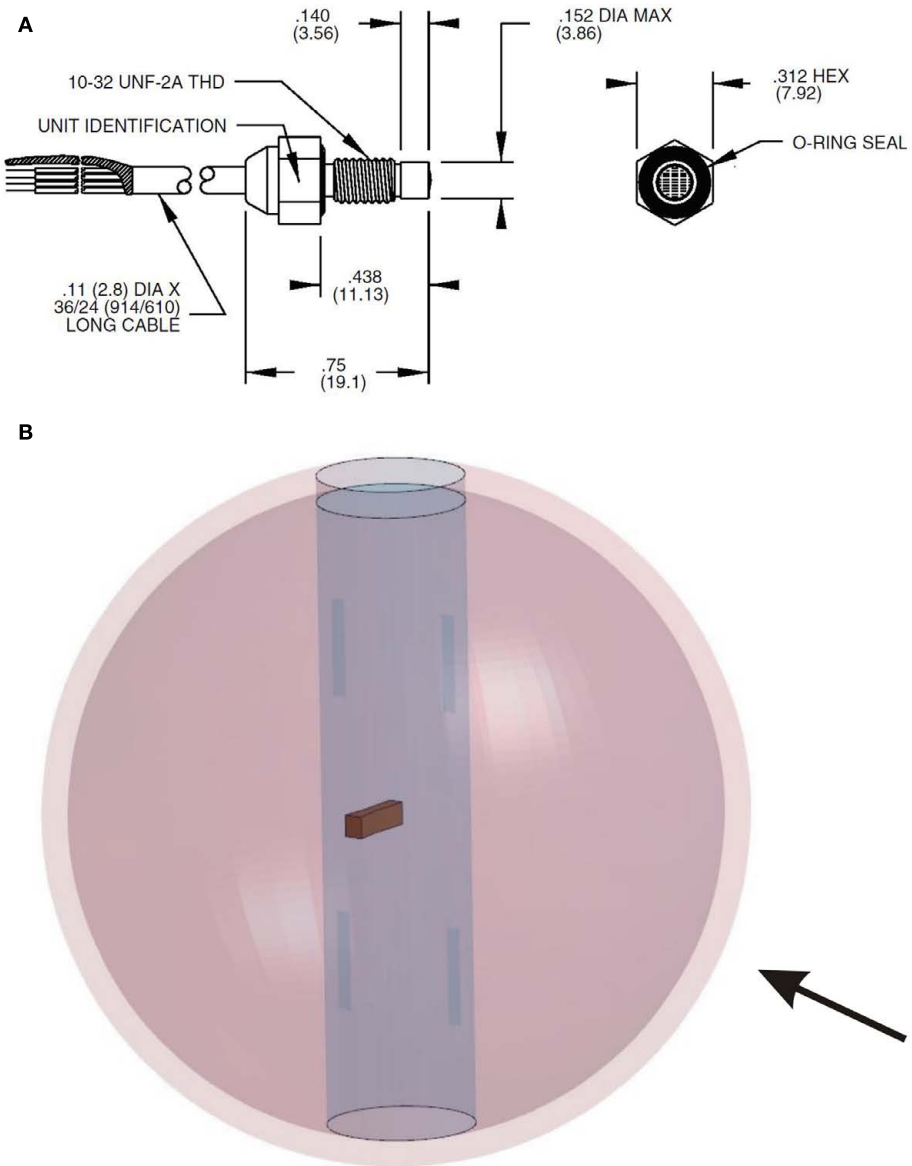

FIGURE 17 | (A) Endevco pressure gage; **(B)** full surrogate FE model with gage.

a viscoelastic shear model, instead of the elastic material model used in this study, might only lead to a modest improvement.

- Because of the small deformation and displacement of the surrogate skull upon blast loading, an uncoupled simulation approach (CFD + FE) for the FSI between air blast and surrogate is justifiable. The CFD simulations agree with the shock tube blast experiments, with the advantage over the experiments that the pressure can be obtained anywhere in the domain, whereas the number of experimental measurements is limited.
- A high frequency component is observed in the simulated internal pressure, which corresponds to the reflections of the pressure wave against the sphere's free boundaries. This effect is not seen in the experiments, and further investigation is needed to explain these differences. To the author's knowledge there is no evidence in literature of the application of the pressure gages used in the experiments to viscoelastic materials. Hence, it is recommended to validate the gages' performance in gelatin, under a known pressure-time load.
- Simulations revealed that the influence of the gages is limited and only introduces a high frequency component. Mesh fineness remains to be investigated, since the pressure field created around the gages may require a finer mesh discretization.
- Strain rates observed in the simulations and experiments are moderate. Hence, standard tests can be performed for material characterization (e.g., dynamic tensile tests), without the need of high strain rate tests (e.g., SHB).

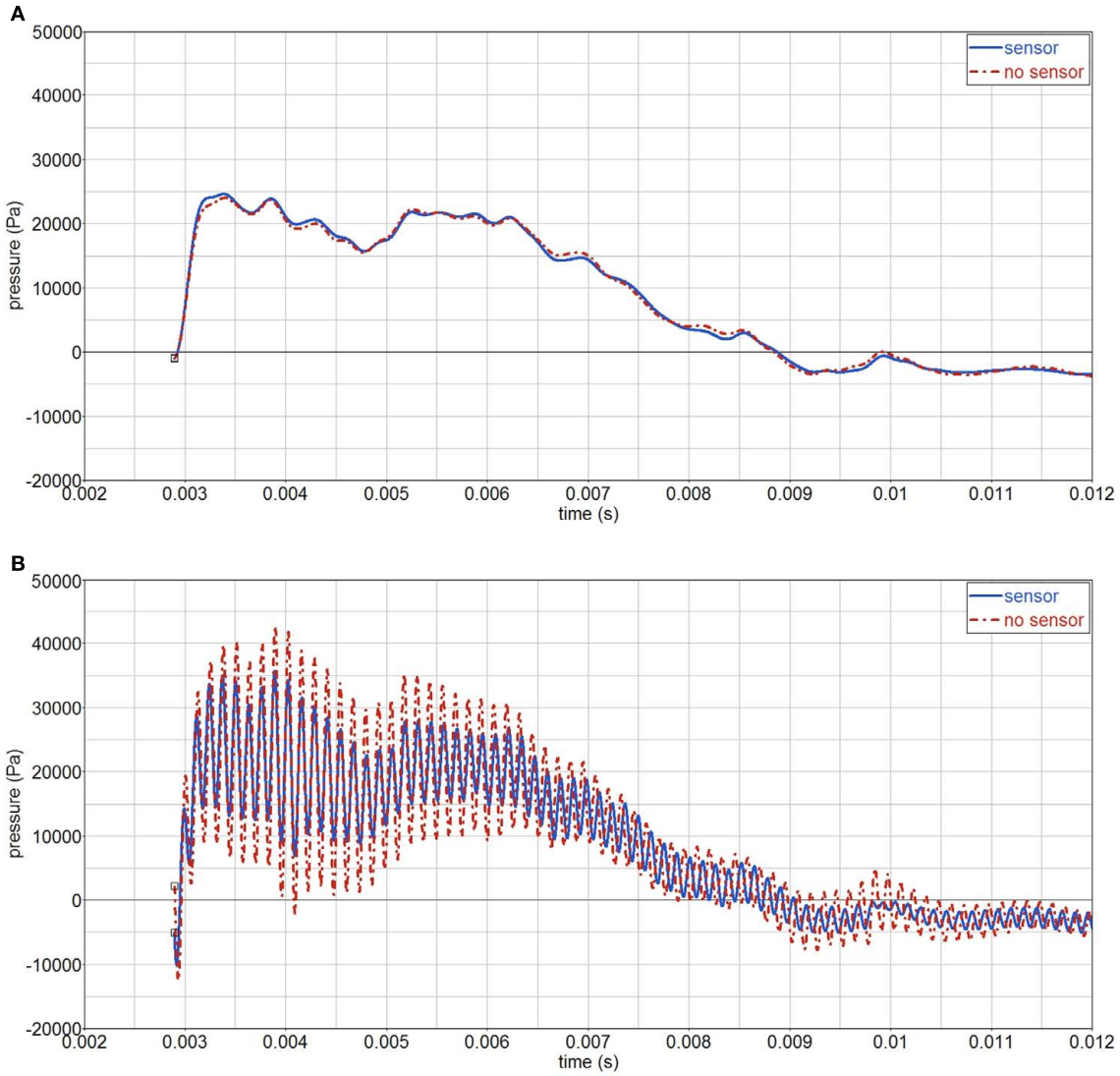

FIGURE 18 | Influence of the gage on pressure-time curves, in the middle of sphere (P2). (A) 4 kHz filter; **(B)** 8 kHz filter.

ACKNOWLEDGMENTS

The authors would like to thank TNO, in particular the department of Physical Protection and Survivability, for providing the framework to do the experiments and the simulations; as well as the Dutch Ministry of Defense for funding this research project.

REFERENCES

Alley, M. D., Schimizze, B. R., and Son, S. F. (2011). Experimental modeling of explosive blast-related traumatic brain injuries. *Neuroimage* 54(Suppl. 1), S45–S54.

Axelsson, H., Hjelmqvist, H., Medin, A., Persson, J. K. E., and Suneson, A. (2000). Physiological changes in pigs exposed to a blast wave from a detonating high-explosive charge. *Mil. Med.* 165, 119–126.

Bass, C. R., Rafaels, K. A., and Salzar, R. S. (2008). Pulmonary injury risk assessment for short-duration blasts. *J. Trauma* 65, 604–615.

Cernak, I., and Noble-Haeusslein, L. J. (2009). Traumatic brain injury: an overview of pathobiology with emphasis on military populations. *J. Cereb. Blood Flow Metab.* 30, 255–266.

Chafi, M. S., Karami, G., and Ziejewski, M. (2009). Numerical analysis of blast-induced wave propagation using fsi and ale multi-material formulations. *Int. J. Impact Eng.* 36, 1269–1275.

Cronin, D. S., Salisbury, C., Worswick, M. J., Pick, R. J., Williams, K. V., and Bourget, D. (2000). "Appropriate material selection for surrogate leg models subjected to blast loading," in *Proceedings Explomet 2000*, eds L. Murr and M. Meyer, Albuquerque, NM.

Garo, A., Hrapko, M., Van Dommelen, J. A. W., and Peters, G. W. M. (2007). Towards a reliable characterisation of the mechanical behaviour of brain tissue: the effects of post-mortem time and sample preparation. *Biorheology* 44, 51–58.

Grujicic, M., Bell, W. C., Pandurangan, B., and He, T. (2010). Blast-wave impact-mitigation capability of polyurea when used as helmet suspension-pad material. *Mater. Des.* 31, 4050–4065.

Long, J. B., Bentley, T. L., Wessner, K. A., Cerone, C., Sweeney, S., and Bauman, R. A. (2009). Blast overpressure in rats: recreating a battlefield injury in the laboratory. *J. Neurotrauma* 26, 827–840.

Moore, D. F., Jrusalem, A., Nyein, M., Noels, L., Jaffee, M. S., and Radovitzky, R. A. (2009). Computational biology – modeling of primary blast effects on the central

nervous system. *Neuroimage* 47(Suppl. 2), T10–T20.

Moss, W. C., King, M. J., and Blackman, E. G. (2009). Skull flexure from blast waves: a mechanism for brain injury with implications for helmet design. *Phys. Rev. Lett.* 103, 108702.

Mott, D. R., Schwer, D. A., Young, T. R., Levine, J., Dionne, J.-P., Makris, A., and Hubler, G. (2008). "Blast-induced pressure fields beneath a military helmet," in *MABS*, Oslo.

Papazoglou, S., Rump, J., Klatt, D., Hamhaber, U., Braun, J., and Sack, I. (2006). "Influence of the transducer near field in MR elastography wave images," in *International Society of Magnetic Resonance in Medicine*, Seattle, Washington.

Richmond, D. R., and Axelsson, H. (1990). Air blast and underwater blast studies with animals. *J. Trauma* 6(Suppl. 2), 229–234.

Säljö, A., Arrhen, F., Bolouri, H., Mayorga, M., and Hamberger, A. (2008). Neuropathology and pressure in the pig brain resulting from low-impulse noise exposure. *J. Neurotrauma* 25, 1397–1406.

Säljö, A., Mayorga, M., Bolouri, H., Svensson, B., and Hamberger, A. (2011). Mechanisms and pathophysiology of the low-level blast brain injury in animal models. *Neuroimage* 54(Suppl. 1), S83–S88.

Scherer, M., and Schubert, M. (2009). Traumatic brain injury and vestibular pathology as a comorbidity after blast exposure. *Phys. Ther.* 89, 980–992.

Taylor, P. A., and Ford Corey, C. (2009). Simulation of blast-induced early-time intracranial wave physics leading to traumatic brain injury. *J. Biomech. Eng.* 131, 061007.

van den Berg, A. C. (2009). "Blast": a compilation of codes for the numerical simulation of the gas dynamics of explosions. *J. Loss Prev. Process Industries* 22, 950–4230.

Zhu, F., Wagner, C., Dal Cengio Leonardi, A., Jin, X., Vande-Vord, P., Chou, C., Yang, K., and King, A. (2011). Using a gel/plastic surrogate to study the biomechanical response of the head under air shock loading: a combined experimental and numerical investigation. *Biomech. Model. Mechanobiol.* 1–13. 1617–7959.

Conflict of Interest Statement: The authors declare that the research was conducted in the absence of any commercial or financial relationships that could be construed as a potential conflict of interest.

Received: 14 February 2011; accepted: 28 August 2011; published online: 19 September 2011.

Citation: Mediavilla Varas J, Philippens M, Meijer SR, van den Berg AC, Sibma PC, van Bree JLMJ and de Vries DVWM (2011) Physics of IED blast shock tube simulations for mTBI research. Front. Neur. ***2****:58. doi: 10.3389/fneur.2011.00058*

This article was submitted to Frontiers in Neurotrauma, a specialty of Frontiers in Neurology.

frontiers in
NEUROLOGY

PERSPECTIVE ARTICLE
published: 23 November 2010
doi: 10.3389/fneur.2010.00146

Report of a consensus meeting on human brain temperature after severe traumatic brain injury: its measurement and management during pyrexia

Charmaine Childs[1]*, Tadeusz Wieloch[2], Fiona Lecky[3], Graham Machin[4], Bridget Harris[5] and Nino Stocchetti[6]

[1] *Yong Loo Lin School of Medicine, National University of Singapore, Singapore*
[2] *Laboratory for Experimental Brain Research, Wallenberg Centre for Neuroscience, Lund, Sweden*
[3] *Trauma Audit Research Network, Salford Royal NHS Foundation Trust, University of Manchester, Greater Manchester, UK*
[4] *Temperature Group, National Physical Laboratory, Middlesex, UK*
[5] *School of Clinical Sciences and Community Health, Royal Infirmary, The University of Edinburgh, Edinburgh, UK*
[6] *Terapia Intensiva Neuroscienze, Ospedale Policlinico, Istituiti di Ricovero e Cura a Carattere Scientifico, Milano, Italy*

Edited by:
Marten Risling, Karolinska Institutet, Sweden

Reviewed by:
Mattias Sköld, Karolinska Institutet, Sweden
Guy Clifton, Uniformed University of the Health Sciences, USA

****Correspondence:***
Charmaine Childs, Yong Loo Lin School of Medicine, Alice Lee Centre for Nursing Studies, National University of Singapore, Block E3A, Level 3, 7 Engineering Drive 1, Singapore 117574. e-mail: charmaine_childs@nuhs.edu.sg

Temperature disturbances are common in patients with severe traumatic brain injury. The possibility of an adaptive, potentially beneficial role for fever in patients with severe brain trauma has been dismissed, but without good justification. Fever might, in some patients, confer benefit. A cadre of clinicians and scientists met to debate the clinically relevant, but often controversial issue about whether raised brain temperature after human traumatic brain injury (TBI) should be regarded as "good or bad" for outcome. The objective was to produce a consensus document of views about current temperature measurement and pyrexia treatment. Lectures were delivered by invited speakers with National and International publication track records in thermoregulation, neuroscience, epidemiology, measurement standards and neurocritical care. Summaries of the lectures and workshop discussions were produced from transcriptions of the lectures and workshop discussions. At the close of meeting, there was agreement on four key issues relevant to modern temperature measurement and management and for undergirding of an evidence-based practice, culminating in a consensus statement. There is no robust scientific data to support the use of hypothermia in patients whose intracranial pressure is controllable using standard therapy. A randomized clinical trial is justified to establish if body cooling for control of pyrexia (to normothermia) vs moderate pyrexia leads to a better patient outcome for TBI patients.

Keywords: brain temperature, measurement, pyrexia, fever, cooling

INTRODUCTION

PYREXIA AFTER TRAUMATIC BRAIN INJURY: IS IT GOOD OR BAD FOR PATIENT OUTCOME?

For patients with severe traumatic brain injury (TBI) temperature management is undertaken for two reasons; (a) for neuroprotection (b) for control of pyrexia. In the case for cerebral neuroprotection, results in rodents provide convincing evidence that if body (or brain) temperature is lowered such that animals are rendered hypothermic during a brief period of transient cerebral ischemia, infarct size is smaller compared to the "normothermic" or hyperthermic animal (Busto et al., 1987; Kim et al., 1996; Yanamoto et al., 1999). The starting point to begin hypothermic neuroprotection may well be a normal temperature (which in the rat under thermoneutral conditions is 38°C Stoner, 1974). Hypothermia holds promise as a neuroprotective therapy after ischemic stroke (Lyden et al., 2006) but as the role of ischemia remains controversial as a mechanism of brain damage after TBI (Coles, 2004; Vespa, et al., 2005) the benefit of hypothermia for neuroprotection in this patient group remains speculative (Abate et al., 2008).

To date there is no robust evidence that control of pyrexia, using antipyretic drugs or body cooling is beneficial after severe TBI. Nevertheless current opinion favors treatment for control of pyrexia (Kilpatrick et al., 2000) because of the commonly held view that a mild to moderate rise in temperature is harmful (Manno and Farmer, 2004). We can add a third common assumption that, for all practical purposes, body temperature is an adequate surrogate measure of brain temperature even though there are well documented observations showing brain-body dissociation (Mellergard, 1994; Stone et al., 1995; Henker et al., 1998; Rumana et al., 1998; Childs et al., 2005).

Guidelines for the best approach to temperature measurement do not exist. The most recent (2007) Brain Trauma Foundation (BTF) recommendations for therapeutic hypothermia after TBI (Bullock and Povlishock, 2007) are based on the lowest level of evidence only (Cook et al., 1995; also refer to Center for Evidence Based Medicine www.cebm-net/). Until we can "close the loop" on our understanding of the impact of pyrexia on outcome (good or bad in the case of TBI patients; Childs, 2008) treatment will continue to be underpinned by weak, inconclusive evidence of benefit. This paper aims at summarizing current knowledge in the field and in particular two clinically relevant issues:

(a) In the critical care setting, what should future recommendations be: direct measurement of brain temperature or to continue using body core temperature surrogates?

(b) Should therapeutic control of temperature be advocated as a treatment panacea or should it be "on prescription"?

MANCHESTER CONSENSUS MEETING

A cadre of clinician-scientists were invited to participate in a debate about the clinically relevant, but often controversial issue: "Is raised brain temperature; good or bad after human TBI?" Interlinked, "bench to bedside" lectures, were presented followed by workshop discussions, the content of which forms this consensus document.

LITERATURE FRAMEWORK

WHAT ARE THE POSSIBILITIES FOR ACCURATE MEASUREMENT OF TEMPERATURE IN PATIENTS?

The essential background role that calibration, traceability and accreditation play in ensuring reliable temperature measurement was discussed. Particular emphasis was given to ensuring measurements were reliably linked to the International temperature scale of 1990 (ITS-90; Preston-Thomas, 1990). ITS-90 is essentially a "recipe" of how to realize a temperature scale that is close to thermodynamic values through the calibration of specified thermometers (platinum resistance thermometers, PRTs) at defined temperature references known as fixed points. The primary fixed points are generally the freezing points of pure materials or triple points (e.g., of water). A triple point is a unique point on a materials phase diagram where solid, liquid, and vapor coexist. The calibrated PRT is then used as a reference for the calibration of other more "practical" sensors, e.g., *in situ* mini sensors of the type used in everyday health care practice. In addition, special radiance sources are constructed to derive their temperature from calibrated PRTs. These can be used to calibrate clinical infra-red (tympanic, temporal artery, thermal imaging) thermometers.

Using the triple point of two high performance organic fixed-point temperature reference substances, Diphenyl-ether (DPE; nominally 26°C), and ethylene carbonate (EC; nominally 36°C), (both substances having temperature uncertainties of 0.005°C) the performance (reliability, reproducibility, and measurement error) of clinical thermometers used for deep body temperature measurement were tested for traceability of the thermometers to ITS-90 and for maximum confidence in the measurements. The results showed that all the temperature sensors tested (brain and core body thermistors) performed within the manufacturer's stated tolerances (Childs and Machin, 2009; Machin and Childs, 2010).

In recent years, new techniques have emerged for non-invasive temperature measurement. Proton magnetic resonance spectroscopy (^{1}HMRS) can be utilized for absolute internal temperature (Childs et al., 2007). However, there is currently no established approach to calibrate measurements in a systematic way but two independent temperature measurement techniques can be used for MR thermometry: PRTs and phantom-based, organic triple point, temperature cells. Early results and field trials are promising (Vescovo et al., 2010). A novel, quasi-spherical, temperature phantom has been developed and built suitable for use at field strengths of 1.5 and 3 Tesla "phantom" material is placed at the center, surrounded by a reference source of the organic fixed-point material, which for clinical measurement consists of either DPE or EC.

THE ROLE OF TEMPERATURE IN THE DAMAGED BRAIN

In most animal species, the response to local and systemic inflammation and infection is a rise in body temperature. Fever, with its long evolutionary history has been shown to confer benefit for the host in terms of bacterial killing and increased immunity. Over the years, studies have been conducted in numerous species (Kluger, 1979) and the survival benefit of fever is evident (Romanovsky and Szekely, 1998). It is also clear that mortality increases if the febrile response to inflammation is prevented or blocked (Griesman and Mackowiak, 2002; Schulman et al., 2005).

In patients, fever is a common sign of inflammation and trauma and for the most part is widely thought to have a beneficial role in "fighting" infection. However, if the injury damages brain (and specifically ischemic cells) tolerance to heat is low (Brinnel et al., 1987). The prevailing view in neurocritical care rather favors the opinion that raised temperature after TBI is bad and that low temperature is innocuous and beneficial.

Studies in animals show that below normal temperature preserves, and high temperature accelerates damage in ischemic neurones (Yanamoto et al., 1999). There is evidence to support the case for therapeutic neuroprotection by induction of hypothermia in ischemic brain (cardiac arrest; Lyon et al., 2010) and neonatal hypoxic encephalopathy (Shankaran et al., 2008) but the evidence is not as compelling after human stroke (Schwab et al., 1998) and the value of mild or moderate hypothermia remains speculative in patients with brain trauma (Sydenham et al., 2009). On balance therefore, the view is that raised temperature due to fever has biological benefit if the brain is intact but once damaged (specifically by ischemia) any protective benefits of a "true" fever may be outweighed by the presumed increased vulnerability of CNS tissue to damage by heat (Haveman et al., 2005; Van Der Zee et al., 2008).

The uncertainty about the role of fever after TBI presents a dilemma for the clinician. How can appropriate evidence-based decisions be made when there is a lack of robust data to underpin practice? Which patients should be a priority for treatment of pyrexia and which patients are at low risk of temperature-related secondary damage? With the increasing interest and use of therapeutic hypothermia, even in the absence of clear benefit, at least in humans we may now need to question the potential for "good" and "bad" effects of deliberate hypothermia, as well as the potentially "good" and "bad" effects of fever (Clifton et al., 2001; Hutchinson et al., 2008). Since there is an abundant literature on the use of therapeutic hypothermia, still without a definitive answer about its benefits, it is timely to give thought to the apparently "unthinkable"; that there may be TBI patients for whom a moderate rise in temperature might not be harmful and who might not need aggressive temperature control.

TEMPERATURE AS A MARKER OF SECONDARY BRAIN DAMAGE

Of the many factors contributing to the quality of a patient's outcome after TBI, body temperature has only recently been considered for its prognostic significance. The problem is that any relationship between body (or brain) temperature, particularly with respect to sub-normal temperature and outcome is confounded by other important variables such as brain injury severity, age, gender, peripheral trauma, and a number of co-existing physiological responses (e.g., pupil size, intracranial pressure). At

the time of admission, approximately 10% of patients presenting with TBI were hypothermic (McHugh et al., 2007). From results of the International TBI data collaboration on modeling prognostic indicators of outcome after TBI (IMPACT; Maas et al., 2007), it was recognized that any relationship between (brain) temperature and outcome would be confounded by other important variables (if not measured and adjusted for). During the years spanning 1982–1998, the IMPACT methods were to merge data from randomized trials and large observational studies of TBI patients treated in an ICU setting. Univariate analysis of 26 predictors for outcome at 6 months were analyzed in 8719 patients. Hypoxia, hypotension, and spontaneous hypothermia were significant prognostic markers of adverse outcome. However, the strength of the association between hypothermia on admission to the Emergency Department (ED) and adverse outcome after TBI was lessened after adjustment for other confounders such as age, GCS, motor score and pupil size and reactivity. In view of the results, the adverse outcomes associated with spontaneous hypothermia do not lend support for "continued" body cooling of the TBI patient on arrival to the ED and before transfer to ICU. Despite the large numbers of patients studied from the IMPACT database, there is still uncertainty about how best to manage body temperature after acute TBI.

IS THERAPEUTIC HYPOTHERMIA A DOUBLE-EDGE SWORD?

From studies of experimental ischemia in rodents, the mechanisms of neuroprotection by hypothermia appear to be multifactorial. The degree of neuroprotection afforded will depend on the severity of the insult and the timing, depth and duration of hypothermia after the onset of cerebral ischemia. As the pathological mechanisms involved are known to be complex, they may of themselves act as a double-edged sword, having both beneficial and deleterious effects on the ischemic animal brain (Endress et al., 2008). Of the biochemical pathways involved in "hypothermia-induced neuroprotection," glutamate and calcium ions are major players in neuronal excitotoxicity but they are also essential for normal brain function and a key driving force for the reorganization and synaptogenesis involved in tissue repair after injury (Wieloch and Nikolich, 2006). In this same vein, nitric oxide (NO) derived from endothelia may increase blood flow, so aiding healing, whilst neuronal and inducible NO synthase (NOS) may contribute to inflammation with the formation of oxidants and free radicals. This raises questions about whether or not hypothermia (which may act to ameliorate inflammation) is exclusively beneficial. Perhaps at times hypothermia could be disadvantageous (Goss et al., 1995). Hypothermia might be protective early during recovery but if induced later, might impede repair.

From the point of view of effects on coagulation, hypothermia is regarded as a major risk factor for morbidity and mortality. It is a well recognized supposition that free blood in the ventricles after subarachnoid hemorrhage may play a role in vasospasm and development of high fever (Grande et al., 2009). However, whilst experimental hypothermia (32°C) has been shown to inhibit coagulation function in swine (Martini, 2007) and in hypothermic (33.8°C) post-laparotomy surgical patients with blood loss (Bernabei et al., 1992) the induction of hypothermia after severe TBI in patients with comparable (33°C) body temperature did not show a significant difference in coagulation parameters (although a tendency toward lower platelet counts was observed in the hypothermic group) compared to normothermic patients (Tokutomi et al., 2004).

PYREXIA: HOW DOES IT INFLUENCE BRAIN OXYGENATION AND CHEMISTRY?

Altered temperature is a sign of inflammation rather than a disease itself. What seems certain in the light of the recent studies is that high temperature after TBI is common, especially in those presenting with a GCS of 9 or less (Stocchetti et al., 2002). The threshold for fever has been widely debated but practice parameters for evaluating new fever onset in critical care developed by O'Grady et al. (1998) allow a level of uniformity in describing fever. Stocchetti et al. (2005) show that 78% of patients had temperatures above 38.3°C, the Critical Care Society threshold for fever, despite antibiotic and antipyretic treatment. Pyrexia had a significantly different distribution depending on the severity of damage, with patients with the most severe brain trauma more likely to have an early and consistent pyrexia than those patients with GCS >8. Pyrexia prolonged the length of ICU stay (LOS).

For apyrexial patients, LOS was an average of 8 days whereas pyrexial patients stayed in ICU for significantly longer (average 14 days). An important concern with regard to the impact of raised temperature after TBI is that of effects on intracranial pressure (ICP). Although Rossi et al. (2001) were unable to show a clear relationship between average ICP and brain temperature (a finding supported recently from the groups of LeRoux's (Spiotta et al., 2008) and Childs et al. (2009) it was noted, that during the febrile episode, ICP was significantly increased. That a rise in brain temperature during fever was accompanied by a rise in ICP (and concomitant increase in SjO_2) may suggest that the increase in brain temperature has effects more on increasing CBF (and possibly cerebral blood volume) than it does on increasing cerebral metabolism ($CMRO_2$). The limited number of patients studied and the lack of direct cerebral blood flow monitoring make it possible only to suggest (from the SJO_2 measurements) that a mismatch between CBF and $CMRO_2$ may be occurring during fever. Of course the rise in ICP and temperature may be epiphenomenon of different inflammatory processes or due to effects of raised temperature *per se*, possibly due to mechanisms other than "true" fever. Here "central" fever or neurogenic hyperthermia due to damage to the central thermoregulatory pathways may precipitate cerebral oedema as temperature exceeds 40°C. As Cremer and Kalkman (2007) suggest, neurological abnormalities of a temperature increase above the fever threshold, which has long been regarded to be 41°C (DuBois, 1949), is associated with disturbed conscious level, brain oedema, and a high mortality. The possibility of a combination of pathological events linking raised temperature with brain swelling and intracranial hypertension has been observed in rodents (Sharma and Hoopes, 2003).

Significant reductions in mean brain tissue oxygen content ($PbtO_2$) occur as brain temperature is lowered from 37°C to 34°C. Gupta et al. (2002) however show that at temperatures within the normal to moderate fever range (37–38.9°C) $PbtO_2$ is relatively unchanged. More recent data lends further support to the view that raised brain temperature does not bring about a reduction in brain tissue oxygen (Spiotta et al., 2008). Using commercially available systems (Licox, Integra Neuroscience, Plainsboro, NJ, USA) for brain tissue partial

pressure of oxygen overall brain temperature and brain tissue oxygen were poorly correlated suggesting that the relationship between human brain temperature and brain oxygen is complex.

Against this background of uncertainty about the role of raised temperature; whether it could be harmful to injured neurones or whether it could be an adaptive response and therefore of some benefit to the patient, the impact of pyrexia on neurochemistry and cerebral oxygenation after acute brain injury was presented. Brain tissue temperature, partial pressure of oxygen (Licox Systems, Integra Neurosciences, Plainsboro, NJ, USA) and microdialysis (CMA, Sweden) for brain glucose, lactate, pyruvate, and glutamate were measured in a mixed neurocritical care population. Despite a rise in brain temperature of the order of 1.3°C, no significant changes from baseline in any of the measured variables (including ICP, CPP, brain tissue pH, CO_2, glucose, lactate, pyruvate, ratio) were observed. However it was noted that brain tissue oxygen partial pressure (reflecting the balance between cerebral oxygen delivery and consumption) rose significantly and the arterio-venous difference in oxygen content ($AJDO_2$) dropped significantly from 4.2 to 3.8 vol% ($p < 0.05$). These data suggest that oxygen supply to the brain during fever in patients with non-ischemic brain trauma (TBI) remains adequate during the febrile event.

Appropriate, and safe, translation of research evidence obtained in experimental studies to the patient is of key importance for evidence-based practice (Sacho and Childs, 2008). Despite the weight of opinion that raised temperature is both frequent and harmful, results from Stocchetti's group showing that a rise in average brain temperature (from 38 to 39°C) was not associated with abnormal neurochemistry requires an explanation particularly as pyrexia appeared to be well tolerated in the small patient population studied and, furthermore, did not exacerbate ICP readings (**Table 1**). This is of particular importance currently, in view of the recent evidence that many of the treatments used to lower the temperature of the body are associated with adverse side effects (Seule et al., 2009). In the current clinical climate, translational medicine is pivotal in establishing: (a) whether results obtained in one clinical pathology (e.g., stroke) translate to other clinical conditions (e.g., severe brain trauma) and (b) whether studies in animals are an appropriate model for safe translation of results from the bench to the bedside.

BRAIN TEMPERATURE AND OUTCOME AFTER TBI: TRACING THE EVIDENCE FROM BENCH

Although new possibilities for non-invasive temperature measurement are on the horizon, the day to day delivery of accurate estimation of body, and in the case of brain trauma, brain tissue temperature, remain one of the most common clinical measurement activities. Despite the interest in temperature and outcome after TBI, there is no universal definition of the threshold for an increased temperature or where and how temperature should be measured. The European Brain Injury Consortium guidelines recommend avoiding hyperthermia but do not define this (Maas et al., 1997). The most recent Brain Trauma Foundation Guidelines do not mention fever thresholds or discuss the management of increased temperature [except in the context of hypothermia (level III recommendation only); Cook et al., 1995]. In practice most clinicians contend that normothermia is beneficial after TBI and, anecdotally, in the view of some, therapeutic hypothermia is warranted. However, Aiyagari and Diringer in a recent systematic review of fever control in brain injury concluded that: "… the answer to the critical question: Does fever control improve outcome is not known?". The definitive study has not been performed (Aiyagari and Diringer, 2007). Two recent systematic reviews of therapeutic hypothermia for TBI have not shown clear benefit (Peterson et al., 2008; Sydenham et al., 2009). On this basis, decisions about how best to approach the management of temperature have not achieved equipoise.

Even so, current opinion is that raised temperature after TBI is associated with worse outcome. There is some support for this view in a recent systematic review and meta-analysis on pooled data from patients with stroke and TBI (Greer et al., 2008). However, only 17% of the patient cohort had TBI. Of the eight adult TBI studies, four failed to show a significant relationship between temperature and mortality (Jeremitsky et al., 2003; Geffroy et al., 2004, (and Glasgow Outcome Score, GOS), Andrews et al., 2002; Soukup et al., 2002). The relationship between temperature and outcome after TBI may not be entirely clear cut as shown recently in an observational study of the relationship between temperature and outcome in patients with severe TBI (Childs et al., 2006).

In the relationship between temperature and outcome there are potentially confounding factors such as severity of injury (Jeremitsky et al., 2003) and, because temperature is a symptom,

Table 1 | Changes in intracranial pressure, cerebral perfusion pressure, pH, and jugular bulb oxygen saturation before and after the development of pyrexia.

	Fever onset					Fever lysis				
	ICP (mmHg)	CPP (mmHg)	Pb_tO_2 (mmHg)	pH_{br}	SJO_2	ICP (mmHg)	CPP (mmHg)	Pb_tO_2 (mmHg)	pH_{br}	SJO_2
Baseline (T_{br} 38.0°C)	16 (4)	71 (10)	32 (21)	7.19 (0.06)	0.69 (0.05)					
Pyrexia (T_{br} 39.3°C)	17 (6)	71 (100)	37 (22)*	7.16 (0.06)	0.71 (0.06)					
Pyrexia (T_{br} 39.2°C)						18 (6)	71 (6)	24 (14)	7.10 (0.09)	0.70 (0.05)
Baseline (T_{br} 38.0°C)						16 (5)**	72 (8)	25 (18)	7.13 (0.09)**	0.67 (0.08)*

Table adapted from Stocchetti et al. (2005)
Data (baseline to fever onset, n = 14). Data expressed as mean (SD)
Changes in T_{br}, intraparenchymal brain temperature; ICP, intracranial pressure; CPP, cerebral perfusion pressure; Pb_tO_2, brain tissue oxygen content; pH_{br}, brain tissue Ph; and SJo_2, jugular saturation at the superior jugular bulb in 13 patients with severe TBI before (baseline) and on developing fever (pyrexia).
**p < 0.05 vs baseline, ** p < 0.001 vs pyrexia. Note the significant increase in Pb_tO_2 with pyrexia.*

the reason(s) for a rise in temperature may include the acute inflammatory response to injury, infection and/or neurogenic fever (Thompson et al., 2003). The problem is that the underlying cause of raised temperature may be impossible to determine with certainty. Furthermore, there is likely to be a complex interplay with other influences on temperature, for example hypotension, blood sugar, hydration, and sleep (Mekjavic and Eiken, 2006). Adding to the complexity of probing the root to the relationship between temperature and outcome is the variability in temperature site, the frequency of the measurement interval *per se*, the duration of temperature monitoring, the frequency of raised (or lowered) temperature, the use of therapeutic temperature interventions and the time-interval to follow-up and outcome assessments.

Decision tree analysis has been used to explore predictors of outcome at 12 months (Jones et al., 1994; McQuatt 1998; Andrews et al., 2002). Logistic regression analysis in a patient sub-set showed duration of pyrexia to be significantly associated with mortality at 12 months ($p = 0.014$; Jones et al., 1994). However the decision tree analysis for GOS prediction showed a small group of patients in whom "more" pyrexia was not associated with worse outcome, nor "less" pyrexia with better outcome (McQuatt, 1998). The emerging hypothesis from some of the decision trees is that pyrexia may not always be detrimental. Further assessment and investigation is warranted (Andrews et al., 2002).

These results are supported by data from our own group (CC) where burden of pyrexia (% time spent with brain temperature ≥37.5°C) during the period of intraparenchymal monitoring was significantly greater in survivors compared with non-survivors ($p = 0.02$; **Figure 1**). In the first of two observational studies, Childs et al. (2006) (**Figure 2**), used logistic regression to explore for linear and quadratic relationships between initial (and 48 h average) brain temperature and survival at 3 months. No evidence of an association between initial brain temperature and risk of death was found. From statistical modeling, and assuming a linear relationship between brain temperature and death at 3 months, patients with higher mean brain temperature were less likely to die OR (95% confidence interval, CI) for death per 1°C change in temperature was 0.31 (0.09–1.1, $p = 0.06$). On the other hand, fitting a quadratic relationship to the data suggested that low and high end temperatures were associated with an increased risk of death. Unlike studies in human stroke where high admission temperature predicts poor outcome (Reith et al., 1996), results in a population of severe TBI patients did not support such a relationship.

In our subsequent study of the temporal pattern of brain temperature, 35 of 67 patients with severe TBI had a brain temperature >37.5°C for 60–100% of time during the first 5 days. Therapeutic temperature management with body cooling was minimal. There were four deaths only (11%) in this "persistent pyrexia" group. More patients died in the group who did not develop pyrexia. Statistical modeling of the relationship between brain temperature and probability of death at 30 days revealed the lowest probability of death to be in patients with brain temperature in the range 36–38.5°C. Taking in to account the severity of brain injury using pupil size and reactivity as a marker, the predicted probability of death increased as brain temperature dropped below 36°C. For those patients with "abnormal" pupillary responses, the probability of death was rather constant across the range 34–39°C (Sacho et al., 2010). Small sample size limits the impact of the findings but even so, the results do raise important questions; not least the question of whether a

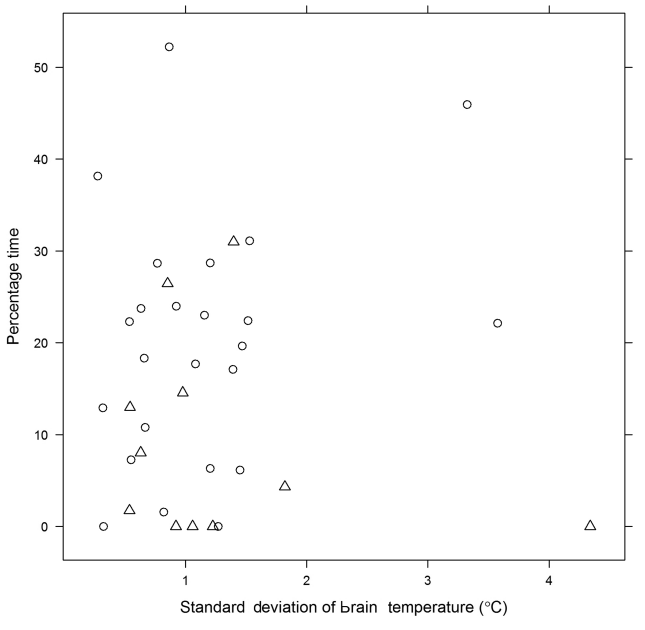

FIGURE 1 | Percentage (%) time during the period of neuro-monitoring that patients with severe TBI (n = 36) had brain temperature ≥37.5°C. Figure shows data from survivors (O) and non-survivors (Δ) plotted with respect to standard deviation of mean brain temperature.

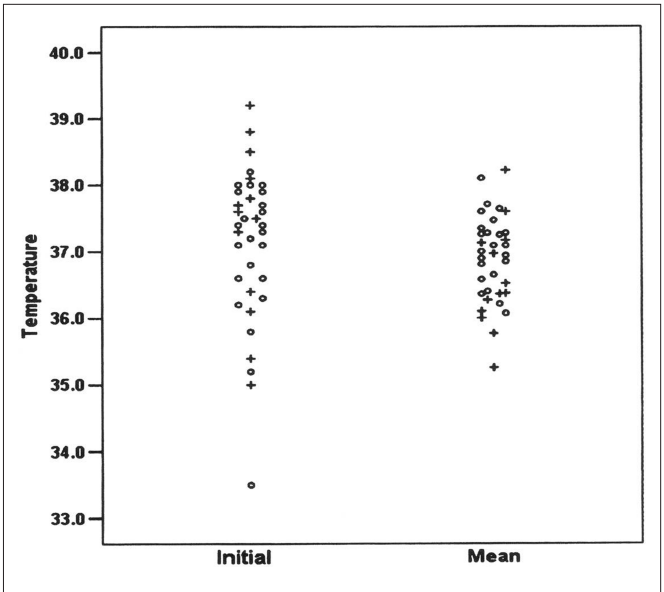

FIGURE 2 | The initial brain temperature (ºC) at time of insertion of combined intracranial pressure/temperature sensor (left column) and mean brain temperature measured during the first 48 h after injury (right column) in 37 patients with severe TBI admitted to ICU for medical management of their brain injury. Symbols represent survivors (O) and non-survivors (+). (Reproduced with permission).

1–2°C rise in temperature commonly thought to cause secondary injury in the damaged (ischemic) brain is deleterious for all patients with severe TBI.

PROCESS: QUESTIONS POSED AT THE ROUNDTABLE WORKSHOP

Having discussed the background literature and debated the role of temperature in the injured human brain, the participants worked together in four groups to discuss two issues relevant to neurocritical care management after TBI:

(a) What should future recommendations for temperature measurement be: direct measurement of brain temperature or body core temperature surrogates?

(b) Should therapeutic control of temperature be advocated as a treatment panacea or "on prescription"?

From the discussions, the participants arrived at a level of agreement for each issue and the summary opinion provided the basis for this consensus document (**Table 2**).

The conclusions drawn from the meeting were: there is, as yet, no robust scientific data to support the use of therapeutic control of temperature by induction of hypothermia in patients whose ICP is controllable using standard therapy. A randomized clinical trial is justified to establish if body cooling for control of pyrexia (to normothermia) vs moderate pyrexia leads to a better patient outcome for TBI patients.

Table 2 | Summary of workshop discussions and the participants' recommendations and consensus.

Workshop objective	Discussion points	Concerns expressed	Recommendations	Consensus
To discuss future recommendations for temperature measurement in patients with severe TBI.	Do opportunities exist for improvement in measurement accuracy? What are the range of differences between brain and body temperature and how much do they vary?: see Kirk et al. (2009) What are the benefits of brain temperature monitoring?	Value of common body temperature sites (Johnston et al., 2006; axilla/skin folds/rectal/oesophageal) as surrogates for brain temperature should be questioned due to poor measurement practice No published guidelines available for standardization of depth (or positioning) of the brain temperature sensor In view of evidence that differences exist between brain and body temperature, this should be sufficient justification for direct brain temperature monitoring	Need for improved measurement reliability in thermometry practice Support for greater use of multi-modality monitoring If the objective of neuro-monitoring is to prevent secondary damage-"normal" brain rather than "damaged" brain tissue should be the focus for monitoring A possible benefit of brain temperature monitoring is the potential to "titrate" brain temperature to ICP	Standardization in temperature measurement is a key objective for the future Lack of confidence in rectal temperature as a surrogate for brain temperature is attributed to poor measurement practice notably: site and depth of thermistor insertion. Brain temperature monitoring should be encouraged as a "gold" standard if intracerebral monitoring is warranted Goal for the future: to build a body of evidence on brain temperature about absolute and trend change differences between brain and different core sites There is a need to understand the role of brain temperature as a biomarker for outcome
To discuss whether therapeutic control of temperature should be advocated as a treatment panacea or undertaken "on prescription"	What is the evidence that therapeutic control of body/brain temperature is beneficial for all neurosurgical patients?	The effect of *not cooling* patients with high brain temperature (i.e., >39°C) on survival of injured neurones is unknown. Treatments/ therapies to manipulate brain/body temperature to normal/below normal, levels are justified only as an adjunct therapy for those patients with refractory intracranial hypertension where clinicians are "struggling" to gain control of pressure increases within the brain.	Overwhelming support was given to a more "prescriptive" or "tailored" approach to the use of cooling interventions Patients with refractory ICP may benefit from body cooling.	The "selection" of patients for therapeutic hypothermia was a preferred approach to temperature management Whole body/internal cooling is not justifiable for temperature control *per se*.

ACKNOWLEDGMENTS

Our thanks go to the Manchester Conference delegates and workshop participants†: Iain Chambers, Paul Dark, Ian Geraghty, Chris Griffiths, Arun Gupta, Stephen Hopkins, Nicola Johnston, Andrew King, Andrew Levick, Richard Protheroe, Raphael Sacho, Martin Smith, Gareth Thomas, Christos Tolias, Pippa Tyrrell, Andy Vail, Elena Vescovo, Chris Whitehead. We also with to thank Dr Dannielle Kirk, Dr Anna McGlone, Mrs Sharon Hulme, and Ms Nicole Burden, who kindly transcribed the workshop discussions. I would also like to thank Mrs Denise Fieldhouse for facilitating the afternoon workshop and for her clarity and drive in helping achieve our consensus statement. My sincere thanks also go to my colleague, Mr Timothy Rainey for his help and assistance with the conference organization. Thanks are also due to the generous support of our sponsors; Irwin Mitchell Solicitors, Integra Neurosciences, Raumedic®, Eden Medical Ltd and Lambda photometrics. Thanks are also due to Dr Chen Nan for assistance with data analysis. I would like to thank all the speakers and participants for helping make the day a rewarding and successful venture.

REFERENCES

Abate, M. G., Cadore, B., and Citerio, G. (2008). Hypothermia in adult neurocritical care patients: a very "hot" strategy not to be hibernated yet! *Minerva Anestesiol.* 74, 425–430.

Aiyagari, V., and Diringer, M. N. (2007). Fever control and its impact on outcomes: what is the evidence? *J. Neurol. Sci.* 261, 39–46.

Andrews, P. J., Sleeman, D. H., Statham, P. F., McQuatt, A., Corruble, V., Jones, P. A., Howells, T. P., and Macmillan, C. S. (2002). Predicting recovery in patients suffering from traumatic brain injury by using admission variables and physiological data: a comparison between decision tree analysis and logistic regression. *J. Neurosurg.* 97, 326–336.

Bernabei, A. F., Levison, M. A., and Bender, J. S. (1992). The effects of hypothermia and injury severity on blood loss during trauma laparotomy. *J. Trauma.* 33, 835–839.

Brinnel, H., Cabanac, M., and Hales, J. R. S. (1987). "Critical upper levels of body temperature, tissue thermosensitivity and selective brain cooling in hyperthermia," In *Heat Stress: Physical Exertion and Environment*, eds I. R. S. Hales and D. A. B. Richards (Amsterdam: Excerpta Medica), 209–240.

Bullock, R. M., and Povlishock, J. T. (2007). Guidelines for the management of severe traumatic brain injury. Brain trauma foundation guidelines. *J. Neurotruma* 24(Suppl. 1), S-1–S-106.

Busto, R., Dietrich, W. D., Globus, M. Y-T., Scheinberg, P., and Ginsberg, M. D. (1987). Small differences in intraischemic brain temperature critically determine the extent of ischaemic neuronal injury. *J. Cereb. Blood Flow Metab.* 7, 729–738.

Childs, C. (2008). Human brain temperature: regulation, measurement and relationship with cerebral trauma: part 1. *Br. J. Neurosurg.* 22, 486–496.

Childs, C., Hiltunen, Y., Patankar, T., and Kauppinen, R. (2007). Determination of regional brain temperature using proton magnetic resonance spectroscopy to determine brain-body temperature differences in healthy human subjects. *Magn. Reson. Med.* 57, 59–66.

Childs, C., and Machin, G. (2009). Reliability issues in human brain temperature measurement. *Crit. Care* 13, R106. doi: 10.1186/cc7943.

Childs, C., Sacho, R. H., and King, A. T. (2009). Brain hyperthermia after traumatic brain injury does not reduce brain oxygen (letter to the editor). *Neurosurgery* 64(3), E577.

Childs, C., Vail, A., Leach, P., Rainey, T., Protheroe, R., and King, A. (2006). Brain temperature and outcome after severe traumatic brain injury. *Neurocrit. Care* 5, 1–5.

Childs, C., Vail, A., Protheroe, R., King, A. T., and Dark, P. M. (2005). Differences between brain and rectal temperature during routine critical care of patients with severe traumtic brain injury. *Anaesthesia* 60, 759–765.

Clifton, G. L., Choi, S. C., Miller, E. R., Levin, H. S., Smith, Jr. K. R., Muizelaar, J. P., Wagner, Jr. F. C., Marion, D. W., and Luerssen, T. G. (2001). Lack of effect of induction of hypothermia after acute brain injury. *N. Engl. J. Med.* 344, 556–563.

Coles, J. P. (2004). Regional Ischaemia after head injury. *Curr. Opin. Crit. Care* 10, 120–125.

Cook, D. J., Guyatt, G. H., Laupacis, A., Sackett, D. L., and Goldberg, R. J. (1995). Clinical recommendation using levels of evidence for antithrombotic agents. *Chest* 108, 227–230.

Cremer, O. L., and Kalkman, C. J. (2007). Cerebrla pathophysiology and clinical neurology of hyperthermia in humans. *Prog. Brain Res.* 162, 153–169.

DuBois, E. F. (1949). Why are fever temperatures over 106oF rare? *Am. J. Med. Sci.* 27, 361–368.

Endress, M., Engelhardt, B., Koistinaho, J., Lindvall, O., Mearis, S., Mohr, J. P., Planas, A., Rothwell, N., Schwaninger, M., and Schwab, M. E. (2008). Improving outcome after stroke: overcoming the translational Medicine roadblock. *Cerebrovasc. Dis.* 25, 268–278.

Geffroy, A., Bronchard, R., Merckx, P., Seince, P. F., Faillot, T., Albaladejo, P., and Marty, J. (2004). Severe traumatic head injury in adults: which patients are at risk of hyperthermia? *Intensive Care Med.* 30, 785–790.

Goss, J. R., Styren, S. D., Miller, P. D., Kochanek, P. D., Palmer, A. M., Marion, D. W., and DeKosky, S. T. (1995). Hypothermia attenuates the normal increase in interleukin 1beta NNA and nerve growth factor following traumatic brain injury in the rat. *J. Neurotrauma* 12, 159–167.

Grande, P.-O., Reinstrup, P., and Romner, B. (2009). Active cooling in traumatic brain-injured patients: a questionable therapy? *Acta Anesthesiol. Scand.* 53, 1233–1238.

Greer, D. M., Funk, S. E., Reaven, N. L., Ouzounelli, M., and Uman, G. C. (2008). Impact of fever on outcome in patients with stroke and neurological injury. *Stroke* 39, 3029–3035.

Griesman, L. A., and Mackowiak P. A. (2002). Fever: beneficial and detrimental effects of antipyretics. *Curr. Opin. Infect. Dis.* 15, 241–245.

Gupta, A. K., Al-Rawi, P. G., Hutchinson, P. J., and Kirkpatrick, P. J. (2002). Effect of hypothermia on brain tissue oxygenation in patients with severe brain injury. *Br. J. Anesth.* 88, 188–192.

Haveman, J., Sminia, P., Wondergem, J., Van Der Zee, J., and Hulshof, M. C. C. M. (2005). Effects of hyperthermia on the central nervous system: what was learnt from animal studies? *Int. J. Hyperthermia* 21, 473–487.

Henker, R. A., Brown, S. D., and Marion, D. W. (1998). Comparison of brain temperature with bladder and rectal temperatures in adults with severe head injury. *Neurosurgery* 42, 1071–1075.

Hutchinson, J. S., Ward, R. E., Lacroix, J., Hebert, P. C., Barnes, M. A., Bohn, D. J., Dirks, P. B., Doucette, S., Fergusson, D., Gottesman, R., Joffe, A. R., Kirpalani, H. M., Meyer, P. G., Morris, K. P., Moher, D., Singh, R. N., and Skippen, P. W. (2008). Hypothermia theraphy after traumatice brain injury in children. *N. Engl. J. Med.* 358, 2447–2456.

Jeremitsky, E., Omert, L., Dunham, M., Protech, J., and Rodtiguez, A. (2003). Harbingers of poor outcome the day after severe brain injury: hypothermia, hypoxia and hypotension. *J. Trauma* 54, 312–319.

Johnston, N. J., King, A. T., Protheroe, R., and Childs, C. (2006). Body temperature management after severe traumatic brain injury: methods and protocols usd in the United Kingdom and Ireland. *Resuscitation* 70, 254–262.

Jones, P. A., Andrews, P. J. D., Midgley, S., Anderson, S. I., Piper, I. R., Tocher, J. L., Housley, A. M., Corrie, J. A., Slattery, J., Dearden, N. M., and Miller, J. D. (1994). Measuring the burden of secondary insults in head-injured patients during intensive care. *J. Neurosurg. Anesthesiol.* 6, 4–14.

Kilpatrick, M. M., Lowry, D. W., Firlik, A. D., Yonas, H., and Marion, D. W. (2000). Hyperthermia in the neurosurgical intensive care unit. *Neurosurgery* 47, 850–856.

Kim, Y., Busto, R., Dietrich, W. D., Kraydieh, S., and Ginsberg, M. D. (1996). Delayed postischaemic hyperthermia in awake rats worsens the histpathological outcome of transient focal ischaemia. *Stroke* 27, 2274–2281.

Kirk, D., Rainey, T., Vail, A., and Childs, C. (2009). Infra-red thermometry: the reliability of tympanic and temporal artery readings fro predicting brain temperature after severe traumatic brain injury. *Crit. Care* 13, R81. doi: 10.1186/cc7898.

Kluger, M. J. (1979). *Fever: Its Biology, Evolution and Function*. Princeton: Princeton University Press.

Lyden, P. D., Krieger, D., Yenari, M., and Dietrich, W. D. (2006). Therapeutic hypothermia for acute stroke. *Int. J. Stroke* 1, 9–19.

Lyon, R. M., Robertson, C. E., and Clegg, G. R. (2010). Therapeutic hypothermia in the emergency department following out-of-hospital cardiac arrest. *Br. Med. J.* 27, 418–423.

Maas, A. I., Dearden, M., Teasdale, G. M., Braakman, R., Cohadon, F., Iannotti, F., Karimi, A., Lapierre, F., Murray, G., Ohman, J., Persson, L., Servadei, F., Stocchetti, N., and Unterberg, A. (1997). EBIC-guidelines for management of severe head injury in adults. European Brain Injury Consortium. *Acta Neurochir. (Wien)* 139, 286–294.

Maas, A. I. R., Marmarou, A., Murray, G. D., Teasdale, T. W., and Steyerberg, E. W. (2007). Prognosis and clinical trial design in traumatic brain injury: the IMPACT study. *J. Neurotrauma* 24, 232–238.

Machin, G., and Childs, C. (2010). A systematic performance evaluation of brain and body temperature sensors using ultra-stable temperature references. *J. Med. Eng. Technol.* 34, 192–199.

Manno, E. M., and Farmer, J. C. (2004). Acute brain injury: if hypothermia is good, then is hyperthermia bad? *Crit. Care Med.* 32, 1611–1612.

Martini, W. Z. (2007). The effects of hypothermia on fibrinogen metabolism and coagulation function in swine. *Metab. Clin. Exp.* 56, 214–221.

McHugh, G. S., Butcher, I., Steyerberg, E. W., Lu, J., Mushkudiani, N., Marmarou, A., Maas, A. I. R., and Murray, G. D. (2007). Statistical approaches to the univariate prognostic analysis of the IMPACT database on traumatic brain injury. *J. Neurotrauma* 24, 251–258.

McQuatt, A. (1998). *Using Machine Learning Techniques to Predict Clinical Ooutcome*. MD Thesis, Edinburg University, Edinburgh.

Mekjavic, I. B., and Eiken, O. (2006). Contribution of thermal and nonthermal factors to the regulation of body temperature in humans. *J. Appl. Physiol.* 100, 2065–2072.

Mellergard, P. (1994). Monitoring of rectal, epidural, and intraventricular temperature in neurosurgical patients. *Acta Neurochir.* 60, 485–487.

O'Grady, N. P., Barie, P. S., Bartlett, J., Bleck, T., Garvey, G., Jacobi, J., Linden, P., Maki, D. G., Nam, M., Pasculle, W., Pasquale, M. D., Tribett, D. L., and Masur, H. (1998). Practice parameters for evaluating new fever in critically ill adult patients. *Crit. Care Med.* 26, 392–408.

Peterson, K., Carson, S., and Carney, N. (2008). Hypothermia treatment for traumatic brain injury: a systematic review and meta-analysis. *J. Neurotrauma* 25, 62–71.

Preston-Thomas, H. (1990). The international temperature scale of 1990 (ITS90). *Metrologia* 27, 3–10.

Reith, J., Jorgensen, H. S., Pederson, P. M., Nakayama, H., Raaschou, H. O., Jeppesen, L. L., and Olsen, T. S. (1996). Body temperature in acute stroke: relation to stroke severity, infarct size, mortality and outcome. *Lancet* 347, 422–425.

Romanovsky, A. A., and Szekely, M. (1998). Fever and hypothermia: two adaptive thermoregulatory responses to systemic inflammation. *Med. Hypotheses* 50, 219–226.

Rossi, S., Zanier, E. R., Mauri, I., Colombo, A., and Stocchetti, N. (2001). Brain temperature, body core temperature and intracranial pressure in acute cerebral damage. *J. Neurol. Neurosurg. Psychiatr.* 71, 448–454.

Rumana, C. S., Gopinath, S. P., Uzura, M., Valadka, A. B., and Roberston, C. S. (1998). Brain temperature exceeds systemic temperature in head-injured patients. *Crit. Care Med.* 26, 562–567.

Sacho, R. H. Vail, A, Rainey, T., King, A. T., and Childs, C. (2010). The effect of spontaneous alterations in brain temperature in outcome: a prosepctive observational cohort study in patients with severe traumatic brain injury. *J. Neurotrauma*. doi: 10. 1089/neu.2010.1384 [ahead of print].

Sacho, R. S., and Childs, C. (2008). The significance of altered temperature after traumatic brain injury: an analysis of investigations in experimental and human studies: part 2. *Br. J. Neurosurg.* 22, 497–507.

Schulman, C. I., Namias, N., Doherty, J., Manning, R. J., Li, P., Alhaddad, A., Lasko, D., Amortegui, J., Dy, C. J., Dlugasch, L., Baracco, G., and Cohn, S. M. (2005). The effect of antipyretic therapy upon outcomes in critically ill patients: a randomised controlled trial. *Surg. Infect.* 6, 369–375.

Schwab, S., Schwartz, S., Aschoff, A., Keller, E., and Hacke, W. (1998). Moderate hypothermia and brain temperature in patients with severe middle cerebral artery infarction. *Acta Neurochir.* 71, 131–134.

Seule, M. A., Muroi, C., Mink, S., Yonekawa, Y., and Keller, E. (2009). Therapeutic hypothermia in patients with aneurysmal subarachnoid hemorrhage, refractory intracranial hypertension, or cerebral vasospasm. *Neurosurgery* 64, 86–93.

Shankaran, S., Pappas, A., Laptook, A. R., McDonald, S. A., Ehrenkranz, R. A., Tyson, J. E., Walsh, M., Goldberg, R. N., Higgins, R. D., and Das, A. (2008). Outcomes of safety and effectiveness in a multicenter randomized, controlled trial of whole body hypothermia fro neonatal hypoxi-ischaemic encephalopathy. *Pediatrics* 122, e791–e798.

Sharma, H. S., Hoopes, P. J. (2003). Hyperthermia induced pathophysiology of the central nervous system. *Int. J. Hyperthermia* 19, 325–354.

Soukup, J., Zauner, A., Doppenberg, E. M. R., Menzel, M., Gilman, C., Young, H. F., and Bullock, R. (2002). The importance of brain temperature in patients with severe head injury: relationship to intracranial pressure, cerebral perfusion pressure, cerebral blood flow and outcome. *J. Neurotrauma* 19, 559–571.

Spiotta, A. M., Stiefel, M. F., Heuer, G. C., Bloom, S., Maloney-Wilensky, E., Yang, W., Grady, M. S., and LeRoux, P. D. (2008). Brain hyperthermia after traumatic brain injury does not reduce brain oxygen. *Neurosurgery* 62, 864–872.

Stocchetti, N., Protto, A., Lattuada, M., Magnoni, S., Longhi, L., Ghisoni, L., Egidi, M., and Zanier, E. R. (2005). Impact of pyrexia on neurochemistry and cerebral oxygenation after acute brain injury. *J. Neurol. Neurosurg. Psychiatr.* 76, 1135–1139.

Stocchetti, N., Rossi, S., Zanier, E. R., Colombo, A., Beretta, L., and Citerio, G. (2002). Pyrexia in head injured patients admitted to intensive care. *Intensive Care Med.* 28, 1555–1562.

Stone, J. G., Young, W. L., Smith, C. R., Solomon, R. A., Wald, A., Ostapkovich, N., and Shrebnick, D. B. (1995). Do standard monitoring sites reflect true brain temperature when profound hypothermia is rapidly induced and reversed? *Anaesthesiology* 82, 344–351.

Stoner, H. B. (1974). Inhibition of thermoregulatory non-shivering thermogenesis by trauma in cold-acclimated rats. *J. Physiol.* 238, 657–670.

Sydenham, E., Robers, I., and Alderson, P. (2009). Hypothermia for traumatic head injury. *Cochrane Database Syst. Rev.* CD001048.

Thompson, H. J., Pinto-Martin, J., and Bullock, M. R. (2003). Neurogenic fever after traumatic brain injury: an epidemiologocal study. *J. Neurol. Neurosurg. Psychiatr.* 74, 614–619.

Tokutomi, T., Miyagi, T., Morimoto, K., Karukaya, T., and Shigemori, M. (2004). Effect of hypothermia on serum electrolyte, inflammation, coagulation and nutritional parameters in patients with severe traumatic brain injury. *Neurocrit. Care* 1, 171–182.

Van Der Zee, J., Vujaskovic, Z., Kondo, M., and Sugahara, T. (2008). The Katoda Fund International Forum 2004-clinical group comsensus. *Int. J. Hyperthermia* 24, 111–122.

Vescovo, E., Levick, A. P., Childs, C., Zhao, S., Machin, G., Rainey, T., and Williams, S. R. (2010). High precision calibration of MRS thermometry using validated temperature standards. *Proc. Int. Soc. Magn. Reson. Med*. (in press).

Vespa, P., Bergsneider, M., Hattori, N., Wu, H.-M., Hiang, S.-C., Martin, N. A., Glenn, T. C., McArthur, D. L., and Hovda, D. A. (2005). Metabolic crisis without brain ischaemia is common after traumatic brain injury: a combined microdialysis and positron emission tomography study. *J Cereb. Blood Flow Metab.* 25, 763–774.

Wieloch, T., and Nikolich, K. (2006). Mechanisms of neuronal plasticity following brain injury. *Curr. Opin. Neurobiol.* 16, 258–264.

Yanamoto, H., Nagata, I., Nakahara, I., Tohnai, N., Zhang, Z., and Kikuchi, H. (1999). Combination of intraischaemic and postischaemic hypothermia provides potent and persistent neuroprotection against temporary focal ischaemia in rats. *Stroke* 30, 2720–2726.

Conflict of Interest Statement: The authors declare that the research was conducted in the absence of any commercial or financial relationships that could be construed as a potential conflict of interest.

Received: 28 September 2010; accepted: 01 November 2010; published online: 23 November 2010.

Citation: Childs C, Wieloch T, Lecky F, Machin G, Harris B and Stocchetti N (2010) Report of a consensus meeting on human brain temperature after severe traumatic brain injury: its measurement and management during pyrexia. Front. Neur. 1:146. doi: 10.3389/fneur.2010.00146

This article was submitted to Frontiers in Neurotrauma, a specialty of Frontiers in Neurology.

frontiers in NEUROLOGY

ORIGINAL RESEARCH ARTICLE
published: 21 January 2011
doi: 10.3389/fneur.2010.00158

Pivotal role of anterior cingulate cortex in working memory after traumatic brain injury in youth

Fabienne Cazalis[1,2]*, Talin Babikian[1], Christopher Giza[3], Sarah Copeland[3], David Hovda[3] and Robert F. Asarnow[1]

[1] *Psychiatry and Biobehavioral Sciences, University of California Los Angeles David Geffen School of Medicine, Los Angeles, CA, USA*
[2] *Department of Anatomy, Ross University School of Medicine, Roseau, Commonwealth of Dominica*
[3] *Department of Neurosurgery, University of California Los Angeles David Geffen School of Medicine, Los Angeles, CA, USA*

Edited by:
Marten Risling, Karolinska Institutet, Sweden

Reviewed by:
Hans Lindå, Karolinska Institutet, Sweden
Frank Krueger, George Mason University, USA

****Correspondence:***
Fabienne Cazalis, Department of Anatomy, Ross University School of Medicine, P.O. Box 266, Roseau, Commonwealth of Dominica.
e-mail: fcazalis@rossu.edu

In this fMRI study, the functions of the anterior cingulate cortex (ACC) were studied in a group of adolescents who had sustained a moderate to severe traumatic brain injury (TBI). A spatial working memory task with varying working memory loads, representing experimental conditions of increasing difficulty, was administered. In a cross-sectional comparison between the patients and a matched control group, patients performed worse than Controls, showing longer reaction times and lower response accuracy on the spatial working memory task. Brain imaging findings suggest a possible double-dissociation: activity of the ACC in the TBI group, but not in the Control group, was associated with task difficulty; conversely, activity of the left sensorimotor cortex (lSMC) in the Control group, but not in the TBI group, was correlated with task difficulty. In addition to the main cross-sectional study, a longitudinal study of a group of adolescent patients with moderate to severe TBI was done using fMRI and the same spatial working memory task. The patient group was studied at two time-points: one time-point during the post-acute phase and one time-point 12 months later, during the chronic phase. Results indicated that patients' behavioral performance improved over time, suggesting cognitive recovery. Brain imaging findings suggest that, over this 12-month period, patients recruited less of the ACC and more of the lSMC in response to increasing task difficulty. The role of ACC in executive functions following a moderate to severe brain injury in adolescence is discussed within the context of conflicting models of the ACC functions in the existing literature.

Keywords: traumatic brain injury, diffuse axonal injury, functional MRI, working memory, anterior cingulate cortex, executive functions, adolescent

INTRODUCTION

Anterior cingulate cortex (ACC) activity is reportedly related to task difficulty, in healthy subjects (Botvinick et al., 2004) as well as in clinical populations, such as patients with post-traumatic stress disorder (Shaw et al., 2009) or patients with traumatic brain injury (TBI) (Rasmussen et al., 2008; Kohl et al., 2009). The exact role of the ACC in executive functions is still debated, with most prominent theories suggesting a role in cognitive control, including error detection, conflict monitoring, and/or task switching (Botvinick et al., 2004; Kerns et al., 2004; Ullsperger and Von Cramon, 2004; Carter and van Veen, 2007; Hyafil et al., 2009).

Executive function is affected by TBI, independently of the presence/absence of cortical lesions (Metting et al., 2007; Sanchez-Carrion et al., 2008). It has been suggested that it is diffuse axonal injury – commonly observed after TBI – that disrupts integrative networks and that is the main cause of executive functions impairment following TBI (Ghajar and Ivry, 2008; Niogi et al., 2008). This makes TBI a very interesting neuropsychological model for studying the role of ACC in executive functions.

In this study, we investigated ACC activation in relation to task difficulty, using a working memory task in adolescent patients with moderate to severe TBI. Our hypotheses were consistent with the literature: we expected that patients in the cross-sectional study would present lower performance than controls, notably with longer reaction times, and an alteration of their pattern of cerebral activation as compared to controls. We also expected patients in the longitudinal study to exhibit improvement of performance at Time 2 as compared to Time 1, as well as a change in brain imaging.

MATERIALS AND METHODS

This fMRI study of working memory in adolescents with TBI was conducted in two stages. First, a cross-sectional design compared youth with TBI to matched Controls. Secondly, a longitudinal study was conducted on a subset of the adolescent TBI patients who were reevaluated 12 months after their initial exam.

The spatial working memory task was parametrically designed in order to allow study of the effect of working memory load (WML) on brain activation.

PATIENTS

Participants included in this study presented with the following characteristics: 13–18 years of age; normal vision (contact lenses were accepted); right handedness; English skills sufficient enough to understand instructions; no previous history of major neurological, developmental, or psychiatric disorders (as stated by the parents of the patients during the inform consent process); and safety compliance to MRI. Recruitment and consent processes were approved by the UCLA Institutional Review Board (IRB).

Traumatic brain injury patients were recruited from two Pediatric ICUs within Los Angeles County (UCLA Medical Center and Harbor-UCLA Medical Center) as well as a local rehabilitation facility. Patients presented with moderate to severe non-penetrating TBI. Glasgow Coma Scale score (at intake at Emergency Department or post-resuscitation) was between 3 and 12, although three patients with GCS > 12 were included, since they presented with abnormalities on clinical imaging and therefore were classified as having moderate TBI. Severe TBI was defined by a GCS of 8 or less. All TBI patients exhibited diffuse axonal injury, as identified on FLAIR and T2 star MRI sequences. **Tables 1 and 2** describe the study groups.

PARADIGM DESCRIPTION

During the functional MRI exam, subjects performed a parametric cognitive task in an event-related design. They received instructions for the task prior to the exam. Participants responded by pressing a four-button keyboard that was placed under the subject's right hand. Responses and response times (RTs) were recorded.

The task was an original non-verbal spatial working memory task that required participants to reproduce visual sequences (**Figure 1**). A set of four positions was presented on the screen, as shown in **Figure 1**. Photographs of fruits and vegetables appeared sequentially, forming a spatio-temporal sequence that subjects were instructed to reproduce using the keyboard. Each picture was sufficiently detailed to be identifiable but sufficiently complex to prevent verbal description (Pepin Press, 2006a,b). The use of non-verbal material was *sine qua non* to avoid bilingualism being a confound, since exclusion of bilingual children was not a reasonable option (more than half of the children of Los Angeles, California, are bilingual, according to http://www.mla.org). The task was programmed using Matlab (The MathWorks Inc.).

Table 1 | Description of TBI and Control groups for the cross-sectional study.

	TBI	Controls
Number of subjects (males/females)	11 (9/2)	12 (4/8)
Mean age (years) ± SD (range)	16.0 ± 1.5 (14–18)	15.4 ± 1.5 (13–18)
Mean delay post-injury (months) ± SD (range)	7.0 ± 2 (3–17)	
Mean Glasgow coma scale score ± SD (range)	9.0 (3–15)	

Table 2 | Description of TBI group for the longitudinal study.

	Longitudinal TBI
Number of subjects (males/females)	6 (5/1)
Mean age (years) ± SD (range) at Time 1	16.7 ± 0.7 (15.8–17.4)
Mean age (years) ± SD (range) at Time 2	17.7 ± 0.8 (16.7–18.5)
Mean delay post-injury (months) ± SD (range) at Time 1	4.5 ± 1.0 (3–6)
Mean delay post-injury (months) ± SD (range) at Time 2	16.5 ± 3.1 (14–22)
Mean Glasgow coma scale score ± SD (range)	9.4 ± 5.1 (3–14)

The task included four conditions that were defined by the number of items to be manipulated in working memory, i.e., WML: Baseline (1 item); Low WML (3 items); Intermediate WML (4 items); High WML (5 items). There were 30 trials per condition. Conditions were alternated pseudo-randomly.

MRI EXAM

The MRI exam was conducted on a 3-T scanner (Siemens, Allegra) and included the following sequences:

- Structural T2 (TE = 56; TR = 4040 ms; FOV = 200 mm; voxel size = 0.8 mm × 0.8 mm × 5.0 mm; 25 slices of 5 mm; distance of 1.3 mm; axial orientation; order of acquisition = interleaved)
- EPI BOLD (TE = 30 ms; TR = 2000 ms; FOV = 200 mm; voxel size = 3.125 mm × 3.125 mm × 3 mm; 33 slices; axial orientation; order of acquisition = interleaved; 500 volumes acquired)
- T2* 3D flash (48 slices, voxel size = 1 mm × 0.5 mm × 2 mm; FOV = 256 mm; TR = 57 ms; TE = 20 ms; flip angle = 20°)
- A 3D volume structural sequence was acquired on a 1.5-T scanner (Siemens, Sonata) on the same day as functional scanning: MP-RAGE sequence (180 sagittal slices; FOV = 256 mm, voxel size = 1 mm × 1 mm × 1 mm; TR = 1900 ms; TE = 4.4 ms; TI = 1100 ms; flip angle = 15°)

BEHAVIORAL DATA PROCESSING

Two behavioral measures were used for statistical analyses: response accuracy and RT. Performance on both of these measures was recorded for each of the four conditions, representing WML [1-3-4-5]. Two groups were compared in the cross-sectional study: TBI and Control groups. For the Control group, behavioral

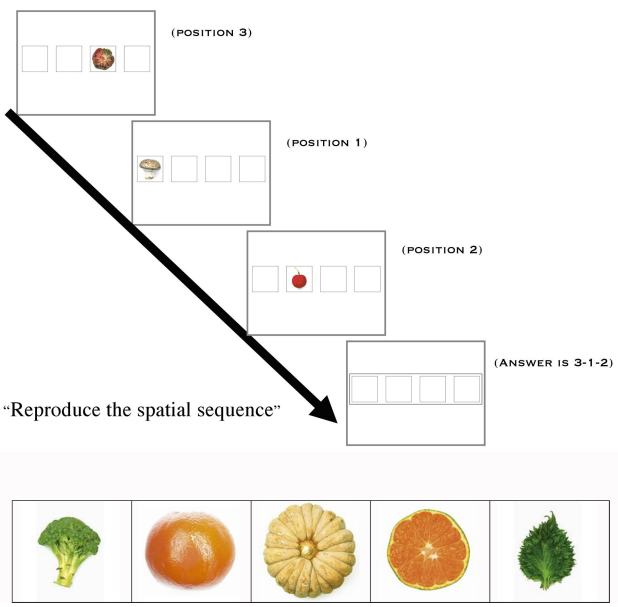

FIGURE 1 | Working memory task and examples of pictures used in the task.

data was available for 11 subjects. A subset of the TBI subjects, for whom data was available at two time-points, was included in the longitudinal study.

Cross-sectional study

Non-parametric Spearman correlations (two-tailed) were used to determine associations between the behavioral measures of response accuracy and RT with WML. A linear mixed model with *post hoc* (LSD) analyses were used to characterize case/control differences, with the between subject factor of Group (TBI or Control) and the within-subject factor of WML [1-3-4-5].

Longitudinal study

Because of the small sample size of the subgroup of the subjects for whom longitudinal data was acquired, simple paired *t*-tests were used for within-group comparison between Time 1 and Time 2.

MRI DATA PROCESSING

Functional MRI data were preprocessed and processed using the FSL package (Smith et al., 2004; Woolrich et al., 2009).

Preprocessing

Preprocessing included motion correction, brain extraction, spatial smoothing (FWHM = 5 mm), and high pass temporal filtering (66 s).

Processing: first-level analysis

Data were processed at the individual level according to their event-related design, for a total of five events-lists. Correct trials constituted the first four events, corresponding to the number of items loaded in working memory (WML): WML = 1 ("Baseline"); WML = 3 ("Low WML"); WML = 4 ("Intermediate WML"); WML = 5 ("High WML"). Failed and missed trials were assembled together in a fifth event that was excluded from analysis. Whitening was appended to data estimation, after convolution with double Gamma hemodynamic response function. Temporal derivative was applied, as well as temporal filtering. Four contrasts were used for this study:

- "Low WML" (Low WML versus Baseline)
- "Intermediate WML" (Intermediate WML versus Baseline)
- "High WML" (High WML versus Baseline)
- "WML increase" (High WML versus Low WML)

Individual activation maps were registered on the standard MNI space through the following steps: structural T2 was the initial image (linear – normal search – 7 DOF), 3D structural volume was the main structural image (linear – normal search – 12 DOF) and the MNI template ("avg152T1_brain" in FSL) was the standard space (linear – normal search – 12 DOF).

Processing: higher-level analysis

Higher-level analyses were processed at the group level (TBI and Control), using a fixed effects model. The measures for the cross-sectional study were: "mean Control group" and "mean TBI group" for the above-mentioned four contrasts. The contrasts for the longitudinal study were "mean TBI group Time 1" and "mean TBI group Time 2." In addition to a voxel threshold of $p = 0.05$, all maps were thresholded at the cluster level ($Z = 1.8$) in order to correct for multiple comparison. The template space was used as background for rendering.

Qualitative analysis

A complete list of all activated areas was compiled, using anatomical atlases (Mai et al., 2004; Ratiu and Talos, 2006) for correct determination of areas.

Quantitative analysis: regions of interest

Our choice for the regions of interest (ROI), determined by our working hypothesis, included the ACC. In an ideally large study, we would have compared the ACC activity with all the areas reportedly involved in spatial working memory processing (Wager and Smith, 2003; D'Esposito, 2008). However, because of the sample size of our study, we focused on the comparison of ACC with the left sensorimotor cortex (lSMC) because involvement of this later area has been well demonstrated in spatial working memory studies (Shaw et al., 2009) as well as in studies of mental imagery (Fiehler et al., 2008; Hanakawa et al., 2008; Sack et al., 2008).

We defined two spherical ROI according to their MNI coordinates and radius length (mm):

- Left sensorimotor cortex: $x = -40$; $y = -32$; $z = 56$; $r = 20$
- Anterior cingulate cortex : $x = 0$; $y = 34$; $z = 28$; $r = 14$

Regions of interests were used as masks in order to retrieve individual time-series values within these areas, using the "avwmeants" function included in the FSL package, hence obtaining the intensity of the betas based on the GLM model.

Statistical analyses were conducted for each ROI:

- Within-subjects differences between contrasts were explored using repeated measures ANOVAs. One-tailed *t*-tests were used for *post hoc* analyses.
- Within-subjects correlations between each ROI's levels of activation and WML (3, 4, or 5 items) were calculated using non-parametric Spearman correlations.
- Between subjects differences for each ROI were assessed using one-tailed *t*-tests.
- For the longitudinal study, within-subjects changes over time for each ROI were assessed using paired *t*-tests.

RESULTS

The first part of this section describes the cross-sectional study (TBI group versus Control group); the second part describes the longitudinal study (TBI group at Time 1 versus Time 2).

CROSS-SECTIONAL STUDY

Behavioral results: within-group analysis

Spearman correlation coefficients indicated a decline in both accuracy and RT with increasing WML in the control group. A decline in accuracy with increasing WML was observed for the TBI group, but no such effects were noted for RT (**Table 3**).

Behavioral results: between-groups analysis

Linear mixed model analyses for response accuracy indicated significant main effects of Group ($F = 9.635$, $p = 0.003$) and WML ($F = 17.356$, $p < 0.001$). There were no Group by WML interactions ($F = 1.213$, $p = 0.321$). *Post hoc* analyses with LSD corrections using one-tailed statistics suggested statistically significant effects (all $p < 0.10$) between all pairwise comparisons of WML. This suggests that our spatial working memory task is not only sensitive in detecting case/control differences but also shows the expected dose–response relationship between response accuracy and WML, with less accurate responding observed with increasing WML.

Similarly, linear mixed model analyses for RT indicated significant main effects of Group ($F = 28.188$, $p < 0.001$) and WML ($F = 2.767$, $p = 0.052$). There were no Group by WML interactions ($F = 0.173$, $p = 0.914$). *Post hoc* analyses with LSD corrections using one-tailed statistics suggested statistically significant effects (all $p < 0.10$) between the following pairwise comparisons of WML: 1 versus 4 and 5; 3 versus 4 and 5, indicating significant differences in RT from the baseline and easy conditions (load of 1 and 3) compared to the harder and more demanding conditions (load of 4 and 5). The Control group performed faster than the TBI group, regardless of WML. Also, across groups, participants were faster on the higher, and thus more difficult, WML trials (4 and 5) compared to the easier trials (1 and 3), with the longest time taken on the Baseline condition (WML of 1) in both groups. Results are summarized in **Figure 2**.

Post hoc analysis (see **Table 4**) show groups differences for accuracy and RTs in all conditions, with the exception of accuracy during the Baseline condition (WML = 1). Both groups were indeed close to 100% accuracy on the Baseline condition (96 and 99%, respectively for TBI and Controls).

Table 3 | Within-groups performance effects.

	TBI group	Control group
Correlation between WML and accuracy	$r = -0.645$; $p < 0.001$*	$r = -0.843$; $p < 0.001$*
Correlation between WML and response time	$r = -0.179$; $p = 0.244$	$r = -0.403$; $p = 0.007$*

**Statistically significant result.*

Imaging results and qualitative analysis: network recruited by the spatial working memory task

Differences between groups were visible on statistical maps for each condition. In all cases, however, a common network of activated areas was observed in both groups, as follows: cingulate cortex (anterior and posterior); frontal cortex, including: frontal gyri (superior, middle, and inferior) and precentral gyrus; parietal cortex, including: supramarginal gyrus, angular gyrus, parietal lobule, and post-central gyrus; temporal cortex (medial and inferior temporal gyri); occipital cortex; subcortical structures, including: head of caudate nucleus, parahippocampal gyrus, putamen, thalamus and insula.

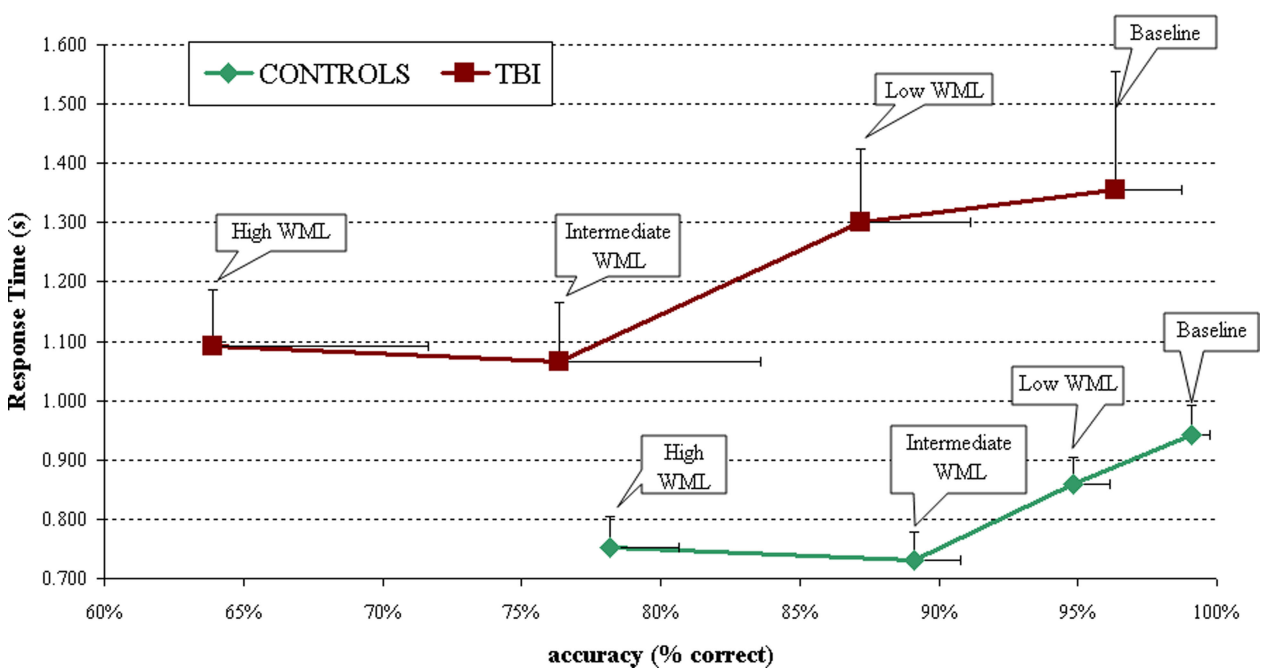

FIGURE 2 | Behavioral results for the cross-sectional study.

Imaging results and quantitative analysis of regions of interest: within-subjects effect of working memory load

Two ROI, ACC and lSMC, were defined as described in the section "Materials and Methods" and compared with regards for WML. Comparison of "Low WML" to "High WML" contrasts for the TBI group showed significant difference for the ACC ($p = 0.049$) but not for the lSMC ($p = 0.127$). The opposite was observed in the Control group, where the comparison of "Low WML" to "High WML" showed no difference for the ACC ($p = 0.387$) but a significant difference was observed for the lSMC ($p = 0.005$). **Figure 3** illustrates these results.

Table 4 | *p* values for TBI and Control groups comparisons on the behavioral measures.

	Baseline	Low WML	Intermediate WML	High WML
Accuracy	0.139	0.040*	0.051	0.048*
RT	0.028*	0.002*	0.004*	0.003*

**Statistically significant result.*

In the TBI group, activity in the ACC was associated (as a trend) with WML ($r = 0.327$; $p = 0.06$) but activity in lSMC was not ($r = -0.210$; $p = 0.24$). In the Control group, the opposite was observed: activity in the ACC was not correlated with WML ($r = 0.052$; $p = 0.76$) but correlation of the activity in the lSMC was significant, albeit in a negative direction ($r = -0.462$; $p = 0.005$).

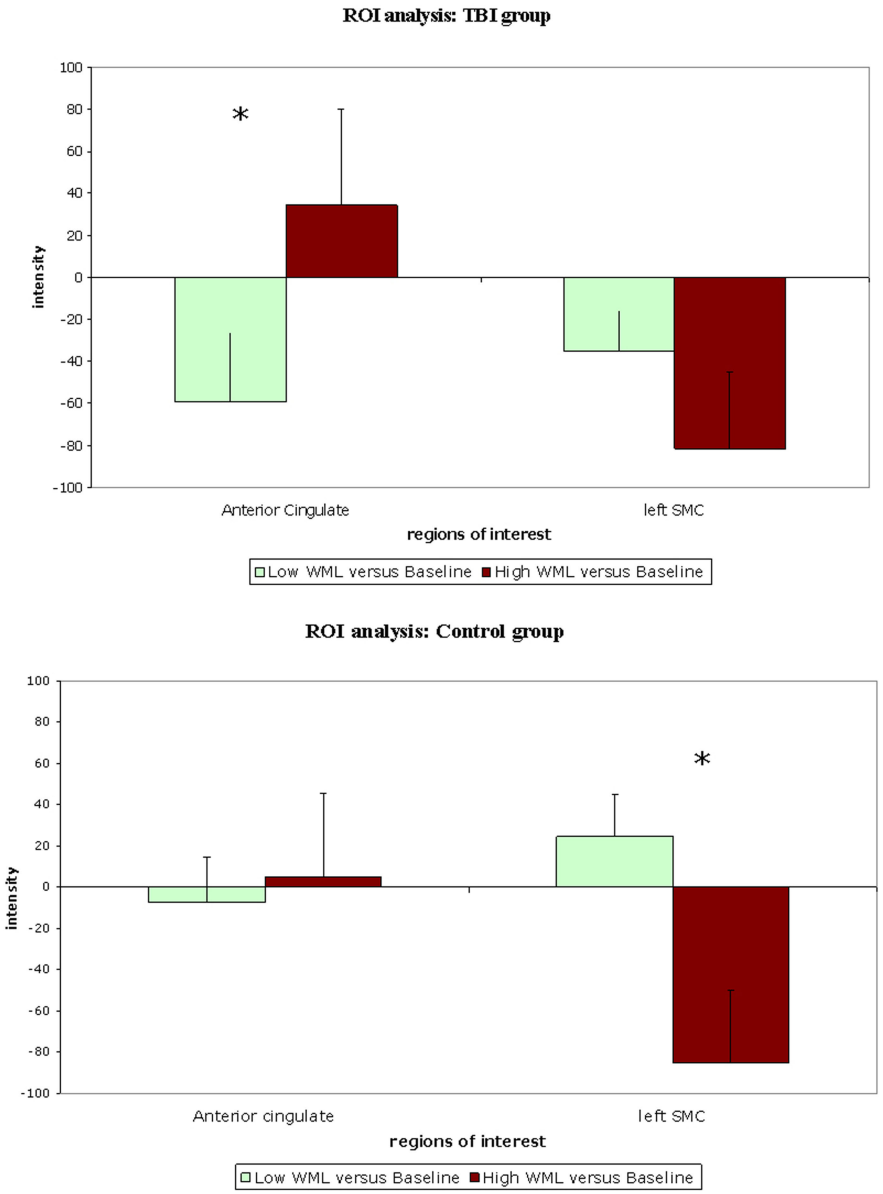

FIGURE 3 | Comparison of activation in regions of interest for "Low WML" (green) and "High WML" (brown) contrasts in traumatic brain injury group and Control group respectively.

Imaging results and quantitative analysis of regions of interest: between-subjects effect of working memory load

The use of a parametric task allowed us to examine the effect of WML by analyzing the contrast "WML increase" (WML = 5 items versus WML = 3 items). For the ACC region, a significant group difference was observed ($p = 0.038$), with the TBI group exhibiting more activation than the Control group. There was no observed group difference for this contrast, however, for the lSMC region ($p = 0.356$).

LONGITUDINAL STUDY

Behavioral results

As summarized in **Table 5** and **Figure 4**, the TBI patients' performances were compared between Time 1 and Time 2 (approximately 12 months apart).

Imaging results

Activation was observed in the ACC and the head of caudate nucleus for the "Time 1 versus Time 2" contrast, while activation of lSMC was observed for the contrast "Time 2 versus Time 1," as shown in **Figure 5**.

Table 5 | *p* values for Time 1 versus Time 2 behavioral data for the TBI patients.

	Accuracy	RT
Baseline	0.394	0.103
Low WML	0.117	0.047*
Intermediate WML	0.263	0.049*
High WML	0.289	0.032*

**Statistically significant result.*

Between Time 1 and Time 2, the change of activation in ACC was not significant ($p = 0.321$) but the activation of lSMC was significantly increased at Time 2 as compared to Time 1 ($p = 0.032$).

DISCUSSION

CROSS-SECTIONAL STUDY: PERFORMANCE

Adolescent TBI patients showed worse behavioral performance (higher RTs and poorer accuracy) than Controls on the spatial working memory task. This finding is consistent with an extended literature of cognition after brain injury, which reports that pediatric patients with moderate to severe TBI experience psychomotor slowing and impaired working memory (see Babikian and Asarnow, 2009 for a review). It is important to note that the composition of the groups may have influence this result because gender was not equally distributed across the TBI and Control groups. Education level was not tested and difference of education level between groups cannot be excluded.

CROSS-SECTIONAL STUDY: BRAIN IMAGING

In both groups, the spatial working memory task activated a broadly distributed network involving the prefrontal cortex, the cingulate cortex, the pre and post-central gyri, wide areas of the parietal and occipital cortices, medial and inferior temporal gyri, as well as subcortical structures, notably the head of the caudate nucleus. These findings are consistent with literature of spatial working memory (Wager and Smith, 2003; D'Esposito, 2008). Quantitative differences between groups were observed, and this also is consistent with the literature on brain imaging of TBI (Hillary et al., 2002; Cazalis et al., 2006; Niogi et al., 2008).

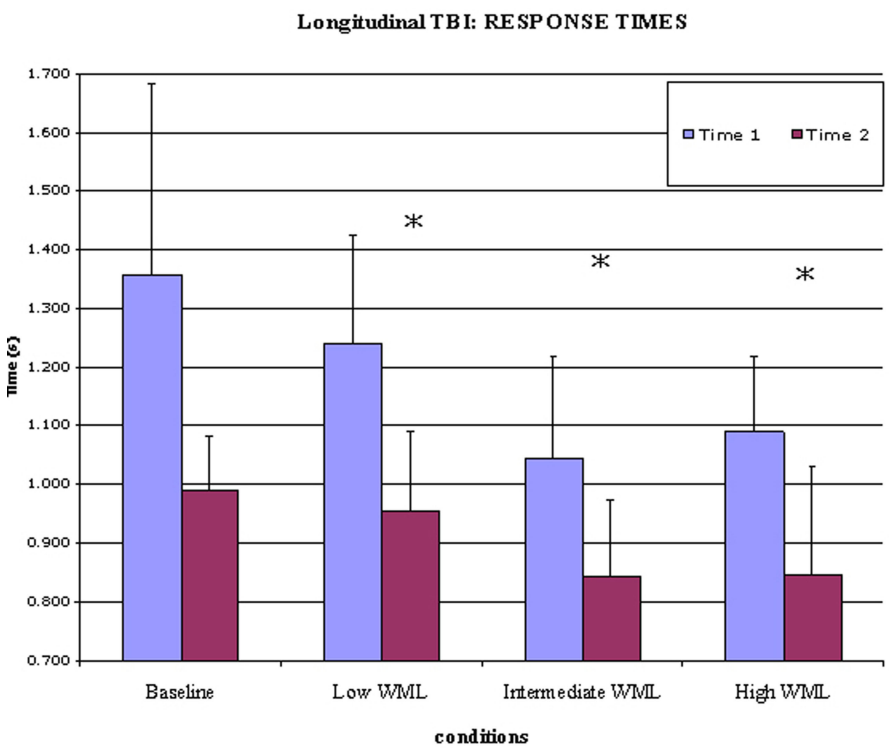

FIGURE 4 | Significant decrease of response times at Time 2 versus Time 1 in TBI patients.

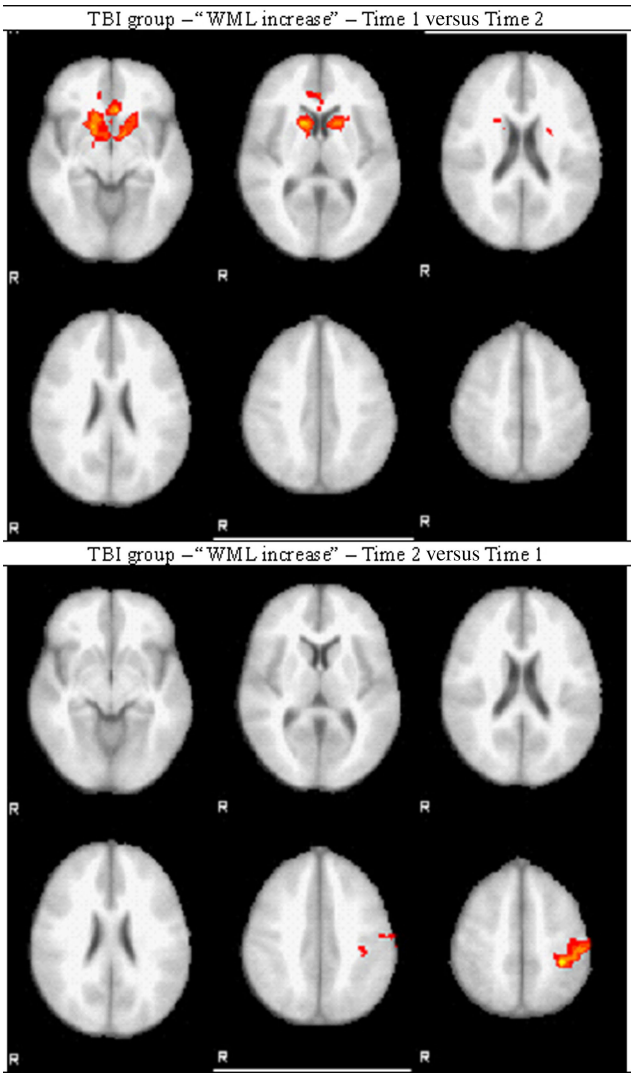

FIGURE 5 | Longitudinal contrasts for TBI patients.

The region of interest analysis was focused on the ACC, in order to understand its role in executive functions after moderate to severe TBI, and on the lSMC as well, because of its established role in spatial working memory.

Quantitative within-subject analyses of ROI activity in response to WML showed that, in the TBI group, ACC was significantly more activated when WML increased, while there was no change of lSMC activation. In the Control group, the opposite was observed: there was no change in ACC activation between conditions while lSMC activation decreased when WML increased. Our interpretation of those results is that Control subjects and TBI patients do not rely on recruiting the same cortical areas in response to increasing WML: Control subjects showed decreased activation of lSMC while TBI patients showed increased activation of ACC. Corroborating this result, correlation analysis showed that ACC activation was associated (as a trend) with WML in TBI patients but not in Controls, and that lSMC activation was correlated (inversely) in Controls but not in TBI patients. This double dissociation suggests that ACC activation depends on WML in TBI patients but not in Controls, while lSMC activation depends on WML in Controls but not in TBI patients.

Between-subject analysis, that compared TBI and Control groups for "WML increase," showed that ACC activation was significantly increased in the TBI group as compared to the Control group. In contrast, there was no difference between groups regarding lSMC activation. These results brought supplementary precisions to the findings above: ACC activation in TBI significantly increased in response to task difficulty as compared to Controls. Control subjects apparently responded to difficulty by decreasing activation of lSMC, while such decrease could not be observed in TBI patients who showed very low lSMC activation from the beginning.

Our interpretation of these results is that, although TBI patients and Control subjects seemed to use similar cognitive processes and neural networks in order to solve a spatial working memory task, there were notable differences between groups in the way these networks were recruited in response to difficulty, i.e., increasing WML in our case. Such differences, which were strongly suggested by the differences of performance during task solving, were revealed by comparing activation of two of the areas composing this network: ACC and lSMC.

While measure of clear differences between TBI and Control groups is an encouraging finding, we are aware that this may be only one part of a larger picture and that further research should be done with larger samples in order to determine the behavior of other areas involved in processing of items in spatial working memory, such as intraparietal cortex and dorsolateral prefrontal cortex.

LONGITUDINAL STUDY: PERFORMANCE

Six TBI patients were able to return for a second experimental session an average of 12 months after Time 1. While they did not show improvement in accuracy, their RTs were significantly decreased at Time 2. Recovery of cognitive functions after TBI has been extensively studied and our results are highly consistent with the existing literature. A recent meta-analysis of cognitive outcome after TBI (Babikian and Asarnow, 2009) showed that there is substantial recovery of processing speed in TBI patients over time, while recovery of working memory was noted in patients presenting with the most severe TBI.

LONGITUDINAL STUDY: BRAIN IMAGING

Within-subject analysis was a comparison of "WML increase" (WML of 5 items versus WML of 3 items) between Time 1 and Time 2. ACC and the head of caudate nucleus were more activated post-acutely as compared to the chronic phase, while lSMC was more activated in the chronic phase as compared to the post-acute phase; that is after a period of time allowing for recovery. These results, despite the small sample size, confirm our cross-sectional findings suggesting that prior to recovery, TBI patients significantly recruit ACC region for working memory, but they switch to lSMC recruitment following a period of recovery. Quantitative analyses of ROI activation in response to difficulty confirmed the increase of lSMC recruitment after recovery. This should be interpreted with regard to the cross-sectional study, which demonstrated a decreased recruitment of lSMC in response to difficulty (WML

increase) in Controls while lSMC activation was consistently low in the TBI group. The fact that we observed more lSMC activation in TBI patients at Time 2 as compared to Time 1 suggests that they recovered the ability to use this area, although it is unclear if it follows the activation pattern observed in Controls. Moreover, it is important to note that because there was no longitudinal control group, we cannot exclude that such changes would not be due to recovery but simply to the fact that patients were one year older at Time 2, or may even have emerged by chance. This limitation, as well as the low number of subjects, makes the results of this longitudinal study difficult to interpret, but nevertheless encouraging, because they do show a change of activation pattern overtime, which parallels improvement in behavioral performance. It is reasonable to postulate that the changes of brain activation and behavioral performance observed in the TBI group between Time 1 and Time 2 result in the TBI group resembling the Control group over time, suggesting normalization and recovery.

FUNCTIONS OF ANTERIOR CINGULATE CORTEX

Over the last decade, several theories of ACC functions have been proposed, with some overlapping and some contradicting elements. Activation in ACC is observed in solving of difficult problem, multiple response management, conflict management, attention monitoring, and error detection (Botvinick et al., 2004; Ullsperger and Von Cramon, 2004; Declerck et al., 2006; Carter and van Veen, 2007; Hyafil et al., 2009; Ursu et al., 2009). In our study, only correct trials were included in brain imaging processing, therefore activation of the ACC cannot be attributed to error detection. In their study, Ursu et al. (2009) showed that there may be activation of ACC in presence of conflict even if the subject is not aware of such a conflict. Due to the structure of the task used in our study, it is not likely that the observed ACC activation was due to response override or conflict management. Magno et al. (2006) have indeed suggested that ACC activity is not related to error but to evaluation of difficulty. Furthermore, another study has shown that increased ACC activity was independent of anticipated error or conflict (Aarts et al., 2008). Finally, a study of TBI patients showed that ACC activity is increased with cognitive fatigue as experienced during effortful tasks (Kohl et al., 2009). This suggests that models of ACC functioning should include the broader concept of task difficulty – also described as challenging, effortful or demanding cognitive tasks –, thus encompassing concepts of error detection and conflict management.

Botvinick et al. (2004) have proposed an integrative hypothesis of ACC monitoring attention that applies to our results. According to their theory, activation of the ACC is associated with compensatory adjustment in response to tasks "experienced as cognitively difficult," considering that "conflict might serve as an index of the demand for mental effort," but that difficulty can occur in absence of conflict. While TBI subjects in our study did not perform as well as Controls despite exhibiting the highest ACC activation, this is not sufficient to exclude a compensatory adjustment. The compensatory adjustment theory, however, is used to explain studies showing that ACC activation is associated with higher performance (Botvinick et al., 2001; Garavan et al., 2002; Kerns et al., 2004). The results of our study apparently contradict those results, since TBI patients exhibited worse performance than Controls. However, in a previous fMRI study, we have shown that adult patients with severe TBI who perform very poorly on a planning task with working memory components exhibited reduced activation of the ACC as compared to severe TBI patients who were able to perform as well as Control subjects (Cazalis et al., 2006). Similar results were described by Kohl et al. (2009) as a coping mechanism. It is therefore reasonable to assume that those TBI patients in our current study, who were able to complete the task, may have recruited ACC in a compensatory adjustment fashion, in order to avoid poorer performance.

Alternatively, other studies of individual performance and cortical activation variability suggest that activity in ACC could reflect the ability of the individual to succeed at the task, in which case ACC activation could be seen as a predictor of performance. In a review of PET studies, Paus et al. (1998) argued that ACC activation positively reflects the level of difficulty of a task, which is itself indicative of the level of performance. In a study of a planning task, Cazalis et al. (2003) showed that subjects with poorer performance exhibited greater activation of the ACC than subjects with better performance. Hahn et al. (2007) have shown that ACC activity is dependent on performance (RTs). In two studies of verbal working memory, Osaka et al. (2003, 2004) found greater ACC activation in individuals with higher verbal working memory spans. Although it is difficult to transpose verbal WM and spatial WM, these studies interestingly confirm the dependence of ACC activation on performance. Furthermore, another study of anatomical variation of ACC demonstrated an association between a specific (leftward) morphological pattern of paracingulate sulcus folding and higher performance in demanding cognitive tasks (Fornito et al., 2004).

Such accumulation of results, including conflicting data, may lead the reader to a broad vision of ACC as a backup system that takes over problem solving when the executive system is overloaded. In simple words, ACC could be the ace up the prefrontal cortex's sleeve, meant to be used when executive functions are impaired or overloaded, whether by physical disconnection as in TBI or simply by a high level of difficulty. As a backup system, its efficiency would be limited, but would be involved in improving performance up to a certain limit, and would remain activated after this limit has been reached. This hypothesis is compatible with the concept of compensatory adjustment and would explain why some studies show that individuals with ACC lesions are still able to solve difficult problems (di Pellegrino et al., 2007). Furthermore, as suggested by our results, a double dissociation between ACC and lSMC activation in response to difficulty could account for the conflicting literature regarding the role of ACC.

CONCLUSION

While our study provides yet another small brick to the construction of ACC understanding, it is noteworthy that the ACC is involved in so many apparently distinct functions that one may have to reconsider the existing theoretical framework before one can reach firm conclusions. One aspect that deserves further consideration is the structure–function relationship that exists at the level of the ACC (Koski and Paus, 2000; Margulies et al., 2007; Orr and Weissman, 2009) as it exists in other regions. For example, one appealing model has been proposed that connects the

structure of dorsolateral prefrontal cortex to its functions, with concrete action planning being closer to motor areas and more abstract planning being more rostral (Koechlin and Jubault, 2006; Badre and D'Esposito, 2007), consistently with the perception–action model that was developed by Fuster (2005). A similarly innovative proposition was made by Postle (2006), stating that working memory is an emergent function rather than an embedded function, a theory also supported by Zimmer (2008). The ACC occupies a strategic location in the brain and therefore has the capacity of integrating of a wide variety of inputs. Indeed, ACC activity has been associated with a wide variety of mental functions, such as attention (Brocki et al., 2009), motivation (Ullsperger and Von Cramon, 2004), sexuality (Stoléru et al., 1999), pain (Robinson et al., 2009), executive functions (Mansouri et al., 2009), among others.

Most models, deeply influenced by Cartesian heritage, draw a scientific line between emotional and intellectual processes, despite our knowledge that these functions are highly interdependent. In order to fully understand how one cerebral area can process such diverse information, we may have to rethink those categories and investigate their potential interconnections. A neurophenomenological approach would suggest that all inputs processed by one area have to share either a common architecture or require a common processing (Allman et al., 2001). Therefore, seeking the common ground of these inputs would provide essential information on the fundamental roles of the ACC. It is likely that such an integrative theory would help unifying the current models of ACC functions.

ACKNOWLEDGMENTS

We want to thank Bernard Mendiburu for Matlab programming and support, Russell Poldrack for help with study design, Trent Thixton for help with brain imaging, Tarman Aziz for proofreading, Claudia Kernan and Nina Newman for patients' assessment and consenting, all the RAPBI members for discussion and feedback. This work was supported by the UCLA Brain Injury Research Center (Christopher Giza, Robert F. Asarnow), The Della Martin Foundation, Winokur Family Foundation/Child Neurology Foundation (Christopher Giza), UCLA Faculty Grants Program.

REFERENCES

Aarts, E., Roelofs, A., and van Turennout, M. (2008). Anticipatory activity in anterior cingulate cortex can be independent of conflict and error likelihood. *J. Neurosci.* 28, 4671–4678.

Allman, J. M., Hakeem, A., Erwin, J. M., Nimchinsky, E., and Hof, P. (2001). The anterior cingulate cortex: the evolution of an interface between emotion and cognition. *Ann. N. Y. Acad. Sci.* 935, 107–117.

Babikian, T., and Asarnow, R. (2009). Neurocognitive outcomes and recovery after pediatric TBI: meta-analytic review of the literature. *Neuropsychology* 23, 283–296.

Badre, D., and D'Esposito, M. (2007). FMRI evidence for a hierarchical organization of the prefrontal cortex. *J. Cogn. Neurosci.* 19, 1–18.

Botvinick, M. M., Braver, T. S., Barch, D. M., Carter, C. S., and Cohen, J. D. (2001). Conflict monitoring and cognitive control. *Psychol. Rev.* 108, 624–652.

Botvinick, M. M., Cohen, J. D., and Carter, C. S. (2004). Conflict monitoring and anterior cingulate cortex: an update. *Trends in Cogn. Sci.* 8, 539–546.

Brocki, K., Clerkin, S. M., Guise, K. G., Fan, J., and Fossella, J. A. (2009). Assessing the molecular genetics of the development of executive attention in children: focus on genetic pathways related to the anterior cingulate cortex and dopamine. *Neuroscience* 164, 241–246.

Carter, C. S., and van Veen, V. (2007). Anterior cingulate cortex and conflict detection: an update of theory and data. *Cogn. Affect. Behav. Neurosci.* 7, 367–379.

Cazalis, F., Feydy, A., Valabregue, R., Pelegrini-Issac, M., Pierot, L., and Azouvi, P. (2006). fMRI study of problem-solving after severe traumatic brain injury. *Brain Inj.* 20, 1019–1028.

Cazalis, F., Valabregue, R., Pelegrini-Issac, M., Asloun, S., Robbins, T. W., and Granon, S. (2003). Individual differences in prefrontal cortical activation on the Tower of London planning task: implication for effortful processing. *Eur. J. Neurosci.* 17, 2219–2225.

Declerck, C. H., Boone, C., and De Brabander, B. (2006). On feeling in control: a biological theory for individual differences in control perception. *Brain Cogn.* 62, 143–176.

D'Esposito, M. (2008). "Working memory," in *Handbook of Clinical Neurology*, eds P. J. Vinken and G. W. Bruyn (Amsterdam: Elsevier), 237–247.

di Pellegrino, G., Ciaramelli, E., and Ladavas, E. (2007). The regulation of cognitive control following rostral anterior cingulate cortex lesion in humans. *J. Cogn. Neurosci.* 19, 275–286.

Fiehler, K., Burke, M., Engel, A., Bien, S., and Rösler, F. (2008). Kinesthetic Working Memory and Action Control within the Dorsal Stream. *Cereb. Cortex* 18, 243–253.

Fornito, A., Yucel, M., Wood, S., Stuart, G. W., Buchanan, J. A., Proffitt, T., Anderson, V., Velakoulis, D., and Pantelis, C. (2004). Individual differences in anterior cingulate/paracingulate morphology are related to executive functions in healthy males. *Cereb. Cortex* 14, 424–431.

Fuster, J. M. (2005). *Cortex and Mind: Unifying Cognition*. New York: Oxford University Press.

Garavan, H., Ross, T. J., Murphy, K., Roche, R. A. P., and Stein, E. A. (2002). Dissociable executive functions in the dynamic control of behavior: inhibition, error detection, and correction. *Neuroimage* 17, 1820–1829.

Ghajar, J., and Ivry, R. B. (2008). The predictive brain state: timing deficiency in traumatic brain injury? *Neurorehabil. Neural. Repair* 22, 217–227.

Hahn, B., Ross, T. J., and Stein, E. A. (2007). Cingulate activation increases dynamically with response speed under stimulus unpredictability. *Cereb. Cortex* 17, 1664–1671.

Hanakawa, T., Dimyan, M. A., and Hallett, M. (2008). Motor planning, imagery, and execution in the distributed motor network: a time-course study with functional MRI. *Cereb. Cortex*. 18, 2775–2788.

Hillary, F., Steffener, J., Biswal, B., Lange, G., DeLuca, J., and Ashburner, J. (2002). Functional magnetic resonance imaging technology and traumatic brain injury rehabilitation: guidelines for methodological and conceptual pitfalls. *J. Head Trauma Rehabil.* 17, 411–430.

Hyafil, A., Summerfield, C., and Koechlin, E. (2009). Two mechanisms for task switching in the prefrontal cortex. *J. Neurosci.* 29, 5135–5142.

Kerns, J. G., Cohen, J. D., MacDonald, A. W. III, Cho, R. Y., Stenger, V. A., and Carter, C. S. (2004). Anterior cingulate conflict monitoring and adjustments in control. *Science* 303, 1023–1026.

Koechlin, E., and Jubault, T. (2006). Broca's area and the hierarchical organization of human behavior. *Neuron* 50, 963–974.

Kohl, A. D., Wylie, G. R., Genova, H. M., Hillary, F. G., and DeLuca, J. (2009). The neural correlates of cognitive fatigue in traumatic brain injury using functional MRI. *Brain Inj.* 2, 420–432.

Koski, L., and Paus, T. (2000). Functional connectivity of the anterior cingulate cortex within the human frontal lobe: a brain-mapping meta-analysis. *Exp. Brain Res.* 133, 55–65.

Magno, E., Foxe, J. J., Molholm, S., Robertson, I. H., and Garavan, H. (2006). The anterior cingulate and error avoidance. *J. Neurosci.* 26, 4769–4773.

Mai, J. K., Paxinos, G., and Assheuer, J. K. (2004). Atlas of the Human Brain, 2nd Edn. San Diego, CA: Academic Press.

Mansouri, F. A., Tanaka, K., and Buckley, M. J. (2009). Conflict-induced behavioural adjustment: a clue to the executive functions of the prefrontal cortex. *Nat. Rev. Neurosci.* 10, 141–152.

Margulies, D. S., Kelly, A. M., Uddin, L. Q., Biswal, B. B., Castellanos, F. X., and Milham, M. P. (2007). Mapping the functional connectivity of anterior cingulate cortex. *Neuroimage* 37, 579–588.

Metting, Z., Rödiger, L. A., De Keyser, J., and van der Naalt, J. (2007). Structural and functional neuroimaging in mild-to-moderate head injury. *Lancet Neurol.* 6, 699–710.

Niogi, S. N., Mukherjee, P., Ghajar, J., Johnson, C. E., Kolster, R., Lee, H., Suh, M., Zimmerman, R. D., Manley, G. T., and McCandliss, B. D. (2008). Structural dissociation of attentional control and memory in adults with and without mild traumatic brain injury. *Brain* 131, 3209–3221.

Orr, J. M., and Weissman, D. H. (2009). Anterior cingulate cortex makes 2 contributions to minimizing distraction. *Cereb. Cortex* 19, 703–711.

Osaka, M., Osaka, N., Kondo, H., Morishita, M., Fukuyama, H., Aso, T., and Shibasaki, H. (2003). The neural basis of individual differences in working memory capacity: an fMRI study. *Neuroimage* 18, 789–797.

Osaka, N., Osaka, M., Kondo, H., Morishita, M., Fukuyama, H., and Shibasaki, H. (2004). The neural basis of executive function in working memory: an fMRI study based on individual differences. *Neuroimage* 21, 623–631.

Paus, T., Koski, L., Caramanos, Z., and Westbury, C. (1998). Regional differences in the effects of task difficulty and motor output on blood flow response in the human anterior cingulate cortex: a review of 107 PET activation studies. *Neuroreport* 9, R37–R47.

Pepin Press. (2006a). *The Agile Rabbit Visual Dictionary of Vegetables*, Agile Rabbit Editions. Amsterdam: Pepin Press.

Pepin Press. (2006b). *The Agile Rabbit Visual Dictionary of Fruits*, Agile Rabbit Editions. Amsterdam: Pepin Press.

Postle, B. R. (2006). Working memory as an emergent property of the mind and brain. *Neuroscience* 139, 23–38.

Rasmussen, I.-A., Xu, J., Antonsen, I. K., Brunner, J., Skandsen, T., Axelson, D. E., Berntsen, E. M., Lydersen, S., and Håberg, A. (2008). Simple dual tasking recruits prefrontal cortices in chronic severe traumatic brain injury patients, but not in controls. *J. Neurotrauma* 25, 1057–1070.

Ratiu, P., and Talos, I.-F. (2006). *Cross-Sectional Atlas of the Brain*. Cambridge, MA: Cambridge Harvard University Press.

Robinson, M., Edwards, S., Iyengar, S., Bymaster, F., Clark, M., and Katon, W. (2009). Depression and pain. *Front. Biosci.* 1, 5031–5051.

Sack, A. T., Jacobs, C., Martino, F. D., Staeren, N., Goebel, R., and Formisano, E. (2008). Dynamic premotor-to-parietal interactions during spatial imagery. *J. Neurosci.* 28, 8417–8429.

Sanchez-Carrion, R., Fernandez-Espejo, D., Junque, C., Falcon, C., Bargallo, N., Roig, T., Bernabeu, M., Tormos, J. M., and Vendrell, P. (2008). A longitudinal fMRI study of working memory in severe TBI patients with diffuse axonal injury. *Neuroimage* 43, 421–429.

Shaw, M. E., Moores, K. A., Clark, R. C., McFarlane, A. C., Strother, S. C., Bryant, R. A., Brown, G. C., and Taylor, J. D. (2009). Functional connectivity reveals inefficient working memory systems in post-traumatic stress disorder. *Psychiatry Res.* 172, 235–241.

Smith, S. M., Jenkinson, M., Woolrich, M. W., Beckmann, C. F., Behrens, T. E. J., Johansen-Berg, H., Bannister, P. R., De Luca, M., Drobnjak, I., Flitney, D. E., Niazy, R. K., Saunders, J., Vickers, J., Zhang, Y., De Stefano, N., Brady, J. M., and Matthews, P. M. (2004). Advances in functional and structural MR image analysis and implementation as FSL. *Neuroimage* 23(Suppl. 1), S208–S219.

Stoléru, S., Grégoire, M., Gérard, D., Decety, J., Lafarge, E., Cinotti, L., Lavenne, F., Le Bars, D., Vernet-Maury, E., Rada, H., Collet, C., Mazoyer, B., Forest, M. G., Magnin, F., Spira, A., and Comar, D. (1999). Neuroanatomical correlates of visually evoked sexual arousal in human males. *Arch. Sex. Behav.* 28, 1–21.

Ullsperger, M., and Von Cramon, D. Y. (2004). Neuroimaging of performance monitoring: error detection and beyond. *Cortex* 40, 593–604.

Ursu, S., Clark, K. A., Aizenstein, H. J., Stenger, V. A., and Carter, C. S. (2009). Conflict-related activity in the caudal anterior cingulate cortex in the absence of awareness. *Biol. Psychol.* 80, 279–286.

Wager, T. D., and Smith, E. E. (2003). Neuroimaging studies of working memory: a meta-analysis. *Cogn. Affect. Behav. Neurosci.* 3, 255–274.

Woolrich, M., Jbabd, S., Patenaude, B., Chappell, M., Makni, S., Behrens, T., Beckmann, C., Jenkinson, M., and Smith, S. M. (2009). Bayesian analysis of neuroimaging data in FSL. *Neuroimage* 45(Suppl.), S173–S186.

Zimmer, H. D. (2008). Visual and spatial working memory: from boxes to networks. *Neurosci. Biobehav. Rev.* 32, 1373–1395.

Conflict of Interest Statement: The authors declare that the research was conducted in the absence of any commercial or financial relationships that could be construed as a potential conflict of interest.

Received: 05 October 2010; paper pending published: 05 November 2010; accepted: 16 December 2010; published online: 21 January 2011.

*Citation: Cazalis F, Babikian T, Giza C, Copeland S, Hovda D and Asarnow RF (2011) Pivotal role of anterior cingulate cortex in working memory after traumatic brain injury in youth. Front. Neur. **1**:158. doi: 10.3389/fneur.2010.00158*

This article was submitted to Frontiers in Neurotrauma, a specialty of Frontiers in Neurology.